Intro
Therma

Techniqu

INTRODUCTION TO THERMAL ANALYSIS

Hot Topics in Thermal Analysis and Calorimetry

Volume 1

Series Editor:

Judit Simon, *Budapest University of Technology and Economics, Hungary*

Introduction to Thermal Analysis

Techniques and Applications

Edited by

Michael E. Brown

Chemistry Department,
Rhodes University,
Grahamstown, South Africa

KLUWER ACADEMIC PUBLISHERS
NEW YORK, BOSTON, DORDRECHT, LONDON, MOSCOW

eBook ISBN: 0-306-48404-8
Print ISBN: 1-4020-0472-9

Created in the United States of America

Visit Kluwer Online at: http://kluweronline.com
and Kluwer's eBookstore at: http://ebooks.kluweronline.com

CONTENTS

4. DIFFERENTIAL THERMAL ANALYSIS (DTA) AND DIFFERENTIAL SCANNING CALORIMETRY (DSC)

5. THERMOPTOMETRY

6. THERMOMECHANOMETRY

7. COMBINATION OF THERMAL ANALYSIS TECHNIQUES

PREFACE TO THE FIRST EDITION, CHAPMAN & HALL, LONDON, 1988

The aim of this book is, as its title suggests, to help someone with little or no knowledge of what thermal analysis can do, to find out briefly what the subject is all about, to decide whether it will be of use to him or her, and to help in getting started on the more common techniques. Some of the less-common techniques are mentioned, but more specialized texts should be consulted before venturing into these areas.

This book arose out of a set of notes prepared for courses on thermal analysis given at instrument workshops organized by the S.A. Chemical Institute. It has also been useful for similar short courses given at various universities and technikons. I have made extensive use of the manufacturers' literature, and I am grateful to them for this information. A wide variety of applications has been drawn from the literature to use as examples and these are acknowledged in the text. A fuller list of the books, reviews and other literature of thermal analysis is given towards the back of this book. The ICTA booklet 'For Better Thermal Analysis' is also a valuable source of information.

I am particularly grateful to my wife, Cindy, for typing the manuscript, to Mrs Heather Wilson for the line drawings, and to Professor David Dollimore of the University of Toledo, Ohio, for many helpful suggestions.

Michael E. Brown

Grahamstown 1987

ABOUT THE FIRST EDITION OF THIS BOOK...

"... a readable basic textbook covering material rarely seen in general analytical texts, at a level where the reader may gain an adequate overview of the information to be obtained from the various methods. (…) This book is a valuable starting point for those wishing to explore the field."

Peter C. Uden, University of Massachusetts
in Journal of the American Chemical Society (1990)

"Brown's work is a convenient and easy-to-read first book for those intending to use thermal analysis methods; it is a practical help in getting started."

György Pokol
in Journal of Thermal Analysis (1990)

"...an excellent, well-balanced, notably clear and thoroughly up-to-date introduction to the various techniques and methods of Thermal Analysis..."

Slade Warne, University of Newcastle (Australia)
in Canadian Mineralogist (1989)

"This excellent monograph in the field of thermal analysis does exactly what its title suggest. (…) Any student of thermal analysis would be well recommended to obtain a copy."

F.W. Wilburn
in NATAS Notes (1989)

"This is a book that many people will use and about which the author has a right to be proud. I have already started using it in teaching undergraduate and graduate courses and in planning laboratory experiments."

David Dollimore, University of Toledo
in Analytical Chemistry (1989)

PREFACE TO THE SECOND EDITION

Preparation of this Second Edition has made me very aware of how many things have changed since 1987. The greatest changes have been in the tasks that can now be comfortably handled by computers and their ever-growing range of accessories. The availability of sophisticated word processing and graphics packages, plus scanners and excellent printers, has, however, resulted in much greater responsibility being thrust upon authors for the preparation of camera-ready copy, a phrase that now causes scientists to leave their lab benches and become permanently attached to their computer screens. The number of people that the author can now blame for any remaining mistakes (although my wife, Cindy, has done her utmost to track these down) has decreased drastically to one!

In this Edition, relatively small sections of the First Edition have withstood the changes of 14 years. One of the most embarrassing parts of the First Edition, that has now disappeared without trace, is the Appendix of lots of programs written in Applesoft BASIC. Would that I had had the advice of Professor Bernhard Wunderlich in advance of the appearance of that Edition.

A sad aspect of the intervening years has been the death of Professor David Dollimore, whose helpful comments were acknowledged in the First Edition. My many collaborations with Dr Andrew Galwey of Belfast have continued and many of the aspects of Chapter 10 on kinetics owe a great deal to discussions with him over the years. I also am grateful to Mr Emmanuel Lamprecht and Dr Cheryl Sacht for commenting on some of the chapters.

This Edition will undoubtedly be criticized, even more than the First, by nomenclature purists. I have tried to indicate the complexity and unresolved nature of the nomenclature question and have made much, but certainly not exclusive, use of the logical scheme developed by Dr Wolfgang Hemminger and his ICTAC Nomenclature Committee. Instrument manufacturers have, however, had a large (and uncontrollable) part in the development of nomenclature and this is taken into account.

What will any future edition look like? The range of information on the Internet and the ease with which this information can be updated is impressive, but an alarming prospect for "old-timers".

Michael E. Brown
Grahamstown 2001

INTRODUCTION

1.1 Definition and History

What do bread and chocolate, hair and finger-nail clippings, coal and rubber, ointments and suppositories, explosives, kidney stones and ancient Egyptian papyri have in common? Many interesting answers could probably be suggested, but the connection wanted in this context is that they all undergo interesting and practically important changes on heating.

The study of the effect of heat on materials obviously has a long history, from man's earliest attempts at producing pottery, extracting metals (about 8000 BC) and making glass (about 3400 BC) through the philosophical discussions of the alchemists on the elements of fire, air, earth and water, to early work on the assaying of minerals (about 1500 AD), followed by the development of thermometry and calorimetry [1,2]. Only in the late 19th century did experiments on the effect of heat on materials become more controlled and more quantitative. Much of this work depended upon the development of the analytical balance which has its own interesting history [3,4]. Some milestones in the development of thermal measurements are given in Table 1.1.

Excellent accounts of the basic, but difficult, concepts of "heat" and "temperature" and the development of temperature scales have been given by Wunderlich [5] and by Schuijff [6]. A detailed thermodynamic background to thermal analysis and calorimetry has been provided by van Ekeren [7]. In very brief summary, *heat* is one of the forms in which energy can be transferred. Such transfer requires a temperature difference and three mechanisms of transfer have been identified: conduction, convection and radiation. The laws of thermodynamics deal with thermal equilibrium (zeroth), conservation of energy (first), direction of spontaneous processes including heat transfer (second), and the reference point for entropy measurements (third).

To provide useful qualitative and quantitative information on the effect of heat on materials, experiments have to be carefully planned, and use is often made of sophisticated equipment. The following formal definition of *thermal analysis* was originally provided by the International Confederation for Thermal Analysis and Calorimetry (ICTAC).

PREVIOUS

THERMAL ANALYSIS (TA) refers to a group of techniques in which a property of a sample is monitored against time or temperature while the temperature of the sample, in a specified atmosphere, is programmed.

A recent discussion of the above ICTAC definition by Hemminger and Sarge [8,9] points out some of the difficulties and suggests some modification to:

NEW

THERMAL ANALYSIS (TA) means the analysis of a change in a property of a sample, which is related to an imposed temperature alteration.

Hemminger and Sarge [8,9] explain that: (a) "analysis" means much more than "monitoring"; (b) in most experiments it is a *change* in a property, rather than the property itself which is monitored and (c) it is the temperature of the sample's environment (e.g. a furnace), rather than the actual sample temperature which is programmed. A "temperature alteration" includes: (i) a stepwise change from one constant temperature to another; (ii) a linear rate of change of temperature; (iii) modulation of a constant or linearly changing temperature with constant frequency and amplitude; and (iv) uncontrolled heating or cooling. The direction of change may involve either heating or cooling and the above modes of operation may be combined in any sequence. Isothermal experiments, other than at ambient temperature, are included in this definition under mode (i), where the first constant temperature is usually ambient temperature and the change is to the desired isothermal experimental conditions. The temperature may also be programmed to maintain a constant rate of reaction, such a mode is a sample-controlled programme (Chapter 3).

Hemminger and Sarge [8,9] state that the qualification concerning the "specified atmosphere" should not be part of the general definition, but is an operational parameter similar to other parameters such as crucible material, etc. They also distinguish between "thermoanalytical techniques" and "thermoanalytical methods". The techniques are characterized by the suffix "*-metry*", while the more comprehensive methods, which include the evaluation and interpretation of the measured property values, are indicated by adding "*analysis*". For example the technique of *differential thermometry* involves measurement of the difference in temperature of a sample and some reference material, but the interpretation of the observations made is part of the method of *differential thermal analysis.*

The proposals of Hemminger and Sarge have yet to obtain official recognition (August 2001) and acceptance by the various bodies concerned with thermal analysis and calorimetry. The proposals are described here because of their elegance as a logical system. Practical nomenclature, however, is determined by general acceptance and factors such as the role of journal editors in insisting on particular usage. Manufacturers also play a significant role in the terms used in their patents, instrument manuals and application sheets.

Because there are many properties of the sample which can be measured, the number of techniques (and associated methods) is quite large. The main sample properties used and the associated primary techniques are listed in Table 1.2. *Absolute* values of the sample property may be recorded, or the *difference* in the property of the sample compared to the same property of a reference material may be more convenient to measure, or the *rate of change* of the sample property with temperature (or time) may be of interest (derivative measurements). Further techniques (and methods) derived from those in Table 1.2. are listed in Table 1.3. Care is needed in interpreting the new terminology in terms of the familiar older names, particularly in the manufacturers' literature. When the pressure of the atmosphere in the apparatus is above ambient, the abbreviated technique is sometimes prefaced by HP for "high pressure", e.g. HPDTA.

The range of samples is enormous, limited usually, but not necessarily, to initially solid substances. Studies on liquids provide less information of interest and studies on gases are not usually included under thermal analysis. The temperature programme to which the sample is subjected is most often a constant heating (or cooling) rate and the atmosphere is usually an inert gas, but studies in reactive gases also provide a wealth of information.

Like most techniques based on relatively simple principles, the interpretation of results is not always as straightforward and, hence, it is important to combine information from several techniques whenever possible.

Table 1.1
Some milestones in the development of thermal measurements

DATE	PERSONS	DEVELOPMENTS
1714	Fahrenheit	Mercury thermometer and temperature scale
1742	Celsius	Temperature scale
1760	Black	Ice calorimeter
-1784	Lavoisier & Laplace	-ditto-
1782	Wedgwood	Pyrometer
1822	Seebeck	Thermoelectric effect
1826	Becquerel	Thermocouple development
-1836	Pouillet	-ditto-
-1886	Le Chatelier	-ditto-
1848	Kelvin	Absolute temperature scale
1871	Siemens	Resistance thermometer
1892	Le Chatelier	Optical pyrometer
1899	Austen-Roberts	DTA
1907	Henning	Dilatometry
1915	Honda	Thermobalance

The establishment of the International Confederation of Thermal Analysis (ICTA) in Aberdeen in 1965 and its growth and influence are important factors in the history of thermal analysis and are fascinatingly described, from personal experience, by Dr Robert Mackenzie [10]. ICTA became ICTAC in 1992 by adding Calorimetry to its title.

1.2 Thermal Analysis Instruments

All thermal analysis instruments have features in common. These are illustrated in Figure 1.1. The *sample,* contained in a suitable sample pan or crucible, is placed in a *furnace* and subjected to some desired temperature programme. During this procedure, one or more properties of the sample are monitored by use of suitable *transducers* for converting the properties to electrical quantities such as voltages or currents. The variety of the techniques to be discussed stems from the variety of physical properties that can be measured and the variety of transducers that can be used.

Measurements are usually continuous and the heating rate is often, but not necessarily, linear with time. The results of such measurements are *thermal analysis curves* and the features of these curves (peaks, discontinuities, changes of slope, etc.) are related to *thermal events* in the sample. ("Thermogram" is not a recommended term for a thermal analysis curve, because of its medical usage.) The thermal events which may be detected are described in Chapter 2.

Fig. 1.1
A generalized thermal analysis instrument and the resulting thermal analysis curve.

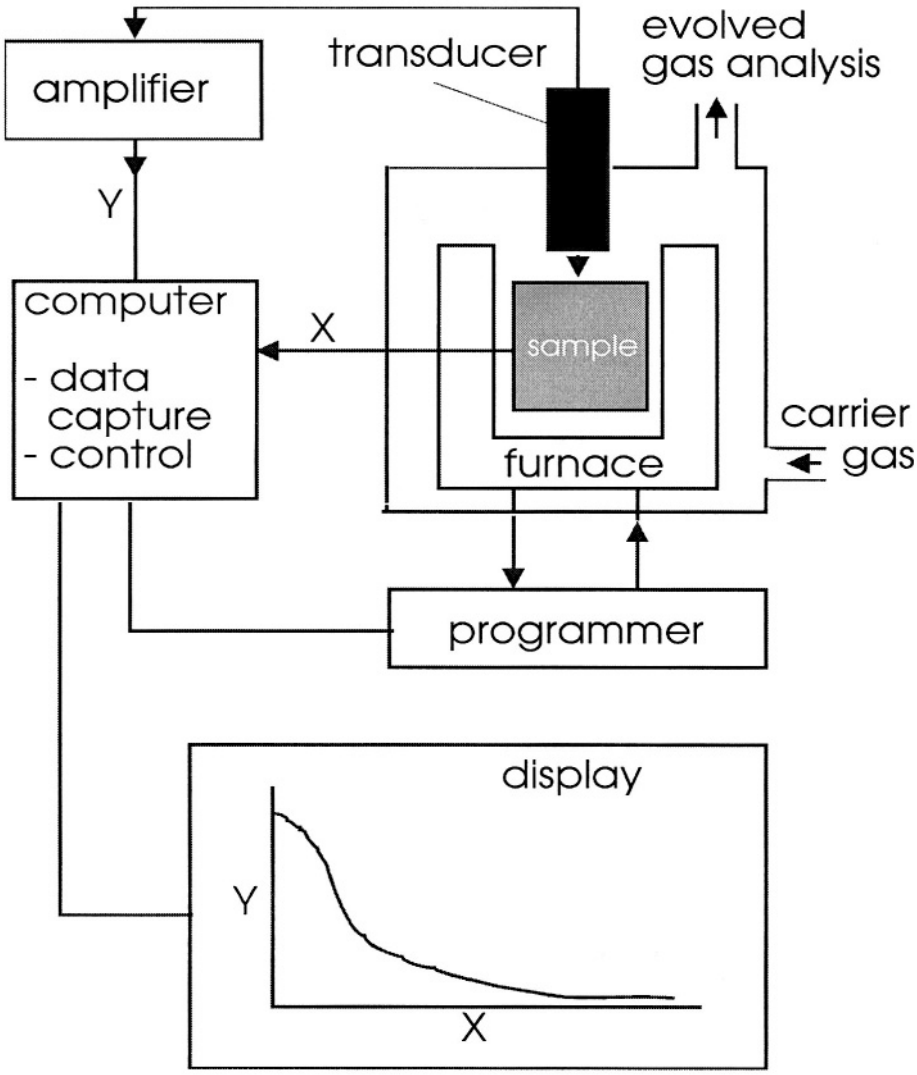

Table 1.2

THE PRIMARY THERMAL ANALYSIS (TA) TECHNIQUES AND METHODS

Property	Techniques	Methods	Abbreviations
Temperature	Thermometry	Heating or cooling curve analysis	
Temperature difference	Differential Thermometry	Differential Thermal Analysis	DT and DTA
Heat flow difference	Differential Scanning Calorimetry		DSC
Mass	Thermogravimetry	Thermogravimetric Analysis	TG and TGA
Dimensions or mechanical properties	Thermomechanometry	Thermomechanical Analysis	TM and TMA
Pressure	Thermomanometry	Thermomanometric Analysis	
Electrical properties	Thermoelectrometry	Thermoelectrical Analysis	TE and TEA
Magnetic properties	Thermomagnetometry	Thermomagnetic Analysis	
Optical properties	Thermoptometry	Thermoptometric Analysis	TO and TOA
Acoustic properties	Thermoacoustimetry	Thermoacoustimetric Analysis	TAA
Gas exchange	Thermally Stimulated Exchanged Gas Measurement	Thermally Stimulated Exchanged Gas Analysis	EGM and EGA
Chemical composition, crystal structure	various - see Table 1.3.		

Table 1.3

SPECIAL TECHNIQUES DERIVED FROM THE PRIMARY THERMAL ANALYSIS TECHNIQUES

Primary Technique	Special Techniques (Methods)	Property or conditions	Abbreviations
Thermomechanometry	Thermodilatometry (Thermodilatometric Analysis)	dimension (negligible force)	TD
	Static Force Thermomechanometry (Static Force Thermomechanical Analysis)	dimension (static force)	sf-TM and sf-TMA
	Dynamic Force Thermomechanometry (Dynamic Force Thermomechanical Analysis)	dimension (dynamic force)	df-TM and df-TMA
	Modulated Force Thermomechanometry (Modulated Force Thermomechanical Analysis)	dimension (modulated force)	mf-TM and mf-TMA

continued

Table 1.3 (continued)

SPECIAL TECHNIQUES DERIVED FROM THE PRIMARY THERMAL ANALYSIS TECHNIQUES

Primary Technique	Special Techniques (Methods)	Property or conditions	Abbreviations
Thermoptometry	Thermomicroscopy (Thermomicroscopic Analysis)	visual appearance	
	Thermoluminescence Measurement (Thermoluminescence Analysis)	emitted radiation	TLM
	Thermophotometry (Thermophotometric Analysis)	intensity of total reflected or transmitted radiation	
	Thermospectrophotometry (Thermospectrophotometric Analysis)	reflected or transmitted radiation of specific wavelength(s)	

continued

Table 1.3 (continued)

SPECIAL TECHNIQUES DERIVED FROM THE PRIMARY THERMAL ANALYSIS TECHNIQUES

Primary Technique	Special Techniques (Methods)	Property or conditions	Abbreviations
Thermoelectrometry	Thermally Stimulated Current Measurement	no superimposed electric field	TSCM
	(Thermally Stimulated Current Analysis)		TSCA
	(Alternating Current Thermoelectrical Analysis)	alternating electric field	ac-TEA
	(Dielectric Thermal Analysis)	dielectric properties	DETA
Thermoacoustimetry	Thermosonimetry	acoustic emission	TS
	Thermosonimetric Analysis		TSA

continued

Table 1.3 (continued)

SPECIAL TECHNIQUES DERIVED FROM THE PRIMARY THERMAL ANALYSIS TECHNIQUES

Primary Technique	Special Techniques (Methods)	Property or conditions	Abbreviations
Thermally Stimulated Exchanged Gas Measurement	Thermally Stimulated Exchanged Gas Detection	total amount of gas	EGD
	Thermally Stimulated Exchanged Gas Determination	composition of gas	EGA
	Thermally Stimulated Emanation Measurement (Emanation Thermal Analysis)	radioactive gas released	ETA
various	Thermodiffractometry Thermodiffractometric Analysis	crystal structure	

References

1. R.C. Mackenzie, Thermochim. Acta, 73 (1984) 249, 307; 92 (1985) 3; 148 (1989) 57; J. Thermal Anal., 40 (1993) 5, Israel J. Chem., 22 (1982) 203.
2. J.O. Hill (Ed.), "For Better Thermal Analysis and Calorimetry", 3rd Edn, ICTA, 1991.
3. C.J. Keattch and D. Dollimore, "An Introduction to Thermogravimetry", Heyden, London, 2nd Edn, 1975.
4. R. Vieweg, "Progress in Vacuum Microbalance Techniques", Vol. 1, (Eds T Gast and E. Robens), Heyden, London, 1972, p.l.
5. B. Wunderlich, “Thermal Analysis”, Academic Press, Boston, 1990.
6. A. Schuijff, “Calorimetry and Thermal Analysis of Polymers”, (Ed. V.B.F. Mathot), Hanser Publishers, Munich, 1994, Ch.l.
7. P.J. van Ekeren, “Handbook of Thermal Analysis and Calorimetry”, Vol.1, (Ed. M.E. Brown), Elsevier, Amsterdam, 1998, Ch.2.
8. W. Hemminger and S.M. Sarge, “Handbook of Thermal Analysis and Calorimetry”, Vol.1, (Ed. M.E. Brown), Elsevier, Amsterdam, 1998, Ch.l.
9. W. Hemminger, Recommendations of the ICTAC Nomenclature Committee, ICTAC NEWS, December 1998, p.106-122.
10. R.C. Mackenzie, J. Thermal Anal., 40 (1993) 5.

THERMAL EVENTS

2.1 Introduction

The *sample* referred to in the definition of thermal analysis in Chapter 1, is very often in the *solid* state, at least at the start of the investigation. The thermal behaviour of liquids can also be studied using special techniques (see below), but gases are not normally the principal reactants in thermal analysis experiments.

2.2 The Solid State

The main characteristic feature of the solid state is the relatively ordered arrangement of the constituent atoms, molecules or ions. Just as the concept of an "ideal gas" is useful in describing the behaviour of real gases, the concept of a "perfect solid" or "perfect crystal" is useful as the reference point for real solids. A perfect (crystalline) solid has a completely ordered arrangement of its constituents, while real solids have imperfections of many kinds. When the order present is marginally greater than for liquids, but considerably less than in a perfect crystal, the substance is sometimes referred to as a "non-crystalline solid". When liquids composed of complex molecules or ions (e.g. sucrose or silicates and a vast number of organic polymers) are cooled rapidly a *glass* may be formed. A glass resembles a solid in many of its physical properties, e.g. rigidity, but differs in that the constituents do not show the regular (lattice) arrangement of a crystalline solid. Glasses are thus examples of non-crystalline solids. They do not melt at a sharply-defined temperature, but soften over a temperature interval. This transition from the rigid glassy state to a more flexible form is known as the *glass transition* and the temperature interval over which this change occurs, known as the *glass transition temperature,* T_g, [6], is of tremendous importance in the practical use of polymers.

Crystalline solids may be classified according to the dominant bonding forces between the constituents in the crystal, i.e. as molecular, covalent, ionic or metallic crystals [2,7].

In *molecular crystals* the identity of each individual molecule is preserved. The van der Waals attractive forces between molecules, which give the solid its coherence, are weak compared with the (usually covalent) bonds between the atoms comprising each molecule. On heating, most molecular solids melt without chemical changes of the constituents. Some compounds may be unstable because of molecules with considerable internal strains or containing several reactive groups, as in many explosives, and decomposition may occur at temperatures below

the melting point. The size and shape of the constituent molecule has a very marked effect on the order possible when molecules are packed closely together. Large molecules (macromolecules), especially non-linear and relatively rigid molecules, seldom form very ordered arrangements. Thermal analysis has played an important role in exploring the properties of such high-polymers [6,8],

In *covalent crystals,* each constituent atom is linked to its neighbours through directed covalent bonds. The crystal structure is determined by the arrangement in space of these bonds. Such solids are hard and have high melting points, e.g. diamond, silicon carbide, etc.

In *ionic crystals,* ions of opposite charge are packed as efficiently as possible, subject to the additional influence of thermal energy. Because of the non-directional nature of electrostatic forces, the structures adopted are determined by: (i) the relative numbers of cations and anions, (ii) the relative sizes of positive and negative ions and (iii) the ionic shapes. Molecules of water (or solvent) of crystallization, may be incorporated in the crystal structure. Dehydration usually precedes decomposition but some overlap of these processes may occur.

Metals (and alloys) are usually close-packed arrangements of similar sized spheres. Each atom has a high coordination number. The valence electrons from each atom have freedom to migrate in an applied field so that metals are good conductors of electricity, e.g., copper, iron, lead, etc.

In many crystalline substances there may be several bond types, e.g. the vast number of coordination compounds. Loss of water from a crystal containing a hydrated cation involves the rupture of coordinate bonds and the associated hydrogen bonds.

2.3 Reactions of Solids

When a single pure solid substance, A, is heated in an inert atmosphere, the resultant increase in molecular, atomic or ionic motion may lead to changes in crystal structure, sintering, melting or sublimation [1,2]. Some substances may decompose forming new molecular fragments, some or all of which may be volatile at the temperatures reached.

In a perfect solid at zero kelvin the constituent units, whether they be atoms, molecules or ions, form a completely and perfectly ordered three-dimensional array. This structural arrangement is the result of the interaction of the bonding forces amongst the units (and the zero-point energy). At higher temperatures, thermal energy results in increased vibration and rotation of the constituents. These motions, although random, are limited in extent and each constituent remains in the vicinity of its original site.

As a solid is heated, the amplitudes of the vibrations of the lattice constituents are increased and eventually a temperature will be reached where one (or more) of the following changes will occur, (i) *Phase transition*: a new arrangement of constituents may become more stable than the original [3,4]. (ii) *Melting*: When sufficient energy becomes available, the forces of attraction between constituents become insufficient to maintain the ordered arrangement of the solid and the system relaxes to the more disordered arrangement of constituents in a liquid [5]. For some complex molecules the change from solid to liquid may occur in stages. The

structures of intermediate order are known as *liquid crystals.* (iii) *Sublimation*: When the kinetic energy of the constituents increases very rapidly, direct transition to the disordered arrangement of a gas may occur, without the intermediate formation of a liquid phase, (iv) *Thermal decomposition*: When the bonding forces *within* constituent molecules or ions are weaker than those *between* the atoms constituting these units, increasing the temperature may result in bond redistribution and the formation of products chemically different from the reactant. Such chemical processes are referred to as thermal decomposition (or crystolysis) [2].

These processes, some of which are reversible, are represented symbolically in Table 2.1 below. It is not unusual for melting or sublimation to occur concurrently with thermal decomposition. During thermal decompositions that are accompanied by melting, the reaction usually proceeds more rapidly in the liquid than in the crystalline state.

Table 2.1
Thermal events on heating a single solid, A, in an inert atmosphere

		ΔH	sign	ΔMass
A (s,structure 1) → A (s,structure 2)	Phase transition	yes	+ or -	no
A (s) → A (ℓ)	Melting	yes	+	no
A (glass) → A (rubber)	Glass transition	no	no	no
A (s) → A (g)	Sublimation	yes	+	yes
A (s) → B (s) + gas or gases	Thermal decomposition	yes	+ or –	yes

2.4 Decomposition of Solids

Decomposition of a single pure solid substance A may be represented [1,2] as:

$$A(s) \rightarrow B(s) + C(g)$$

Numerous examples of such decompositions exist, e.g.

$$BaCl_2.2H_2O(s) \rightarrow BaCl_2(s) + 2H_2O(g)$$
$$CaCO_3(s) \rightarrow CaO(s) + CO_2(g)$$
$$BaN_6(s) \rightarrow Ba(s) + 3N_2(g)$$

In any real crystal of A there will be imperfect regions [2,7] within which the constituents are more reactive than in the bulk of the solid. The crystal surfaces are very important regions of relative imperfection on account of the less symmetrical bonding in these regions. At a suitably high temperature, decomposition can be initiated by redistribution of the bonding within

imperfect regions. These initially isolated regions of product, still embedded in a matrix of original reactant, are usually sufficiently mobile to reorganize into *nuclei* of product phase B. Mechanisms of nucleation are discussed in references [1,2]. Part of the surface of the product solid remains in contact with the crystal from which it was formed and this reactive reactant/product interface is important in discussions of solid state decomposition mechanisms [1,2]. Further decomposition results from either the *formation* of further nuclei, or through the *growth* of the existing nuclei by addition of further product across the reactant/product interface. Growth cannot continue indefinitely and nuclei eventually impinge on each other so that growth ceases along areas of contact, or growth may cease if contact is lost between product and the remaining reactant.

2.5 Reaction with the Surrounding Atmosphere

The sample may react with the surrounding atmosphere [9], e.g.

$$2Ag(s) + \tfrac{1}{2}O_2(g) \rightarrow Ag_2O(s)$$
$$CuO(s) + H_2(g) \rightarrow Cu(s) + H_2O(g)$$
$$Ni(s) + 4CO(g) \rightarrow Ni(CO)_4(g)$$
$$C(s) + O_2(g) \rightarrow CO_2(g)$$

The decomposition of organic polymers in inert atmospheres to produce fragments of lower molecular mass is called *thermal degradation* and is usually an endothermic process, in contrast to the (exothermic) *oxidation* in air or oxygen. Very rapid exothermic reactions can lead to self-sustaining *combustion* or, in the extreme, *explosion.*

2.6 Solid-Solid Interactions

When more than one solid substance is present initially, there are correspondingly more possibilities for interaction on heating. New phases, such as solid solutions or eutectic mixtures, may form, as well as new compounds formed by addition or double decomposition reactions [10], e.g.

$$Fe_2O_3(s) + MgO(s) \rightarrow MgFe_2O_4(s)$$
$$NaCl(s) + AgBr(s) \rightarrow AgCl(s) + NaBr(s)$$

The above changes are nearly always accompanied by enthalpy changes, and sometimes also by changes in mass (see Table 2.1), so they may be studied using one or more of the thermal analysis techniques introduced in Chapter 1 and described in greater detail in the following chapters.

References

1. M.E. Brown, D. Dollimore and A.K. Galwey, “Reactions in the Solid State”, Comprehensive Chemical Kinetics, Vol.22, Elsevier, Amsterdam, 1980.
2. A.K. Galwey and M.E. Brown, “Thermal Decomposition of Ionic Solids", Elsevier, Amsterdam, 1999.
3. C.N.R. Rao and K.J. Rao, “Phase Transitions in Solids”, McGraw-Hill, New York, 1978.
4. J.W. Christian, “Transformations in Metals and Alloys”, Pergamon, Oxford, 1965; Vol. l, 2nd Edn, 1975.
5. A.R. Ubbelohde, “Melting and Crystal Structure”, Clarendon, Oxford, 1965; “The Molten State of Matter”, Interscience, New York, 1978.
6. B. Wunderlich, “Thermal Analysis”, Academic, San Diego, 1990, p.95.
7. A.R. West, "Solid State Chemistry and its Applications", Wiley, Chichester, 1984, Ch.12.
8. E.A. Turi (Ed.), “Thermal Characterization of Polymeric Materials”, 2nd Edn, Vols 1 and 2, Academic, San Diego, 1997.
9. J. Szekely, J.W. Evans and H.Y. Sohn, "Gas-Solid Reactions", Academic, New York, 1976.
10. H. Schmalzried, "Solid State Reactions", Verlag Chemie, Weinheim, 2nd Edn, 1981.

THERMOGRAVIMETRY (TG)

3.1 Introduction

Measurements of changes in sample *mass* with temperature (*thermogravimetry,* see Table 1.2) are made using a thermobalance (sometimes referred to as a thermogravimetric analyzer). (Note that *mass* is a measure of the amount of matter in a sample, whereas *weight* refers to the effect of the gravitational force on a mass and thus varies from one geographical location to another.) A thermobalance is a combination of a suitable electronic microbalance with a furnace, a temperature programmer and computer for control, that allows the sample to be simultaneously weighed and heated or cooled in a controlled manner, and the mass, time, temperature data to be captured. The balance should be in a suitably enclosed system so that the nature and pressure of the atmosphere surrounding the sample can be controlled (see Figure 3.1). Care is usually taken to ensure that the balance mechanism is maintained at, or close to, ambient temperature, in an inert atmosphere.

3.2 The Balance

Several types of balance mechanism are possible [1-4]. Null-point weighing mechanisms are favoured in TG as they ensure that the sample remains in the same zone of the furnace irrespective of changes in mass. Various sensors have been used to detect deviations of the balance beam from the null-position, e.g. in the Cahn RG electrobalance (Figure 3.2.) an electro-optical device has a shutter attached to the balance beam. The shutter partly blocks the light path between a lamp and a photocell. Movement of the beam alters the light intensity on the photocell and the amplified output from the photocell is used to restore the balance to its null-point and, at the same time, is a measure of the mass change. The restoring mechanism is electromagnetic. The beam has a ribbon suspension and a small coil at the fulcrum, located in the field of a permanent magnet. The coil exerts a restoring force on the beam proportional to the current from the photocell.

The sensitivity of a thermobalance and the maximum load which it can accept, without damage, are related. Typical values are maximum loads of 1 g and sensitivities of the order of 1 μg.

Figure 3.1
A schematic thermobalance.

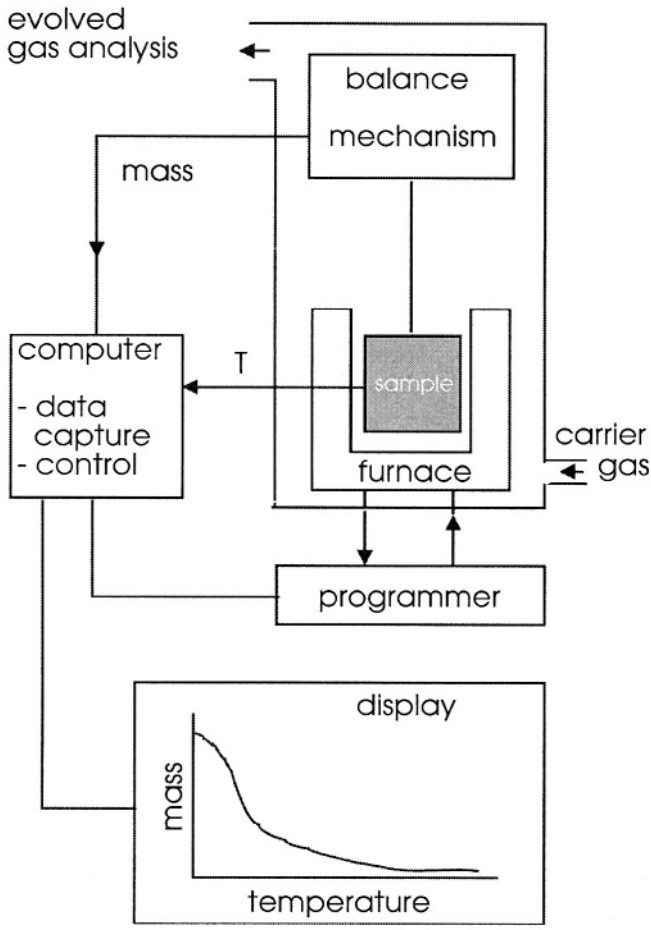

Electrobalances suitable for simultaneous DTA-TG are available. The electrical signals for simultaneous measurements are usually taken off the balance beam near the fulcrum so as to minimize disturbance of the balance mechanism. Simultaneous measurements are described in Chapter 7.

The use of quartz crystal microbalances has also been suggested [5-10]. Sensitivities of the order of 0.1 ng have been reported [4], but stability and operating temperature range are limited.

Figure 3.2
The Cahn electrobalance. (With the permission of Cahn Instruments, Inc.)

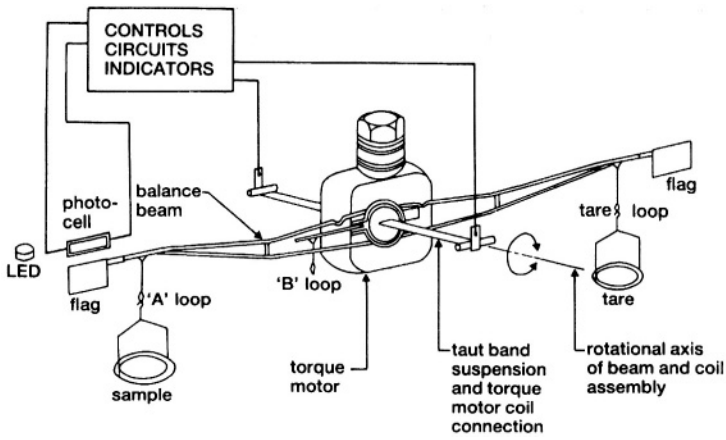

Software usually provides for electrical taring and for scale expansion to give an output of mass loss as a percentage of the original sample mass. The output may be differentiated numerically, with respect to time or temperature, to give a derivative thermogravimetric (DTG) curve.

3.3 Heating the Sample

In conventional thermobalances, there are three main variations in the position of the sample relative to the furnace as shown in Figure 3.3. The sample may be suspended from the balance beam and hang down into a furnace or controlled-temperature environment. The suspension system needs protection by baffles or cooling to prevent rising hot gas from affecting the balance mechanism. Alternatively, the sample may be placed upon a rigid vertical support above the balance beam and the furnace suitably modified for this position. Heat convection is then less of a problem, but the mass of the sample support required is a disadvantage. The third major configuration is when the sample support is a horizontal extension of the balance beam and the furnace is also arranged horizontally. Problems of condensation of evolved volatiles on the sample supports are decreased, but thermal expansion of the beam material has to be minimized.

Figure 3.3
Main variations in the position of the sample relative to the furnace.

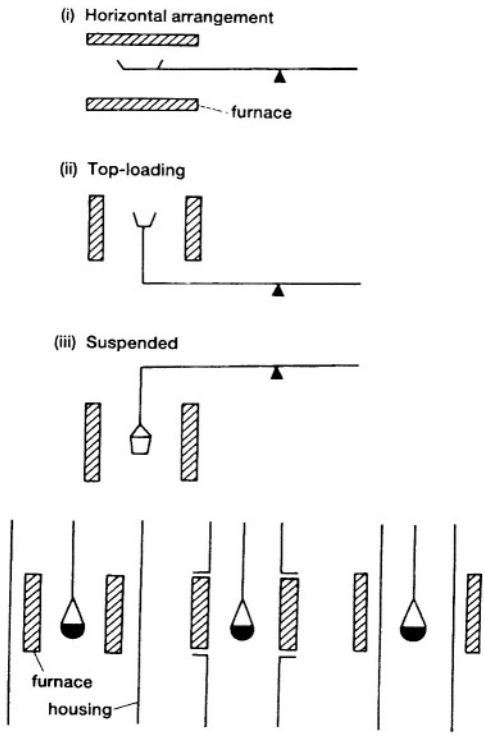

The furnace is normally an electrical resistive heater and may also, as shown in Figure 3.3, be within the balance housing, part of the housing, or external to the housing. The internal arrangement is suitable for small furnaces and both heating and cooling rates can be high, allowing a rapid turnaround time during use of the instrument.

The furnace should (i) be non-inductively wound, (ii) be capable of reaching 100 to 200°C above the maximum desired working temperature, (iii) have a uniform hot-zone of reasonable length, (iv) reach the required starting temperature as quickly as possible, (i.e. have a low heat capacity), (v) not affect the balance mechanism through radiation or convection. Transfer of

heat to the balance mechanism should be minimized by inclusion of radiation shields and convection baffles. The materials used for construction of the resistance elements are governed by both the temperature range that is to be used and the nature of the gaseous environment in the furnace. Beyond the maximum limits of rhodium (about 1800°C), molybdenum (2200°C) or tungsten (2800°C) elements may be used, but only in non-oxidizing atmospheres. The working life of a resistive furnace is limited and can be increased by limiting the time of operation at high temperatures to the minimum possible for the information required.

Manufacturers market a variety of furnaces and modular control systems to combine with their balance [3], e.g. a Nichrome or Kanthal based furnace in conjunction with fused silica refractories for operation up to 1000°C, and a platinum/rhodium or $MoSi_2$ based furnace combined with alumina refractories for operation to 1500-1700°C. Protective circuits to prevent thermal runaway in the event of thermocouple failure are also a necessity.

The magnetic field generated by the resistive heating must be considered when working with magnetic samples [3]. To minimize the magnetic field, it is common to wind the furnace in a bifilar fashion by having the direction of flow for the electrical current opposite in each half of the winding.

Steinheil [11] described a vacuum microbalance system, for use at high temperatures (1600 to 2400°C) which incorporated induction heating by a high-frequency electromagnetic field, but did not allow weighing during actual heating because of the electromagnetic forces acting on the sample.

Furnaces containing electrical resistive heaters rely mainly on heating of the sample by conduction, through solid or gas, with inevitable large temperature gradients, especially when dealing with samples of low thermal conductivity such as polymers and inorganic glasses. Heating by radiation becomes significant only at high temperatures in such furnaces, but alternative heating systems using either infrared or microwave radiation have been considered.

For infrared heating [3,12,13] the light from several halogen lamps is focused onto the sample by means of elliptic or parabolic reflectors. Heat transfer is virtually instantaneous, provided that the path between lamp and sample, which includes the balance container, is transparent to the radiation. Temperatures of over 1400°C may be achieved at heating rates of up to 1000°C/min and control within ± 0.5°C. If infrared-absorbing gases are evolved from the sample during heating, the heat flux reaching the sample will change, particularly if these gases condense on the surfaces of the balance container which are in the radiation pathway.

Karmazin *et al.* [14,15] have suggested the use of microwaves to generate heat uniformly within the sample. Such a process would have the immediate advantage of allowing for use of larger and more representative samples than are often used in thermal analysis. Temperature measurement and power control both present problems in using microwaves. A thermocouple may be positioned in the waveguide if its orientation is such that it collects no energy itself from the microwaves, and its size is small compared to the guide so that reflected waves are negligible. The thermocouple is then used [14] for power control via a microcomputer system.

The use of lasers for heating and infrared pyrometers for remote temperature measurement in the in situ thermal analysis of bulk materials has also been suggested [16].

3.4 The Atmosphere

Thermobalances are normally housed in glass or metal systems [17], to allow for operation at pressures ranging from high vacuum (about 10^{-4} Pa) to high pressure (about 70 bar), of inert, oxidizing, reducing or corrosive gases [18]. Microbalances are affected by a variety of disturbances [1,3,4,17]. One correction which may have to be made is for buoyancy arising from lack of symmetry in the weighing system. If the asymmetry can be measured in terms of a volume *V,* the mass of displaced gas (assuming ideal gas behaviour) is $m = pM\ V/RT$ (where p is the pressure and M the molar mass). The buoyancy thus depends not only on the asymmetry *V,* but also on the pressure, temperature and nature of the gas. Attempts may be made to reduce V to zero, or a correction may be calculated, or an empirical correction may be applied by heating an inert sample under similar conditions to those to be used in the study of the sample of interest [4]. Gallagher [3] has pointed out that the masses of 1 cm^{-3} of air, hydrogen and carbon dioxide, at room temperature and pressure, are about 120 g, 9 g and 196 g, respectively. Very accurate work requires allowance for these differences. Generally, during the evolution of volatile products the buoyancy effects will change.

At low pressures (10^{-2} to 270 Pa), a particular problem is thermomolecular flow [1] which results when there is a temperature gradient along the sample holder and support. This gradient causes 'streaming' of molecules in the direction hot cold, i.e. up the suspension as a rule, giving spurious mass changes. Thermomolecular flow may be minimized: (i) by working outside the pressure range by adding inert gas, or (ii) by careful furnace design and sample placement, including use of a symmetrical balance design with twin furnaces, or (iii) by determination of corrections required, using an inert sample, as is done for buoyancy corrections.

The sample may be heated in a small container with a restricted opening. Decomposition then occurs in a self-generated atmosphere [19] of gaseous decomposition products. The inhibiting or catalytic effects of these products on the decomposition can then be studied. Garn and co-workers [20,21] have described the design and use of furnaces for carrying out reactions in controlled atmospheres of ligand. Such systems are essential for studying the thermodynamic reversibility of dissociations of coordination compounds.

At atmospheric pressure, the atmosphere can be static or flowing. A flowing atmosphere has the advantages that it: (i) decreases condensation of reaction products on cooler parts of the weighing mechanism, (ii) flushes out corrosive products, (iii) decreases secondary reactions, and (iv) acts as a coolant for the balance mechanism. The balance mechanism should, however, not be disturbed by the gas flow. It is possible for the balance mechanism to be protected by an inert gas atmosphere, while a corrosive gas or vapour is passed over the sample (e.g. H_2O vapour for dehydration studies).

The choice of purge gas is determined not only by its reactivity, or lack of reactivity, towards the sample, but also by cost, availability, purity, density, and thermal conductivity. It may be necessary to decrease the amount of residual oxygen in a nominally “inert” gas stream. Passage over heated titanium turnings or powder is effective. The density of a purge gas can be used

to minimize back-streaming [3]. If the balance is above the furnace and sample, then denser argon is preferable to helium, but the reverse holds for the opposite configuration of balance and furnace [22]. The high thermal conductivity of a purge gas such as helium can significantly affect heat transfer compared to gases such as argon or nitrogen.

Measurement and/or control of the flow rate of the purge gas selected can be done using various devices, including floats and tubes, or soap-film bubble towers, or more expensive mass flow controllers [3]. Valves for programmed switching of gas streams, e.g. to change from an inert to an oxidizing atmosphere, as in the proximate analysis of coal, are also available.

The balance mechanism may need to be protected from reactive gases (incoming reactants or volatile products) by passing an independent stream of inert purge gas through the balance chamber.

Reactive gas streams can be prepared by incorporating volatile liquid or solid species into the purge gas by passing the gas stream through the liquid, or over the solid, at the appropriate temperature and rate.

Many decompositions are reversible if a supply of the gaseous products of reaction is maintained. Such studies thus require careful control of the surrounding atmosphere and should include runs at reduced pressures. Reducing the pressure, though, worsens the heat exchange, causing problems in temperature measurement.

The noise level of TG traces at pressures above about 20 kPa usually increases as the temperature increases, on account of thermal convection [1,23,24]. The use of dense carrier gases at high pressures in hot zones with large temperature gradients gives the most noise. Variations in the flow rate of the gas do not affect the noise level much, but may shift the weighing zero. Noise levels also increase as the radius of the hangdown tube increases. Thermal convection, and hence noise, can be reduced by altering the gas density gradient by introducing a low density gas, such as helium, above the hot region. Alternatively, and more practically, baffles can be introduced in the hangdown tube. A series of close-fitting convoluted baffles was found to be most successful [25]. Even with the baffles it was found that changes in ambient temperature caused non-turbulent gas movements in the hangdown tube and hence apparent changes of mass. Sample containers should be of low mass and of inert material (e.g. platinum containers may catalyze some reactions). Samples should generally be thinly spread to allow for ready removal of evolved gases. Results should be checked for sample-holder geometry effects.

Build up of electrostatic charge on glass housings is another source of spurious mass effects. Methods proposed for dealing with this problem include use of weak radioactive sources for ionization of the balance atmosphere, coating of glassware with a sputtered metal film or other metal shielding, and the use of various commercial sprays or solutions. Wiping the outside of the glassware with ethanol is reasonably effective.

3.5 The Sample

Although solid samples may be nominally of the same chemical composition, there may be considerable differences in their behaviour on heating. These differences arise from structural differences in the solid, such as the defect content, the porosity and the surface properties, which are dependent on the way in which the sample is prepared and treated after preparation. For example, very different behaviour will generally be observed for single crystals compared to finely ground powders of the same compound [26]. In addition to the influence of defects on reactivity [27], the thermal properties of powders differ markedly from those of the bulk material.

As the amount of sample used increases, several problems may arise. The temperature of the sample becomes non-uniform through slow heat transfer and through either self-heating or self-cooling as reaction occurs. Exchange of gas with the surrounding atmosphere is also decreased. These factors may lead to irreproducibility. Even when the sample material is inhomogeneous and hence a larger sample becomes desirable (e.g. coal and mineral samples), the sample mass should be kept to a minimum and replicates examined for reproducibility if necessary. Small sample masses also protect the apparatus in the event of explosion or deflagration. The sample should be powdered where possible and spread thinly and uniformly in the container [26].

3.6 Temperature Measurement

The sample temperature, T_s, will usually lag behind the furnace temperature, T_f, and T_s cannot be measured very readily without interfering with the weighing process. The lag, $T_f - T_s$, may be as much as 30°C, depending upon the operating conditions. The lag is marked when operating in vacuum or in fast-flowing atmospheres and with high heating rates. Temperature measurement is usually by thermocouples (see section 3.6.1.) and it is advisable to have separate thermocouples for measurement of T_s and for furnace regulation. (Platinum resistance thermometers are used in some controllers).

3.6.1 Thermocouples

The commonly used thermocouple types [28] are identified by letter designations originally assigned by the Instrument Society of America (ISA) and adopted as an American Standard in ANSI C96.1-1964. The upper temperature limits for use are dependent upon the diameter of the wire used. Values given in brackets (°C) refer to 24 gauge (0.51 mm) wire in conventional closed-end protecting tubes [28]. The reference junction of the thermocouple must be held at a fixed and defined temperature. Traditionally this was 0°C, established by an ice bath. Modern instruments use an isothermal block maintained at a temperature slightly above typical room temperatures and the software uses appropriately adjusted temperature versus voltage curves used to convert the signal into temperature.

Factors such as stability, sensitivity (V/C), and cost determine the choice of thermocouple. Stability can be improved, at the expense of increased response time, by enclosing the thermocouple in a inert sheath. The response time and lifetime of the thermocouple are strongly influenced by the diameter of the wire. Larger diameters add to the mechanical strength and lifetime, but also decrease the sensitivity and increase the response time [3]. The long term stability of a thermocouple depends upon its composition being maintained. At high temperatures, diffusion and/or vaporization can make the two metals or alloys more similar and thus decrease the sensitivity.

Type B - Platinum-30 percent rhodium (+) versus platinum-6 percent rhodium (-) (1700°C). Recommended for continuous use in oxidizing or inert atmospheres and short term use in vacuum. They should not be used in reducing atmospheres, nor those containing metallic or nonmetallic vapors, unless suitably protected.

Type E - Nickel-10 percent chromium (+) versus constantan (-) (430°C). Type E thermocouples develop the highest emf per degree of all the commonly used types and are often used primarily because of this feature. Recommended for use in oxidizing or inert atmospheres. In reducing atmospheres, alternately oxidizing and reducing atmospheres, marginally oxidizing atmospheres, and in vacuum they are subject to the same limitations as Type K thermocouples. They are suitable for subzero temperature measurements since they are not subject to corrosion in atmospheres with high moisture content.

Type J - Iron (+) versus constantan (-) (370°C). These are suitable for use in vacuum and in oxidizing, reducing, or inert atmospheres, but the rate of oxidation of the iron thermoelement is rapid above 540°C and the use of heavy-gauge wires is recommended when long life is required at the higher temperatures. Bare thermocouples should not be used in sulfurous atmospheres above 540°C. Possible rusting and embrittlement of the iron wire makes its use less desirable than Type T for low temperature measurements.

Type K - Nickel-10 percent chromium (+) versus Nickel-5 percent (aluminium, silicon) (-) (870°C). (NOTE: Silicon, or aluminium and silicon, may be present in combination with other elements.). Recommended for continuous use in oxidizing or inert atmospheres. Suitable for temperature measurements as low as -250°C. May be used in hydrogen or cracked ammonia atmospheres, but should *not* be used in: atmospheres that are reducing or alternately oxidizing and reducing unless suitably protected with protection tubes; sulfurous atmospheres unless properly protected; and vacuum except for short time periods (vaporization of chromium from the positive element will alter calibration).

Type R - Platinum-13 percent rhodium (+) versus platinum (-) (1480°C).
Type S - Platinum-10 percent rhodium (+) versus platinum (-) (1480°C).

Types R and S thermocouples are recommended for continuous use in oxidizing or inert atmospheres. They should not be used in reducing atmospheres, nor those containing metallic or nonmetallic vapors, unless suitably protected. They may be used in a vacuum for short periods of time, but greater stability will be obtained by using Type B thermocouples for such applications. Continued use of Types R and S thermocouples at high temperatures causes excessive grain growth which can result in mechanical failure of the platinum element. Calibration changes also are caused by diffusion of rhodium from the alloy wire into the platinum, or by volatilization of rhodium from the alloy.

Type T - Copper (+) versus constantan (-) (200°C). They are resistant to corrosion in moist atmospheres and are suitable for subzero temperature measurements. They can be used in a vacuum and in oxidizing, reducing, or inert atmospheres.

3.6.2 Resistance Thermometers

The electrical resistances of metallic conductors increase with rising temperature [29]. Temperature coefficients for different metals are not very different. Platinum wire of high purity and small diameter (25 to 650 m), annealed so that it is strain-free and protected against contamination, is commonly used for temperature measurement in the range 120 to 1300°C, although evaporation causes the zero to drift above about 980°C.

The relationship [29] for the temperature, t (°C), is:

$$t = (r_t / r_o - 1) / \alpha + \delta (t / 100 - 1) t / 100 + \beta (t / 100 - 1) (t / 100)^3$$

where r_t is the observed resistance in ohms at t°C, r_o is the resistance at 0°C and α, β and δ are constants for the particular resistance element determined by calibration.

3.7 Temperature Control

Controlling the temperature of the sample is the most difficult and critical aspect of thermogravimetry [3]. The three fundamental aspects are: (i) heat transfer to (and from) the sample; (ii) determination of the actual sample temperature, and (iii) feedback and control of the furnace temperature. Adjustment of the temperature of the sample's surroundings is the main means of controlling the temperature of the sample.

Cooling the sample in a controlled manner is generally more difficult than the heating process. The purge gas has a natural cooling effect and this effect may be increased by passing the gas through a refrigerant. The desired amount of cooling is obtained by balancing the cooling effect of the flowing atmosphere against the energy input from the furnace heater.

Precise control of the sample's temperature requires that the furnace, controller, sensor, and system geometry be carefully matched and optimized [3]. A furnace system must respond rapidly to control commands but not be susceptible to unstable oscillations.

Because any direct contact between the temperature sensor and the sample will interfere with the measurement of the sample mass, the true temperature of the sample is seldom measurable. Indirect measurements of temperature, such as by optical means, measure the temperature of only that portion of the sample or its holder on which the optics are focused [3].

Separate sensors are thus usually used for control of the furnace and for measurement of the sample temperature. The latter thermocouple is positioned as close to the sample as possible without interfering with the weighing process. The larger the size of the uniformly heated zone of the furnace, the less critical is the placement of the thermocouple. Thermal expansion of both the sample suspension system and the thermocouple can cause contact problems as the system is heated.

Furnace control is based on comparison of the temperature of the furnace thermocouple with a set time-temperature programme. Power to the furnace is supplied so as to maintain the difference between the thermocouple reading and the control setting at a minimum. The offset between the furnace temperature and the true sample temperature has to be determined by a suitable calibration procedure (see below).

The most common temperature programme is a *linear* heating or cooling ramp. *Isothermal* programmes are used to measure changes in mass as a function of time and are often used in kinetic studies (see Chapter 10). More complex temperature programmes may contain combinations of linear and isothermal segments. Other possibilities include programmes to produce a *constant rate* of change of mass with time or temperature, or to separate complex changes in mass with the highest possible resolution. Modulated temperature techniques developed recently, particularly for differential scanning calorimetry, DSC (see Chapter 4), superimpose another function, e.g., a sine wave, on an underlying linear heating ramp [30-32]. These types of programme and their advantages are discussed further below.

Proportional integral derivative (PID) control [3], rather than simple "on - off" switching of power to the furnace in response to the difference between the thermocouple reading and the control setting, is generally used to produce too satisfactory programmed temperature or heating/cooling rates for measurement of the processes under investigation. Departures from heating or cooling progammes may be related to inappropriate PID values, or simple inability of the furnace to keep up with programmed rate.

3.8 Sample Controlled Thermal Analysis (SCTA) (or Controlled Rate Thermal Analysis, CRT A)

In "conventional" thermal analysis, the temperature programme is chosen by the experimenter and proceeds irrespective of any changes undergone by the sample. A group of methods has been developed in which the response of the sample to the initial heating programme is used as feedback to the control system to influence the continuation of the temperature programme in some way. The simplest method is to set a rate of mass loss and use the difference between the set value and the observed rate of mass loss as the input signal to the furnace controller. The historical development of these methods has been reviewed by Reading [33].

In the early 1960s Rouquerol [34] and Paulik and Paulik [35] independently developed methods for holding the rate of reaction at a constant value by using the measured mass loss or pressure of evolved gas as feedback to the furnace temperature controller. The temperature-time profiles that result are important in understanding what has occurred [36]. Often they correspond to almost isothermal conditions during much of the reaction, so the techniques have also been called *quasi-isothermal* [37], for example the study by Paulik and Paulik of the decomposition of calcium carbonate [37]. The principle of the CRTA approach is compared with conventional thermal analysis in Figures 3.4 and 3.5 [38].

Closely-related techniques [39], particularly useful in obtaining kinetic information (see Chapter 10), are those involving either a temperature jump (Figure 3.6) or a rate jump (Figure 3.7). In stepwise isothermal analysis [40] upper and lower limits are set for the reaction rate and when the rate falls below the minimum set value, typically 0.08% of the maximum rate of loss at a normal linear heating rate, the temperature is increased (at a generally fast linear rate) until the reaction rate exceeds the maximum set value. The temperature is then held constant until the reaction rate again falls below the minimum.

Figure 3.4
Control system for conventional thermal analysis.

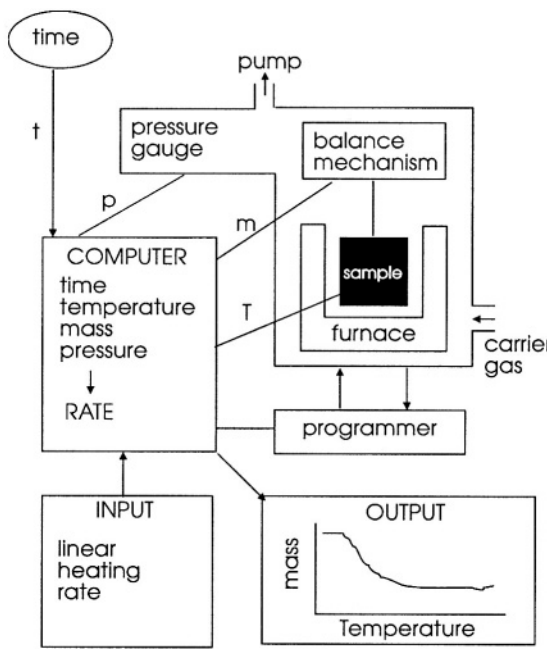

Figure 3.5
Control system for constant rate thermal analysis (CRTA).

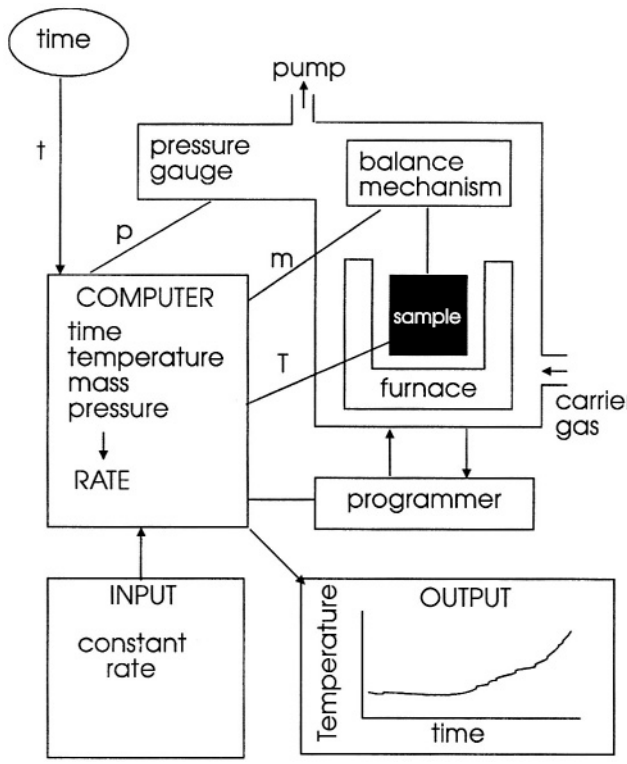

Figure 3.6
Control system for the temperature-jump method.

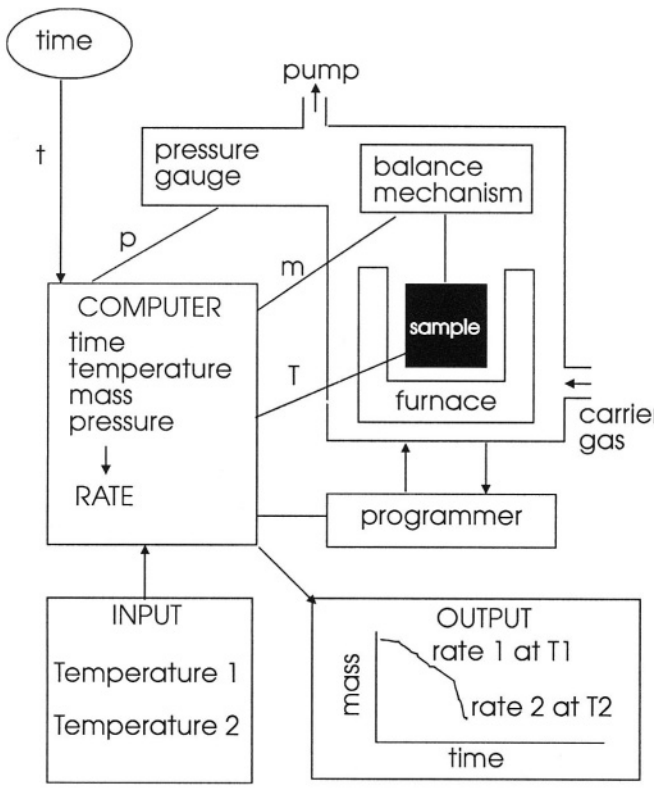

Figure 3.7
Control system for the rate-jump method.

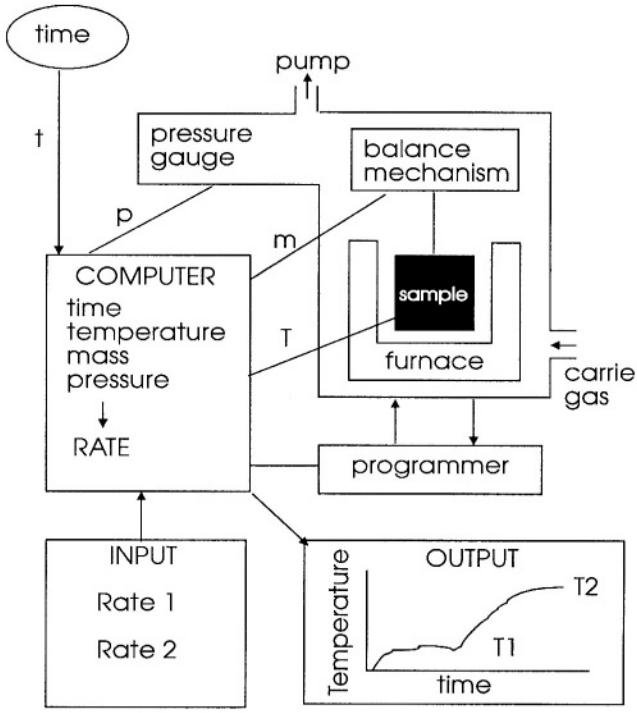

A method developed fairly recently by TA Instruments, known as high resolution, *Hi-Res TG* [41] or *dynamic rate TG* [42], produces a marked decrease in the heating rate when the system crosses the upper threshold set for the rate. The changes in heating or cooling rates are controlled by adjustment of the values of two numerical parameters, referred to as resolution and sensitivity. An example of the output from Hi-res TG using $CuSO_4.5H_2O$ [41] is shown in Figure 3.8.

Figure 3.8
Hi-Res TG and DTG of $CuSO_4.5H_2O$ [41]. (With permission of the Journal of Thermal Analysis and Calorimetry.)

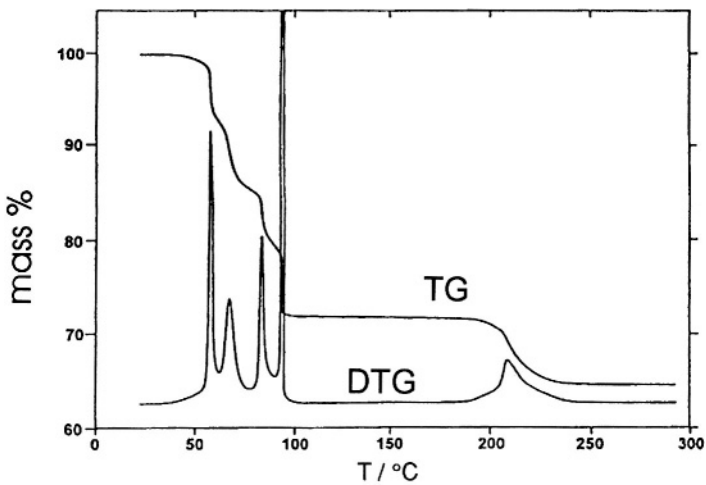

The problems of consistent and acceptable nomenclature for the variety of techniques described above have been reviewed by Reading [33]. The term *sample controlled thermal analysis* (SCTA) for all methods where the transformation undergone by the sample in some way influences the course of the temperature programme it experiences, has now been proposed.

Use of SCTA methods can provide a more uniform reaction environment than usually exists in conventional TA. Pressure and temperature gradients within the sample can be a problem, particularly for rapid, strongly endothermic decompositions. These gradients can be minimized by using small sample masses and setting slow decomposition rates, if adequate sensitivity is available. Isothermal experiments suffer particularly in comparison with SCTA [43] because often the reaction rate can be too rapid at the beginning of the experiment and far too slow near the end for the reaction to be complete in a realistic time. In linear rising temperature experiments, the rate goes through a maximum near the midpoint of a reaction step. Lowering the heating rate to decrease this maximum rate gives unduly long experiments. In SCTA, provided that the temperature gradients at the rate chosen are acceptable, obtaining undistorted results will take the minimum time possible. Barnes et al. [44] have compared SCTA methods and supported the claims of enhanced resolution over conventional TG.

Because SCTA usually provides better control of the sample environment, it is often used as a method of preparing porous or finely divided solids by thermal decomposition [45], especially for use in catalysis [46]. The results of SCTA are also sometimes preferred for measuring kinetic parameters (see Chapter 10).

For maximum resolution of multi-stage reactions the dynamic rate method may be suitable. Reading has pointed out [33] that the slowest heating rate should be applied during the transition from one stage to another, in contrast to the usual method where the heating rate decreases during a reaction and then increases during the passage from one stage to another. The required algorithm takes the rate of change of temperature into account (Figure 3.6).

Reading [33] has speculated on future developments and has suggested algorithms that look at the shapes of curves of reaction rate against time rather than simply at peak heights. The aim is always to avoid long times being spent on large peaks because of a threshold value set too low, or small peaks being missed because of a threshold value set too high.

The use of modulated temperature programmes in TG, similar to those described in Chapter 4 for differential scanning calorimetry, is another interesting recent development [32].

3.9 Calibration

The *precision* (reproducibility) of a measurement of a quantity depends upon factors such as the instrumentation, the homogeneity of the sample, and experimental techniques. Good precision is required for determination of the true value of the quantity (*accuracy*), but systematic errors may produce constant offsets in the experimental measurements, rather than the random fluctuations that determine precision. To detect and eliminate these systematic errors, calibration is required. For TG, both mass and temperature calibrations are required.

3.9.1. Mass Calibration [3]

Calibration masses in a wide range of sizes and several classes of accuracy may be obtained from the national standards organizations or commercial suppliers. Class M standards are used by standards organizations for certification of other classes of mass pieces. A 100 mg Class S mass has a tolerance of ± 0.025 mg or 250 ppm, while a Class S-1 mass has a tolerance of twice that. Changes in buoyancy resulting from changing temperature usually have to be determined from blank runs under essentially identical conditions. Gallagher [3] warns that, at very high temperatures (above about 1300°C for platinum) vaporization of metal from the sample suspension system may give an unexpected mass loss.

3.9.2. Temperature Calibration

For TG measurements to be meaningful, careful calibration of temperature at the sample position is essential. An ingenious method of temperature calibration [47] for small furnaces, makes use of the Curie points of a range of metals and alloys. On heating a ferromagnetic material, it loses its ferromagnetism at a characteristic temperature known as the Curie point, T_C. If a magnet is positioned below the furnace containing the suspended sample of ferromagnetic material, as shown in Figure 3.9(a), the total downward force on the sample, at temperatures below the Curie point, is the sum of the sample weight and the magnetic force. At the Curie point the magnetic force is reduced to zero and an apparent mass-loss is observed, Figure 3.9(b). By using several ferromagnetic materials, a multi-point temperature calibration may be obtained (Figure 3.9(c)). The calibration is an example of the use of thermomagnetometry (TM) (see further below). The extrapolated end point of the magnetic effect is equated to T_C. The derivative (DTM) curve, which is more sensitive, may also be used [3]. The Standardization Committee of ICTAC has certified five materials and marketed them through NIST (USA) [48].

An alternative method, known as the "fusible link" method [49,50] uses inert mass-pieces that are suspended from the balance in place of the sample by links of thin fusible wire. When the temperature is raised through the melting point, the link melts and drops from its support, causing a momentary detectable disturbance in the mass signal.

Whichever of the above methods is used, the final stage of calibration is to correlate the known transition temperatures with the "apparent" temperatures measured using the instrument's temperature sensor in its normal operating position.

Even with careful temperature calibration, T_s may still not be accurately known, because slow heat transfer may cause self-heating or self-cooling from strongly exothermic or endothermic processes in relatively large samples.

Early attempts to use the mass losses associated with some thermal decomposition reactions for temperature calibration were unsuccessful because of the slow rates of most of such reactions. Brown *et al.* [51] have proposed some peroxo coordination compounds, which undergo explosive decomposition over a very narrow temperature range, as possible temperature standards. The temperatures of onset of decomposition can be determined by the sharp exotherms in their DTA or DSC curves. These DTA or DSC instruments would have been calibrated in the normal way using the melting points of appropriate pure metal standards. The DSC and TG curves of the glycine (gly) complex $K_2[Mo_2O_2(O_2)_4(gly)].2H_2O$ are shown, as an example, in Figure 3.10 [51].

Simultaneous TG-DTA instruments can be calibrated by measuring temperatures directly in the DTA system [52-54]. A suitable pair of pure metals, whose melting points should bracket the magnetic transition, are placed in the sample pan alongside the magnetic material. The measured melting points are used to construct a correction curve for the observed Curie temperatures, T_C [3] Some of the magnetic materials used as temperature standards in TG are listed in Table 3.1 [3]. In a series of simultaneous TG-DTA experiments [52-54], nickel gave the best result, but its standard deviation of 5.4°C is not good enough for a reference standard. A certification programme is in progress [3] to use cobalt- and nickel-based alloys to provide a series of standards in the temperature range of 160 to 1130°C.

3.10 Presentation of TG Data

Results from TG experiments can be presented in a variety of graphical ways (see Figure 3.11) [3,55]. *Mass* or *mass percent* is usually plotted as the ordinate (Y-axis) and *temperature* or *time* as the the abscissa (X-axis). Mass percent has the advantage that results from different experiments can be compared on normalized sets of axes. When time is used as the abscissa, a second curve of temperature versus time needs to be plotted to indicate the temperature programme used.

Figure 3.9
Temperature calibration using magnetic standards [47].
(a) A magnet positioned below the furnace containing a sample of ferromagnetic material adds to the total downward force on the sample, at temperatures below the Curie point.
(b) At the Curie point the magnetic force is reduced to zero and an apparent mass-loss is observed.
(c) By using several ferromagnetic materials, a multi-point temperature calibration may be obtained.

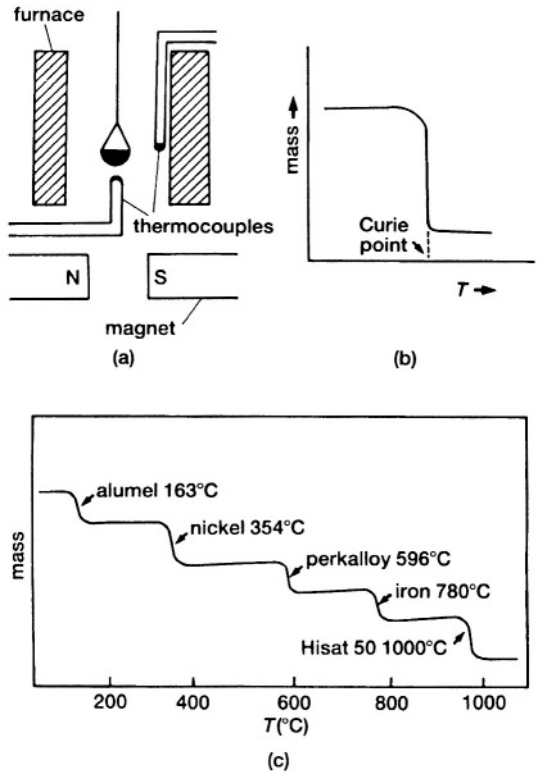

Figure 3.10
Temperature calibration using explosive decomposition [51].
The DSC (a) and TG (b) curves of the glycine (gly) complex, $K_2[Mo_2O_2(O_2)_4(gly)].2H_2O$.
(With the permission of Thermochimica Acta.)

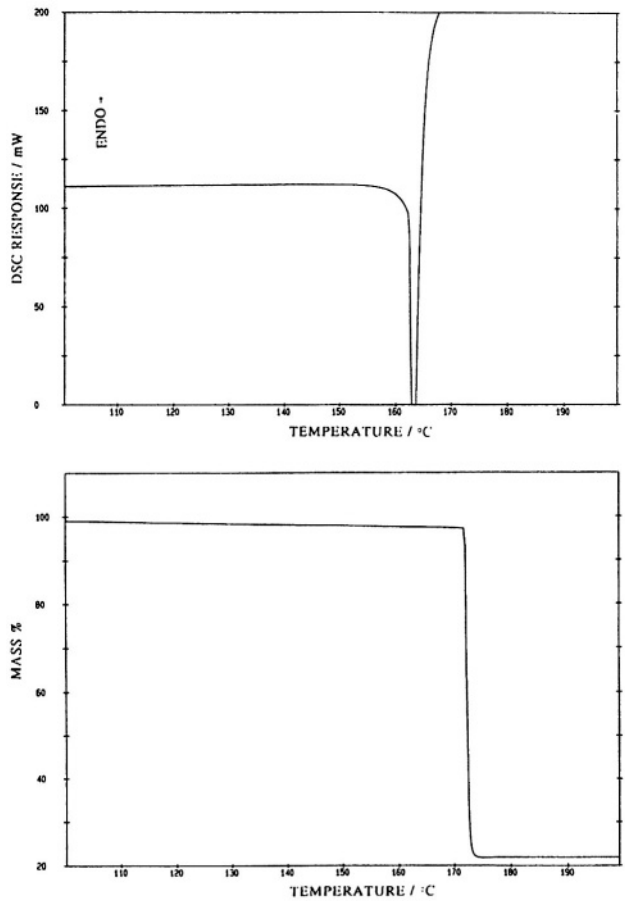

Derivative plots showing the rate of mass change as a function of time or temperature (derivative thermogravimetry, DTG) are useful in attempting to resolve overlapping processes and for some methods of kinetic analysis (see Chapter 11). DTG curves are also readily comparable with other derivative measurements such as DTA, DSC, or EGA. Derivative plots usually show increased noise, so some form of smoothing may be needed (see Appendix).

Table 3.1.
Suggested magnetic materials for use as temperature standards in TG [3].

Material	Recommended T_C/°C	Source
Monel	65	Perkin-Elmer[a]
Alumel	163	Perkin-Elmer
Permanorm 3	266.3 ± 6.6	ICTAC-NIST
Nickel	354	Perkin-Elmer
	354.4 ± 5.4	ICTAC-NIST
Numetal	393	Perkin-Elmer[a]
	386.2 ± 7.4	ICTAC-NIST
Nicroseal	438	Perkin Elmer[a]
Permanorm 5	458.8 ± 7.6	ICTAC-NIST
Perkalloy	596	Perkin-Elmer
Trafoperm	753.8 ± 10.2	ICTAC-NIST
Iron	780	Perkin-Elmer
Hisat-50	1000	Perkin-Elmer

[a] No longer supplied.

3.11 Automation of TG

Thermal analysis equipment does not generally lend itself to full automation in the sense of analysis of sample after sample without operator intervention [56]. Thermogravimetry is frequently used for routine quality control types of analyses and there is thus a demand for equipment which can run multiple samples, either simultaneously or sequentially. If there is some means of changing the sample automatically, the required heating/cooling programme and the switching of carrier gas is readily implemented on modern instruments. A multi-specimen 'carousel' thermobalance has been designed by Ferguson *et al.* [57] (see Figure 3.7.), which allows twenty specimens, mounted on arms radiating from a central shaft, to be weighed sequentially. There is obviously a limit to the sorts of treatment which the samples can receive between weighings, but they can all be exposed to a similar environment.

Figure 3.11
Presentation of TG Data [55]. (With the permission of ASTM.)
(a) Assignment of the extrapolated onset temperature, T_{onset} , from the TG curve.

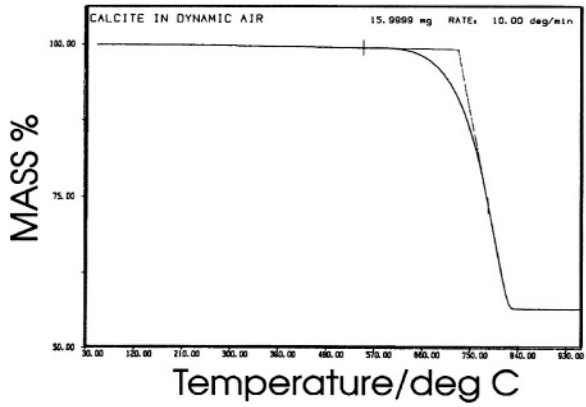

(b) Percentage mass loss assignment from the TG curve.

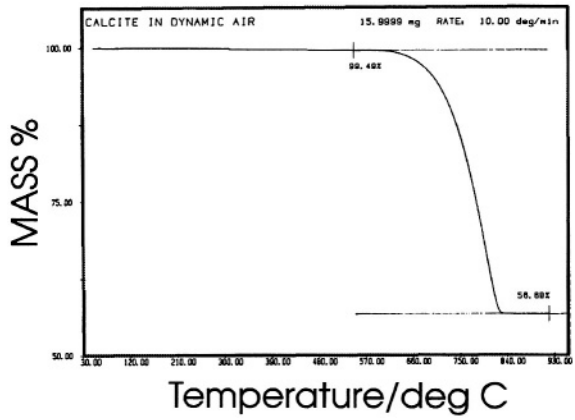

The LECO Model TGA-500, operates in a similar fashion [3]. It can operate one or two furnace systems simultaneously and have as many as 19 specimens per furnace. TA Instruments also use a carousel of identical sample holders to supply the samples, but each sample is run individually, in sequence, under any set of programmed experimental conditions.

Figure 3.12
A multi-specimen 'carousel' thermobalance designed by Ferguson et al. [57]. (With the permission of John Wiley and Sons, Chichester.)

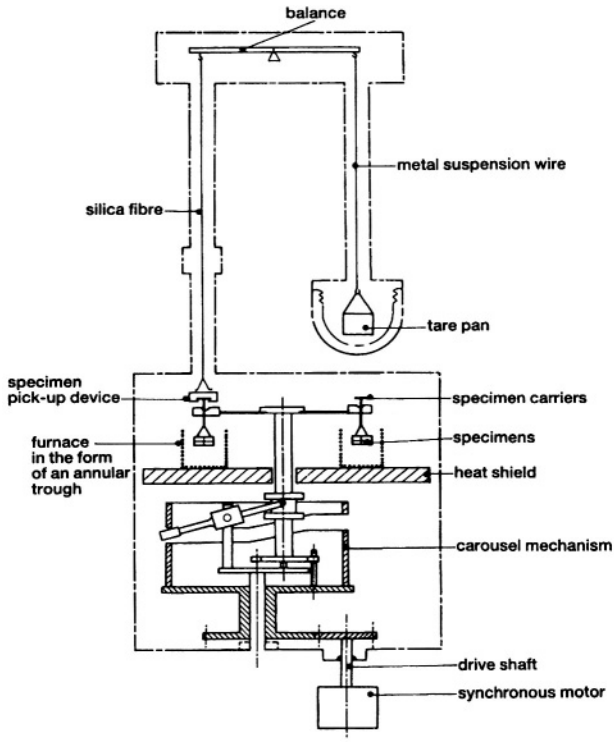

3.12 Thermomagnetometry (TM)

3.12.1. Introduction

When a sample is placed in a magnetic field, it may experience either attractive or repulsive forces. Attractive forces arise from three types of property of the sample: antiferromagnetism, paramagnetism and ferromagnetism (with ferromagnetism causing the strongest interaction). The diamagnetic properties of a sample, arising from the orbital motion of electrons, and hence present in all samples, but sometimes swamped by the other magnetic properties, give rise to weak repulsive forces. Antiferromagnetism occurs in only a few transition-metal compounds.

The volume magnetic susceptibility of a sample is defined as $\chi = M/H$, where M is the magnetization and H is the magnetic field strength. The mass magnetic susceptibility, s, then $= \chi / \rho$, where ρ is the density of the sample. Materials in which χ is positive are called paramagnetic, and those for which χ is negative are called diamagnetic.

Different types of magnetic behaviour can be distinguished by their temperature dependence. For paramagnetic samples, the magnetic susceptibility decreases with absolute temperature according to the Curie-Weiss law: $\chi = C/(T - \theta)$, where C is the Curie constant and θ is the Weiss constant. The susceptibility of diamagnetic materials does not change much with temperature, while ferromagnetic materials have high susceptibilities at temperatures below what is known as the Curie point. Above their Curie points, ferromagnetic materials become paramagnetic and these magnetic transitions are used for temperature calibration of TG systems (see Section 3.8.2.).

Gallagher and Warne have provided recent reviews of thermomagnetometry in general [58,59]and its applications to minerals [60] and inorganic materials [61].

The strength of the magnetic field used for TM [3] depends on the purpose of the measurement. When determining magnetic transition temperatures, T_C, a strong field may not be necessary or even desirable, provided that the apparent mass change is detectable. However, when attempting to detect the formation of magnetic intermediates or final products during the course of a reaction, the sensitivity of detection increases with the strength of the magnetic field gradient at the sample position. This strength depends on the strength of the magnet as well as its position relative to the sample. A large furnace may cause problems in bringing the magnet close enough to the sample, and increasing the strength of the magnetic field may affect the accuracy of the balance mechanism.

3.12.2. Apparatus

Both the apparatus used, and the techniques and precautions required for thermomagnetometry are basically those required for thermogravimetry (TG), with the addition of means of producing a strong magnetic field ($>10^4$ gauss) around the sample. The apparent mass of the sample is then the sum of the actual sample mass and the magnetic force. Allowance obviously has to be made for the effect of the field on the sample container, which should thus have a low magnetic susceptibility e.g. quartz. The magnetic field may be applied periodically so that measurements of actual mass (TG) and apparent mass (TM) can be compared. Interference of

the magnetic field with the balance mechanism is avoided by use of long suspension wires and suitable magnetic screening. Some applications of TM are described below.

3.13 Interpretation of TG and DTG Curves

Actual TG curves obtained may be classified into various types [62] as illustrated in Figure 3.13. Possible interpretations of the curves shown in Figure 3.13 are as follows:

Type (i) curves: The sample undergoes no decomposition with loss of volatile products over the temperature range shown. No information is obtained, however, on whether solid phase transitions, melting, polymerisation or other reactions involving no volatile products have occurred. Use of some of the other techniques (Table 1.2) is necessary to eliminate these possibilities. Assuming that these possibilities are eliminated, the sample would then be known to be stable over the temperature range considered. This could be good news if a heat resistant material was being sought, or bad news if potential explosives were being tested!

Type (ii) curves: The rapid initial mass-loss observed is characteristic of desorption or drying. It could also arise, when working at reduced pressures, from effects such as thermomolecular flow or convection (Section 3.4.). To check that the mass-loss is real, it is advisable to rerun the sample, which should then produce a type (i) curve, unless the carrier gas contained moisture or was very readily readsorbed on the sample at the lower temperature.

Type (iii) curves: represent decomposition of the sample in a single stage. The curve may be used to define the limits of stability of the reactant, to determine the stoichiometry of the reaction, and to investigate the kinetics of reaction (see Chapter 10).

Type (iv) curves: indicate multi-stage decomposition with relatively stable intermediates. Again, the temperature limits of stability of the reactant and of the intermediates can be determined from the curve, together with the more complicated stoichiometry of reaction.

Type (v) curves: also represent multi-stage decomposition, but in this example stable intermediates are not formed and little information on all but the stoichiometry of the overall reaction can be obtained. It is important to check the effect of heating rate on the resolution of such curves. At lower heating rates, type (v) curves may tend to resemble type (iv) curves more closely, while at high heating rates both type (iv) and type (v) curves may resemble type (iii) curves and hence the detail of the complex decomposition is lost.

Type (vi) curves: show a gain in mass as a result of reaction of the sample with the surrounding atmosphere. A typical example would be the oxidation of a metal sample.

Type (vii) curves: are not often encountered. The product of an oxidation reaction decomposes again at higher temperatures (e.g., $2Ag + O_2 \rightarrow Ag_2O \rightarrow 2Ag + O_2$).

Resolution of the individual stages of more complex TG curves can be improved by examining the derivative DTG curves (Figure 3.14).

Figure 3.13
The main types of thermogravimetric (TG) curves. (Based on C. Duval, *Inorganic Thermogravimetric Analysis*, Elsevier, Amsterdam, 2nd Edn, 1963, and T. Daniels, *Thermal Analysis*, Kogan Page, London, 1973, with permission.)

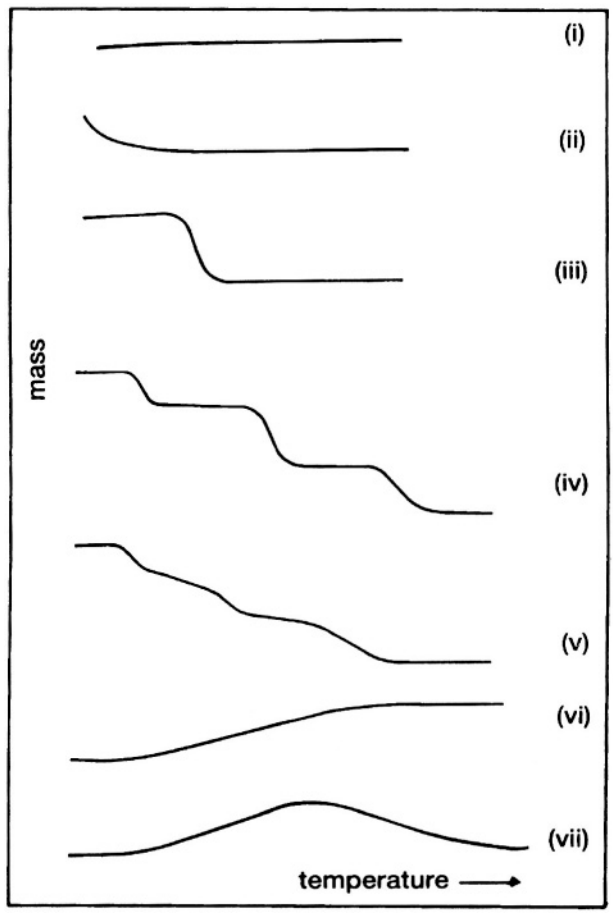

Figure 3.14
Comparison of TG and DTG curves.

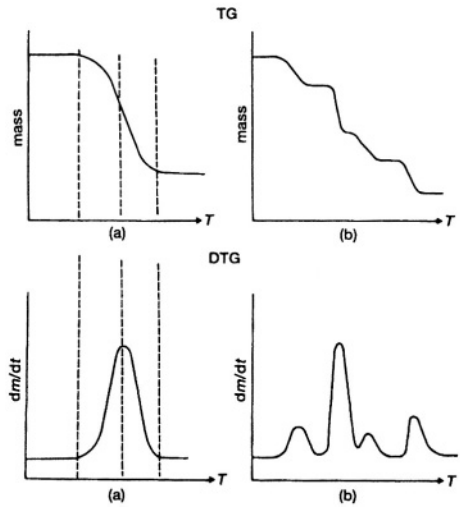

3.14 Applications of Thermogravimetry (TG)

Applications of TG are limited, to some extent, in that not all of the thermal events, listed in Chapter 2, are accompanied by changes in mass. For desorption, decomposition and oxidation processes, however, much valuable information can be obtained from TG alone. Much of the earlier work in TG was on the accurate definition of conditions for drying or ignition of analytical precipitates [62]. Examples of TG curves for $CuSO_4.5H_2O$ and for $CaSO_4.2H_2O$ [63] are given in Figures 3.15 and 3.16. The mass losses define the stages, and the conditions of temperature (and surrounding atmosphere) necessary for preparation of the anhydrous compounds, or intermediate hydrates, can be established immediately. At higher temperatures, the sulfates will decompose further. Knowledge of the thermal stability range of materials provides information on problems such as the hazards of storing explosives, the shelf-life of drugs and the conditions for drying tobacco and other crops. By using an atmosphere of air or oxygen, the conditions under which oxidation of metals and degradation of polymers become catastrophic can be determined.

Figure 3.15
TG curve for $CuSO_4.5H_2O$

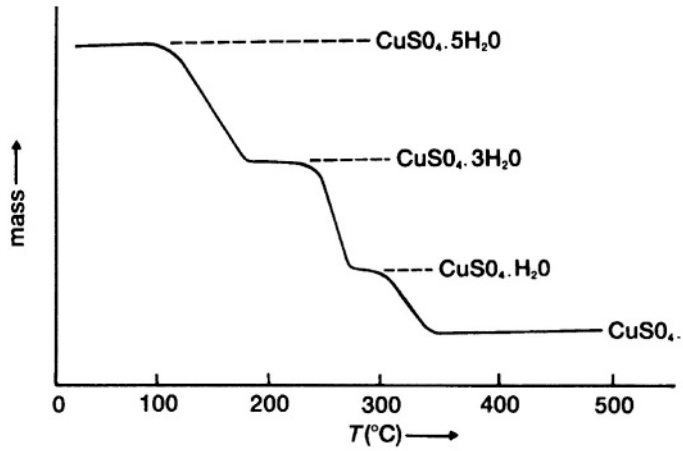

Figure 3.16
TG curves for $CaSO_4.2H_2O$ [63]. (With the permission of Wiley-Heyden Ltd.)

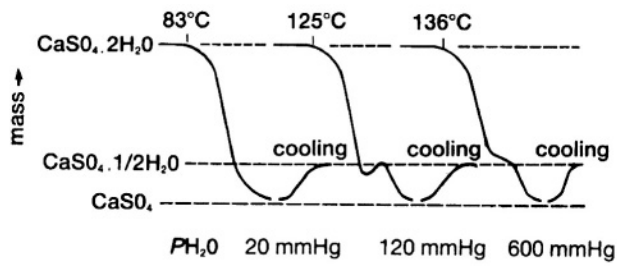

TG curves for more complex materials, such as minerals and polymers, are not always immediately interpretable in terms of the exact reactions occurring. Such curves can, however, be used for "fingerprint" purposes. The TG curve obtained on a given apparatus, under specified conditions, is compared with a bank of reference curves accumulated on the apparatus concerned. Some sets of reference curves have been published [64] but, as mentioned earlier, comparison is best when curves from the same instrument are available.

The reactions corresponding to the mass losses can best be determined, or confirmed, by simultaneous evolved gas analysis (EGA) (Chapter 9). For example, in Figure 3.15, the appearance of traces of SO_3, SO_2 and O_2 in the evolved gases would indicate the onset of sulfate decomposition. A complementary technique, such as hot-stage microscopy (HSM) (Chapter 5) may provide information on the mechanism of dehydration or decomposition, by showing up the formation and growth of decomposition nuclei, or progress of the reactant/product interface inwards from crystal surfaces.

A very routine application of TG is the proximate analysis of coal [65-67] which involves stepwise temperature increases as well as changes in the gaseous atmosphere as indicated in Figure 3.17.

Figure 3.17
Proximate analysis of coal using TG, followed by determination of iron pyrites using thermomagnetometry (see below) [65]. (With the permission of Wiley-Heyden Ltd.)

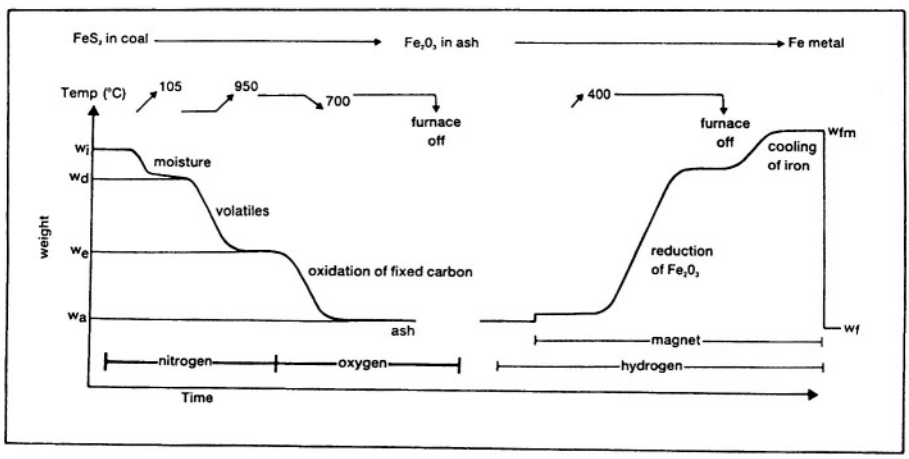

When the process occurring is clearly defined, e.g. the stoichiometric dehydration of a definite hydrate, the kinetics of the reaction can be determined from the TG curves (or from a series of isothermal curves of mass-loss against time, obtained at different temperatures). Details of some of the kinetic analyses that have been suggested are given in Chapter 10. Values of activation energies, obtained in this way, have been used to extrapolate to conditions of very slow reaction at low temperatures (in predicting shelf-lives of materials, resistance to weathering, and in estimating rates of natural processes, e.g. petroleum genesis over geological times) and to very fast reaction at high temperatures (behaviour of propellants and explosives).

In addition to the use of a thermobalance for magnetic susceptibility measurements, as mentioned above, a thermobalance may also be used to measure the vapour-pressure of a sample, e.g. a metal, by determining the rate of mass-loss through a calibrated orifice in a Knudsen cell; for accurate density measurements; for determining surface areas by adsorption, and for particle-size analysis by sedimentation.

3.15 Applications of Thermomagnetometry (TM)

The major applications of TM have been to ferromagnetic samples where the magnetic effects are strongest. For example, TM has been used [68] to examine the spinel phases formed during the thermal decomposition of siderite ($FeCO_3$). The TM and TG curves shown in Figure 3.18 for siderite samples heated in nitrogen, show the onset of decomposition at around 400°C. As the wustite (FeO) originally formed is oxidized by evolved CO_2, magnetite (Fe_3O_4) is formed. The apparent mass gain in the TM curve occurs as the magnetite nuclei grow and crystallize. When the temperature rises beyond the Curie point of magnetite, the TM trace coincides with the TG trace in the absence of a magnetic field. In oxygen, the wustite is oxidized so rapidly to haematite that the strongly magnetic spinel phase never has a chance to form. The conditions for optimization of the formation of the ferrite $NiFe_2O_4$ from decomposition of the NiFe citrate have also been determined through use of TM [69].

Figure 3.18
TM and TG curves shown in for siderite samples heated in nitrogen and in oxygen [68]. (With the permission of Thermochimica Acta.)

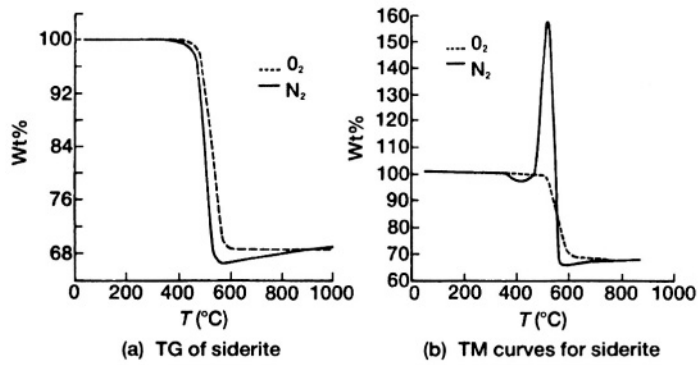

A novel use of TM is to study reactions in sealed systems [70], e.g. corrosion, provided that there is at least one ferromagnetic reactant or product. Figure 3.19 shows the apparatus used and the results obtained for the corrosion of carbon steel in an ammoniated EDTA solution.

Another application is in the determination of pyrite in coal [65],usually in combination with EGA. The residual ash from normal proximate analysis is heated in a reducing atmosphere (H_2/N_2) in the presence of a magnetic field (see Figure 3.17). From the apparent changes in mass, as the Fe_2O_3 is reduced to Fe and the product is cooled, the pyrites content can be calculated [65].

Figure 3.19
TM studies of the corrosion of carbon steel in an ammoniated EDTA solution [70].
(With the permission of John Wiley and Sons, Chichester.)

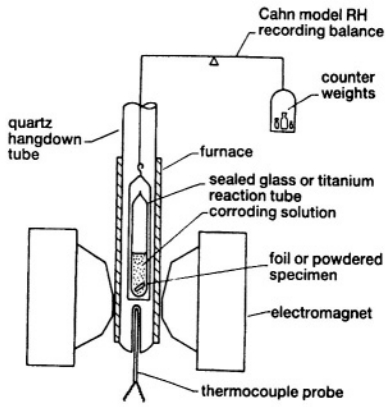

(a) TM apparatus as used for aqueous corrosion work

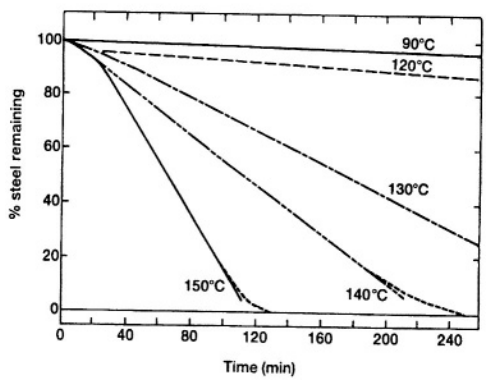

References

1. A.W. Czanderna and S.P. Wolsky, "Microweighing in Vacuum and Controlled Environments", Elsevier, Amsterdam, 1980.
2. C.J. Keattch and D. Dollimore, "An Introduction to Thermogravimetry", Heyden, London, 2nd Edn, 1975.
3. P.K. Gallagher, "Handbook of Thermal Analysis and Calorimetry", Vol.1, (Ed. M.E. Brown), Elsevier, Amsterdam, 1998, Ch.3.
4. P.K. Gallagher, "Thermal Characterization of Polymeric Materials", (Ed. E.A. Turi), Academic Press, San Diego, 2nd Edn, 1997, Ch.1.
5. J.P. Termeulen, F.J. Van Empel, J.J. Hardon, C.H. Massen and J.A. Poulis, "Prog. Vacuum Microbalance Techniques", Vol.1, (Eds T. Gast and E. Robens), Heyden, London, 1972, p.41.
6. F. Boersma and F.J. Van Empel, "Prog. Vacuum Microbalance Techniques", Vol.3, (Eds C. Eyraud and M. Escoubes), Heyden, London, 1975, p.9.
7. D.E. Henderson, M.B. DiTaranto, W.G. Tonkin, D.J. Ahlgren, D.A. Gatenby and T.W. Shum, Anal. Chem., 54 (1982) 2067.
8. V.B. Okhotnikov and N.Z. Lyakhov, J. Solid State Chem., 53 (1984) 161.
9. J.C.A. Offringa, C.G. de Kruif, P.J. van Ekeren and M.G.H. Jacobs, J.Chem. Thermodyn. (1983) 681.
10. B.J. Mulder, J.Phys.E : Sci.Instrum., 17 (1984) 119.
11. E. Steinheil, "Prog. in Vacuum Microbalance Techniques", Vol.1, (Eds T. Gast and E. Robens), Heyden, London, 1972, p.1 11.
12. A. Kishi, K. Takaoka and M. Ichihasi, Proc. 5th ICTA, (Ed. H. Chihara), Heyden, London, 1977, p.554.
13. A. Maesono, M. Ichihasi, K. Takaoka and A. Kishi, Proc. 6th ICTA, (Ed. H.G. Wiedemann), Birkhauser, Basel, 1980, Vol.1, p.195.
14. E. Karmazin, R. Barhoumi, P. Satre and F. Gaillard, J.Thermal Anal., 30 (1985) 43; 29 (1984) 1269.
15. E. Karmazin, R. Barhoumi and P. Satre, Thermochim. Acta, 85 (1985) 291.
16. P. Cielo, J. Thermal Anal., 30 (1985) 33.
17. E. Robens, Vacuum, 35 (1985) 1.
18. S. Inderijarso, J.S. Oklany, A. Millington, D. Price and R. Hughes, Thermochim. Acta, 277 (1996) 41.
19. A.E. Newkirk, Thermochim. Acta, 2 (1971) 1.
20. P.D. Garn and A.A. Alamalhoda, Thermochim. Acta, 92 (1985) 833; Proc. 7th ICTA, (Ed. B. Miller), Wiley, New York, 1982, Vol.1, p.436.
21. P.D. Garn and H.E. Kenessy, J. Thermal Anal., 20 (1981) 401.
22. J. Czarnecki and D. Thumin, Proc. 17th NATAS (Ed. C.M. Earnest), 1988, p.93.

23. A.M. Koppius, J.A. Poulis, C.H. Massen and P.J.A. Jansen, "Prog. Vacuum Microbalance Techniques", Vol.1. (Eds T. Gast and E. Robens), Heyden, London, 1972,p.181.
24. J.W. Schurman, C.H. Massen and J.A. Poulis, "Prog. Vacuum Microbalance Techniques", Vol.1, (Eds T.Gast and E. Robens), Heyden, London, 1972, p.189.
25. M.G.C. Cox, B. McEnaney and V.D. Scott, "Prog. Vacuum Microbalance Techniques", Vol.2, (Eds S.C. Bevan, S.J. Gregg and N.D. Parkyns), Heyden, London, 1973, p.27.
26. H.R. Oswald and H.G. Wiedemann, J. Thermal Anal., 12 (1977) 147.
27. V.V. Boldyrev, M. Bulens and B. Delmon, "The Control of the Reactivity of Solids", Elsevier, Amsterdam, 1979.
28. "Manual on the Use of Thermocouples in Temperature Measurement", American Society for Testing and Materials, ASTM Special Technical Publication 470A, 1974.
29. H. Dean Baker, E.A. Ryder and N.H. Baker, "Temperature Measurement in Engineering", Vol.2, Omega Press, Stamford, 1975, Ch.1.
30. D. Chen and D. Dollimore, Thermochim. Acta, 272 (1996) 75.
31. R.L. Blaine, Proc. 25th NATAS, (Ed. R.J. Morgan), 1997, p.485.
32. R.L. Blaine and B.K. Hahn, J. Thermal Anal., 54 (1998) 695.
33. M. Reading, in "Handbook of Thermal Analysis and Calorimetry, Vol. 1, (Ed. M.E. Brown), Elsevier, Amsterdam, 1998, Ch.8.
34. J. Rouquerol, Bull. Soc. Chim. Fr., (1964) 31.
35. J. Paulik and F. Paulik, Anal. Chim. Acta, 56 (1971) 328.
36. J. K. Arthur and J. P. Redfern, J. Therm. Anal., 38 (1992) 1645.
37. F. Paulik and J. Paulik, Thermochim. Acta, 100 (1986) 23.
38. J. Rouquerol, Thermochim. Acta, 144 (1989) 209.
39. O. Toft Sorensen, Thermochim. Acta, 50 (1981) 163.
40. P.K. Gallagher, in "Handbook of Thermal Analysis and Calorimetry", Vol. 1, (Ed. M.-E. Brown), Elsevier, Amsterdam, 1998, Ch.4.
41. P. S. Gill, S. R. Sauerbrunn, and B. S. Crowe, J. Therm. Anal., 38(1992)255.
42. S.R. Sauerbrunn, P.S. Gill and B.S. Crowe, Proc. 5th ESTAC, (1991) O-6.
43. J. Rouquerol, F. Rouquerol, P. Llewellyn, M. Pijolat, M/Soustelle and V. Bouineau, Proc. 12th ICTAC (2000), paper O.14, in press.
44. P. A. Barnes, G. M. B. Parkes, and E. L. Charsley, Anal. Chem., 66 (1994) 2226.
45. J. Rouquerol and M. Ganteaume, J. Thermal Anal., 11 (1977) 201.
46. P.A. Barnes and G.M.B. Parkes, Proceedings of the 6th Int. Symp. on the Scientific Bases for the Preparation of Catalysts, Louvain-la-Neuve, (Ed. G. Poncelet *et al.),* (1995) 859.
47. S.D. Norem, M.J. O'Neill and A.P. Gray, Thermochim. Acta, 1 (1970) 29.

48. P.D. Garn, O. Menis and H.G. Wiedemann, Proc. 6th ICTA, (Ed. H.G. Wiedemann), Vol.1, Birkhäeuser, Basel, 1980, p.201.
49. A.R. McGhie, Thermochim. Acta, 55 (1983) 987.
50. A.R. McGhie, J. Chiu, P.G. Fair and R.L. Blaine, Thermochim. Acta, 67 (1983)241.
51. M.E. Brown, T.T. Bhengu and D.K. Sanyal, Thermochim. Acta, 242 (1994) 141.
52. P.K. Gallagher, Z. Zhong, E.L. Charsley, S.A. Mikhail, M. Todoki, K. Tanaguchi and R.L. Blaine, J. Thermal Anal., 40 (1993) 1423.
53. B.J. Weddle, S.A. Robbins and P.K. Gallagher, Pure Appl. Chem., 67 (1995) 1843.
54. E.M. Gundlach and P.K. Gallagher, J. Thermal Anal., 49 (1997) 1013.
55. C.M. Earnest, "Compositional Analysis by Thermogravimetry", (Ed. C.M. Earnest), ASTM, Philadelphia, 1988, STP 997, p.1.
56. E.J. Millett, J. Phys. E., Sci. Instr., 9 (1976) 794.
57. J.M. Ferguson, P.M. Livesey and D. Mortimer, "Prog. Vacuum Microbalance Techniques", Vol.1, (Eds T. Gast and E. Robens), Heyden, London 1972, p.87.
58. P.K. Gallagher, J. Thermal Anal., 49 (1997) 33.
59. S. St.J. Warne and P.K. Gallagher, Thermochim. Acta, 110 (1987) 269.
60. S. St.J. Warne, Thermochim. Acta, 192 (1991) 19.
61. P.K. Gallagher, Thermochim. Acta, 214 (1993) 1.
62. C. Duval, "Inorganic Thermogravimetric Analysis", Elsevier, Amsterdam, 2nd Edn., 1963.
63. H.G. Wiedemann, J. Thermal Anal., 12 (1977) 147.
64. G. Liptay (Ed.), "Atlas of Thermoanalytical Curves", Vol.1 (1971), Vol.2 (1973), Vol.3 (1974), Vol.4 (1975), Vol.5 and Cumulative Index (1976), Heyden, London.
65. D. Aylmer and M.W. Rowe, Proc. 7th ICTA, (Ed. B. Miller), Wiley, Chichester, 1982, Vol.2, p. 1270.
66. S. St.J. Warne, "Thermal Analysis in the Geosciences", (Eds W. Smykatz-Kloss and S. St.J. Warne), Springer-Verlag, Berlin, 1991, p.62-83.
67. H.G. Wiedemann, R. Riesen, A. Boiler and G. Bayer, "Compositional Analysis by Thermogravimetry", (Ed. C.M. Earnest), ASTM, Philadelphia, 1988, STP 997, p.227.
68. P.K. Gallagher and S. St.J. Warne, Thermochim Acta, 43 (1981) 253.
69. H. Tzehoval and M. Steinberg, Israel J. Chem., 22 (1982) 227.
70. R.G. Charles, Proc. 7th ICTA, (Ed. B. Miller), Wiley, Chichester, 1982, Vol.1, p264.

DIFFERENTIAL THERMAL ANALYSIS (DTA) AND DIFFERENTIAL SCANNING CALORIMETRY (DSC)

4.1 Classical DTA [1,2]

Differential thermal analysis, DTA, is the simplest and most widely used thermal analysis technique. The difference in temperature, ΔT, between the sample and a reference material is recorded while both are subjected to the same heating programme. In 'classical' DTA instruments, represented schematically in Figure 4.1., a single block with symmetrical cavities for the sample and reference is heated in the furnace. The block is chosen to act as a suitable heat-sink, and a sample-holder of low thermal conductivity is included between the block and the sample to ensure an adequate differential temperature signal during a thermal event.

Should an endothermic thermal event (ΔH positive, such as melting) occur in the sample, the temperature of the sample, T_s, will lag behind the temperature of the reference, T_r, which follows the heating programme. If the output from the thermocouples, $\Delta T = T_s - T_r$, is recorded against T_r (or the furnace temperature, $T_f - T_r$), the result will be similar to Figure 4.1(c)). If an exothermic process (ΔH negative such as oxidation) occurs in the sample, the response will be in the opposite direction. Since the definition of ΔT as $T_s - T_r$ is rather arbitrary, each DTA curve should be marked with either the *endo* or *exo* direction. The negative peak, shown in Figure 4.1(c), is called an *endotherm* and is characterized by its onset temperature. The temperature at which the response is at a maximum distance from the baseline, ΔT_{max}, is often reported but is very dependent upon the heating rate, β, used in the temperature programme and factors such as the sample size and the thermocouple position. The *area* under the endotherm (or exotherm) is related to the value of the enthalpy change, ΔH, for the thermal event (for a more detailed interpretation, see Section 4.7).

The reference material should have the following characteristics: (i) It should undergo no thermal events over the operating temperature range. (ii) It should not react with the sample holder or thermocouple, (iii) Both the thermal conductivity and the heat capacity of the reference should be similar to those of the sample. Alumina, Al_2O_3, and carborundum, SiC, have been extensively used as reference substances for inorganic samples, while for organic compounds, especially polymers, use has been made of octyl phthalate and silicone oil.

Both solid samples and reference materials are usually used in powdered form. The particle-size and the packing conditions influence results. A common technique for matching the thermal properties of the sample to those of the reference, is to use the reference material

as a diluent for the sample. There must obviously be no reaction of the sample with the reference material.

Figure 4.1
Differential thermal analysis (DTA). (a) Classical apparatus (S = sample; R = reference); (b) heat-flux configuration; (c) typical DTA curve. (Note the DTA convention that endothermic responses are represented as negative, i.e. downward peaks.)

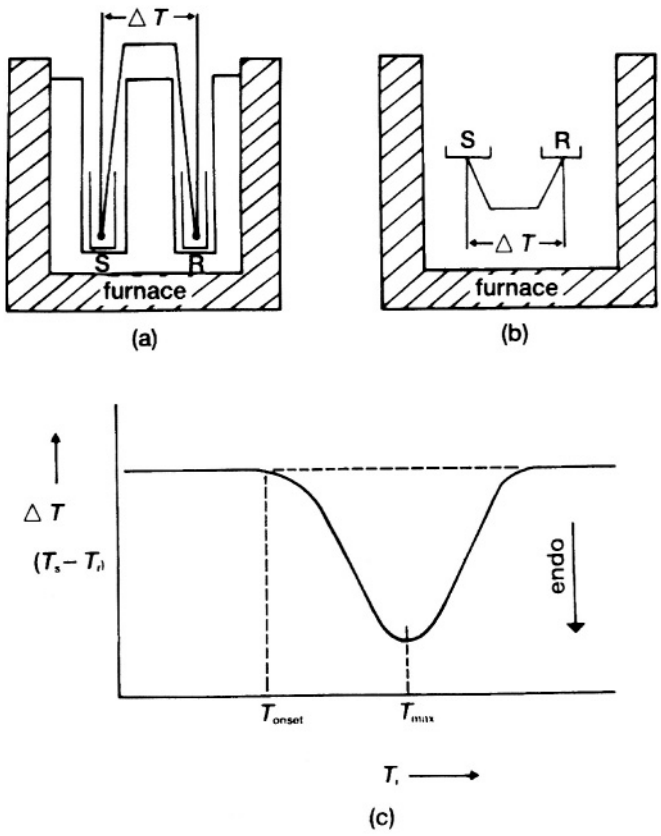

The furnace system is usually purged with an inert gas and the possibilities of atmosphere control are similar to those discussed for TG (Chapter 3).

4.2 Calorimetric DTA or heat-flux DSC [3]

In 'calorimetric' DTA, (also known as Boersma DTA), the sample and reference, in similar holders, usually flat pans, are placed on individual thermally conducting bases. The thermocouple junctions are attached to these bases and are thus not directly in the sample or reference material. This configuration has the advantage that the output signal is less dependent upon the thermal properties of the sample (see above), but response is slower (see Figure 4. l(b)).

The temperature range of DTA depends on the materials used for the furnace windings and for the thermocouples.

4.3 Differential Scanning Calorimetry (DSC) [4-8]

In power-compensated differential scanning calorimetry (pc-DSC), the aim is to maintain the sample and a reference material at the same temperature $(\Delta T = T_s - T_r \approx 0)$ throughout the controlled temperature programme. Any difference in the independent supplies of power to the sample and the reference is then recorded against the programmed (reference) temperature. The apparatus is shown schematically in Figure 4.2(a), and an example of a resulting DSC curve in Figure 4.2(b). There are many similarities between DSC and DTA, including the superficial appearance of the thermal analysis curves obtained, but the principle of power-compensated DSC is distinctly different to that of heat-flux DSC (see Sections 4.2 and 4.4).

Thermal events in the sample thus appear as deviations from the DSC baseline, in either an endothermic or exothermic direction, depending upon whether more or less energy has to be supplied to the sample relative to the reference material. Again, these directions should be clearly marked on the record, to avoid later confusion. In DSC, endothermic responses are usually represented as being positive, i.e. above the baseline, corresponding to an increased transfer of heat to the sample compared to the reference. Unfortunately this is exactly the opposite convention to that usually used in DTA, where endothermic responses are represented as negative temperature differences, below the baseline, as the sample temperature lags behind the temperature of the reference.

The operating temperature range of power-compensated DSC instruments is generally more restricted than that of DTA instruments. The Perkin-Elmer DSC-7, for example, has a maximum temperature of 726°C (999 K). Low temperature attachments are available for extending the operating range of the DSC to as low as -175°C. At low temperatures the instrument has to be protected from moisture condensation.

Figure 4.2
Differential scanning calorimetry (DSC). (a) Apparatus (S = sample; R = reference); (b) typical DSC curve. (Note the DSC convention is opposite to the DTA convention in that endothermic responses are represented as positive, i.e. upward peaks.)

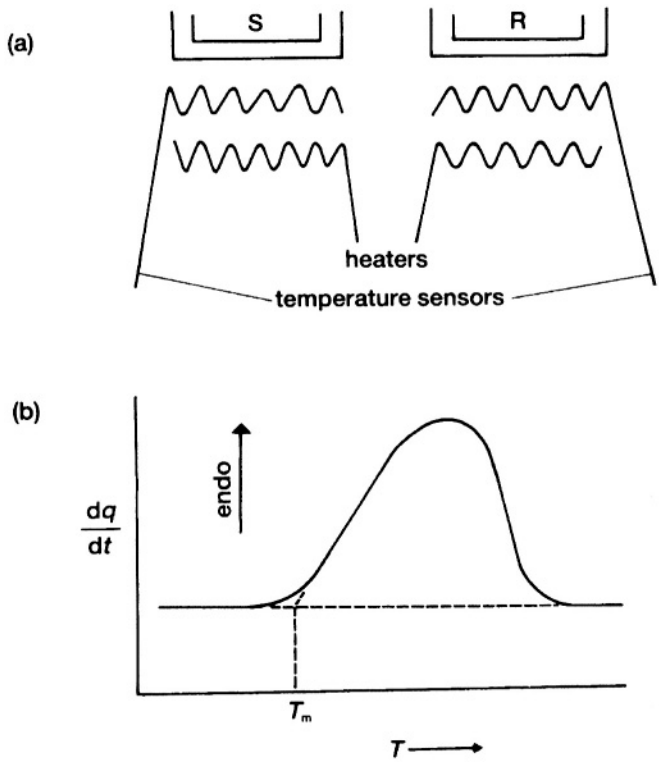

4.4 Comparison of the Principles of DTA and DSC [3,9,10]

A schematic diagram of a differential thermal apparatus is given in Figure 4.3 together with definitions of the terms needed for comparison of classical DTA, heat-flux DSC and power-compensated DSC.

Figure 4.3
Differential thermal apparatus. (From S.C. Mraw, Rev. Sci. Instr., 53 (1982) 228, with permission of the American Institute of Physics.)

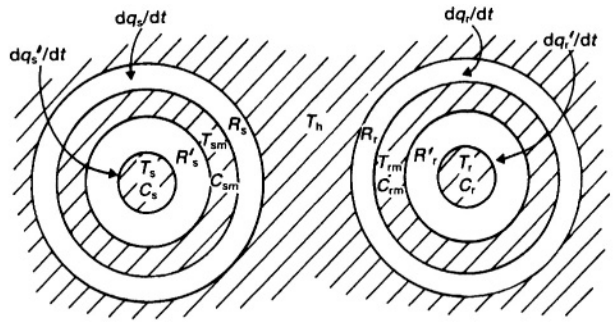

T_h = temperature of heat source

T_S	=	actual sample temperature	T_r	=	actual reference temperature
T_{sm}	=	measured sample temperature	T_{rm}	=	measured reference temperature
C_S	=	heat capacity of sample + pan	C_r	=	heat capacity of reference + pan
C_{sm}	=	heat capacity of monitoring station	C_{rm}	=	heat capacity of monitoring station

R'_s, R_s, R_r and R'_r are thermal resistances
The dq/dt terms are heat flows

For an ideal instrument, the heat capacities and thermal resistances would be matched, i.e. $C_{rm} = C_{sm}$; $R_r = R_s = R$ and $R_r' = R_s' = R'$. Note that $R \neq R'$ and $C_s \neq C_r$. It is further assumed that $C_s > C_r$ and that heat flow is governed by Newton's law:

$$dq / dt = (1/R)\ \Delta T$$

Heat flow to the sample side, heats both (i) the sample monitoring station and (ii) the sample:

$$dq_s / dt = C_{sm}(dT_{sm} / dt) + C_s(dT_s / dt)$$

also

$$dq_s' / dt = C_s(dT_s / dt)$$

so

$$dq_s / dt = C_{sm}(dT_{sm} / dt) + dq_s' / dt$$

Applying Newton's law:

$$dq_s / dt = (1/R)(T_h - T_{sm})$$

and

$$dq_s' / dt = (1/R')(T_{sm} - T_s)$$

Similar expressions hold for the reference side.

Classical DTA
Thermocouples are in the sample and in the reference material so that $T_{sm} = T_s$ and $T_{rm} = T_r$, i.e. $R' = 0$. The signal then is:

$$\Delta T = R (dT / dt)(C_s - C_r)$$

and depends upon the difference in heat capacities, the heating rate and the thermal resistance, R. R is difficult to determine as it depends on both the instrument and the properties of the sample and the reference.

Power-compensated DSC
The power is varied to make $T_{sm} = T_{rm}$. Thus $T_h = T_{sm} = T_{rm}$ and $R = 0$, i.e. there is no thermal resistance. The signal is then:

$$\Delta(dq / dt) = (dT / dt)(C_s - C_r)$$

Heat-flux DSC
The conditions are that:

$$T_h \neq T_{sm} \neq T_s \text{ and } R \neq R' \neq 0.$$

The signal:

$$\Delta T = T_{rm} - T_{sm} = R (dT / dt)(C_s - C_r)$$

is of similar form to classical DTA, except that R depends only on the instrument and not on the characteristics of the sample.

4.5 Modulated Temperature Differential Scanning Calorimetry (MTDSC or mt-DSC)

4.5.1 Introduction

Modulated Temperature Differential Scanning Calorimetry (mt-DSC according to the newest nomenclature proposals, Chapter 1, and usually referred to as MTDSC) is a technique [2,6,11 - 16] in which the conventional linear heating programme is modulated by superimposing a sine wave (or other periodic waveform, see below) of small amplitude on the linear rise. Portions of each cycle then involve heating while other portions involve cooling. The overall trend, however, remains a linear change in average temperature with time. The resultant heat flow signal is analyzed to separate the response to the perturbation from the response to the underlying heating programme.

The modulated heating programme may, for example, be of the form:

$$T = T_0 + \beta t + B \sin(\omega t) \quad (1)$$

where T_0 is the starting temperature, β the heating rate, B the amplitude of the modulation and ω its angular frequency ($= 2\pi f$, where f is the frequency).

The contributions to the resulting heat flow can be written in the form [2]:

$$dq/dt = C_{p,t}\,(dT/dt) + f(t,T) \quad (2)$$

where dq/dt is the heat flow into the sample, $C_{p,t}$ is the heat capacity of the sample and $f(t,T)$ is the heat flow arising as a consequence of a "kinetically hindered" event [2]. The form of $f(t,T)$ will be different for different types of process.

Combination of equations (1) and (2) gives:

$$dq/dt = \{\beta C_{p,t} + F(t,T)\} + \{\omega B C_{p,t} \cos(\omega t) + D \sin(\omega t)\} \quad (3)$$

underlying component — cyclic component

The *total* or underlying signal is $\{\beta C_{p,t} + F(t,T)\}$, where $F(t,T)$ is the average of $f(t,T)$ over the interval of at least one modulation, and the *cyclic* signal is $\{\omega B C_{p,t} \cos(\omega t) + D \sin(\omega t)\}$, where D is the amplitude of the kinetically hindered response to the temperature modulation. Both $C_{p,t}$ and D will be slowly varying functions of time and temperature but can be considered effectively constant over the duration of a single modulation. $f(t,T)$ can also give rise to a cosine contribution.

The kinetically hindered responses are usually assumed to show Arrhenius-type behaviour. The cosine response of $f(t,T)$ can be made negligible by adjusting the frequency of modulation and the underlying heating rate, to ensure that there are many cycles over the course of the transition. The amplitude of the temperature modulation is usually restricted to a degree or less so that the kinetic response can be considered to be linear.

The signals derived from a MTDSC experiment (see Figure 4.4) are: (i) the average or underlying signal, equivalent to conventional DSC; (ii) the in-phase cyclic component from which $C_{p,t}$ can be calculated, and (iii) the out-of-phase signal, *D*. $C_{p,t}$ can be multiplied by the heating rate, β, to give (iv) the reversing contribution to the underlying heat flow. Subtraction of (iv) from the underlying signal (i) gives (v) the non-reversing heat flow.

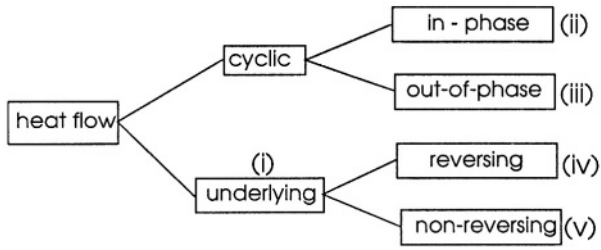

4.5.2 Alternative modulation functions and methods of analysis

Some workers and manufacturers (Perkin-Elmer and Mettler-Toledo) have preferred a square wave or a sawtooth modulation. In some cases they have proceeded with a Fourier transform analysis and taken the first Fourier coefficient (Perkin-Elmer). This then gives equivalent results to the use of a sine wave with a FT analysis [2],

Use of a square wave (Mettler-Toledo) ensures that a steady state is achieved over the isothermal plateau. Because d*T*/d*t* is zero, the signal during this portion must be a non-reversing contribution. The difference between the maxima and the minima generated by the modulation, i.e. the amplitude, gives a measure of the reversing signal. An alternative is to use equal positive and negative heating rates, with a longer duration being given to the positive or negative portions in order to provide a net heating or cooling rate. The sum of the maxima and minima in the heat flow produced by this modulation [2], provides a measure of the non-reversing component (where F(*t,T*) is assumed not to change during the modulation). Again the difference between them is a measure of the reversing signal. The disadvantage of these approaches is that there is only one point per modulation obtained using only part of the data, with the intervening data being lost. This severely compromises accuracy and resolution.

4.5.3 Advantages of mt-DSC [2]

Use of mt-DSC with appropriate frequencies and amplitudes of modulation allows separation of *reversing* processes, such as glass transitions, from *non-reversing* processes such as relaxation endotherms, or cure reactions. Baseline curvature on the cyclic signal is generally very low, thus making it easier to distinguish between baseline effects and real transitions. The signal-to-noise ratio of the cyclic measurement of heat capacity is generally greater, because all drift or noise at frequencies other than that of the modulation is ignored by the Fourier transform analysis. Resolution of processes can be improved because very low underlying heating rates can be used.

Figure 4.4
Separation of the component parts of the MTDSC signal for a run on quenched PET [2].
(With the permission of Elsevier, Amsterdam.)

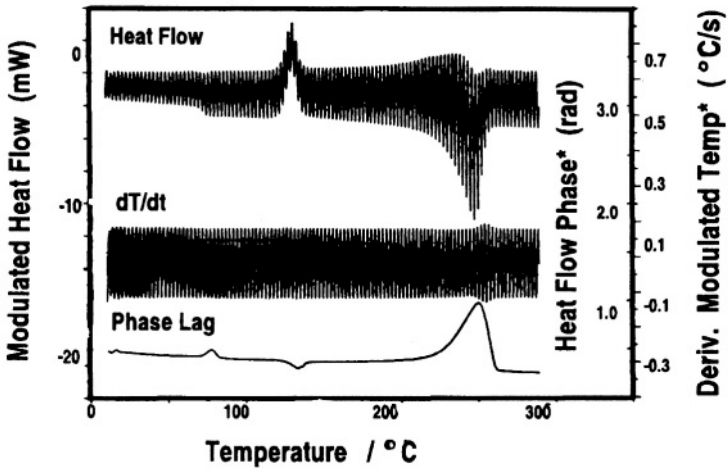

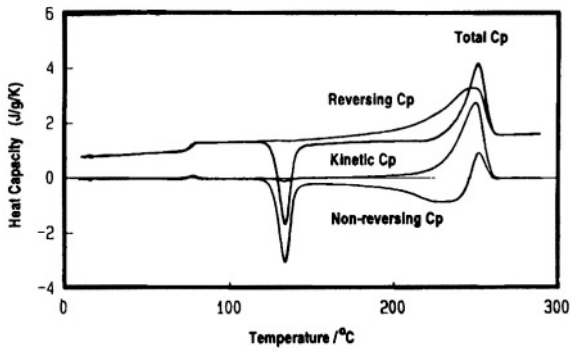

4.6 Sample Containers and Sampling

At temperatures below 500°C (773 K) samples are usually contained in aluminium sample pans. One type of pan has lids which may be crimped (Figure 4.5.) into position, while for volatile samples, pans and press are available which enables a cold-welded seal, capable of withstanding 2-3 bar (220-300 kPa) pressure, to be made. The use of aluminium pans above 500°C will result in destruction of the DSC sample holder, so it is essential to ensure that the hardware or software of the instrument will limit the maximum temperature which may be used by an operator unless he or she has specifically overridden the limit.

Figure 4.5
Sample container presses. (With the permission of Perkin-Elmer Corporation and Mettler Instruments AG.)

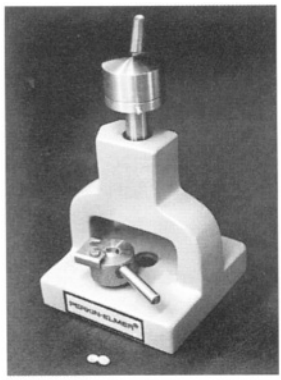

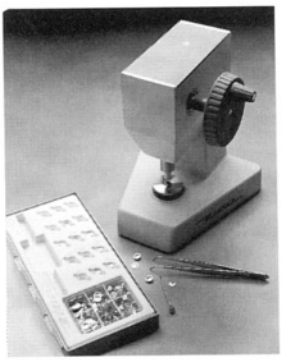

For temperatures above 500°C, or for samples which react with the Al pans, gold or graphite pans are available. Glass sample holders are sometimes suitable. The reference material in most DSC applications is simply an empty sample pan.

The sample-holder assembly is purged by a gas which may be inert or reactive as desired. (The high thermal conductivity of helium makes it unsuitable for thermal measurements although it has advantages for evolved gas analysis (see later)).

Dense powders or discs, cut out of films with a cork borer, are ideal samples. Low density powders, flocks or fibres may be prepacked in a small piece of degreased aluminium foil to compress them. A small syringe is used for filling pans with liquid samples. When volatile products are to be formed on heating the sample, the pan lid should be pierced. This is also necessary when reaction with the purge gas is being investigated.

If the total mass of the sample + pan + lid is recorded before and after a run, further deductions on the processes occurring can be made from any change in mass.

4.7 Quantitative Aspects of DTA and DSC Curves

4.7.1 Characteristics of a DSC Curve [8]

Some characteristic terms are used to describe a measured DSC curve (see Figure 4.6).

Figure 4.6
Definition of zero line, baseline, peak and the characteristic temperatures (definitions see text). T_i, initial peak temperature, T_e, extrapolated peak onset temperature, T_p, peak maximum temperature, T_c, extrapolated peak completion temperature, T_f, final peak temperature [8]. (With the permission of Springer-Verlag, Berlin.)

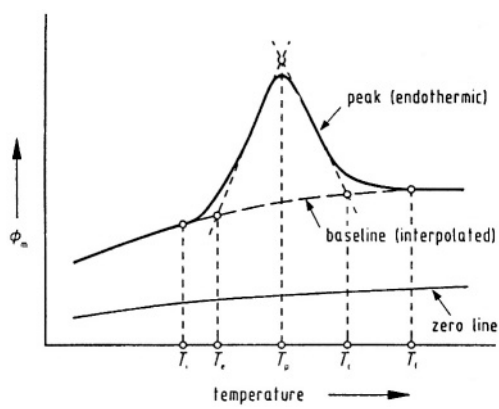

The *zero line* is the curve measured with the instrument empty, i.e. without samples and without sample containers (crucibles), or with the sample containers (crucibles) empty. The (interpolated) *baseline* is the line constructed in such a way that it connects the measured curve before and after a peak, as if no peak had developed. A *peak* in the curve appears when the steady state is disturbed by some production or consumption of heat by the sample. Peaks associated with endothermic processes are plotted upwards (positive direction of heat addition to the system). Some transitions, such as glass transitions, lead to changes in the shape of the DSC curve, rather than to distinguishable peaks.

The characteristic temperatures of a DSC curve are defined as follows [8]:

T_i, *Initial peak temperature*: The peak begins where the curve of measured values begins to deviate from the baseline.

T_e, *Extrapolated peak onset temperature*: Where the line drawn through the almost linear section of the ascending peak slope intersects the baseline.

T_p, *Peak maximum temperature*: Where the **difference** between the DSC curve and the interpolated baseline is a maximum. This not necessarily the absolute maximum of the DSC curve.

T_c, *Extrapolated peak completion temperature*: Where the line through the descending peak slope intersects the baseline.

T_f, *Final peak temperature*: Where the DSC curve returns to the baseline.

4.7.2 The Baseline

The features of interest in DTA or DSC curves are the deviations of the signal from the baseline, and the baseline is not always easy to establish. Initial displacements of the baseline itself from zero, result from mismatching of the thermal properties of the sample and the reference material and asymmetry in the construction of sample and reference holders. In severe cases this may cause a sloping baseline, which may require electrical compensation. After a thermal event, the response will not return to the original baseline if the thermal properties of the high-temperature form of the sample are different from those of the low-temperature form. Many different procedures for baseline construction have been suggested (Figure 4.7) and may be incorporated in the software supplied with an instrument.

It should be immediately obvious whether a DSC or DTA feature is a peak or a discontinuity, provided that the baseline can be established with certainty. Whether a peak is in the exothermic or endothermic direction should be ascertained by comparison with a known melting (endothermic) peak. If there is any suggestion from initial runs that any of the features involve overlapping peaks, then further experiments should be done in which the sample mass and the heating rate are varied to see whether the individual peaks can be resolved.

Figure 4.7
Simpler procedures for baseline construction

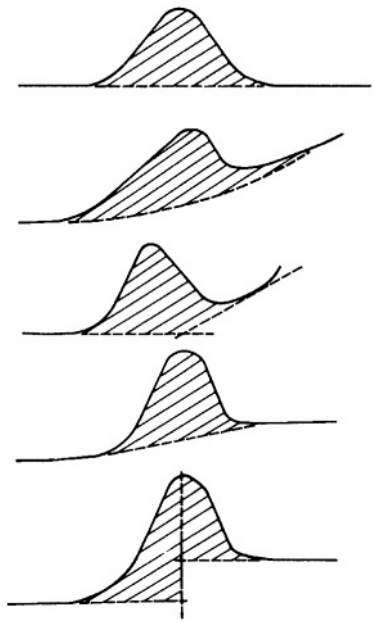

The glass transition in polymers (see Figure 4.8.) is accompanied by an abrupt changes in position of the baseline resulting from the change in heat capacity on going from the glassy to rubber-like states. The enthalpy change, ΔH, for such transitions is zero, which is often regarded as the criterion for a second-order transition, but Wunderlich [17] has emphasized that the glass transition is time dependent and hence is not at thermodynamic equilibrium.

4.7.3 Measurement of enthalpy changes [18]
Once a satisfactory baseline has been defined, the area of the endotherm or exotherm is determined by numerical integration. The measured area, *A,* is assumed to be proportional to the enthalpy change, ΔH, for the thermal event represented.

$$\Delta H = A \times K/m$$

where m is the sample mass and K is the calibration factor. This factor has to be determined by relating a known enthalpy change to a measured peak area. Usually the melting of a pure metal, such as indium, is used for calibration.

Figure 4.8
The glass transition of a printed circuit board (brominated bisphenol A resin). The DSC curve (proportional to the specific heat capacity) is compared with the curve of the linear expansion coefficient (proportional to the first derivative of the TMA curve). (From Mettler Application No. 3402, with permission.)

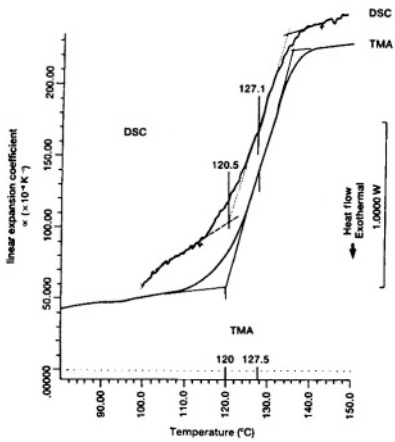

The procedure for the determination of the enthalpy change for a process occurring in the sample, ΔH_s, is then to determine:

$$K = \Delta H_{\text{fusion,calibrant(c)}} \times m_c / A_c$$

and to use this value in

$$\Delta H_s = (K \times A_s)/m_s$$

where A is the area and subscripts c and s refer to calibrant and sample, respectively. Note that the heating rate used in the temperature programme does not enter into the calculations, but, in precise work, should be the same for sample and calibrant.

The calibration factor, K, contains contributions from the geometry and thermal conductivity of the sample/reference system and is thus specific to a particular instrument under one set of operating conditions. For power-compensated DSC, the proportionality constant, K, is virtually independent of temperature, while for DTA or heat-flux DSC, the value of K is markedly dependent upon temperature, so that calibrations have to be carried out over the full operating temperature range of the instrument. Compensation for the temperature dependence of the calibration factor is, however, now usually built into the hardware or software of heat-flux DSC instruments.

The melting point of the standard used for the enthalpy calibration above is usually used at the same time to calibrate the temperature output of the instrument.

4.7.4 Calibration materials

Certified reference materials (CRM) are available from some national laboratories, mainly the UK Laboratory of the Government Chemist (LGC) and the US National Institute of Standards and Technology (NIST) [18]. Table 4.1. lists the transition temperatures and enthalpies of materials recommended as standards [18],

Ideally, the thermal properties of the standard including its transition temperature, should be as close as possible to those of the sample under consideration. The calibrant should [18] also be available in high purity at low cost, be easy to handle and of low toxicity and be chemically and physically stable. The transition of interest should be readily reversible. Enthalpy (and specific heat capacity) data should be known to an order of magnitude better than the DSC reproducibility. Enthalpies of fusion or transition are not generally known to better than $\pm 1\%$, let alone the desired $\pm 0.1\%$[18]. Richardson and Charsley [18] have described experimental procedures in detail. Some important recommendations are that, for melting transitions, the sample should have been premelted to give a thin layer between the pan and its lid; samples should be of minimum size consistent with an adequate signal and should be reweighed at the end of a run to guard against any possible vaporization. Most of the molten metals listed in Table 4.1 will react with aluminium pans. Cammenga *et al.* [19] have discussed sample/pan compatibilities.

Other reference materials and potential calibrants are described in the detailed review by Richardson and Charsley [18]. The International Confederation for Thermal Analysis and Calorimetry (ICTAC) reference materials mainly feature solid/solid transitions. Round-robin comparisons show wide uncertainties in the averaged onset temperatures (Table 4.2) and in determinations of enthalpy changes. ICTAC has a new programme to recertify most of these materials, which should therefore be considered to be *secondary,* or working, standards.

4.7.5 Measurement of heat capacity

DSC can also be used to measure heat capacities of materials. Because heat capacity values are fundamental to thermodynamics, this is an important feature.

$$\Delta H = \int_{T_1}^{T_2} C_p \, dT$$

$$\Delta S = \int_{T_1}^{T_2} (C_p/T) \, dT$$

$$\Delta G = \Delta H - T\Delta S$$

Where C_p is the heat capacity at constant pressure.

Table 4.1
Certified reference materials [18]:
Temperatures (T) and enthalpies of fusion (ΔH_{fus})

	T /°C	T /K	ΔH_{fus}/ J g^{-1}
A. METALS			
Mercury	-38.86	234.29 ± 0.03	11.469 ± 0.008
Indium	156.61	429.76 ± 0.02	28.71 ± 0.08
Tin	231.92	505.07 ± 0.02	60.55 ± 0.13
Tin*	231.91	505.06 ± 0.01	60.22 ± 0.19
Lead	327.47	600.62 ± 0.02	23.00 ± 0.05
Zinc	419.53	692.68 ± 0.02	108.6 ± 0.5
Aluminium	660.33	933.48 ± 0.05	401.3 ± 1.6
Silver*	961.78	1234.93	
B. ORGANIC COMPOUNDS (Temperature uncertainty is ± 0.02)			
4-Nitrotoluene	51.61	324.76	
Biphenyl	68.93	342.08	120.6 ± 0.6
Naphthalene	80.23	353.38	147.6 ± 0.2
	80.30	353.45	
Benzil	94.85	368.00	110.6 ± 0.6
	94.89	368.04	
Acetanilide	114.34	387.49	161.2 ± 0.2
	114.25	387.40	
Benzoic Acid	122.35	395.50	147.2 ± 0.3
	122.24	395.39	
Diphenylacetic Acid	147.17	420.32	146.8 ± 0.1
	147.11	420.26	
Anisic Acid	183.28	456.43	
2-Chloroanthraquinone	209.83	482.98	
Carbazole	245.80	518.95	
Anthraquinone	284.52	557.67	

Unless shown otherwise, all samples are from LGC.
* NIST sample
Supercooling is a problem with many of the organic compounds, especially [18] benzil, diphenylacetic acid, acetanilide and benzoic acid.

Table 4.2
ICTAC reference materials [18]:
Transition (trs) or fusion (fus) temperatures (T)

			Equilibrium value	
	T/°C	T/K	T_x/K*	ΔH_{fus}/(J g^{-1})*
Cyclohexane(trs)	-86.1	187.1 ± 3.5		
Cyclohexane(fus)	4.8	278.0 ± 1.1		
1,2-Dichloroethane(fus)	-35.9	237.3 ± 2.0		
Diphenyl ether(fus)	25.4	298.6 ± 2.2	300.02**	101.15
o-Terphenyl(fus)	55.0	328.2 ± 2.2	329.35§	74.64
Potassium nitrate(trs)	128	401 ± 5	402.0	26.3
(trs)			402.9	50.5
(fus)			607.6	98.2
Indium(fus)	154	427 ± 6	429.7485	28.62
Tin(fus)	230	503 ± 5	505.078	60.40
Potassium perchlorate(trs)	299	572 ± 6	573.1	103.1
Silver sulphate(trs)	424	697 ± 7	Stability problems	
Silica(trs)	571	844 ± 5	Complex transition	
Potassium sulphate (trs)	582	855 ± 7	857	
(fus)			1343	
Potassium chromate(trs)	665	938 ± 7	942.3	
Barium carbonate(trs)	808	1081 ± 8	1082	
Strontium carbonate(trs)	928	1201 ± 7	(1205.9 at 10 K min^{-1}, needs CO_2 purge to stop decomposition)	

*subscript x = trs, solid/solid transition or fus, fusion
** supercools about 60 K
§ supercools (about 90 K) to glass, slow return to original structure

In the absence of a sample, i.e. with empty pans in both holders of Figure 4.9(a), the DSC baseline should be a horizontal line. A sloping baseline may be observed when the sample and reference holders have different emissivities, i.e., if the amount of energy lost by radiation does not vary in the same way with T_1 for both sample and reference. This could occur for a black sample and a shiny reference, so a sloping baseline is often an indication that the sample-holder assembly should be cleaned by heating in air to high temperatures, *with aluminium pans removed.*

When a sample is introduced, the DSC baseline is displaced in the endothermic direction and the displacement, h, is proportional to the total heat capacity, C_p, of the sample. (The total heat capacity = mass x specific heat capacity). This is illustrated in Figure 4.9(a).

$$h \propto C_p \quad \text{or} \quad h = B\beta C_p$$

where β is the heating rate and B the calibration factor. The value of B is determined using a standard substance [18], e.g. sapphire, scanned under similar conditions to the sample (see Figure 4.9(b)). Although the technique is simple in principle, Suzuki and Wunderlich [20] have shown that a great deal of care is necessary to get accurate and reproducible results. Because of the proportionality of the DSC response to the heat capacity of the sample, a shift in baseline after a transition is common (Figure 4.9(c)) and the baseline has to be estimated as shown in Figure 4.7 or by more elaborate procedures [21].

4.7.6 Measurement of thermal conductivity

Thermal conductivity, λ, is an important physical property, particularly with the present emphasis on the efficient use of energy. Numerous methods for measuring thermal conductivity have been published and dedicated commercial instruments are available. Several papers have been published [22-25] in which heat-flux DSC instruments have been used to measure thermal conductivity. An advantage of using DSC is that specific heat capacities, c_p, can be measured in the same instrument and hence, if density values, ρ, are available or can be measured, thermal diffusivities, D, can be calculated from the relationship, $D = \lambda/(\rho\, c_p)$ Chiu and Fair [22] have described an attachment for the DuPont 990 DSC cell, (Figure 4.10), which allows for measurement of thermal conductivity of a sample (in cylindrical form) without modification of the basic instrument. The temperature at the bottom of the sample (T_1) is measured via the output of the DSC, while the temperature at the top of the sample (T_2) is measured with a separate thermocouple in the contact rod. The heat input for the sample is also provided by the DSC. The cell is calibrated with a sample of known thermal conductivity. The output of the DSC operating in the normal mode is used as the baseline. With the sample in position, the DSC cell is brought to the desired measurement temperature, T_1 and when the DSC output is steady with time, the temperature difference across the sample, ΔT_s and the recorder displacement, h_s, are determined. The sample is then replaced by a calibrant, e.g. a standard glass, and the corresponding quantities, ΔT_c and h_c are determined. The thermal conductivity of the sample, λ_s, is then calculated from:

$$\lambda_s = \lambda_c\,(h_s \times \ell_s \times d_c^2 \times \Delta T_c)/(h_c \times \ell_c \times d_s^2 \times \Delta T_s)$$

where ℓ is the length and d the diameter of the sample (subscript s) and calibrant (subscript c) as specified. A sample length of 10 to 25 mm is recommended and a precision of better than 3% is claimed. Sircar and Wells [23] have used the above method in studying elastomer vulcanizates, and Hillstrom [24], a very similar system, for determining the thermal conductivity of explosives and propellants.

Figure 4.9
Measurement of heat capacity using DSC. (a) Displacement of baseline, (b) scan of sample compared to standard, (c) shift in baseline after a transition.

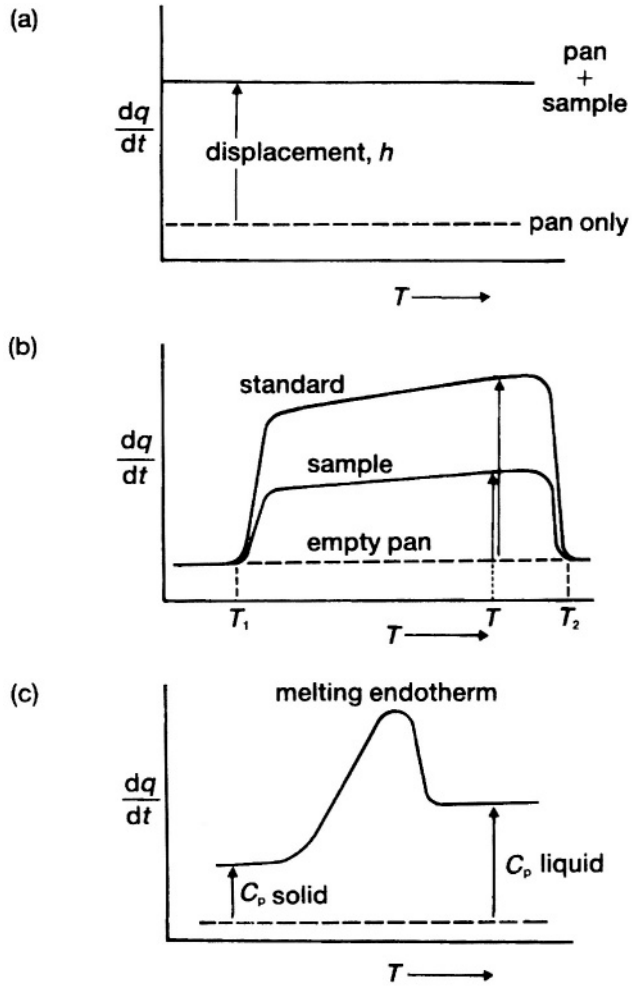

Figure 4.10
Schematic diagram of thermal conductivity cell [22]. (With the permission of Elsevier, Amsterdam.)

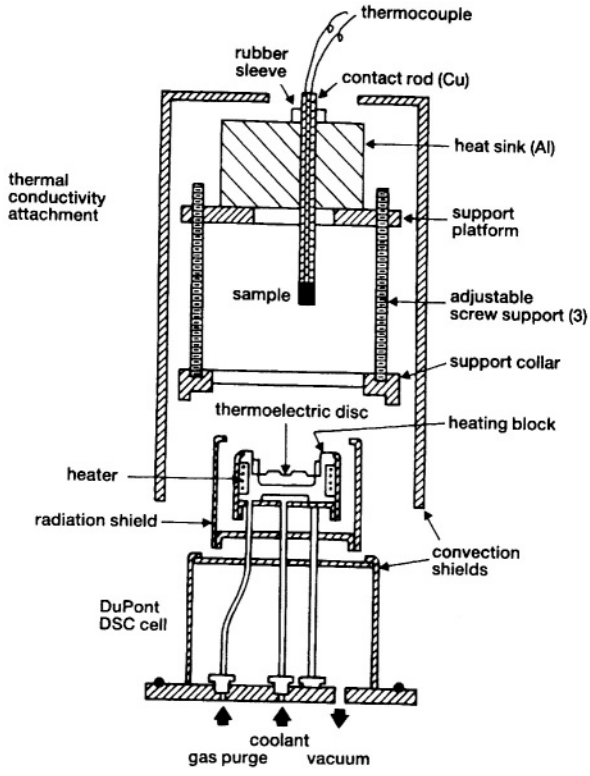

Hakvoort and van Reijen [25] using a DuPont 910 DSC, replaced the temperature sensor on the top of the sample by a disc of pure gallium or indium metal (see Figure 4.11(a)). The temperature at the top of the sample during the melting of the metal is then fixed at the melting point, T_m, of the metal. The y-output scale calibration factor C (in $W\ mV^{-1}$) for the instrument is first determined by melting a weighed sample of the metal placed directly on the sensor, without a sample pan, and measuring the DSC signal, y, with time. The heat of melting, Q_m, is given by:

$$Q_m = \int Q' \, dt = C \int y \, dt$$

so that:

$$Q'_{sensor} = C\,y$$

Two identical cylinders of sample (1-3 mm high, 2-4 mm diameter) are then placed on the

sample and reference positions of the DSC (with silicone grease if necessary). A disc of the metal to be melted (10 to 40 mg and diameter similar to that of the sample) is placed on top of the cylinder on the sample side and the sensor temperature, T_s, and the DSC signal, y are recorded with time as the cell is heated at constant rate. During the melting of the metal, the top of the sample cylinder remains at constant temperature, T_m, while the lower side temperature, T_s, increases at constant rate. The DSC plot obtained is shown in Figure 4.11(b). Two quantities are determined: the slope of the plot of T_s against time, $a = dT_s/dt$; and the slope of the DSC curve, $b = dy/dt$. Combining these quantities, $a/b = dT_s/dy = \beta$. The thermal conductivity, λ, is then calculated from [4]:

$$\lambda = hC/A\,\beta$$

where A is the cross-sectional area of the sample cylinder and h its height.

Boddington *et al.* [26] have carried out a more elaborate modification of a Stanton Redcroft DTA model 673 for measurement of the thermal diffusivity of pyrotechnic compositions.

Figure 4.11
Measurement of thermal conductivity using DSC [25]. (a) Sample geometry, (b) DSC plots, a: T_s against time $\rightarrow dT_s/dt$; b: y against time $\rightarrow dy/dt$; $(dT_s/dt)/(dy/dt) = dT_s/dy = \beta$. (With the permission of Elsevier, Amsterdam.)

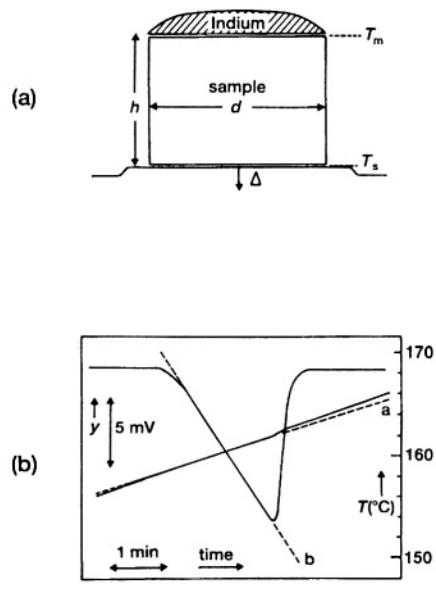

4.8 Interpretation of DSC and DTA curves

At the heart of all thermal analysis experiments lies the problem of correlating the features recorded with the thermal events taking place in the sample. Some aspects of this correlation for TG results have been discussed in Section 3.8. DSC or DTA provides different information and if simultaneous measurements are not possible, the results of parallel experiments, using different techniques such as TG and DSC or DTA, under conditions (e.g. sample mass, heating rate, atmosphere) as closely matched as possible, are most valuable.

Once the main features of the DTA or DSC curve have been established, and baseline discontinuities have been examined, attention can be directed at the correlation of the endothermic or exothermic peaks with thermal events in the sample.

A useful procedure is to test whether the event being monitored is readily reversible on cooling and reheating, or not. Exothermic processes are not usually readily reversible, if at all, in contrast to melting and many solid-solid transitions.

The melting endotherms for pure substances are very sharp (i.e. they occur over a narrow temperature interval) and the melting point, T_m, is usually determined, as shown in Figure 4.2(b), by extrapolation of the steeply rising, approximately linear, region of the endotherm back to the baseline. For impure substances the endotherms are broader and it is possible to estimate the impurity content (up to a maximum of about 3 mole %) from the detailed shape of the melting endotherm (see Chapter 11).

TG and EGD or EGA information is invaluable at this stage in distinguishing between irreversible or slowly-reversible phase transitions and decompositions. Quantitative mass losses and detailed EGA may, in addition, lead to determination of the stoichiometry of decomposition. Account must naturally be taken of the gaseous atmosphere surrounding the heated sample. Dehydration may be found to be reversible on cooling in a moist atmosphere before reheating, and carbonate decompositions are usually reversible in CO_2 atmospheres. Comparison of features observed, under otherwise similar conditions, in inert and oxidising atmospheres is valuable. TG results may show increases in mass corresponding to reaction of the sample with the surrounding atmosphere.

It cannot be over emphasised that as many additional techniques available, such as hot-stage microscopy, conventional elemental analysis, X-ray diffraction (XRD) and the many types of spectroscopy, should be used to confirm suggested interpretations of TA features recorded. Table 4.3 summarises the overall interpretation procedure, but this should NOT be followed blindly. There is no substitute for experience built up by running samples with well-documented behaviour on your own instrument, and also examining the almost legal-type of "proof" of events provided by more-conscientious authors (spurred on by more-demanding editors).

Table 4.3
Interpretation of DSC and DTA experiments

Feature	Peak				Discontinuity	
Direction	*Endothermic*		*Exothermic*			
Reversible	Yes	No	Yes	No	Yes	No
Broad	No	Yes	Usually	Usually	-	-
Mass loss (TG)	No	Yes	No (gain)	Yes	No	-
Gas evolved (EGA)	No	Yes	No	Yes	No	-
Possible interpretation	Solid transition or melting	Dehydration Decomposition (e.g. loss of ligand)	Polymer crystallization Some solid transitions	Decomposition (oxidation)	Glass transition	Electrical disturbance
Further tests	Microscopy	XRD Spectroscopy	XRD	XRD	TMA DMA	check

4.9 Determination of phase diagrams

It is not always easy to detect accurately by eye the onset and completion of melting of binary or more complicated systems. The records obtainable from DSC and DTA runs, under carefully defined sample conditions, and slow heating and cooling rates so that equilibrium is approached, provide a more accurate way of establishing the phase diagram for the melting and solubility behaviour of the system under consideration.

In a binary system of immiscible solids and their completely miscible liquids, with the well-known phase diagram shown in Figure 4.12 (e.g. the benzoic acid/naphthalene system [27,28] or the triphenylmethane/trans-stilbene system [29]), the melting curves of the pure components A and B (with melting points $T_{m,A}$ and $T_{m,B}$) are readily obtained, using DSC or DTA, and should be sharply defined. The melting behaviour of mixtures of A and B will depend upon the histories of the mixtures and, in this discussion, it will be assumed that the mixtures have been prepared in completely molten form initially (without any volatilization or oxidation [30]).

Figure 4.12
Phase diagram for a binary system of immiscible solids and their completely miscible liquids.

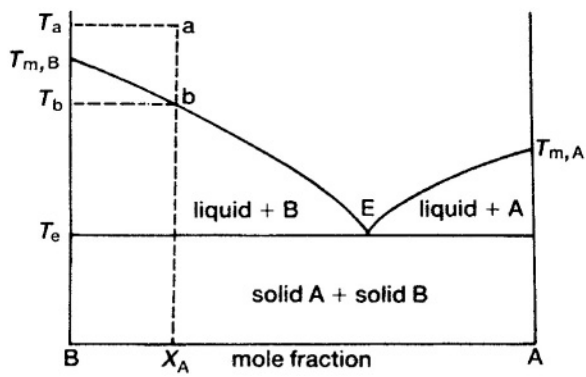

A DSC or DTA record of the slow cooling of such a molten mixture of composition x_A (mole fraction) initially at temperature T_a in Figure 4.12, would show no deviation from the baseline until temperature T_b when solid B begins to crystallize in an exothermic process. This exotherm is not sharp but tails off as crystallization becomes complete (see Figure 4.13). The area under this exotherm will depend upon the amount of B present in the sample of the mixture. As the temperature of the mixture falls further, the eutectic temperature, T_e, is reached and solid A crystallizes in a sharp exotherm (Figure 4.13). If the composition had been chosen to be that corresponding to point E, the DSC or DTA record would have shown only a single sharp exotherm as the eutectic composition solidified. At low concentrations of A, and similarly at low concentrations of B, the formation of the eutectic may be difficult to detect and hence to distinguish from the formation of solid solutions [30].

Figure 4.13
DSC or DTA curve for the slow cooling of a molten mixture of composition x_A initially at temperature T_a in Figure 4.12.

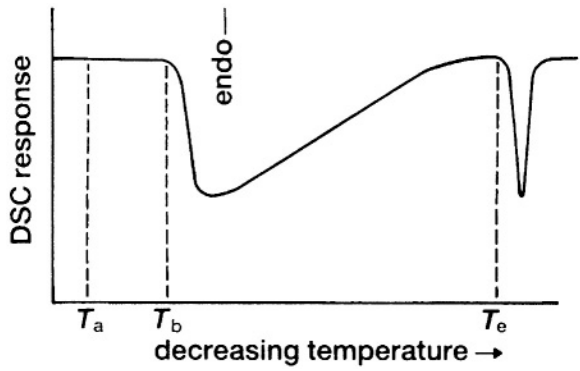

If the mixture, whose cooling curve is shown in Figure 4.13, were to be reheated slowly, the DSC or DTA record should ideally be the endothermic mirror image of that shown. The use of the heating rather than the cooling curve avoids problems of supercooling.

Ideally then, the DSC or DTA traces should be readily relatable to the phase diagram, as illustrated schematically in Figure 4.14.

Figure 4.14
Schematic comparison of DSC or DTA curves with the phase diagram.

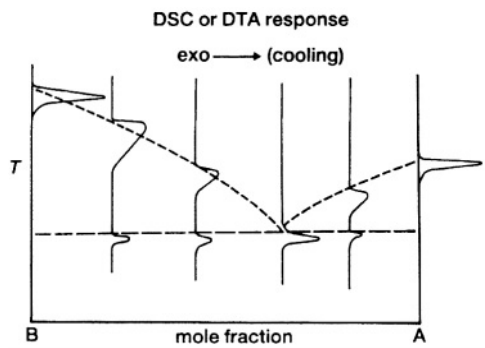

The area under the peak for the eutectic melting is a simple function of concentration (see Figure 4.15) and such a curve may be used to determine the composition of an unknown mixture, e.g. an alloy [31].

Figure 4.15
Relationship between enthalpy of melting and composition.

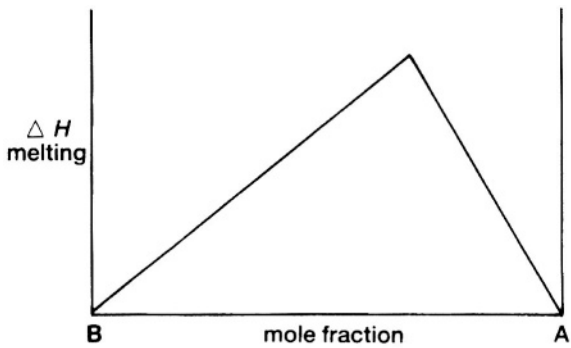

Pope and Judd [30] give an example of a more complicated phase diagram, with incongruently and congruently melting compounds and solid solution, eutectic and liquidus reactions, while Eysel [32] discusses the even more complex Na_2SO_4/K_2SO_4 system. A variety of systems, including ternary systems and phase studies under high pressure, is discussed by Gutt and Majumdar [33], and the theoretical background is covered by Sestak [34]. The phase diagrams for the ternary Ge-Sb-Bi system [35] and the complicated Ag_2Te - Ag_4SSe system, with 17 phase regions [36], serve as illustrations of how successful such studies can be. Combination of DTA with thermomicroscopy can provide additional information over a more limited temperature range.

4.10 General applications of DTA and DSC

The results obtained using DTA and DSC are qualitatively so similar that their applications will not be treated separately. It should be noted that DTA can be used to higher temperatures than DSC (max 725°C) but that more reliable quantitative information is obtained from DSC.

Although DTA and DSC curves may be used solely for "fingerprint" comparison with sets of reference curves, it is usually possible to extract a great deal more information from the curves, such as the temperatures and enthalpy changes for the thermal events occurring. As an example, the DSC curve for $CuSO_4.5H_2O$ is shown in Figure 4.16 for comparison with the TG curve given in Figure 3.10. Note the increase in ΔH of dehydration per mole of H_2O removed.

Figure 4.16
The DSC curve for $CuSO_4.5H_2O$

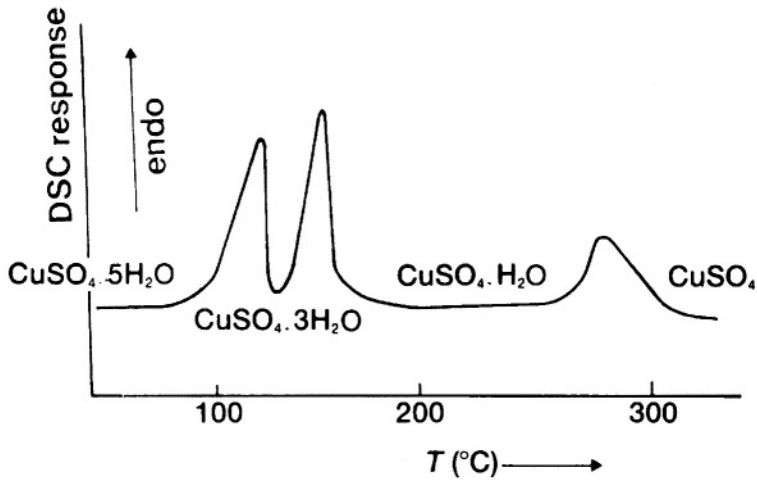

The shape of the melting endotherm can be used to estimate the purity of the sample. The procedure is discussed in detail in Chapter 11.

Detection of solid-solid phase transitions, and due measurement of ΔH for these transitions, is readily done by DSC or DTA. A low temperature attachment permits the range of samples which can be examined, to be extended, as shown by the DSC curve for carbon tetrachloride in Figure 4.17. Satisfactory operation as low as -175°C has been achieved. Condensation of atmospheric moisture can cause problems and has to be reduced. Redfern [39] has reviewed some of the cooling systems available and has discussed some low-temperature applications.

Application of thermal analysis to the study of polymers has been most rewarding [38]. A DSC curve for a typical organic polymer is shown in Figure 4.18. Most solid polymers are formed by rapid cooling to low temperatures (quenching) from the melt and are thus initially in the glassy state. The transition from a glass to a rubber, the *glass transition,* is accompanied by a change in heat capacity, but no change in enthalpy (ΔH=0). The transition thus appears on the DSC curve as a discontinuity in the baseline (see Figure 4.19) at the glass-transition temperature, T_g. As the temperature is slowly increased, the polymer may recrystallise giving the exotherm shown, before melting occurs. At higher temperatures the polymer may decompose (degrade) or oxidise depending upon the surrounding atmosphere.

Figure 4.17
The DSC curve for carbon tetrachloride

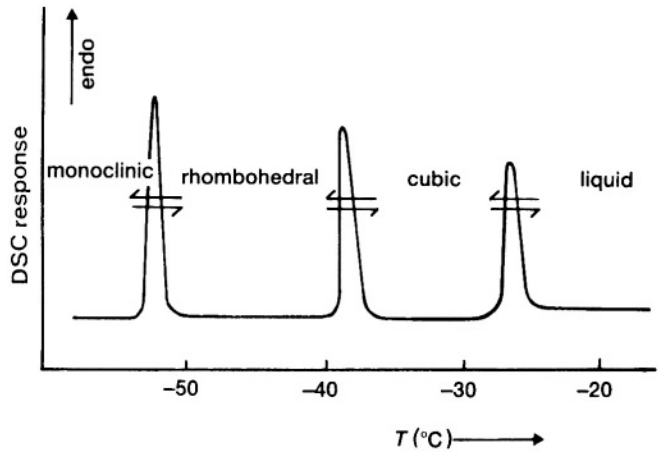

Figure 4.18
A DSC curve for a typical organic polymer

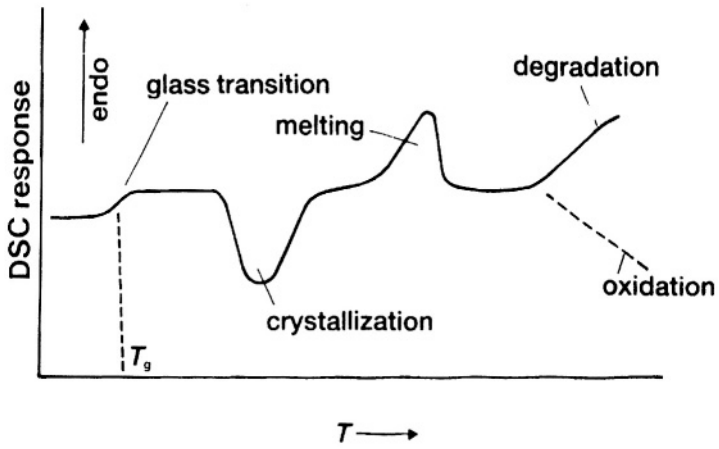

Figure 4.19
Definition of characteristic features of the glass transition. $T_{g,e}$ = the extrapolated onset temperature; $T_{g,½}$ = the half-step temperature at which the heat capacity is midway between the extrapolated heat capacities of the liquid and glassy states; $T_{g,i}$ and $T_{g,f}$ are the initial and final temperatures of the glass transition and $T_{g,f} - T_{g,i}$ is the temperature interval of the glass transition [8]. (With the permission of Springer-Verlag, Berlin.)

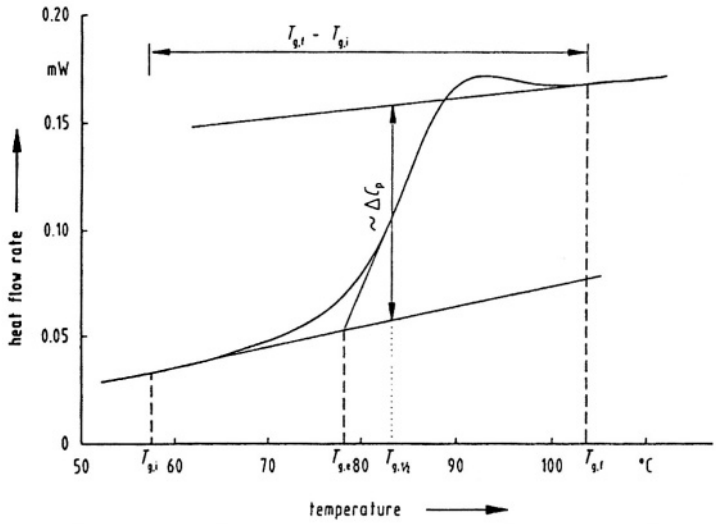

The degradation or oxidation of polymers can be studied using DSC in the isothermal mode. Figure 4.20 shows the effect of stabilizers on the oxidation of polyethylene at 200°C. The crystallisation of polymers can also be studied using isothermal DSC. Several approaches are possible. The molten polymer may be cooled rapidly to a temperature in the crystallisation range, and the crystallisation from the liquid observed, or the temperature may be raised from ambient so that crystallisation from the rubber-like state is observed.

Re-use of plastic waste is obviously most desirable, but is hampered by the problems of identification, sorting and collection. DSC may aid in identification of the constituents of the scrap, as illustrated in Figure 4.21. An example is given in Figure 4.22 of the use of DSC in testing for completeness of curing of epoxy resins. The second scan shows no residual exotherm but indicates the glass-transition temperature for the cured resin.

Figure 4.20
The effect of stabilizers on the isothermal oxidation of polyethylene at 200°C
(B. Cassel, Ind. Res., Aug. 1975, 53-56, with permission.)

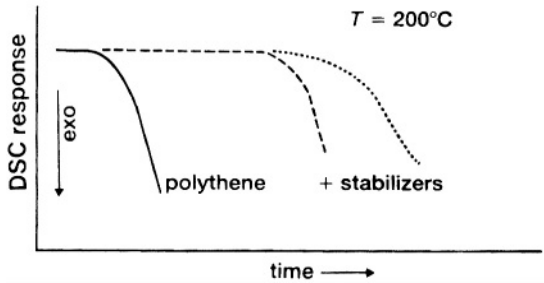

Figure 4.21
DSC used for the identification of the constituents of plastic waste. LPDE=low density polyethylene; HPDE=high density polyethylene; PP=polypropylene; PTFE=poly(tetrafluoroethylene), 'Teflon'.

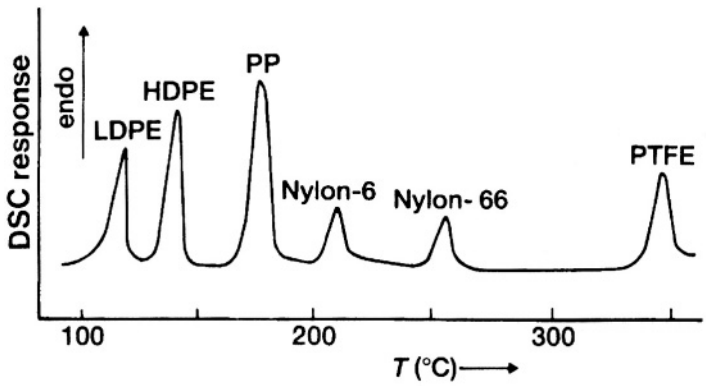

Figure 4.22
The use of DSC in testing for completeness of curing of epoxy resins.

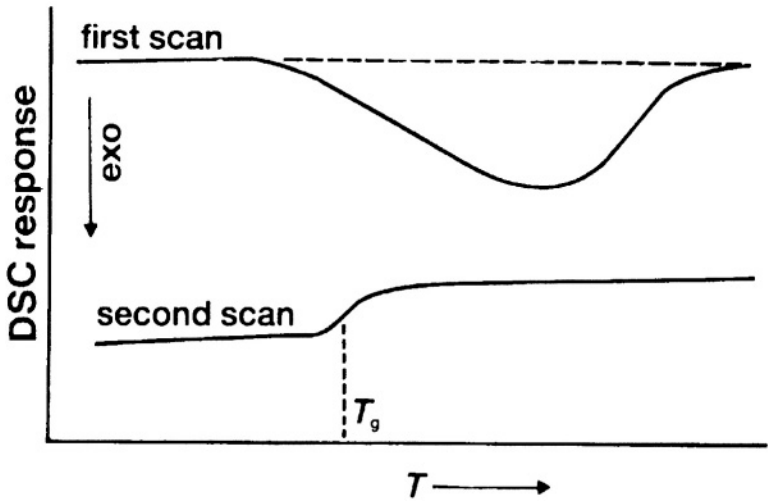

The behaviour of liquid crystals is of practical importance because of the optical phenomena which occur at the transition points, and their proposed role in biological processes. Instead of going directly from solid to liquid at a sharp melting point, liquid crystals form several mesophases between solid and liquid states. The compounds which display this behaviour, generally have large asymmetric molecules with well-separated polar and non-polar regions. In the *smectic* mesophase molecules are aligned and tend to form similarly aligned layers; while in the *cholesteric* mesophase the orientation of the molecular axes shifts in a regular way from layer to layer, and in the *nematic* mesophase molecules are aligned, but layers are not formed (see Figure 4.23). Changes from one mesophase to another can be detected using DSC, and the enthalpies of transition evaluated, as shown for cholesteryl myristate in Figure 4.24.

DSC can also be used to study the liquid → vapour and solid → vapour transitions [39,40] and to measure the enthalpies of vaporisation and of sublimation. In open sample pans these changes are spread out over too wide a temperature interval for an accurate baseline to be determined. The rate of escape of vapour is reduced by partial sealing of the pan. This sharpens up the trace as shown in Figure 4.25.

Figure 4.23
Liquid crystal phases. (Based on W.J. Moore, "Physical Chemistry", 4th Edn, 1972, with the permission of Prentice-Hall, Inc., Englewood Cliffs, New Jersey.)

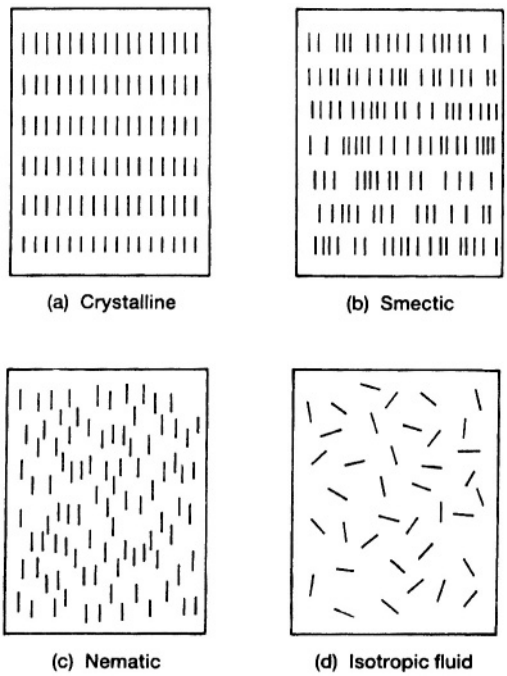

Figure 4.24
DSC curve of a liquid crystal (cholesteryl myristate). (W.P. Brennan and A.P. Gray, Perkin-Elmer Thermal Analysis Application Study, No.13, April 1974, with permission.)

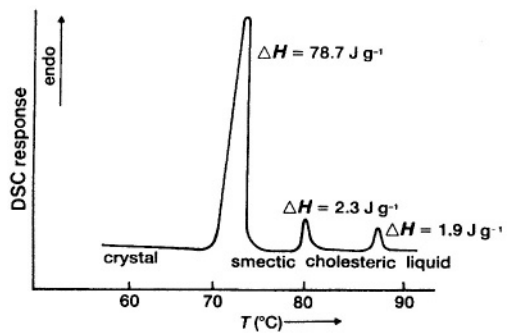

Figure 4.25
DSC curves for water [39,40]. (From Perkin-Elmer Thermal Analysis Newsletter, No.7, 1967, with permission.)

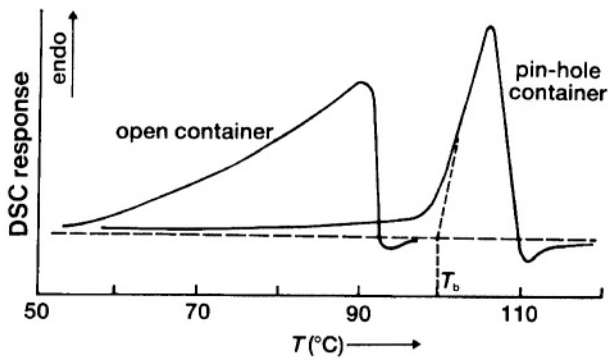

Structural changes in fats and waxes also show up clearly, making the technique (with low temperature attachments) ideal for food chemistry (see Figure 4.26).

Figure 4.26
Butter and margarine - you can tell the difference!

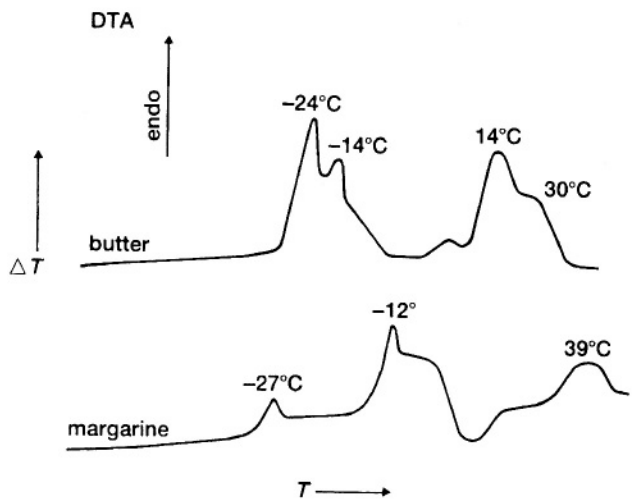

4.11 Automation

Robotic systems for handling several samples without operator intervention are available. The Perkin-Elmer accessory enables 48 samples to be run consecutively on their DSC. The system, shown in Figure 4.27, has a removable sample carousel and a pneumatically controlled sampling arm. The arm, under computer control, automatically selects any desired sample from the carousel, places it in the DSC sample holder and closes the cover. The sample is then subjected to programmed treatment as desired. On completion of this treatment, the sample is removed from the DSC and replaced in the carousel. The sequence in which the samples are handled and their individual treatments can be programmed and the data obtained are stored. The system is obviously at its most efficient when used for quality control with one procedure applied to many similar samples.

Figure 4.27
Perkin-Elmer DSC Robotic System. (With permission.)

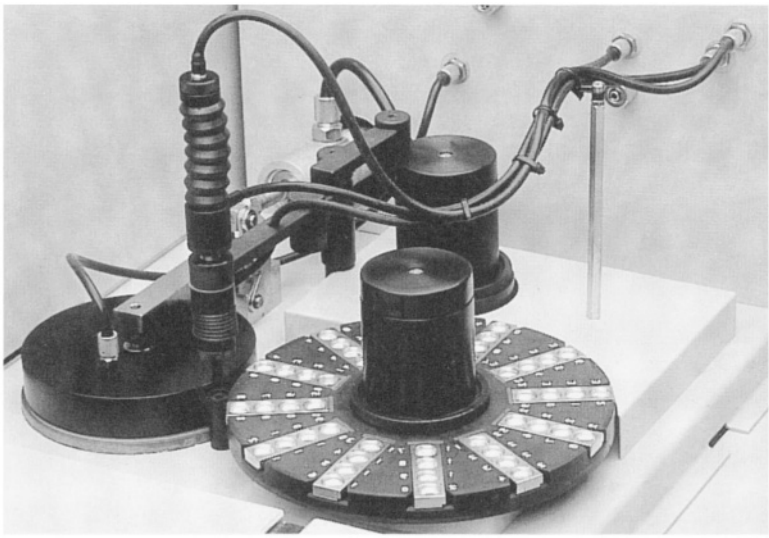

References

1. R.C. Mackenzie, (Ed.), "Differential Thermal Analysis", Vols 1 and 2, Academic Press, London, 1969.
2. P.J. Haines, M. Reading and F.W. Wilburn, “Handbook of Thermal Analysis and Calorimetry”, Vol.1, (Ed. M.E. Brown), Elsevier, Amsterdam, 1998, Ch.5.
3. J. Sestak, V. Satava and W.W. Wendlandt, Thermochim. Acta, 7 (1973) 372.
4. J.L. McNaughton and C.T. Mortimer, "Differential Scanning Calorimetry", Perkin-Elmer Order No.L-604 (Reprinted from IRS, Phys. Chem. Ser.2, Vol.10, Butterworths, 1975).
5. R.L. Fyans, W.P. Brennan and C.M. Earnest, Thermochim. Acta, 92 (1985) 385.
6. P.J. Haines and F.W. Wilburn, “Thermal Methods of Analysis”, (Ed. P.J. Haines), Blackie Academic & Professional, London, 1995, Ch.3.
7. V.J. Griffin and P.G. Laye, “Thermal Analysis - Techniques and Applications”, (Eds E.L. Charsley and S.B. Warrington), Royal Society of Chemistry, Cambridge, 1992, p.17-30.
8. G. Höhne, W. Hemminger and H.-J. Flammersheim, “Differential Scanning Calorimetry”, Springer-Verlag, Berlin, 1996.
9. S.C. Mraw, Rev. Sci. Inst., 53 (1982) 228.
10. Y. Saito, K. Saito and T. Atake, Thermochim. Acta, 99 (1986) 299.
11. J.D. Menczel and L. Judovits (Eds), J. Thermal Anal., (Special Issue), 54 (1998) 409-704.
12. M. Reading, D. Elliott and V. Hill, Proc. 21st NATAS (1992) 145; J. Thermal Anal., 40 (1993) 949; P. S. Gill, S. R. Sauerbrunn and M. Reading, J. Thermal Anal., 40 (1993) 931.
13. M. Reading, Trends Polym. Sci., (1993) 248; M. Reading, A. Luget and R. Wilson, Thermochim. Acta. 238 (1994) 295; M. Reading, Thermochim. Acta, 292 (1997) 979; J. Thermal Anal., 54 (1998) 411.
14. J.E.K Schawe, Thermochim. Acta, 260 (1995) 1; 304/305 (1997) 111; J.E.K Schawe and W. Winter, Thermochim. Acta, 298 (1997) 9.
15. Y. Jin, A. Boller and B. Wunderlich, Proc. 22nd NATAS, (1993) 59; A. Boiler, Y. Jin and B. Wunderlich, J. Thermal Anal., 42 (1994) 277; B. Wunderlich, Y. Jin and A. Boller, Thermochim. Acta, 238 (1994) 277; B. Wunderlich, J. Thermal Anal.,48 (1997) 207.
16. M. Song, A. Hammiche, H.M. Pollock, D.J. Hourston and M. Reading, Polymer, 36 (1995) 3313; 37 (1996) 243; D.J. Hourston, M. Song, H.M. Pollock and A. Hammiche, Proc. 24th NATAS, (1995) 109; K.J. Jones, I. Kinshott, M. Reading, A.A. Lacey, C. Nikolopolous and H.M. Pollock, Thermochim. Acta, 304/305(1997) 187.
17. B. Wunderlich, “Thermal Analysis”, Academic Press, San Diego, 1990, p. 101-103.
18. M.J. Richardson and E.L. Charsley, “Handbook of Thermal Analysis and Calorimetry”, Vol.1, (Ed. M.E. Brown), Elsevier, Amsterdam, 1998, Ch.13.
19. H.K. Cammenga, W. Eysel, E. Gmelin, W. Hemminger, G.W.H. Höhne and S.M. Sarge, Thermochim. Acta, 219 (1993) 333.
20. H. Suzuki and B. Wunderlich, J. Thermal Anal., 29 (1984) 1369.

21. W.P. Brennan, B. Miller and J.C. Whitwell, Ind. Eng. Fundam., 9 (1969) 314.
22. J. Chiu and P.G. Fair, Thermochim. Acta, 34 (1979) 267.
23. A.K. Sircar and J.L. Wells, Rubber Chem. Technol., 55 (1982) 191.
24. W.W. Hillstrom, Thermal Conductivity, 16 (1979) 483.
25. G. Hakvoort and L.L. van Reijen, Thermochim. Acta, 93 (1985) 371; 85 (1985) 319.
26. T. Boddington, P.G. Laye and J. Tipping, Comb. Flame, 50 (1983) 139.
27. M.J. Visser and W.H. Wallace, DuPont Thermogram, 3 (2) (1966) 9.
28. T. Daniels, "Thermal Analysis", Kogan Page, London, 1973, p.119.
29. J.L. McNaughton and C.T. Mortimer, "Differential Scanning Calorimetry", Perkin-Elmer Order No.L-604 (Reprinted from IRS, Phys. Chem. Ser.2, Vol.10, Butterworths, 1975), p.28.
30. M.I. Pope and M.D. Judd, "Differential Thermal Analysis", Heyden, London, 1980, p.53.
31. R.L. Fyans, Perkin Elmer Instrument News, 21 (1) (1970) 1.
32. W. Eysel, Proc. 3rd ICTA,(Ed. H.G. Wiedemann), Birkhauser Verlag, Basel, Vol.2 (1971) 179.
33. W. Gutt and A.J. Majumdar, "Differential Thermal Analysis", (Ed. R.C. Mackenzie), Academic, London, 1972, Vol.2, p.79.
34. J. Sestak, "Thermophysical Properties of Solids", Comprehensive Analytical Chemistry, Vol.XIID, (Ed. G. Svehla), Elsevier, Amsterdam, 1984, p. 109.
35. S. Surinach, M.D. Baro and F. Tejerina, Proc. 6th ICTA, (Ed. H.G. Wiedemann), Birkhauser Verlag, Basel, Vol.1 (1980) p. 155.
36. Z. Boncheva-Mladenova and V. Vassilev, Proc. 6th ICTA, (Ed. W. Hemminger), Birkhauser Verlag, Basel, Vol.2 (1980) p.99.
37. J.P. Redfern, "Differential Thermal Analysis", (Ed. R.C. Mackenzie), Academic, London 1972, Vol.2, p.119.
38. E.A. Turi (Ed.), “Thermal Characterization of Polymeric Materials”, 2nd Edn, Vols 1 and 2, Academic Press, San Diego, 1997.
39. T. Daniels, "Thermal Analysis", Kogan Page, London, 1973, p. 132.
40. J.L. McNaughton and C.T. Mortimer, "Differential Scanning Calorimetry", Perkin-Elmer Order No.L-604 (Reprinted from IRS, Phys. Chem. Ser.2, Vol. 10, Butterworths, 1975), p. 19.

THERMOPTOMETRY

5.1 Introduction

Thermoptometry (also referred to as thermo-optical analysis, TOA) is a group of techniques in which optical properties of a sample are measured as a function of temperature [1]. Under this heading, the major technique is *thermomicroscopy,* i.e. direct observation of the sample. Other techniques involve measurement of total light reflected or transmitted (thermophotometry), light of specific wavelength(s) (thermospectrometry), refractive index (thermorefractometry), or emitted light (thermoluminescence). Wiedemann and Felder-Casagrande [2] have recently reviewed these techniques and also dealt with their historical development, including the important role of W.J. McCrone [3] in the development and popularisation of thermomicroscopy. Wendlandt's book [4] contains an excellent chapter and there is also useful information in references [5,6]. Gallagher's chapter in reference [7] contains much recent information.

To the above techniques must now be added the more recent developments of scanning tunnelling microscopy and atomic force microscopy that have led to the new field of Micro Thermal Analysis described in section 5.10 below.

Table 5.1
Special Techniques derived from Thermoptometry

Special Techniques (Methods)	Property or conditions	Abbreviations
Thermomicroscopy (Thermomicroscopic Analysis)	visual appearance	
Thermoluminescence Measurement (Thermoluminescence Analysis)	emitted radiation	TLM
Thermophotometry (Thermophotometric Analysis)	intensity of total reflected or transmitted radiation	
Thermospectrophotometry (Thermospectrophotometric Analysis)	reflected or transmitted radiation of specific wavelength(s)	

5.2 Thermomicroscopy

It is interesting that the most obvious property of a material, i.e. its outward appearance, is often not examined or monitored during the heating process and yet can provide so much reliable first-hand evidence of the processes occurring. Other thermal analysis techniques give results which have to be associated by inference with thermal events and some processes such as sintering, decrepitation and creeping and foaming of melts are only really detectable by direct observation.

The apparatus required for thermomicroscopy [2] (a schematic diagram is given in Figure 5.1(a)) consists of a microscope with a hot and/or cold stage, a sample holder, gaseous atmosphere control (including, perhaps, vacuum pumps), light sources and a system for recording and processing visual observations, as well as the temperature of the sample.

The main requirement for the microscope is that suitable heat-resistant objective lenses of adequate focal length are available. Controlled temperature stages for microscopes are readily available [2,7] and can cover the temperature range from -180°C up to 3000°C, allowing for study of a wide range of problems, especially phase studies. Some stages are designed to allow combination with other measurement techniques such as DSC or TG (see below). Stages have to be as thin as possible to enable them to fit between the microscope's objective lens and the microscope table. Allowance may have to be made for heating by the illuminating source, or heat filters may be necessary. Movement of the sample holder is essential so that different regions of the sample can be examined and so that blocking of the view of the sample by some sublimation and condensation on the cover plate can be temporarily overcome. Sapphire glass sample pans are recommended [2]. Standard photographic equipment or video cameras can be used for recording observations. Many software packages are available for different types of image analysis.

Sawyer and Grubb [8] have reviewed the use of themomicroscopy in the study of polymers, where overlapping transitions, such as melting and degradation or crystallization and melting, can lead to ambiguities of interpretation. Kuhnert-Brandstatter's book [9] is a classic on the thermomicroscopy of pharmaceuticals.

5.3 Thermophotometry

In thermophotometry, provision is made for measurement of the intensity of the light reflected or transmitted by the sample (a schematic diagram is given in Figure 5.1(b)). If samples are viewed in transmitted light using crossed polars, the only light transmitted is that arising from rotation of the plane of polarization of the light, caused by changes in the crystalline structure of the sample. Melting or the formation of an isotropic structure results in complete extinction of the light.

Figure 5.1
Schematic diagrams of (a) a thermomicroscopy system, and (b) a thermophotometry system (based on reference [2]).

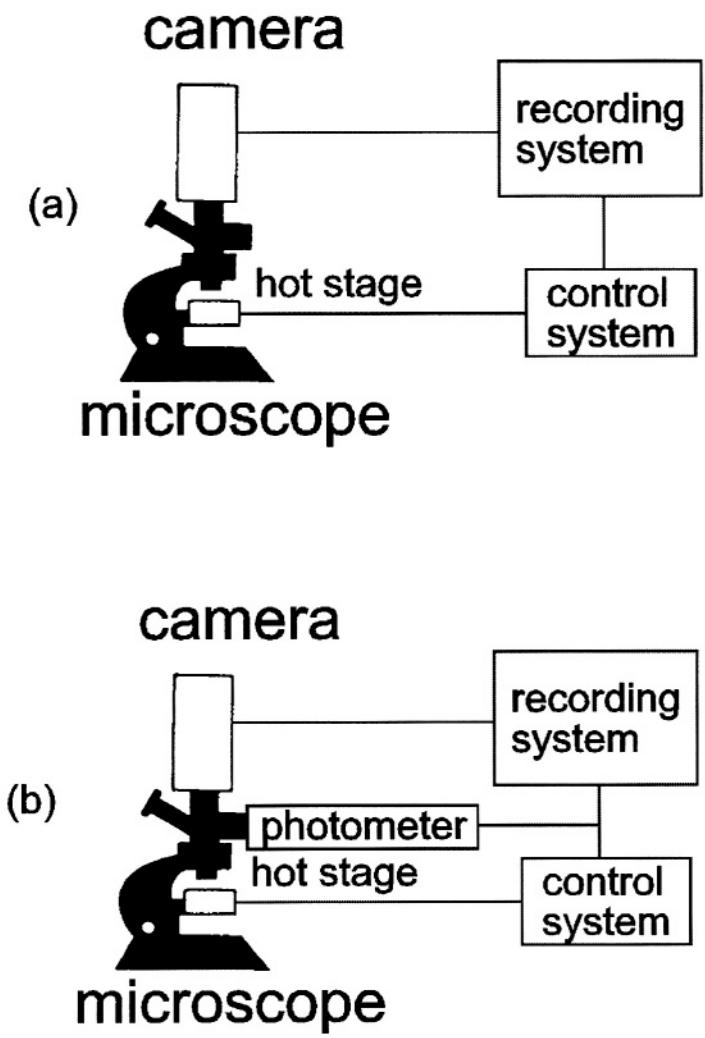

5.4 Thermoluminescence

The technique involving measurement of light actually being emitted by the sample is known as thermoluminescence, TL [1,4]. TL arises from the annealing of defects in the solid sample as the temperature is raised. The defects are present in the sample on account of its previous thermal history, or through irradiation of the sample. TL has been used in radiation dosimetry, archaeological dating, geological activity and evaluation of catalysts, etc.. A simple model of the TL process, descriptions of apparatus and discussion of applications are given in reference [4]. One version of a system used for TL is illustrated in Figure 5.2 [10].

Figure 5.2
Apparatus for thermoluminesence, TL [10]. (With the permission of John Wiley & Sons, Chichester.)

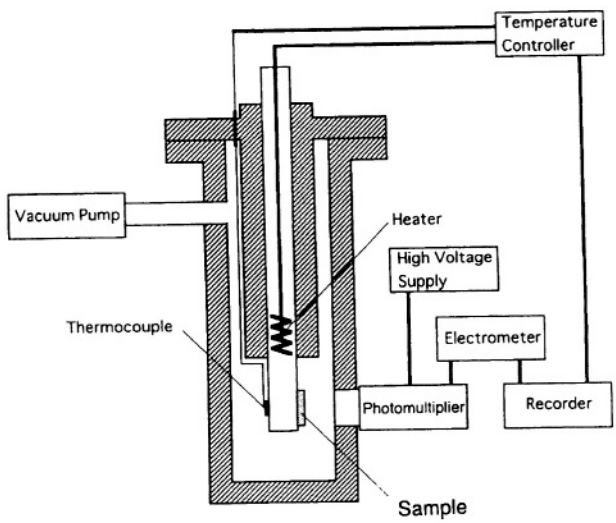

Nuzzio [11] has described the modification of a DuPont 990 Thermal Analyzer for TL measurements. The light-measuring system included filters to absorb heat and to minimize the black-body radiation encountered at temperatures above 400°C. A reference light source was used for calibration. TL measurements could be made under isothermal or increasing temperature conditions. Arrangements for measurements under reduced pressures are also described.

Manche and Carroll [12] modified a Perkin-Elmer DSC-1B for simultaneous TL and DSC, using a matched pair of optical fibres mounted directly above each calorimeter cup.

An example of the use of TL in the authentication and characterization of medieval pottery sherds is provided by the study of Miliani et al. [13] with their TL results illustrated in Figure 5.3.

Figure 5.3
Thermoluminesence curves from medieval pottery sherds of different ages [13]. Samples A and C are about 200 years older and younger than B, respectively. Curves labelled 1, 2 and 3 are instrumental background, natural dose and artificial dose, respectively. (With the permission of Thermochimica Acta.)

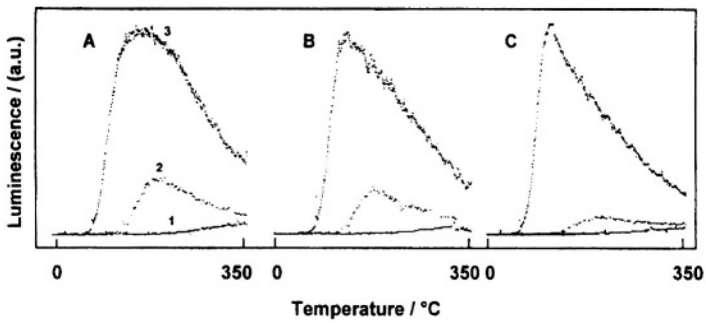

Some polymers when heated in air or oxygen exhibit a low-level light emission that is called oxyluminescence (or chemiluminescence) [4]. The intensity of the light is proportional to the concentration of oxygen in contact with the polymer surface and the presence of stabilizers decreases the intensity. Such measurements can thus provide valuable insights into the oxidative degradation of polymers (and many other organic compounds). Vigorous redox reactions between oxidizing groups and reducing ligands in coordination compounds may also be accompanied by light emission [4,14,15].

5.5 Combination of Thermomicroscopy with DSC (or DTA)

If visual examination can be combined with a quantitative measurement such as DSC or DTA, even more meaningful results can be obtained. The Mettler system [2] (see Figure 5.4) has a heat-flux DSC sensor built from thin-film thermopiles deposited on a special glass disc. The sample is placed in a sapphire crucible and a similar but empty crucible is used as a reference. Sample illumination is by transmitted (normal or polarized) light. The temperature range is from room temperature to 300°C.

Sommer and Jochens [16] have described a micro-thermal analysis system based on the use of a thermocouple as both specimen holder and heating source. The system is easily and cheaply constructed and is particularly useful in phase studies of non-metallic samples.

Figure 5.4
Schematic diagram of a Mettler simultaneous thermomicroscopy-DSC system (based on reference [2]).

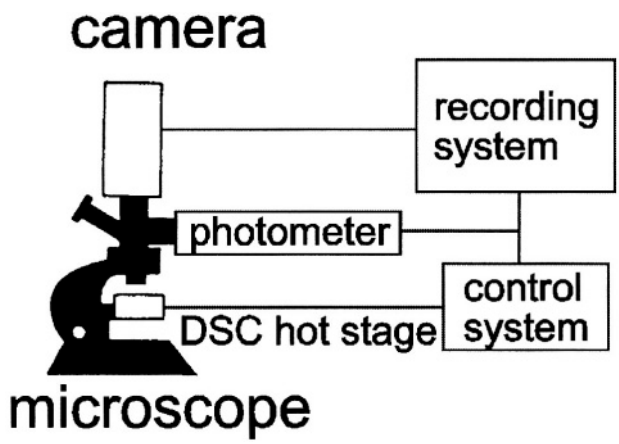

Charsley et al. [17-19] have made excellent use of hot-stage microscopy for determining the ignition temperatures of pyrotechnic compositions. The sample was contained between two microscope cover glasses which rested on a heating block, within an atmosphere-controlled chamber. The block contained a sapphire window for light transmission, and a platinum resistance thermometer for measurement of the temperature and control of the heating or cooling programme. Provision for cooling with liquid nitrogen gave an overall temperature range of -180°C to 600°C. The intensity of the transmitted light was measured using a silicon photodetector.

Haines and Skinner [20] modified a DSC to carry out simultaneous measurements of the intensity of light reflected from the sample. Changes in the surface of the sample may not be accompanied by measurable enthalpy changes, but may show up clearly through changes in reflectance. A binocular microscope was used so that one eyepiece could be used for photographing the actual appearance of the sample, while the photodetector was used on the other eyepiece. The sample was in either an open DSC pan, or else a mica window was crimped into the pan. Changes in the intensity of the reflected light are cumulative so that the curves recorded are related to DSC curves as integral to derivative.

5.6 Combination of Thermomicroscopy with TG

Figure 5.5 is a schematic diagram of a Mettler simultaneous thermomicroscopy-TG system [2], The sample holder for microscopy is attached to a balance by an aluminium oxide capillary. Otherwise the equipment is closely similar to that in Figures 5.1 and 5.4.

Figure 5.5
Schematic diagram of a Mettler simultaneous thermomicroscopy-TG system (based on reference [2]).

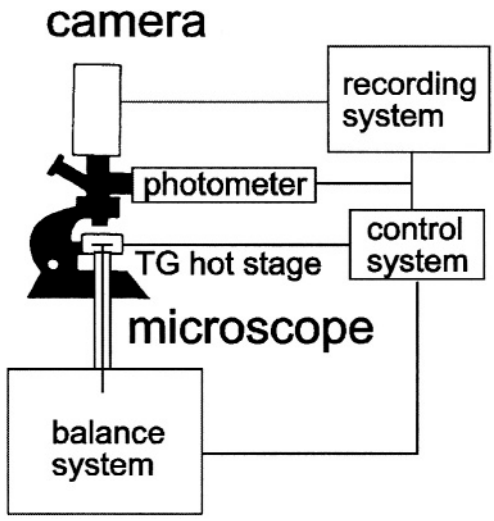

5.7 Other techniques combined with Thermomicroscopy

Gallagher [7] has described some additional combinations of techniques. These include microscopy and X-ray diffraction [21], and DSC combined with an FTIR microscope [22].

5.8 Some applications of the techniques of Thermoptometry

The review by Wiedemann and Felder-Casagrande [2] contains some magnificent examples of the power of microscopic techniques in investigating a wide variety of problems. The micrographs produced are often works of art in their own right Problems tackled so successfully by Wiedemann and his coworkers include the dehydration and hydration of gypsum, $CaSO_4.2H_2O$ to form the industrially important hemihydrate, $CaSO_4.½H_2O$, known as Plaster of Paris [23]; the formation of nuclei of graphite on the surfaces of natural diamonds [24]; the oxidation of graphite flakes [25]; phase transitions in the KNO_3 /$NaNO_3$ series of solid solutions [26]; and polymorphism [27], glass transitions [28] and crystallization in a variety of organic compounds, including explosives [29], Pharmaceuticals [27] and liquid crystals [30].

An example of the results obtained by Haines and Skinner [20] on heating KNO_3 is shown in Figure 5.6. The phase transition from orthorhombic, phase II, to trigonal, phase I, at 128°C and melting at 335°C show up clearly. The phase transition at 128°C for KNO_3 did

Figure 5.6
Thermophotometry curves for potassium nitrate [20]: (a) in transmitted light, (b) in reflected light. (With the permission of Elsevier, Amsterdam.)

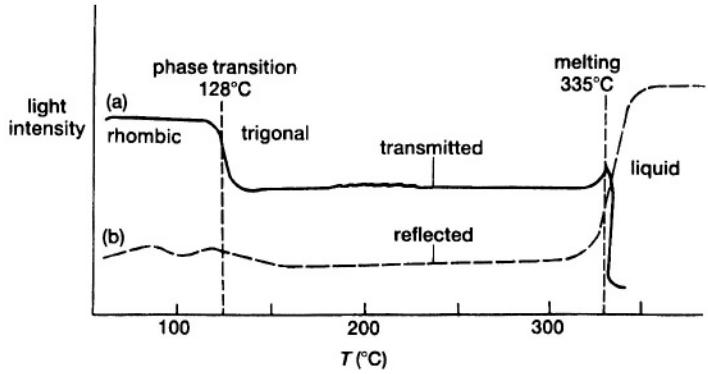

Matzakos and Zygourakis [31] coupled microscopy with TG to obtain a record on video of the pyrolysis of coal at high heating rates (50 K s^{-1}).

Manche and Carroll [12] tested their TL system using mixtures of LiF and KNO_3. LiF is a well-known and extensively-studied thermoluminescent material and KNO_3 was used as the temperature and calorimetric standard and does not normally exhibit thermoluminescence. Ground mixtures were pressed into discs and the discs were irradiated with X-rays. The sample discs, with a preheated disc of LiF as reference, were heated in the modified DSC. The results obtained are shown in Figure 5.7. Areas under the glow curves and the DSC endotherms were measured and were shown to be linear functions of the mass fraction of the individual salts.

5.9 Electron Microscopy

Many of the kinetic studies of mechanisms of decomposition of solids invoke processes of formation and growth of product nuclei. These speculations can often be confirmed or refuted using thermomicroscopy. Use of scanning electron microscopy (SEM), rather than optical microscopy, has the advantages of greater magnification and much increased depth of field as well as providing the possibility of energy-dispersive X-ray analysis of the sample. There are, however, additional problems in the necessity for operating under vacuum and the effect of the electron beam on the sample. Recent developments [7] have led to instruments called environmental SEMs which can operate at pressures as high as 70 torr and have hot stages capable of operating at 1000°C and above.

Figure 5.7
Thermoluminescence (TL) and DSC curves for mixtures of LiF and KNO_3 [12]. (With the permission of the American Chemical Society.)

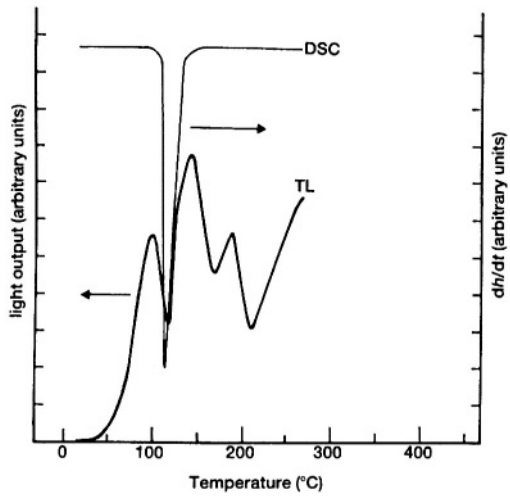

5.10 Micro Thermal Analysis

The development of scanning tunnelling microscopy (STM) [32] and atomic force microscopy (AFM) [33] has made it possible to scan the topography of a solid surface at resolutions down to the scale of individual atoms. Both STM and AFM use extremely fine probe tips which are moved across the sample in a regular scanning pattern. Piezoelectic sensors are used to determine the three-dimensional position of the probe tip. The elevation (z-direction) of the tip is related to the actual features of the surface over which it is moved in the x and y directions. In AFM a very small force is maintained to keep the probe tip in contact with the surface as it traverses, without digging into it. In STM the surface has to be conducting and a small constant tunnelling current is maintained between the probe and the surface. The probe then rides at less than 1 nm above the surface. The tunnelling current depends upon both the surface topography and the local electronic states on the surface. Examination of the same surface using both techniques can reveal any relationships between topographical features and electronic inhomogeneities.

In MicroThermal Analysis (μTA^{TM}) [34-40] thermal analysis is performed on specimens, or regions of specimens, as small as 2×2 μm. The sensor is a very fine, pointed platinum wire mounted on the tip of an atomic force microscope probe (see Figures 5.8 and 5.9). The sample, or sample region, is heated at a linear rate by passing a current through the wire and the resistance of the wire is used simultaneously to measure the sample temperature. Because of the small thermal mass of the sensor, heating rates up to 25°C/s can be used. The imaging capabilities of the AFM are used to map the surface area of interest (see, for

example, Figure 5.10) and to select regions for subsequent thermal analysis. The use of a controlled temperature stage [35] allows the entire sample to be heated or cooled and a thermal probe is then not necessary. Standard AFM contact or non-contact probes can then be used to produce very high resolution images.

Figure 5.8
The TA Instruments 2990 Micro-Thermal Analyzer (μTA) (with permission).

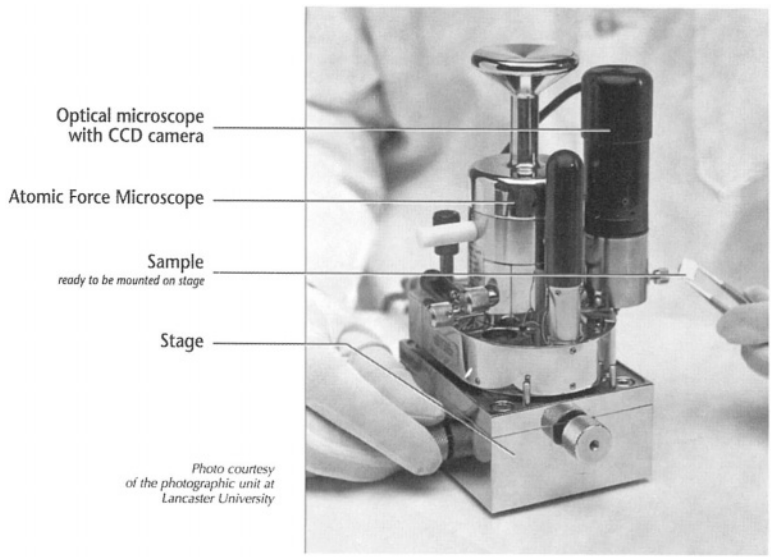

Figure 5.9
Details of a probe for the TA Instruments 2990 Micro-Thermal Analyzer (μTA) (with permission).

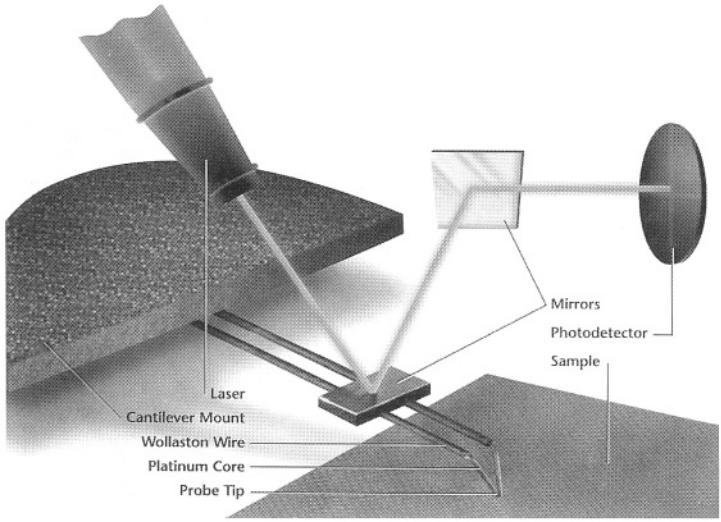

Figure 5.10
3-D thermal conductivity image of a polybutadiene/polyvinyl chloride blend (with permission of TA instruments).

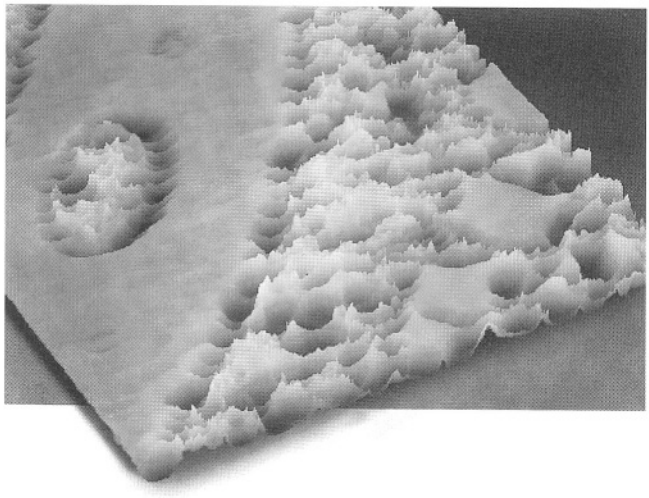

Various TA methods are possible. Micro differential thermal analysis involves comparison of the temperature difference of, or the difference in power supplied to, the sample with respect to a reference. If the probe is loaded with a small force, so that it can penetrate into a melted specimen, micro thermomechanical analysis is possible (see Chapter 6). The use of sinusoidal temperature programmes has led to some modulated μTA techniques. The μTA configuration can be used to pyrolyse selected areas of the sample by rapidly heating the probe to 600-800°C. The evolved gases can be absorbed in a suitable sampling tube placed near to the probe and analysed later by GC-MS [36].

Micro thermal analysis has been mainly used qualitatively for identification of the material being examined, e.g. multi-layer films [34], pharmaceuticals [37] and polymer blends [38].

Temperature calibration [41] is more difficult than in the macro TA versions because the calibrant comes into direct contact with the platinum sensor, so that metals like indium, tin, and zinc are not suitable, and organic compounds and polymers have been used. The sensor is easily cleaned after the experiment by heating in air. Powdered organic materials need to be formed into larger crystals by recrystallization from the melt. The recommended [41] calibrants and their melting temperatures are: biphenyl (69.3°C); benzil (94.5 °C); benzoic acid (122.4 °C); diphenylacetic acid (147.3 °C); anisic acid (183.3 °C), and 2-chloroanthraquinone (209.6 °C). Suitable crystals with smooth flat surfaces can be fixed to the μTA sample mounts using double-sided tape. A two-point calibration procedure is recommended [41].

The μ DTA response for polymers is different to that for pure organic compounds because the organic melt tend to shrink away from the hot probe and lose contact, but the less-mobile polymer materials remain in contact. For polymer studies, calibration using Nylon 6, Nylon 6,6 or polyethylene terephthalate is recommended [41]. Use of polymer films simplifies the calibration procedure.

The precision of temperature measurement depends on the heating rate. The higher heating rates (600 to 1500°C/min) gave better precision than lower rates (120 to 480°C/min) [41].

By controlling the temperature of the tip of the μTA probe [42], the heat flow from the tip to the surface of the sample can be used to map the thermal transport properties of the surface. Such measurements have important applications in microelectronics, cellular biology, polymer science, etc. Calibration is carried out using hard materials of known thermal conductivity [42].

References

1. W. Hemminger and S.M. Sarge, "Handbook of Thermal Analysis and Calorimetry", Vol.1, (Ed. M.E. Brown), Elsevier, Amsterdam, 1998, Ch.1.
2. H.G. Wiedemann and S. Felder-Casagrande, "Handbook of Thermal Analysis and Calorimetry", Vol.1, (Ed. M.E. Brown), Elsevier, Amsterdam, 1998, Ch.10.
3. W.C. McCrone, "Fusion Methods in Chemical Microscopy", Wiley, New York, 1957; Proc. 1st ESTA, (Ed. D. Dollimore), Heyden, London, 1976, p.63; J.H. Kilbourn and W.C. McCrone, Microscope, 33 (1985) 73; W.C. McCrone, J.H. Andreen and S.-M. Tsang, Microscope, 41 (1993) 161.
4. W.W. Wendlandt, "Thermal analysis", Wiley, New York, 3rd Edn, 1986, Ch.9.

5. E.L Charsley, in "Thermal Analysis - Techniques and Applications", (Eds E.L Charsley and S.B. Warrington), Royal Society of Chemistry, Cambridge, 1992, p.68.
6. P.J. Haines, "Thermal Methods of Analysis", Blackie, Glasgow, 1995, p. 186.
7. P.K. Gallagher, in "Thermal Characterization of Polymeric Materials", (Ed. E.A. Turi), Academic Press, New York, 2nd Edn, 1997, Ch.1.
8. L.C. Sawyer and D.T. Grubb, "Polymer Microscopy", Chapman and Hall, New York, 1987.
9. M. Kuhnert-Brandstatter, "Thermomicroscopy in the Analysis of Pharmaceuticals", Pergamon, Oxford, 1971.
10. T. Hatakeyama and Zhenhai Liu, "Handbook of Thermal Analysis", Wiley, Chichester, 1998, p.30.
11. D.B. Nuzzio, Thermochim. Acta, 52 (1982) 245.
12. E.P. Manche and B. Carroll, Anal. Chem., 54 (1982) 1236.
13. C. Miliani, N. Forini, A. Morresi, A. Romani and S. Spigarelli, Thermochim. Acta, 321 (1998) 191.
14. W.W. Wendlandt, "The State-of-the-Art of Thermal Analysis", NBS Spec. Tech. Publ. S80, (Eds O.Menis, H.L. Rook and P.D. Garn), 1980, p.219.
15. W.W. Wendlandt, Thermochim. Acta, 35 (1980) 247; 39 (1980) 313.
16. G. Sommer and P.R. Jochens, Minerals Sci. Eng., 3 (1971) 3.
17. E.L. Charsley, A.C.F. Kamp and J.A. Rumsey, Thermochim. Acta, 92 (1985) 285.
18. E.L. Charsley and A.C.F. Kamp, Proc. 3rd ICTA, (Ed. H.G. Wiedemann), Birkhauser, Basel, 1971, Vol.1, p.499.
19. E.L. Charsley and M.R. Ottaway, Proc. 1st ESTA, (Ed. D. Dollimore), Heyden, London, 1976, p.444.
20. P.J. Haines and G.A. Skinner, Thermochim. Acta, 59 (1982) 343.
21. M. Epple and H.K. Cammenga, Ber. Bunsenges. Phys. Chem., 96 (1992) 1774.
22. S. Lin, C.M. Liao and R.C. Liang, Polym. J. (Tokyo), 27 (1995) 201.
23. H.G. Wiedemann and M. Rossler, Thermochim. Acta, 95 (1985) 145.
24. H.G. Wiedemann and G. Bayer, Z. Anal. Chem., 276 (1975) 21.
25. H.G. Wiedemann and A. Reller, Thermochim. Acta, 271 (1996) 163.
26. H.G. Wiedemann and G. Bayer, J. Thermal Anal., 30 (1985) 1273.
27. H.G. Wiedemann, J. Thermal Anal., 40 (1993) 1031.
28. H.G. Wiedemann, G. Widmann and G. Bayer, Assignment of the Glass Transition, ASTM STP 1249, (Ed. R.J. Seyler), American Society for Testing and Materials, Philadelphia, 1994.
29. H.G. Wiedemann and G. Bayer, Thermochim. Acta, 85 (1985) 271.
30. J. Cheng, Y. Jin, G. Liang, B. Wunderlich and H.G. Wiedemann, Mol. Cryst. Liq. Cryst., 213 (1992) 237.
31. A.N. Matzakos and K. Zygourakis, Rev. Sci. Instr., 64 (1993) 1541.
32. G. Binnig and H. Rohrer, Helv. Phys. Acta, 55 (1982) 726.
33. G. Binnig,, C.F. Quate and C. Gerber, Phys. Rev. Lett., 56 (1986) 930.
34. D.M. Price, M. Reading, A. Caswell, A. Hammiche and H.M. Pollock, Microscopy Anal., 65 (1998) 17.
35. M. Reading, D.M. Price, H.M. Pollock and A. Hammiche, Amer. Lab., 30(1) (1999) 13.

36. A. Hammiche, M. Reading, H.M. Pollock and D.J. Hourston, Rev. Sci. Instr., 67 (1996) 4268.
37. D.Q.M. Craig, R.G. Royall, M. Reading, D.M. Price, T.J. Lever and J. Furry, Proc. 26th NATAS, (1998) 610.
38. M. Reading, D.L. Hourston, M. Song, H.M. Pollock and A. Hammiche, Amer. Lab., 30(1) (1998) 13.
39. T.J. Lever and D.M. Price, Amer. Lab., 30(16) (1998) 15.
40. D.M. Price, M. Reading and T.J. Lever, J. Thermal Anal. Calorim., 56 (1999) 673.
41. R.L. Blaine, C.G. Slough and D.M. Price, Proc. 28th NATAS, (2000) 883.
42. D.M. Price, M. Reading, A. Hammiche and H.M. Pollock, Proc. 28th NATAS, (2000) 586.

THERMOMECHANOMETRY

6.1 Definitions and scope

As described in Chapter 1, several Special Techniques have been developed from the Primary Technique known as *Thermomechanometry* [1]. These are listed and defined in Table 6.1. No standard accepted nomenclature exists at present so the various alternatives in use are given.

Table 6.1

SPECIAL TECHNIQUES DERIVED FROM THERMOMECHANOMETRY

Special Techniques (Methods)	Property or conditions	Abbreviations
Thermodilatometry (Thermodilatometric Analysis)	dimension (negligible force)	TD
Static Force Thermomechanometry (Static Force Thermomechanical Analysis)	dimension (static force)	sf-TM and sf-TMA
Dynamic Force Thermomechanometry (Dynamic Force Thermomechanical Analysis)	dimension (dynamic force)	df-TM and df-TMA
Modulated Force Thermomechanometry (Modulated Force Thermomechanical Analysis)	dimension (modulated force)	mf-TM and mf-TMA

The more familiar names for these techniques include Thermomechanical Analysis (TMA) and Dynamic Mechanical Analysis (DMA).

6.2 Thermodilatometry

6.2.1 Principles

Measurement of the thermal expansion of solids and liquids is a classical physical technique known as *dilatometry.* When special emphasis is put on recording such dimensional changes as a function of temperature, during a controlled temperature programme, the technique is labelled *thermodilatometry* [1,2] and is one of the special techniques derived from thermomechanometry. For solids, we can distinguish between linear and volume expansion, and instruments for measuring the length of a solid sample as a function of temperature are the most common.

Most solids expand on heating. Exceptions include vitreous silica and ZnS at low temperatures. The change in a linear dimension, L, with T is given by:

$$L_2 = L_1 (1 + \int_{T1}^{T2} \alpha \, dT$$

where L_1 is the length at T_1, and L_2 the length at T_2, and α is the coefficient of linear expansion. Over a small temperature interval, ΔT, is approximately constant for many materials, so the *dilation*:

$$L_2 - L_1 = \Delta L = L_1 \, \alpha \, \Delta T \qquad \text{or} \qquad \Delta L/L_1 = \alpha \, \Delta T$$

The value of α is related to the structure and type of bonding in the solid. In general, strong bonding results in low values of α, so the order of expansion coefficients is usually: covalent and ionic materials < metals < molecularly-bonded materials. In some substances, α may vary with direction (anisotropic behaviour). Amongst the materials that may show anisotropy [2] are single crystals, drawn fibres, drawn or blown films, fibre composites, liquid crystals and some metallic glasses. In some anisotropic solids, for example, calcite, the coefficient of expansion in direction of one of the principal axes may be negative.

Measurements of thermal expansion may be classed as either *absolute* or *difference* measurements, as illustrated schematically in Figure 6.1. The pointer and scale are outside the furnace and the movements of the sample and of the reference are transmitted by identical push-rods. Measurements may be made in either the horizontal or vertical position. In horizontal instruments, arrangement has to be made for suitable spring-loading, so that any contraction can be detected. In vertical instruments, the weight of the push-rod and measuring system has to be counterbalanced to avoid compression or deformation of the sample.

Calibration of the system used [2] with a solid of known coefficient of expansion, (aluminium metal, for example) under conditions very similar to those used for the actual sample, is necessary to compensate for the many dimensional changes in the instrument as heating takes place.

Figure 6.1
Thermodilatometry: (a) absolute measurement, (b) difference measurement.

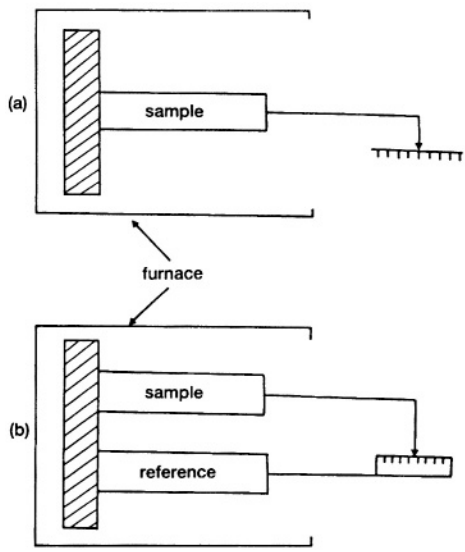

6.2.2 Practical details

Measurement of sample movement obviously has to be more sophisticated than the pointer and scale used in the schematic diagrams. The transducer (Figure 1.1) is usually a linear variable differential transformer (LVDT), the principle of which is illustrated in Figure 6.2. Movement of the core within the coils produces an output with sign dependent upon the direction of the movement, and magnitude giving the movement of the sample. Amplification of the movement is claimed to be as much as 20 000X. Calibration of the LVDT is carried out, initially, using a micrometer screw gauge incorporated in the measuring system.

Safety devices, to prevent damage caused by melting of the sample in the apparatus, are often included. These are activated by rapid sample contractions and power to the furnace is cut off immediately.

Expansion of a standard material can be used as a temperature indicator. Isothermal measurements may be made to study creep or recrystallization processes in the sample (see applications). Changes in volume of liquid samples, contained in a suitable cylinder, can be converted into equivalent linear movement by means of a close-fitting piston attached to a push-rod. A bleed valve on the cylinder ensures that no air is trapped in the liquid.

Figure 6.2
Principle of a linear variable differential transformer (LVDT).

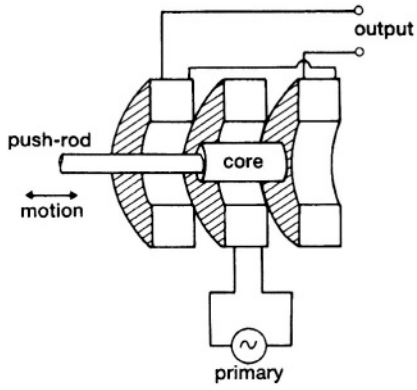

Linseis [3] has described a laser dilatometer based on the principle of a Michelson interferometer. A schematic diagram is given in Figure 6.3. The laser beam is split, after a 90° reflection, into two separate beams. The two beams are directed at reflectors attached to the ends of the sample and reference materials. After total reflection, the beams are recombined and the interference patterns are examined using photodiode detectors and converted to measurements of expansion or shrinkage. These dilation measurements are accurate to one quarter of the wavelength of the laser and involve no mechanical connections with the sample, so very rapid changes of dimension can be examined. The temperature range over which such an optical system can be used is also much greater than for a mechanical system and it is suggested [3] that it will prove useful in examining the expansion coefficients of superconducting materials at liquid helium temperatures.

Karmazsin *et al.* [4] have suggested use of an optoelectronic transducer in place of a LVDT. This has particular advantages for simultaneous thermodilatometric, thermoconductimetric and thermomagnetometric measurements as LVDTs are sensitive to electrical perturbations. A stabilized light source (Figure 6.4) illuminates two photosensitive cells through two rectangular holes of a screen, which is attached to the push-rods of the dilatometer. Movement of the screen alters the relative amount of light received by the two cells. Dimensional variations down to 10^{-8} m could be measured and speed of response was about ten times that of a LVDT. Examples of simultaneous measurements are given [4].

Figure 6.3
Laser dilatometer based on the principle of a Michelson interferometer [3]. (With the permission of John Wiley & Sons, Chichester.)

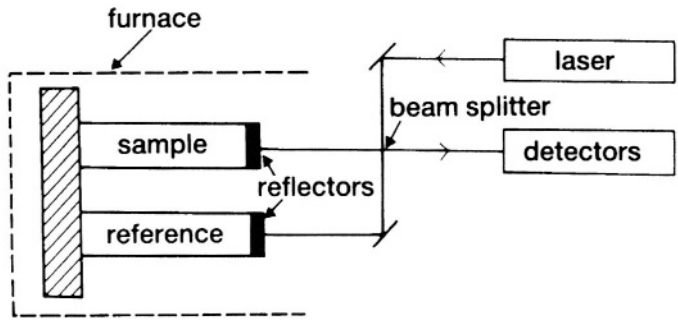

Figure 6.4
Optoelectronic transducer for thermodilatometry [4]. (With the permission of John Wiley & Sons, Chichester.)

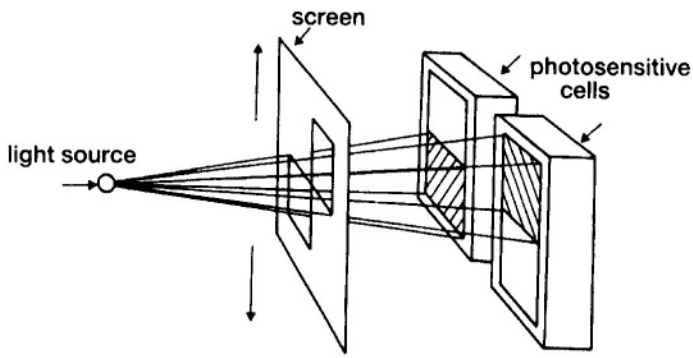

6.2.3 Interpretation of results

Values of the coefficient of expansion, α, may be determined from the slope of a curve of L against T,because:

$$\Delta L/\Delta T = dL/dT = L_1 \alpha$$

Alternatively, the time derivative of the dilation:

$$(dL/dt)(dt/dT) = L_1 \alpha$$

so

$$dL/dt = L_1 \alpha \beta$$

where $\beta = dT/dt$ = the heating rate.

The engineering coefficient of expansion, α', is defined by:

$$\alpha' = (L_T - L_{20})/(L_{20}(T - 20))$$

where L_T and L_{20} are the lengths of the sample at T°C and 20°C, respectively.

Usually it is the discontinuities in the curve of L against T, rather than actual values of α, which are of main interest in thermodilatometry, as these indicate occurrence of thermal events in the sample. These discontinuities are discussed in the applications section below.

6.2.4 Applications of thermodilatometry

A very practical application of TD is in the selection of suitable materials for use as brake-linings [5]. Obviously a low coefficient of expansion, coupled with other qualities such as wear-resistance and a suitable coefficient of friction, is desirable (Figure 6.5).

Wendlandt [6] has used TD to study the change in structure from octahedral to tetrahedral in the cobalt (II) pyridine coordination compound, $Co(py)_2Cl_2$ (Figure 6.6). Another application of TD has been that of Gallagher [7] to the study of the kinetics of sintering of powdered Chromindur alloys (Fe-Cr-Co), used in making high energy magnets. Arrhenius-type plots of $\ln(L/L_o)$ against $1/T$ showed two regions with different activation energies. The values of the activation energies corresponded well with the diffusion energies in the low-temperature face-centred cubic and the high-temperature (>1250°C) body-centred cubic phases.

Figure 6.5
Thermal expansion of brake-lining materials [5]. (With the permission of International Scientific Communications Inc.)

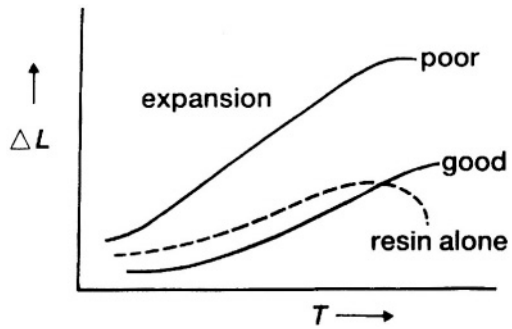

Figure 6.6
Thermodilatometry curve for $Co(py)_2Cl_2$ [6]. (With the permission of *Analytica Chimica Acta*, Elsevier, Amsterdam.)

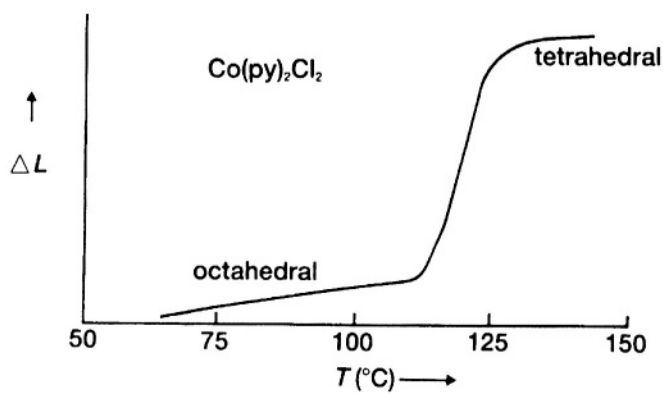

TD has also been used [8] to study the sintering behaviour of kaolins and kaolinitic clays. On heating, kaolin loses structural water at about 550°C and forms the metakaolin structure. Above 960°C this converts to a spinel structure and then above 1100°C to mullite. The mullite formed sinters at higher temperatures. These reactions are accompanied by the shrinkages shown in Figure 6.7. The TD curves of kaolins and kaolinitic clays may be used for their classification [8].

Figure 6.7
Thermodilatometry curve of kaolin (based on Fisher Scientific Co. Bull. 156, p.4, with permission).

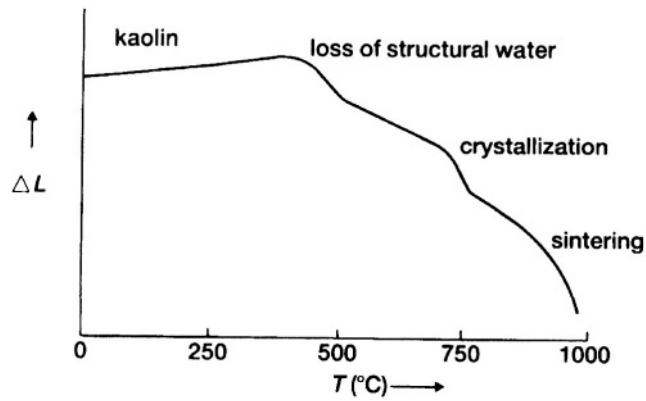

Other applications of TD include studies of the effects of additives on the shrinkage of cellular concretes [9]; the defects in non-stoichiometric oxides [10]; the firing of ceramics and the properties of alloys [11].

6.3 Thermomechanical Analysis (TMA) {Static Force Thermomechanometry (sf-TM)}

6.3.1 Principles [2]

Static Force Thermomechanometry (or Static Force Thermomechanical Analysis, sf-TMA) will be more easily recognised by its less systematic, but well-established name, Thermomechanical Analysis (TMA).

Thermodilatometry is carried out by measuring expansion and contraction under negligible loads. Further information of interest may be obtained by measuring the penetration, i.e. the expansion or contraction of a sample while under compression, as a function of temperature. Alternatively, the extension, i.e. the expansion or contraction of a sample under tension, may be measured as a function of temperature. These techniques, plus flexure and torsional measurements, are classified as thermomechanical analysis (TMA) and are obviously of great practical importance in materials testing (see applications).

6.3.2 Practical details

The apparatus used is based on that for thermodilatometry (Section 6.2). The principles of penetration, extension, flexure and torsional measurements are illustrated in Figure 6.8.

Figure 6.8
Thermomechanical analysis (TMA): (a) penetration, (b) extension, (c) flexure, and (d) torsional measurements.

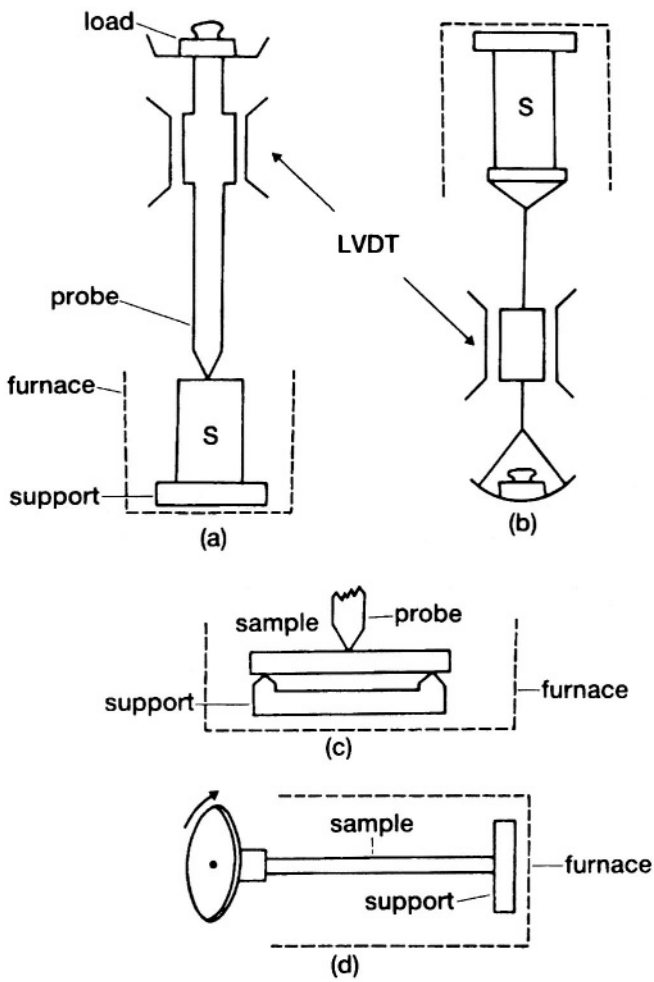

Two main types of experiment are possible: (i) measurement of dilation with temperature at a fixed load, or (ii) measurement of dilation with load at a fixed temperature.

The Shimadzu TMA-50 instrument is illustrated in Figure 6.9. The overall measurement range is ± 2.5 mm about the zero position. The load range is ± 500 g.

Temperature calibration of a TMA instrument can be done using a special sandwich sample built up, as shown in Figure 6.10, from discs of pure metals, separated by alumina discs. As the metals melt, the probe shows step-wise changes in length. The calibration sample can obviously only be used once. Several different designs are available for the probe, e.g. flat, pointed or rounded ends.

Figure 6.9
The Shimadzu TMA-50 instrument (with permission).

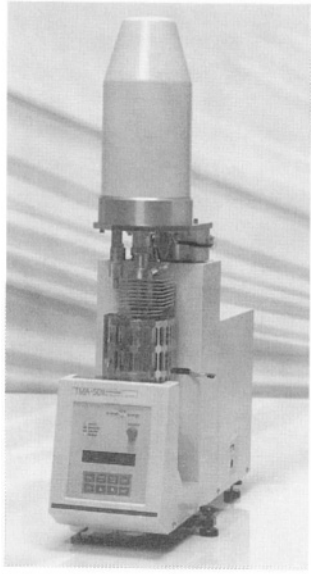

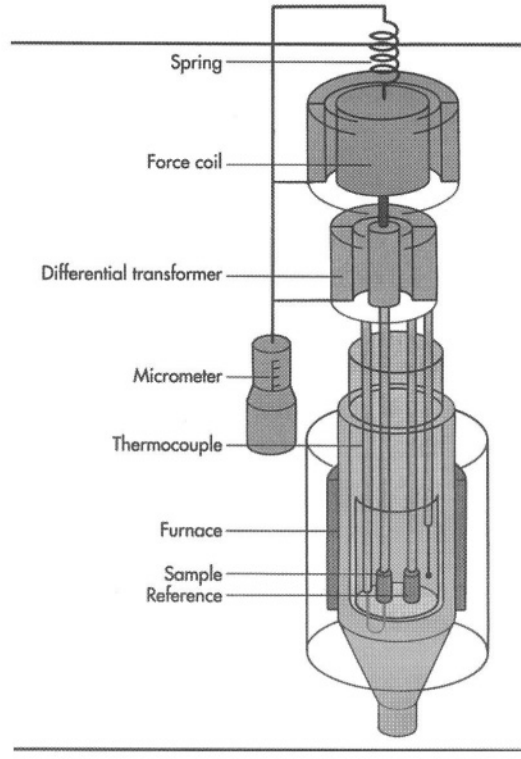

Figure 6.10
Temperature calibration for TMA using discs of pure metals, separated by alumina discs. (With the permission of Mettler-Toledo Instrumente AG.)

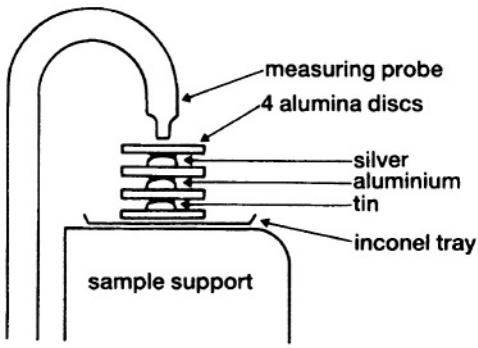

6.3.3 Stress-strain curves

Thermomechanical Analysis (TMA) (or, more precisely, Static Force Thermomechanometry), as described above, involves measurement of the change of a dimension of the sample as the load on the sample is increased, while the temperature is held constant. This is effectively the determination of a stress-strain curve for the sample. The load is related to the applied *stress* (force/area) and the change in dimension is related to the *strain* (elongation/original length).

Different types of materials give different types of stress-strain curves and, of course, the nature of the stress-strain curve for a given material will change as the temperature at which the measurements are made is changed.

The two extremes of behaviour are elastic solids, which obey Hooke's law, i.e., that the applied stress is proportional to resultant strain (but is independent of the rate of strain), and liquids, which obey Newton's law, i.e., that the applied stress is proportional to rate of strain (not the strain itself). Both laws only hold for small values of strain or rate of strain.

Tensile Stress:

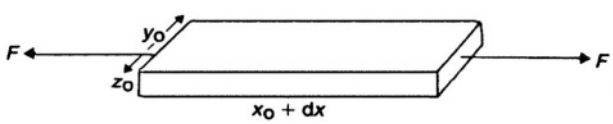

For a sample under tension the tensile stress, σ = force/area = $F / y_o z_o$ and the tensile strain, ϵ = elongation/original length = dx / x_o.

Hooke's law is

$\sigma \propto \epsilon$, or $\sigma = E\,\epsilon$

where E = Young's modulus (units: force/area). For an isotropic body (i.e. properties independent of direction) the changes in length and in width are related by Poisson's ratio:

$\nu_p = (dy/y_o)(x_o/dx)$

for which values range from 0.2 to 0.5.

Shear Stress:

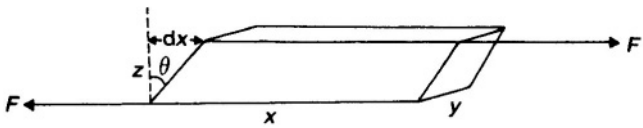

For a sample subjected to a shearing stress, the shear stress, $\sigma_S = Flxy = F/A$, and the shear strain, $\epsilon_S = dx/z = \tan\theta$. Again, Hooke's law is $\sigma_S \propto \epsilon_S$, or $\sigma_S = G\,\epsilon_S$, where G is the shear modulus. $G = \epsilon_S/\sigma_S = F/A \tan\theta$ and for small θ, $\tan\theta \approx \theta$ so $G \approx F/A\,\theta$.

Compression: When a pressure p is applied to a body of original volume, V_o, causing a volume change, ΔV, the stress, $\sigma_B = p$, and the strain $\epsilon_B = -\Delta V/V_o$. Hooke's law is $\sigma_B \propto \epsilon_B$, or $\sigma_B = B\,\epsilon_S$, where B is the bulk modulus. $B = \sigma_B / \epsilon_B = -pV_o/\Delta V$. The compressibility of the sample is defined as $1/B = -\Delta V/V_o$.

Of the three moduli, E, G and B, only two are independent. They are related via Poisson's ratio:

$E = 3B(1 - 2\nu_p) = 2(1 + \nu_p)G$

6.3.4 Viscoelastic behaviour

The stresses applied to liquids are usually shear stresses and Newton's law for viscous liquids is:

$\sigma_S \propto d\,\epsilon_S/dt$

that is, the shear stress is proportional to the *rate* of shear strain, or:

$\sigma_S = \eta\,(d\,\epsilon_S/dt)$

where η is the viscosity coefficient.

Many polymers show behaviour intermediate between elastic solids and viscous liquids and such materials are classified as *viscoelastic*. Shear of viscoelastic materials is described by a combination of Hooke's and Newton's laws. Strains are additive, so when the total shear stress is σ_S:

$$\epsilon_S = \epsilon_{S,elast} + \epsilon_{S,visc}$$

$\epsilon_{S,elast} = \sigma_S / G$ (Hooke's law) and $d\epsilon_{S,visc}/dt = \sigma_S / \eta$ (Newton's law)

Hence

$$d\epsilon_{S,elast}/dt = (1/G)(d\sigma_S/dt)$$

so

$$d\epsilon_S/dt = d\epsilon_{S,elast}/dt + d\epsilon_{S,visc}/dt = (1/G)(d\sigma_S/dt) + \sigma_S/\eta$$

When the shear strain is constant:

$$d\epsilon_S/dt = 0 \quad \text{and} \quad (1/G)(d\sigma_S/dt) = -\sigma_S/\eta$$

which rearranges to:

$$d\sigma_S/\sigma_S = -(G/\eta)\,dt$$

If $\sigma_S = \sigma_o$ at $t = 0$ and $\sigma_S = \sigma$ at $t = t$:

$$\int_{\sigma_o}^{\sigma} (1/\sigma_S)\, d\sigma_S = -(G/\eta)\, t$$

that is:

$$\ln(\sigma/\sigma_o) = -(G/\eta)\,t \quad \text{or} \quad \sigma = \sigma_o \exp(-(G/\eta)\,t)$$

This means that at a fixed strain, if the initial stress is σ_o, this will relax exponentially with time. The relaxation time is η/G.

6.3.5 Stress-strain measurements on polymers

If a viscoelastic sample is subjected to a tensile force, applied at a uniform rate, and the resultant elongation of the sample is measured, a curve of the form shown in Figure 6.11 (a) may be obtained. (The detailed shape will depend upon the rate of application of the stress.) In the region OL, Hooke's law is obeyed and the slope gives Young's modulus, *E*. Beyond the yield point, Y, viscous flow occurs until the maximum elongation is achieved at the break point, B.

The effects of temperature on the stress-strain curves are illustrated in Figure 6.11 (b). As the temperature increases, (i) the modulus of elasticity, *E,* (i.e. slope of OL in Figure 6.11 (a)) decreases; (ii) the yield strength decreases; and (iii) the maximum elongation generally increases.

Figure 6.11
(a) Typical stress-strain curve for a viscoelastic sample [12]. (b) Effect of temperature on stress-strain curves [12]. (Based on Cowie, J. M. G. (1973) *Polymers: Chemistry and Physics of Modern Materials,* Intertext, New York., Ch. 12, with permission of Blackie and Son Ltd., Glasgow.)

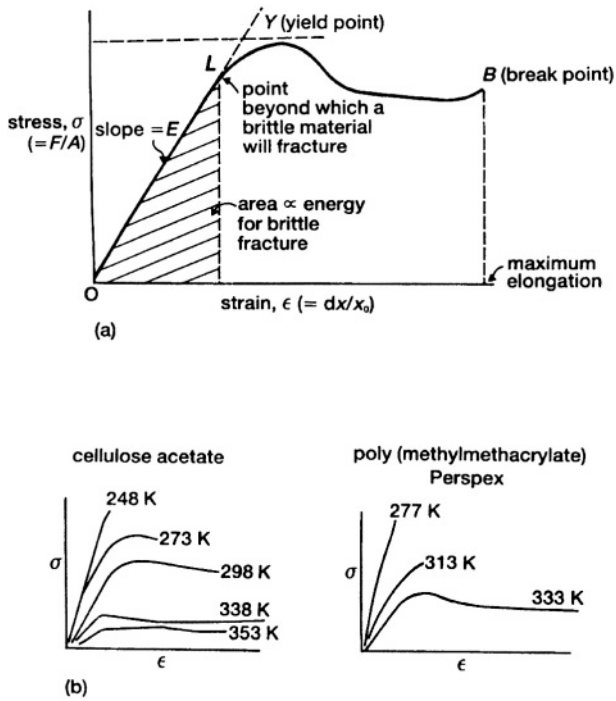

6.3.6 Modulated-Temperature Themomechanical Analysis[13,14]
Application of a modulated-temperature programme to TMA [13,14] provides a method for separating reversible processes such as thermal expansion from irreversible processes such as the deformation arising from creep or dimensional changes arising from orientational relaxations in solids. Depending upon the nature of the sample, measurements can be made under tension (films and fibres) or compression (rods or blocks). Data treatment is similar to that used in modulated-temperature DSC (see Chapter 4).

6.3.7 Applications of TMA

TMA and TD measurements are often carried out on the same sample with the same apparatus. Examples of both expansion and penetration measurements on neoprene rubber [15] are given in Figure 6.12. The coefficient of linear thermal expansion, α, can be determined from the slope of the expansion curve (see Section 6.2). Both the glass-transition (T_g) and melting (T_s) show up clearly. Another example [15] is the use of penetration measurements for testing polyethylene-coated paper (Figure 6.13). The structural transition and the melting show up clearly even though the coating was very thin (< 0.3 mm). Similar measurements have been carried out on paint films [16] and coatings. The behaviour of polymer films and fibres on heating under load is of great practical importance.

Figure 6.12
Expansion and penetration measurements on neoprene rubber [15]. (With the permission of International Scientific Communications Inc.)

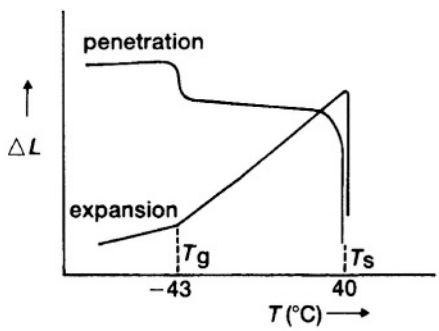

Figure 6.13
The use of penetration measurements for testing polyethylene-coated paper [15]. (With the permission of International Scientific Communications Inc.)

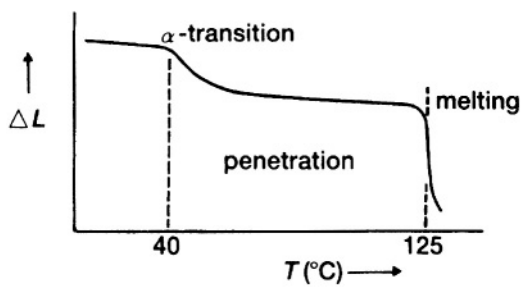

Another interesting application of TMA is a study [17] of the thermomechanical properties of the polymers used as denture bases. The glass-transition temperatures of such polymers are important because there are considerable variations in temperature in the mouth, as well as during the manufacture of dentures. Hugget *et al.* [17] used TMA measurements to monitor the effect of various modifications of the polymerisation of methyl methacrylate on the T_g of the resultant material. The factors expected [18] to increase the T_g of a polymer are: (i) the presence of groups in the backbone which increase the energy required for rotation, e.g. unsaturation and/or long side chains; (ii) secondary bonding between chains e.g. hydrogen bonding; (iii) crosslinking between chains; (iv) molecular mass; (v) copolymerisation, and (vi) plasticisation.

Price and Foster [14] used modulated-temperature TMA to study the behaviour under tension of acrylic fibres manufactured with different degrees of orientation. An average heating-rate of $0.75°C\ min^{-1}$ was used with a 210 s period and an rms amplitude of 1.75°C. The fibres all shrank to different extents on heating but, on deconvolution of the data [14] to separate the contributions from orientational relaxations, they all gave similar values for the coefficient of thermal expansion.

6.4 Dynamic Mechanical Analysis (DMA) {Modulated Force Thermomechanometry (mf-TM)}

6.4.1 Principles

Modulated Force Thermomechanometry is the systematic name proposed [1] for the technique more commonly referred to as Dynamic Mechanical Analysis (DMA) or Dynamic Thermomechanometry (Dynamic Thermal Mechanical Analysis, DTMA) [2,19,20]. In dynamic mechanical analysis (DMA) the sample is subjected to a periodically varying stress (usually sinusoidal of angular frequency, ω). The response of the sample to this treatment can provide information on the stiffness of the material (quantified by its elastic moduli) and its ability to dissipate energy (measured by its damping). For a viscoelastic material, the strain resulting from the periodic stress will also be periodic, but will be out of phase with the applied stress owing to energy dispersion as heat, or damping, in the sample (Figure 6.14 (a)), δ is the phase angle between the stress and the strain. Useful theoretical background is given in [2,12,19-21]. A brief history of the DMA technique is given in the book by Menard [19].

If an elastic sample is vibrated over a range of frequencies and the amplitude of vibration is measured, the *resonance frequency* is that which produces a maximum in a plot of amplitude against frequency. Young's modulus (of elasticity), *E,* is related to the square of the resonance frequency, ν_r.

$$E = c\, L^4\, \rho\, \nu_r^2 / d^2$$

where c is a constant, L is the sample length between clamps, d is the sample thickness and ρ is the sample density. If the sample is allowed to oscillate freely, it will do so at the natural resonance frequency with decreasing amplitude owing to damping. The form of the oscillations is shown in Figure 6.14 (b). The period, *P,* of the oscillations is constant $(= 1/\nu_r)$ and the amplitude (measured from a minimum to the preceding maximum) decays

exponentially. The rate of decay is a measure of how much damping there is. Damping is usually expressed as the logarithmic decrement per cycle:

$$\Delta = \log_{10}(A_1 / A_2) = \log_{10}(A_2 / A_3) = \ldots \text{ etc.}$$

Units used are decibels (dB) i.e. $10 \times \log_{10}(A_1 / A_2)$, e.g. if the amplitude halves, $\log_{10}(A_1 / A_2) = \log 2 = 0.30$. Damping is then 3.0 dB.

For elastic materials, the modulus E is simply the constant ratio between the stress and the resulting strain, but for viscoelastic materials, the modulus is a complex quantity:

$$E^* = E' + iE''$$

where E' is the storage modulus or in-phase component and E'' is the loss modulus or out-of-phase component. The ratio E'/E'' is the tangent of the phase angle, δ.

Damping may be determined from the width of a curve of relative amplitude against frequency (Figure 6.14 (c)), $h = (\nu_2 - \nu_1)/\nu_r$, or by measuring the driving force required to maintain a constant amplitude of vibration at the resonance frequency (forced vibration). Damping depends on the physical state of the sample, e.g. at $T > T_g$, polymers dissipate most of the energy supplied and damping is high. At $T < T_g$, the material stores the energy and damping is low.

6.4.2 Apparatus

A schematic diagram of the TA Instruments DMA 2980 Dynamic Mechanical Analyzer is compared with the more traditional design in Figure 6.15 [21]. The major components of a DMA instrument are the drive motor (which, through the drive shaft, supplies the periodic stress to the sample), the displacement sensor (which measures the amplitude and frequency of the response of the sample), the sample clamping system and the furnace and its associated temperature control system. The DMA 2980 has some new features compared to the traditional design [22]. It uses a non-contact, direct-drive motor to provide the stress over a wide dynamic range (0.0001 to 18 N). It also uses an optical encoder, instead of the traditional linear variable differential transformer (LVDT, see Figure 6.2). The typical resolution of an LVDT [22] is 1 part in 200 000, so to obtain 1 nm resolution, the maximum displacement would be 200 μm. An optical encoder measures displacement from the light diffraction patterns produced when one grating moves relative to another stationary grating. The resolution [22] is 1 nm over the whole displacement range of 25 mm, corresponding to 1 part in 25 000 000. This increased resolution improves the precision of the measured parameters and allows very stiff materials with very small oscillation amplitudes to be studied. With its cooling attachment, the DMA 2980 covers a temperature range of -150 to 600°C.

Figure 6.14
(a) Forced oscillation. (b) Free oscillation with damping. (c) Measurement of damping. (Based on [12] J.M.G. Cowie, "Polymers : Chemistry and Physics of Modern Materials", Intertext, New York, 1973, Ch 12, with permission of Blackie & Son, Glasgow.)

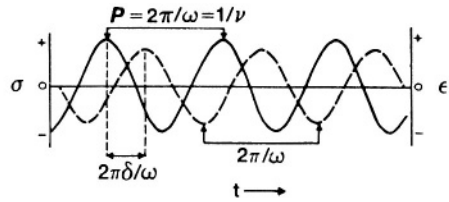

(a) Forced oscillation

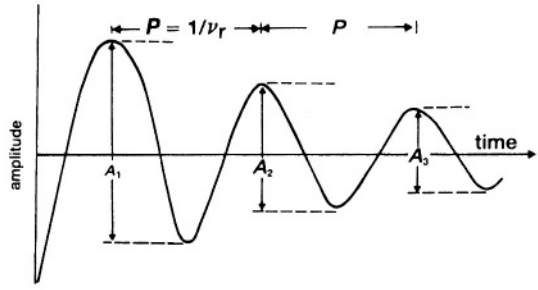

(b) Free oscillation with damping

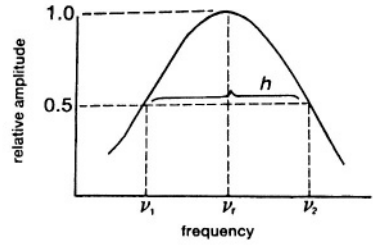

(c) Measurement of damping

Figure 6.15
Comparison of the TA Instruments DMA 2980 Dynamic Mechanical Analyzer with the more traditional type of DMA instrument [21]. (With the permission of TA Instruments.)

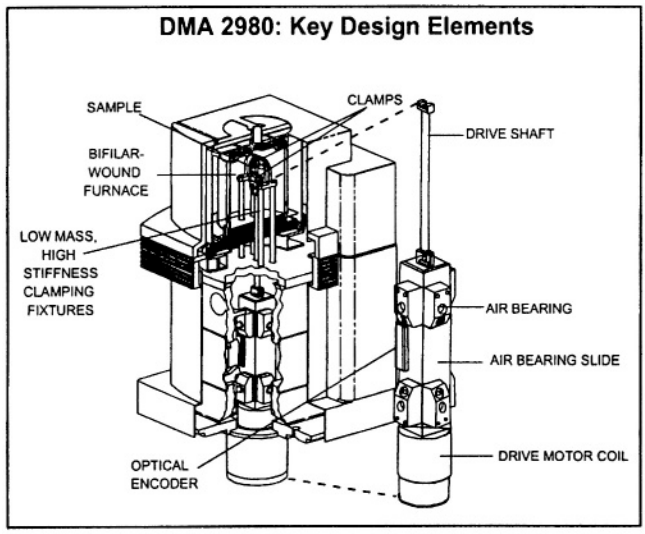

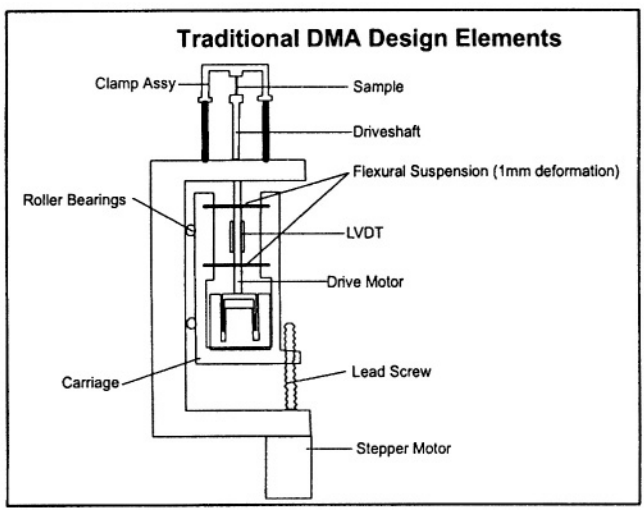

Some of the clamping systems available for most DMA instruments are illustrated in Figure 6.16 [2,20,23]. Clamps should have high stiffness, low mass and be easy to load and adjust [22].

Figure 6.16
Clamping systems for DMA instruments [2,23]. (With the permission of Elsevier, Amsterdam.)

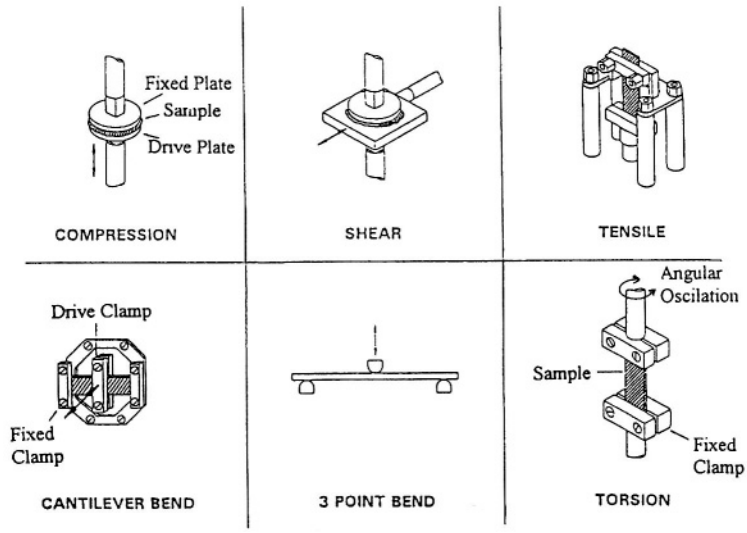

The sample, which is usually in film or fibre form, is clamped in the appropriate sample holder. Although samples should ideally be rigid enough to be tested as a sheet or rod, softer materials, such as thermosets or elastomers can be studied by using specially designed supports [24]. With thin films, buckling deformation can be a problem. Toth *et al.* [25] have developed a special sample clamp assembly which provides an arched sample cross-section. Miller [26] describes a technique for characterizing organic coatings by DMA by coating a multiple filament glass strand. The contribution of the substrate alone is subtracted to give the contribution of the coating. A similar technique using a thin steel strip as substrate can be used in examining the mechanical properties of paints. Liquid samples can be supported on films or absorbed into papers or braids.

6.4.3 Applications of DMA

Changes in Young's modulus indicate changes in rigidity and hence strength of the sample. Damping measurements give practical information on glass transitions, changes in crystallinity, the occurrence of cross-linking, and also shows up the features of polymer chains. The information obtained has been used in various very practical areas such as studies of vibration dissipation, impact resistance and noise abatement.

Typical DMA results [27] on two different samples of polyethylene are shown in Figure 6.17 (a) and (b). The damping curve for linear polyethylene (Figure 6.17 (a)) shows peaks at -95°C and 65°C. The lower temperature peak has been attributed to long chain $(-CH_2-)n$ crankshaft relaxations in the amorphous phase and the higher temperature peak to similar motion in the crystalline phase. The temperatures and relative sizes of the two peaks can be related to the degree of crystallinity of the sample. The damping curve for branched polyethylene (Figure 6.17 (b)) has features at -112°C, -9°C and 45°C. The -112°C and 45°C peaks are explained as above, while the -9°C peak is attributed to $(-CH_3)$ relaxations in the amorphous phase.

Figure 6.17
Typical DMA results [27] for two different samples of polyethylene: (a) linear polyethylene; (b) branched polyethylene. (With the permission of DuPont Analytical Instruments.)

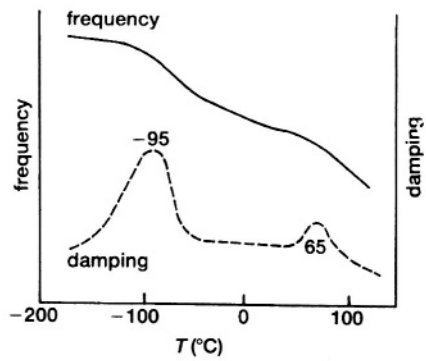

(a) Linear polyethylene

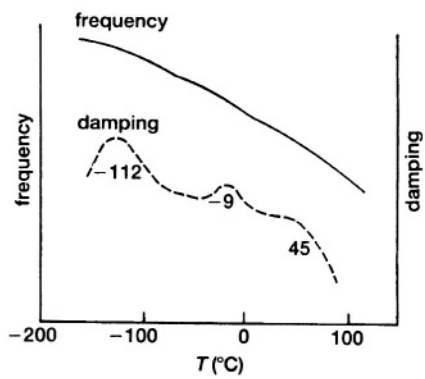

(b) Branched polyethylene

The thermal behaviour of styrene-butadiene-rubber (SBR) is illustrated in Figure 6.18 [27,28]. Various formulations of SBR are used in tyre manufacture. Different styrene-butadiene ratios may be used, or different butadiene isomers, or different additives e.g. carbon black. A high cis-butadiene content lowers the glass transition temperature, T_g, (to as much as -110°C compared to -50°C) giving greater flexibility at low temperatures. The addition of carbon black (Figure 6.18 (c)) increases the modulus of elasticity. The T_g is also slightly increased. The complex damping curve at low temperatures indicates polymer-carbon black interactions and may lead to adverse properties e.g. heat build-up.

Figure 6.18
DMA curves for rubber blends [27,28]:
(a) cis-polybutadiene; (b) styrene-butadiene-rubber (SBR); (c) SBR + carbon black.
(With the permission of DuPont Analytical Instruments.)

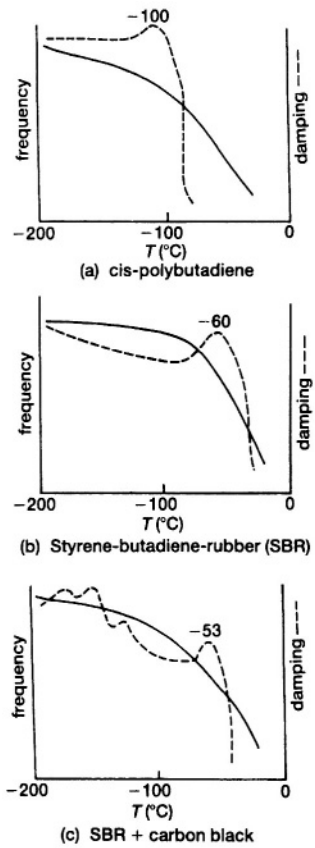

Huson *et al.* [24] have used the changes in height of DMA damping peaks as a measure of the extent of vulcanisation in elastomer blends. Results agreed well with torque rheometer measurements.

Gill [29] has given a general review of the application of DMA to polymer composites. Toth *et al.* [25] have used DMA to study the effect of ageing on paper. Samples were subjected to accelerated ageing at 100°C in air with 50% relative humidity and the DMA curves of original and aged samples were recorded. The increased brittleness of the aged samples showed up in the damping curves.

Schenz *et al.* [30] have designed a sample mold for preparing frozen aqueous solutions for examination by DMA. The DMA technique was found to be very sensitive to second-order transitions. Frozen dilute solutions of sucrose showed two glass transitions at around -32°C, suggesting that as the solutions are frozen, tiny localised inclusions are formed where the concentration differs from the bulk concentration. These inclusions have a T_g higher than that of the bulk solution. DSC was not sensitive enough to detect these details.

Kaiserberger [31] has compared the performance of TMA, DMA and DSC for determining the viscoelastic properties of polymers and concludes that DMA has superior sensitivity in detecting phase transitions of second and higher order.

In addition to the references quoted already, there is some useful information on applications of DMA to polymers in [32] and to food in [33].

References

1. W. Hemminger and S.M. Sarge, "Handbook of Thermal Analysis and Calorimetry", Vol.1, (Ed. M.E. Brown), Elsevier, Amsterdam, 1998, Ch.1.
2. R.E. Wetton, "Handbook of Thermal Analysis and Calorimetry", Vol.1, (Ed. M.E. Brown), Elsevier, Amsterdam, 1998, Ch.6.
3. M. Linseis, Proc. 4th ICTA, Vol.3, Heyden, London, 1975, p.913.
4. E. Karmazsin, P. Satre and M. Romand, Proc. 7th ICTA, Vol. 1, Wiley, Chichester, 1982, p.337.
5. P.F. Levy, Proc. 4th ICTA, Vol.3, Heyden, London, 1975, p.3; Int. Lab., Jan/Feb(1971)61.
6. W.W. Wendlandt, Anal. Chim. Acta, 33 (1965) 98.
7. P.K. Gallagher, Proc. 6th ICTA, Vol.1, Birkhaeuser, Basel, 1980, p. 13.
8. K.H. Schuller and H. Kromer, Proc. 7th ICTA, Vol.1, Wiley, Chichester, 1982, p.526.
9. O. Hoffman, Proc. 8th ICTA, Thermochim. Acta, 93 (1985) 529.
10. V.E. Shvaiko-Shvaikovsky, Proc. 8th ICTA, Thermochim. Acta, 93 (1985)493.
11. W. Hadrich, E. Kaiserberger and H. Pfaffenberger, Ind. Res. Dev., (Oct. 1981) 165.
12. J.M.G. Cowie, "Polymers: Chemistry and Physics of Modern Materials", Intertext, New York, 1973, Ch.12.
13. D.M. Price, Thermochim. Acta, 357/358 (2000) 23; 315 (1998) 11.
14. D.M. Price and G.M. Foster, J. Thermal Anal. Calorim., 56 (1999) 649.

15. P.F. Levy, Proc. 4th ICTA, Vol.3, Heyden, London, 1975, p.3; Int. Lab., Jan/Feb. (1971)61.
16. G. Widmann, Mettler Application No.3401 (1983).
17. R. Huggett, S.C. Brooks and J.F. Bates, Lab. Prac., 33 (11) (1984) 76.
18. J.A. Brydson, "Plastic Materials", Iliffe Brooks Ltd., London, 1969.
19. K.P. Menard, “Dynamic Mechanical Analysis - A Practical Introduction”, CRC Press, Boca Raton, USA, 1999.
20. P.K. Gallagher in “Thermal Characterization of Polymeric Materials” (Ed. E.M. Turi), Academic Press, New York, 2nd Edn, 1997, Ch. 1.
21. B. Wunderlich, “Thermal Analysis”, Academic Press, Boston, 1990, Ch.6.
22. J. Foreman and K. Reed, TA Instruments Thermal Analysis Technical Publication TA-229.
23. R.E. Wetton, J.C. Duncan and R.D.L. Marsh, Amer. Lab., 25 (1993) 15.
24. M.G. Huson, W.J. McGill and P.J. Swart, J. Polym. Sci., Polym. Letters, 22 (1984)143.
25. F.H. Toth, G. Pokol, J. Gyore and S. Gal, Proc. 8th ICTA, Thermochim. Acta, 93 (1985) 405; 80 (1984) 281.
26. D.G. Miller, Int. Lab., (March 1982) 64.
27. DuPont Instruments, Thermal Analysis Review, Dynamic Mechanical Analysis, undated.
28. R.L. Hassel, DuPont Application Brief, TA68.
29. P.S. Gill, Ind. Res. Dev., (March 1983) 104.
30. T.W. Schenz, M.A. Rosolen, H. Levine and L. Slade, Proc. 13th NATAS, 1984, paper 12, p.57.
31. E. Kaiserberger, Proc. 8th ICTA, Thermochim. Acta, 93 (1985) 291.
32. J. Foreman, reprint from American Laboratory, January 1997, TA Instruments TA-236.
33. Thermal Analysis Application Brief, TA Instruments TA-119.

COMBINATION OF THERMAL ANALYSIS TECHNIQUES

7.1 Principles

A truly *simultaneous* thermal analysis technique involves measurements of two or more of the properties in Table 1.1 on the same portion of the sample during a single temperature programme [1,2]. Each of the properties may be monitored continuously, or they may be sampled in a repetitive sequence to allow forthe requirements of data capture. Simultaneous measurements must thus be distinguished from *parallel* measurements, where different portions of the sample are examined using different instruments, and *concurrent* measurements where different portions of the same sample, in different containers, are held within a single furnace and are subjected to a common temperature programme, Figure 7.1. This last option is also used in instruments designed for carrying out one type of measurement on several samples. A simultaneous technique is usually written as the two acronyms linked with a hyphen, e.g. TG-DTA.

Figure 7.1
Combinations of thermal analysis techniques:
(a) simultaneous; (b) concurrent; (c) parallel.

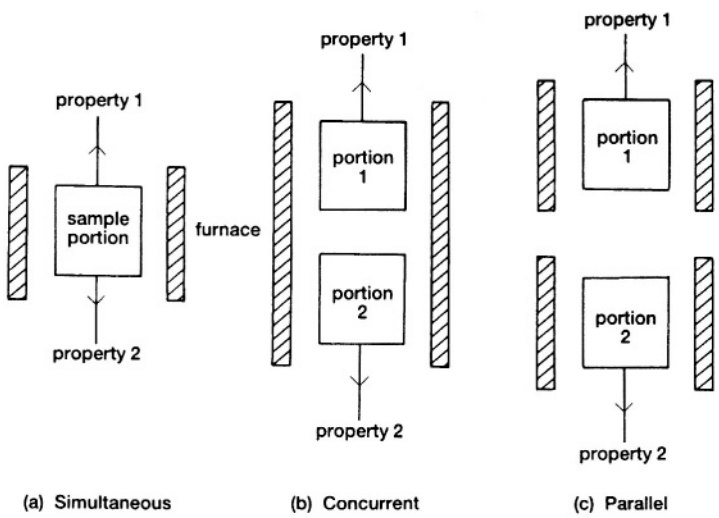

Results of the thermal analysis of a given sample, under a specified set of conditions, on a given instrument, are usually reasonably *repeatable* [3]. Agreement with the results on another portion of the same sample, obtained using the same technique on an instrument of a different make, or a similar instrument in a different laboratory, may be much less *reproducible*. It is even more difficult to compare results of *parallel* measurements from two or more independent thermal analysis techniques, e.g. TG and DTA. The advantages of being able to relate results of different techniques are obvious. For example TG cannot be used to detect melting, while melting and decomposition cannot be distinguished unambiguously using DTA. A substance which melts with accompanying decomposition must thus be studied using both TG and DTA (or DSC). There is usually a synergistic effect in that the total amount of information about the sample that is obtained is greater than the sum of the information obtained from the individual techniques. There are also savings in time and amounts of sample, but generally the sensitivities of the individual techniques are decreased on combination, because of compromises in instrumental design. Some sophisticated techniques, such as power-compensated DSC, do not lend themselves easily to simultaneous measurement of other properties.

Any of the basic TA techniques can be complemented by combination with evolved gas analysis (EGA). Such combination usually has little effect on the sensitivity of the basic technique. EGA is discussed in detail in Chapter 8.

7.2 Equipment

Pioneers in the use of simultaneous methods, based on their instrument called the "Derivatograph", have been J. and F. Paulik [4]. The Derivatograph (Figure 7.2) is an example of one of the first successful combinations, i.e. that of TG with DTA to give TG-DTA. In the Derivatograph and some other instruments, the DTA reference material is not weighed.

In the Netzsch STA 449 TG-DTA system (Figure 7.3) the whole DTA configuration, together with its thermocouple leads, is incorporated into the balance suspension. A variety of different sample modules for the Setaram TG-DTA/DSC system is shown in Figure 7.4. A different approach is used in the Setaram simultaneous TG-DSC 111 (Figure 7.5) [5]. There is no mechanical contact of the TG sample pans with the detectors of the DSC tubes. This is claimed not to affect the quantitative performance of the detectors. The symmetrical configuration of the system and the absence of contact problems are both factors in favour of accurate weighing (Chapter 3).

DTA may be combined with TMA by inserting thermocouples in the sample and in the reference. The Mettler-Toledo TMA/SDTA840 is illustrated in Figure 7.6. DTA/DSC and TG have all been very successfully combined with hot-stage microscopy by Mettler-Toledo (see Chapter 5). Combination of X-ray diffraction with other TA techniques has had some success [6-9]. The simultaneous DSC-XRD system used by Yoshida et al. [9] is shown in Figure 7.7, and results of simultaneous DSC-wide-angle XRD measurements [9] on the crystallization of hexatriacontane ($C_{36}H_{74}$) on cooling at 0.5 $K\ min^{-1}$ from the melt are shown in Figure 7.8.

Figure 7.2
J. and F. Paulik's Derivatograph [4] for simultaneous TG-DTA. 1. sample, 2. reference, 3. furnace, 4. thermocouples. (With the permission of Elsevier, Amsterdam.)

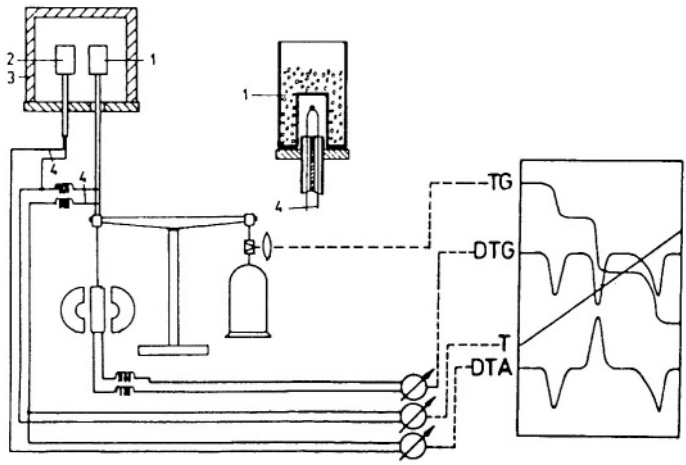

Some of the less-common properties, whose measurement is described in Chapter 9, have been measured simultaneously with more conventional properties.

While dealing with simultaneous measurements, it is worth stressing the importance of *complementary* techniques which can aid in identifying the thermal events occurring in the sample. Complementary techniques include all forms of spectroscopy, X-ray and electron diffraction, optical and electron microscopy and are limited only by the ingenuity of the investigator.

Figure 7.3
The Netzsch STA 449 simultaneous TG-DTA system (with the permission of Netzsch Ltd.).

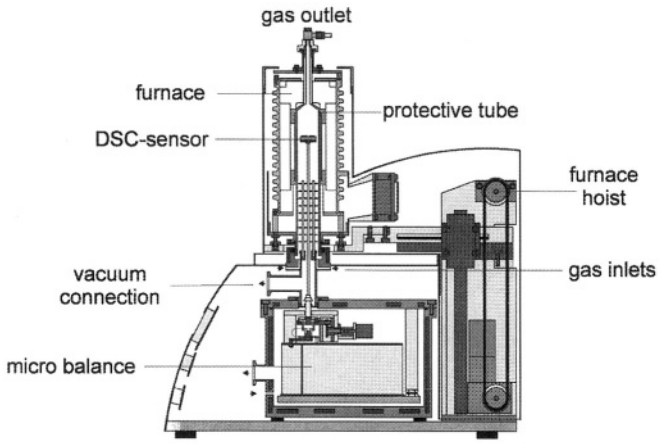

Figure 7.4
Some of the sample holder systems for the Setaram simultaneous TG-DTA/DSC system (with the permission of Setaram Ltd.).

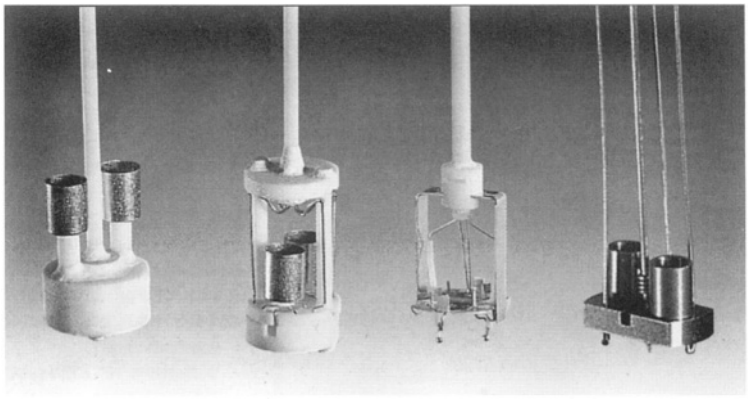

Figure 7.5
The Setaram simultaneous TG-DSC 111 (with the permission of Setaram Ltd.).

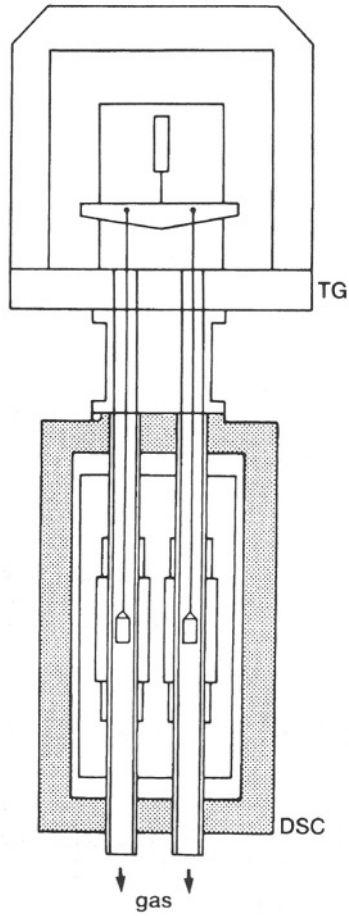

Figure 7.6
The Mettler-Toledo TMA/SDTA840 for simultaneous TMA-DTA (with permission).

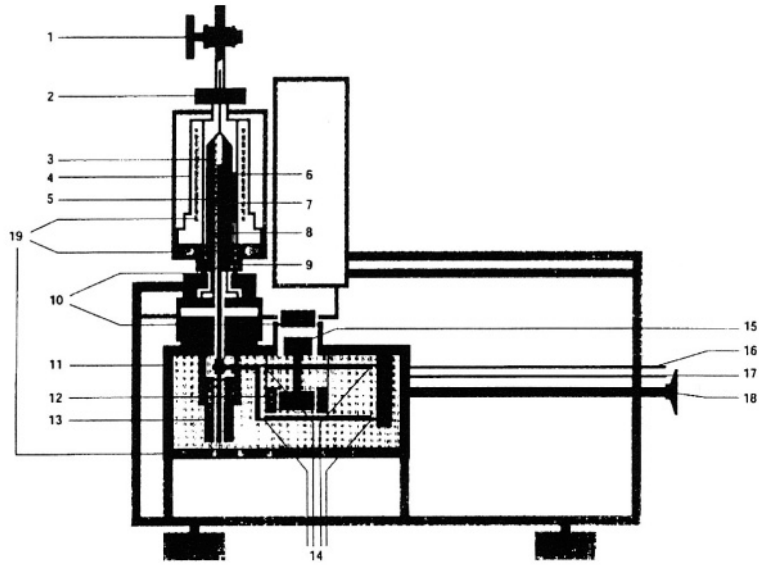

1 Gas outlet stopcock
2 Clamp with screw
3 Furnace windingsg
4 Water-cooled furnace jacket
5 Sample support
6 Furnace temperature sensor
7 Sample temperature sensor
8 Reactive gas capillary
9 Measuring probe
10 Gaskets
11 Thermostated cell housing
12 Force generator
13 Length sensor (LVDT)
14 Bending Bearings
15 Adjustment weights
16 Protective gas inlet
17 Reactive gas inlet
18 Vacuum and purge gas inlet
19 Watercooling

Figure 7.7
The simultaneous DSC-XRD system used by Yoshida et al. [9].
(i) Overall view: a, cooling gas inlet; b, cooling gas outlet; c, gas inlet; d, cooling unit; e, heat sink, f, furnace; g, reference holder; h, sample holder; i, hole for X-ray beam transmission; j, thermocouple; k, bakelite vessel; l, window for X-ray beam transmission; m, silver lid.
(ii) Inside view: n, sample pan; o, aluminium film; p, pan lid; and s, sample.
(With the permission of Thermochimica Acta.)

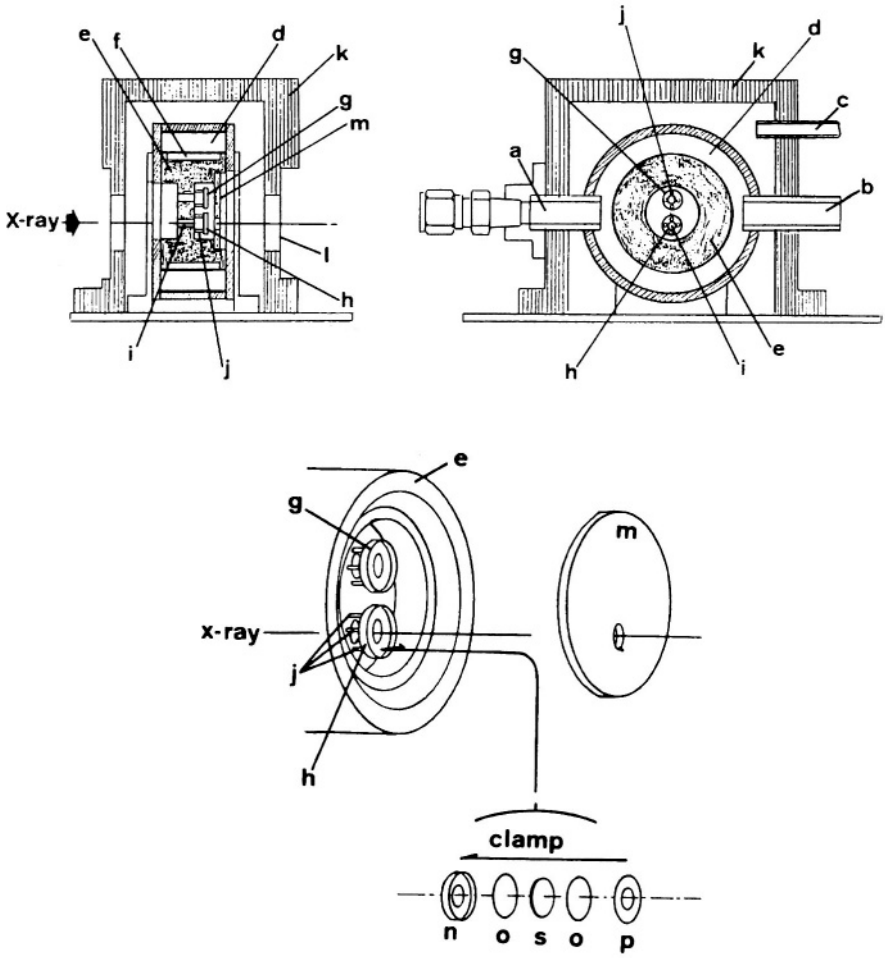

Figure 7.8
Results of simultaneous DSC-wide-angle XRD measurements [9] on the crystallization of hexatriacontane ($C_{36}H_{74}$) on cooling at 0.5 K min^{-1} from the melt using the equipment shown in Figure 7.7. (With the permission of Thermochimica Acta.)

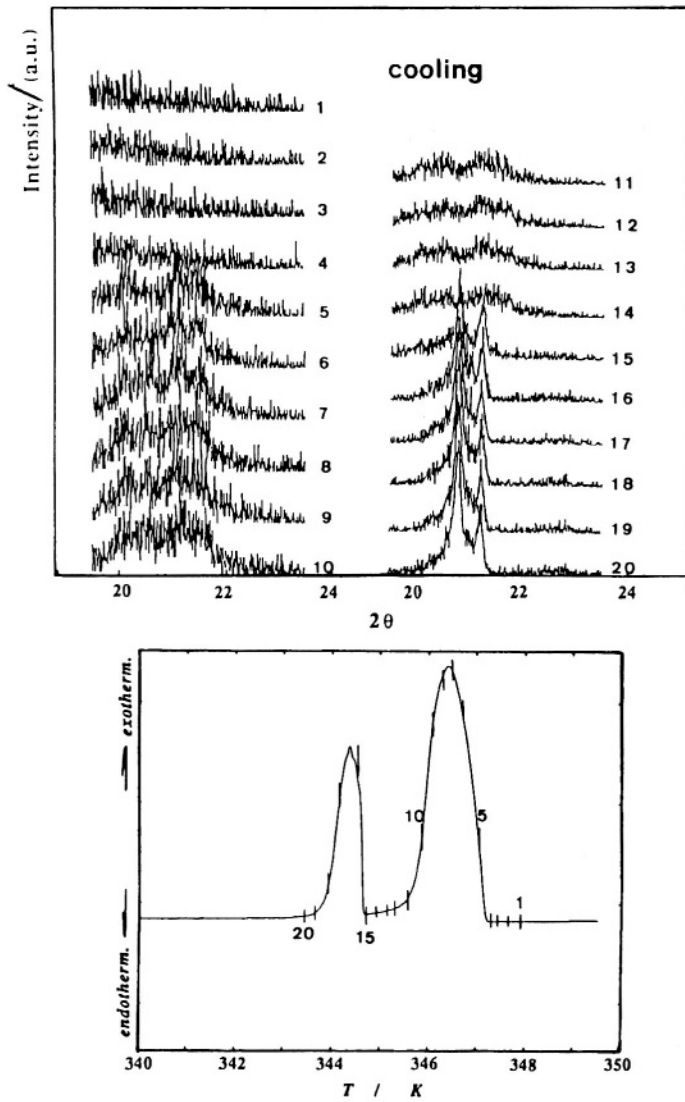

References

1. W. Hemminger and S.M. Sarge,"Handbook of Thermal Analysis and Calorimetry", Vol.1, (Ed. M.E. Brown), Elsevier, Amsterdam, 1998, Ch.1.
2. J. Van Humbeeck, "Handbook of Thermal Analysis and Calorimetry", Vol.1, (Ed. M.E. Brown), Elsevier, Amsterdam, 1998, Ch.11.
3. R.L. Blaine, C.G. Slough and D.M. Price, Proc. 12th ICTAC, (2000), paper O.19.
4. J. Paulik and F. Paulik, "Simultaneous Thermoanalytical Examinations by means of the Derivatograph", "Wilson and Wilson's Comprehensive Analytical Chemistry", Vol.XIIA, Elsevier, Amsterdam, 1981.
5. P. Le Parlouer, Proc. 8th ICTA, Thermochim. Acta, 92 (1985) 371.
6. P.K. Gallagher in "Thermal Characterization of Polymeric Materials" (Ed. E.M. Turi), Academic Press, New York, 2nd Edn, 1997, Ch.1, p97.
7. R. Androsch, M. Stolp and H.-J. Radusch, Thermochim. Acta, 271 (1996) 1.
8. C. Wutz, M. Bark, J. Cronauer, R. Doehrmann and H.G. Zachmann, Rev. Sci. Instr., 66 (1995)1303.
9. H. Yoshida, R. Kinoshita and Y. Teramoto, Thermochim. Acta, 264 (1995) 173.

EVOLVED GAS ANALYSIS (EGA)

8.1 Basic Principles

Many samples, on heating, release gases or vapour through desorption or decomposition. This release is accompanied by thermal effects and, obviously, mass-losses, which, themselves, can be detected by the appropriate thermal analysis technique, e.g. DTA or DSC and TG, respectively. The thermal analysis technique does not, however, identify the gas evolved and, for complex decompositions, such information is essential. It has thus become fairly routine to couple the basic techniques already described with a system for either detecting the evolution of gas (or gases) from the sample (*evolved gas detection,* EGD) or, more satisfactorily, detecting and identifying the gases evolved (*evolved gas analysis,* EGA) [1-4]. The apparatus for EGA will obviously be more complex than that required for EGD. Gas-solid reactions can also be studied by determining the amounts of products formed or reactant gas consumed. A novel technique on this principle is pulsed (gas) thermal analysis [5] (see below).

In practice, the main techniques in current use for EGA are mass spectrometry (MS) or Fourier transform infrared spectroscopy (FTIR). Because of the time intervals required between sampling, gas chromatography (GC) (see below) has declined in usage. If the evolved gas mixtures are so complex that preliminary separation is required, GC may be used for the separation coupled with MS or FTIR for the analysis.

The main thermal analysis technique with which EGA has been coupled is thermogravimetry (TG) and simultaneous techniques (see Chapter 7) are usually indicated by hyphenation, for example TG-MS or TG-FTIR.

The practical aspects of coupling EGA methods with TA instruments have been discussed in considerable detail by Kaiserberger and Post [6]. The gas flow conditions in the combined instruments have to be carefully examined and correlation of the two sets of data obtained from the two techniques by suitable calibration is important. The distribution of an evolved gas in the flow of purge gas depends [6] on the volume ratio, the flow profile and the diffusion coefficients of the species involved. The distribution broadens with increasing time of flow after mixing.

8.2 Evolved Gas Detection (EGD)

EGD has the advantage that measurements of the single property selected for detection of the gas (for example, thermal conductivity, see below) may be completely continuous and hence are readily related to thermal analysis curves. The purge gas from the thermal analysis equipment becomes the carrier for sweeping evolved gases to a detector (Figure

8.1). The detector should be as close as possible to the sample to decrease condensation of vapours, secondary reactions in the gas phase, and time lags between thermal analysis and EGD curves. The most commonly used detectors are those usually found in simpler gas chromatographs, namely: (i) thermal conductivity detectors (TCD, or katharometers), (ii) gas-density detectors, and (iii) ionization detectors. In addition, use has been made of infrared radiometers.

For maximum sensitivity, the measured property, e.g. thermal conductivity, of the evolved gas should differ markedly from that of the carrier (Table 8.1). H_2 and He have very high thermal conductivities and argon very low, making them suitable carriers, but their influence on the thermal effects being examined, must be determined because artefacts have been observed [7]. Flame ionization detectors are particularly sensitive to organic compounds, but do not respond to water vapour. Some separation of gas mixtures is possible by carrying out several EGD runs with suitable cold traps (or even specific absorbents) interposed between the sample and the detector. Alternatively, two similar detectors may be used, one on either side of the trap.

Figure 8.1
Evolved gas detection (EGD)

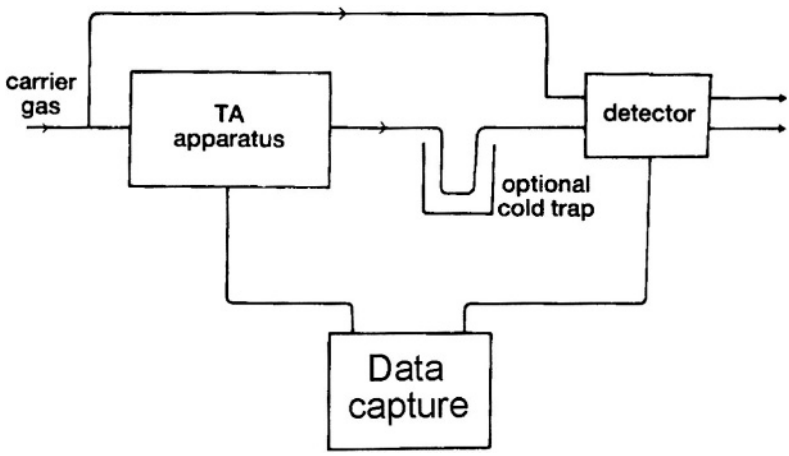

Table 8.1
Thermal conductivities of some gases

Gas	Thermal Conductivity, λ / W m^{-1} K^{-1}		Differences, 100 $\Delta\lambda$ = 100 (λ_{gas} - λ_{ref})	
	T = 300 K	T = 373 K	Ref. N_2	Ref. He
Air	0.0262	0.0301	+0.01	-12.47
Ar	0.0178	0.0213	- 0.83	-13.31
He	0.1509	0.1669	+12.48	-
H_2	0.1869	0.2090	+16.08	+3.60
N_2	0.0261	0.0301	-	-12.48
O_2	0.0266	0.0311	+0.05	-12.43
CO	0.0251	0.0305	- 0.10	-12.58
CO_2	0.0166	0.0212	- 0.95	-13.43
NH_3	0.0246	0.0327	- 0.15	-12.63
N_2O	0.0174	0.0212	- 0.87	-13.35
NO	0.0260		- 0.01	-12.49
NO_2	0.0372 (328 K)		+1.11	-11.37
SO_2		0.0153 (est.)	- 1.1	-13.6
H_2O(g)	0.0181	0.0241	- 0.80	-13.28

Sources:
"Handbook of Chemistry and Physics", ed. R.C. Weast, CRC Press, Boca Raton, 64th Edn, 1984, p.E-2.
"Handbook of Chemistry", ed. N.A. Lange, McGraw-Hill, New York, 10th Edn, 1961, p.1544.
"Gas Effluent Analysis", ed. W. Lodding, Edward Arnold, London, 1967, p.30.
"Fundamentals of Heat Transfer", L.C. Thomas, Prentice-Hall, Englewood Cliffs, 1980, p.665.

8.3 Mass Spectrometry (MS)

Probably the most versatile and fastest means of repetitive gas analysis is mass spectrometry, so the most obvious solution to the problem of identifying the gases evolved from a thermal analysis instrument, is to replace the detector (Figure 8.1) by a mass spectrometer. Emmerich and Kaiserberger [8] have long suggested that the capital already invested in thermal analysis equipment warrants the further expense of adding a mass spectrometer to get the maximum information per run.

The greatest obstacle to routine use of TA-MS has been that mass spectrometers require high vacuum for their operation, while most thermal analysis experiments are carried out at, or just above, atmospheric pressure. The coupling interface [6,9,10] (see Figure 8.2) thus has to allow for the pressure differences in the TA and MS systems while transferring a representative sample of the evolved gases from the TA system.

Figure 8.2
Coupling thermal analysis equipment to mass spectrometers.
(a) Capillary inlet.
(b) Jet separator.

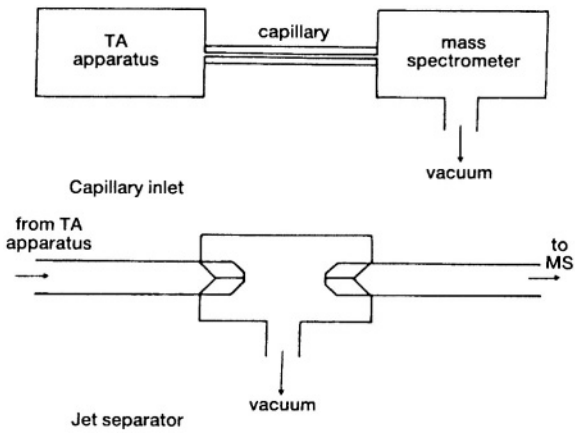

Problems that can arise include: (i) condensation of vapours in the sampling system - attempts to decrease this by heating the system may promote secondary reactions; (ii) the high concentration of carrier gas may swamp the smaller responses of evolved gases - He, with its low mass number, is thus useful as a carrier. Particular problems encountered in high-temperature studies have been discussed [11].

Roduit et al. [12] have examined the influence of mass transfer on the coincidence of TA and MS curves. Quantitative calibration of TA-MS systems by injection of known amounts of a calibration gas into the carrier gas stream, or by decomposition of a solid sample with a simple stoichiometric reaction in the TG system, is discussed by Maciejewski and Baiker [13]. They recommend that the use of helium as carrier gas should be avoided wherever possible because its high diffusivity changes the shape of the MS signal. Stability of the gas flow-rate is essential in quantitative measurements. The problems of condensation of water vapour are also discussed.

Criado *et al.* [14] have calculated the expected EGA curves on the assumption that the partial pressures of the gases generated during thermal decomposition of a sample are proportional to the reaction rate. The apparent reaction order, n, approaches zero as the efficiency of the mass-transfer through the system decreases, but the apparent activation energy remains approximately constant.

Complete mass spectra may be recorded repetitively, or selected mass numbers may be sampled using a suitably programmed system, or a single mass number may be monitored continuously. The results of TA-MS may be presented as a plot of the total ion current (the integral of the signal over the entire mass range scanned) against the temperature, or of the intensity of a peak of fixed mass number against T (Figure 8.3).

Figure 8.3
TG, DTA and MS curves for the thermal decomposition of hydrated cobalt tartrate, $Co(C_4H_4O_6).2.5H_2O$, heated at 5 K min^{-1} in an argon atmosphere [15]. (With the permission of Elsevier, Amsterdam.)

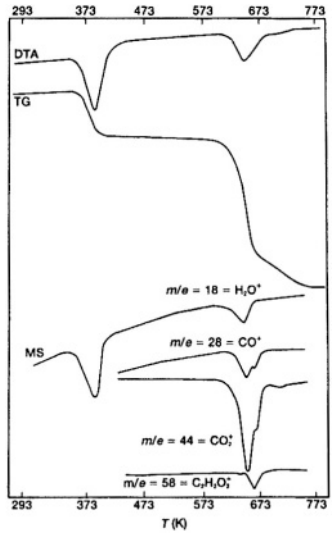

In interpreting the results of MS studies, allowance has to be made for the fragmentation patterns of the parent product molecules. Excessive fragmentation of the gas molecules occurs in some cheaper quadrupole mass spectrometers which do not have a variable ionization potential. Mixtures of CO_2 and CO, for example, may then appear mainly as C^+ and O^+ fragments.

Statheropoulos *et al.* [16] have discussed procedures for the evaluation of the performance of a TG-MS system. These include monitoring the stability of the mass-flow, the gas transfer delay, and any condensation of evolved gases. Sills and He [17] used the oxidation of pyrite to determine transfer times.

8.4 Fourier Transform Infrared (FTIR) Spectroscopy

The potential use of Fourier transform infrared spectrometry (FTIR) for evolved gas analysis was recognized by Liebman et al. [18], who remarked on the specificity and the short measurement times required, as well as warning of the possibilities for interference from the rotational-vibrational fine structure of spectra of small molecules such as H_2O and $HC\ell$. TA-FTIR continues to grow in popularity with the wider availability of FTIR spectrometers. The apparatus for evolved gas analysis by FTIR [1,19] requires (like most simultaneous methods discussed in Chapter 7) that some compromises be made between the ideal requirements for operation of the individual instruments. For example, high

heating rates and low carrier-gas flowrates will give greater concentrations of degradation products in the gas analysis cell, but these conditions are not always the most suitable for accurate thermal analysis. Secondary reactions between gaseous products are also enhanced at low flow-rates, while high flow-rates can cause weighing problems in TG. Kaiserberger and Post [6] deal with the coupling of TA equipment to FTIR instrumentation. In contrast to TA-MS, the whole gas flow from the TA instrument should pass through the gas cell of the FTIR instrument, so the transfer line should not change the flow rate and pressure of the purge gas. The transfer time for the gas to reach the FTIR cell is determined by the flow rate chosen for the TA system and the length of the transfer line. Typically, transfer times will be a few seconds and flow will be laminar.

A gas cell used for FTIR spectroscopy is illustrated in Figure 8.4(c). The gas sampling region of the TG is illustrated in Figure 8.4 (a). FTIR spectra over the full range of the instrument can be recorded, or "windows" selected. The results of TA-FTIR experiments can be presented in several ways. The most common form of presentation is as a plot of the overall integrated intensity of the IR absorption as a function of temperature. This is known as a Gram-Schmidt plot (see Figure 8.5(a)). The areas under these absorption peaks are very dependent upon the nature of the species contributing to the absorption, so, unlike DTG, DSC or DTA curves, the relative amounts of different species cannot be directly inferred from Gram-Schmidt plots. Full or partial IR spectra (see Figure 8.5(b)) at points chosen along the TA curve can be examined and used to identify the species being evolved at that stage.

Morgan [20] has described the use of non-dispersive (i.e. fixed wavelength) infrared analyzers, coupled in series to a DTA apparatus, to measure the amounts of CO_2 and H_2O evolved by minerals and mineral mixtures. (See Figure 8.6.)

8.5 Gas Chromatography (GC)

Another approach to EGA is to precede the detector (Figure 8.1) by a column of a suitable adsorbent, i.e. to pass the evolved gases from the thermal analysis instrument through a gas chromatograph [6]. Sampling, of course, now becomes intermittent because time has to be allowed for the component of the gas mixture with the longest retention time, to be eluted from the column, before the next sample is introduced. This is the main disadvantage of GC because times required for adequate separations may be of the order of several minutes. This means that only a few samplings may be possible during a rapid thermal event, and some events may even be missed completely. The advantage of GC is, however, that by suitable choice of column-packing material, most separations can be achieved and retention times, once determined, provide a simple means of identification. A multiple-loop gas sampling valve has been used [21] to overcome some of the sampling problems. Collection of samples at selected time intervals is followed by later analysis on the reasonable assumption that secondary reactions between evolved gases do not occur in the sample loops.

Figure 8.4
TG-FTIR equipment: (a) the gas sampling region of the TG; (b) the optical layout; (c) a gas cell used for FTIR spectroscopy. (Courtesy of Perkin-Elmer).

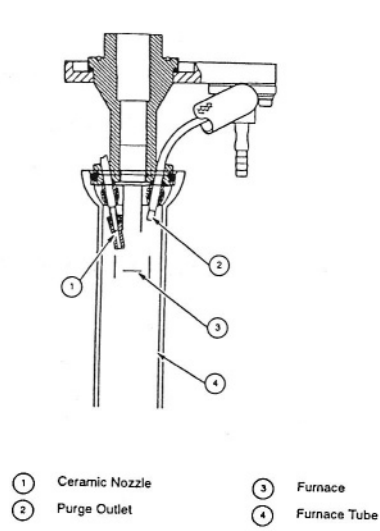

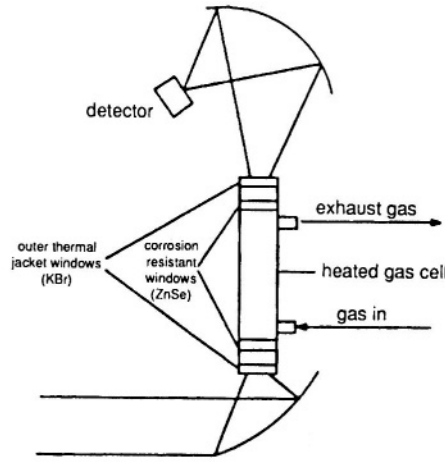

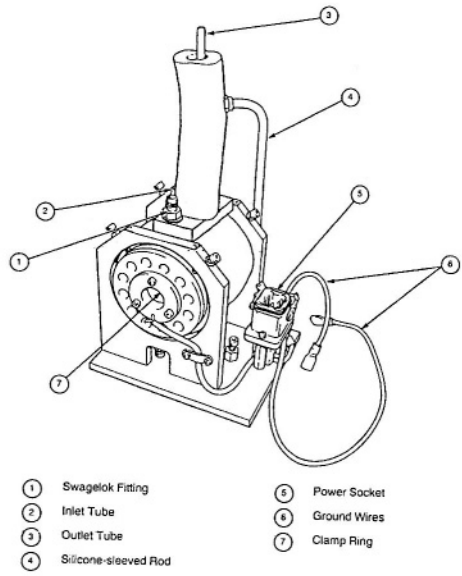

Figure 8.5
Presentation of TG-FTIR results. (Courtesy of Perkin-Elmer.)
(a) The TG curve for the dehydration and subsequent decomposition of calcium oxalate monohydrate, compared with a Gram-Schmidt plot (overall integrated intensity of IR absorption as a function of temperature).
(b) The Gram-Schmidt plot compared with that for the evolution of carbon monoxide.
(c) The Gram-Schmidt plot compared with that for the evolution of carbon dioxide.

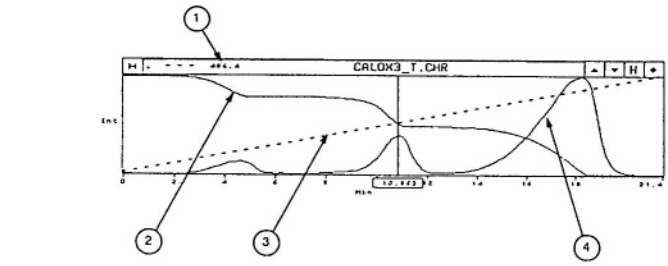

1 Temperature (°C)
2 Weight-Loss Curve
3 Temperature Profile
4 Gram-Schmidt Thermogram

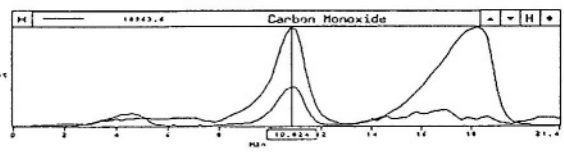

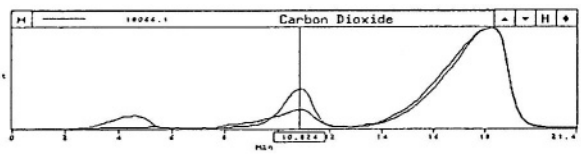

Figure 8.6
DTA and EGA curves for $CuSO_4.5H_2O$ using non-dispersive infrared analyzers [19] for analysis of H_2O and SO_2. (With the permission of Wiley-Heyden Ltd.)

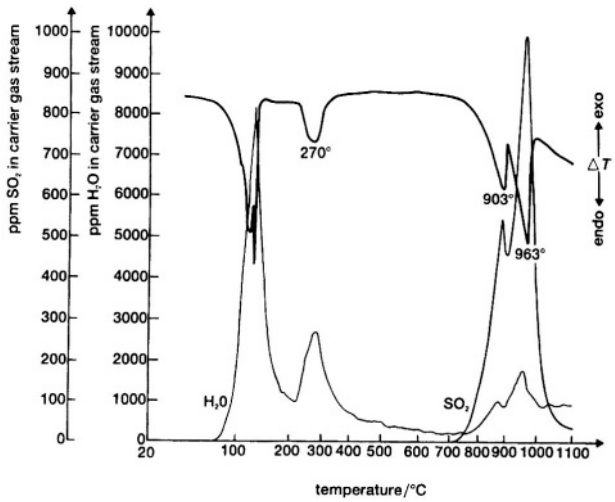

The vast literature of gas-solid chromatography is available in deciding upon a suitable set of analysis conditions for a given sample and its expected products. Two useful references on the analysis of mixtures of the more commonly-encountered gases are the books by Hachenburg [22] and Thompson [23].

A major disadvantage of TG-MS and TG-FTIR, when applied to samples such as polymers which degrade to produce a variety of complex fragments simultaneously, is the lack of separation of products before analysis. The resulting MS or FTIR data are then very difficult to interpret. Lever et al. [24,25] have described the use of sorbent tubes, as an alternative to cold traps, for condensing the gases for later analysis by GC-MS. The suggested name for the technique is Evolved Gas Collection. The collection tube can be coupled to the inlet of the GC-MS and the volatiles are thermally desorbed. A portion of the gas can be readsorbed for further GC-MS experiments. Price et al. [26,27] have used a similar technique in combination with a scanning thermal microscope (see also Chapter 5).

8.6 Special-purpose Detectors

There is no reason, in principle, why any means of analyzing gases should not be coupled to a thermal analysis instrument, and there are reports of the use of absorbents and volumetric methods for the determination of total amounts of evolved gases. Detailed information on the evolution of each component with time is, however, most desirable. Water-vapour is a very common product of thermal decompositions, as well as being a product of the reduction of metal oxides with hydrogen, and special detectors have been

developed to monitor evolution of water, in addition to the use of non-dispersive infrared analyzers described above [20]. Many of the common methods for determining the water content of gases are not entirely suitable when the water content is varying fairly rapidly, on account of slow and/or non-linear detector responses. For EGA the response of the detector should also be selective for water as other products may be evolved simultaneously.

Warrington and Barnes [28] have shown that an electrolytic hygrometer is suitable for continuous water analyses. The hygrometer has two fine platinum wires wound closely, but not in contact, on a PTFE former. The wires are coated with phosphoric acid and the whole element is enclosed in a flow-through glass tube which may be coupled to the outlet of a TA apparatus. At the start, the acid is electrolysed to dryness using a potential of 100 V between the two wires, and, in this state, there is then a negligible current between the two wires. The acid coating absorbs any water from the gas stream passing through the tube and this water is then electrolysed. The electrolysis current is proportional to the water concentration in the gas. Precautions necessary to avoid spurious effects are described [28], and the system was tested on the dehydration of several hydrates and the decompositions of several carboxylic acids.

Gallagher *et al.* [29,30] developed an EGA system based on a Panametrics Model 700 Moisture Analyser in which the moisture content is determined from the dew point of the gas stream and the flow rate. The relationship is non-linear and the computations are described [29]. Allowance has to be made for background moisture in the gas stream and for degassing of the TA apparatus as the temperature rises, as well as loss of moisture by adsorption on cooler surfaces of the system.

Morgan [20] has described an electrolytic detector for SO_2 analysis based on a fuel cell. SO_2 in the carrier gas diffuses through a semi-permeable membrane and is adsorbed on a sensing electrode, producing a current in the circuit which is proportional to the partial pressure of SO_2 in the carrier gas. Calibration using a standard gas mixture is required.

Cote *et al.* [31] have discussed the use of solid electrolytes of K_2SO_4 for analysis of SO_2 and K_2CO_3 for CO_2. The latter has been used in a study of the decomposition of $CaCO_3$.

Chemical conversion agents have been suggested to simplify the final analysis, e.g. use of I_2O_5 to convert CO to CO_2 and of CaC_2 to convert H_2O to C_2H_2 for easier GC analysis. The kinetic aspects of these processes introduce undesirable uncertainties in EGA.

New sensors are regularly being developed and reported in the literature. Some of these will undoubtedly find application in EGA systems of the future.

8.7 Applications of EGA

Knaepen et al. [32] used TG coupled with MS and FTIR, as well as DSC, to study the thermal decompositions of a range of hydrated strontium oxalates, $SrC_2O_4.xH_2C_2O_4.yH_2O$. Their results are illustrated in Figure 8.7. The TG, DTG and DSC curves and the MS traces for water CO and CO_2 are shown. The initial endothermic process is dehydration, while the higher temperature endothermic decomposition stages of the oxalate group give rise to mixtures of CO and CO_2 in different proportions as shown. Detailed decomposition mechanisms were proposed [32].

Figure 8.7
TG, DTG, DSC and MS curves for the thermal decomposition of hydrated strontium oxalates, heated at 10 K min^{-1} in an argon atmosphere [32]. (With the permission of Thermochimica Acta.)

TG and DTG

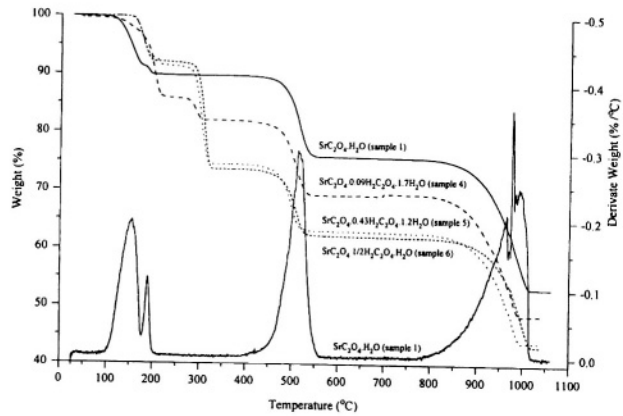

DSC

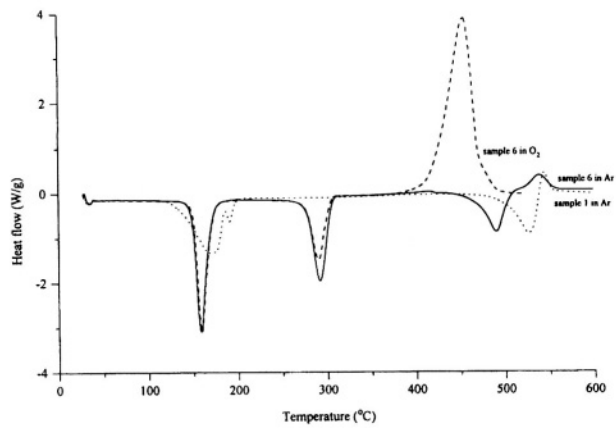

Figure 8.7 Continued
TG, DTG, DSC and MS curves for the thermal decomposition of hydrated strontium oxalates, heated at 10 K min^{-1} in an argon atmosphere [32]. (With the permission of Thermochimica Acta.)

MS

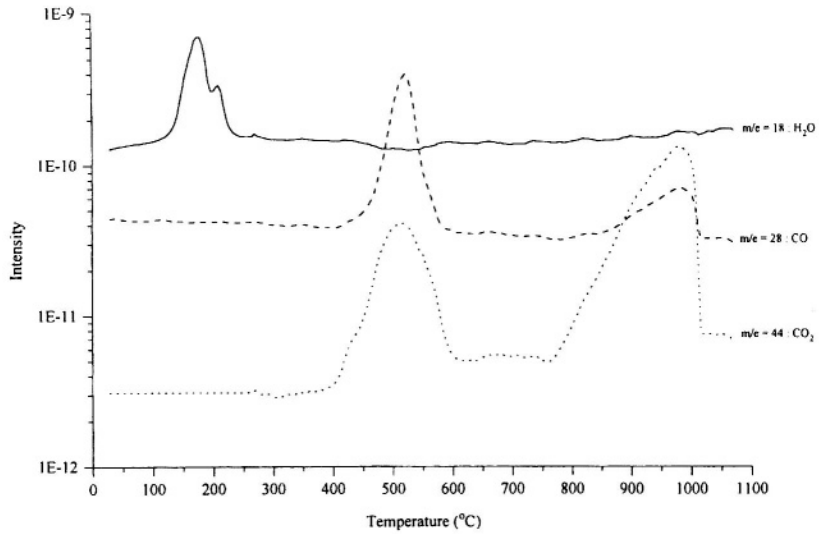

FTIR

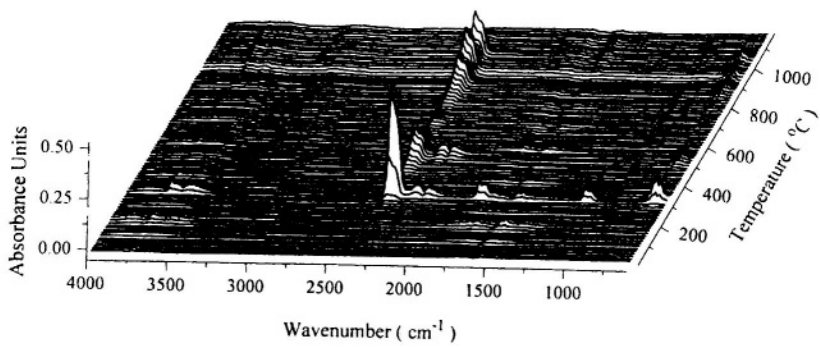

Dei and Guarini [33] used DSC-FTIR to show that a small endothermic event that precedes the main decomposition of commercial $NaHCO_3$ involves the simultaneous evolution of water and CO_2. This was interpreted as water-assisted decomposition of portions of the surface to carbonate.

Raemaekers and Bart [34] have provided a comprehensive review of the applications of TG-MS in polymer analysis, including the characterization of homopolymers, copolymers, polymeric blends and composites, residual monomers, solvents, additives, and toxic degradation products. When using TG-MS for degradation studies (see, for example, Figure 8.8 [35]), slow heating rates are recommended so that kinetic factors can result in some separation of the gaseous products. Polymer identification requires a higher mass number range than needed for most degradation studies. The relative merits of electron impact and chemical ionization techniques are discussed. For complex mixtures, tandem mass spectrometers may be desirable.

Figure 8.8
TG-FTIR of polystyrene heated in 50 mL min^{-1} air at 20 K min^{-1} [35]. (With the permission of Elsevier, Amsterdam.)

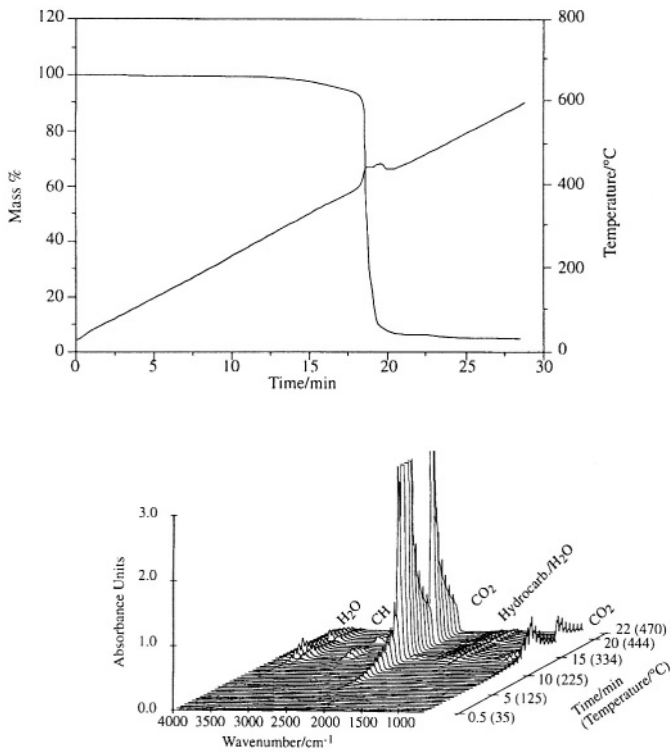

Kettrup *et al.* [36] have described the design of a macro TA-MS system for use in the analysis of samples of environmentally important materials, such as garbage, contaminated soil, etc., where large samples are necessary to obtain representative results. Evolved gases were also adsorbed on suitable resins for subsequent GC-MS. Reggers *et al.* [37] have applied a number of TA - EGA techniques to a variety of waste materials.

Most of the references to the instrumental systems described above also give some examples of their virtually unlimited applications. As a typical example of a practical situation, information on the gaseous products, especially hazardous products such as HCℓ and HCN, formed during the degradation of polymers is essential for the safe use of polymers in high temperature environments.

8.8 Pulsed Gas Thermal Analysis

Maciejewski et al. [5] have introduced a technique which they have named pulse thermal analysis (PTA). Because of possible ambiguity concerning the property of the system to which the 'pulse' refers and hence possible confusion with one of the many variations of modulated temperature techniques (see Chapter 4), the technique will be referred to here as pulsed *gas* thermal analysis. Gallagher [3] has suggested the name 'consumed gas analysis'. The method is based on the injection of a known amount of gaseous reactant into an inert carrier gas stream which then passes over or through a solid reactant in the sample pan of a TG or DSC or DTA instrument. The changes in the composition of the gas stream, as well as any mass (TG) and/or enthalpy changes (DSC or DTA) are monitored and related to incremental extent of reaction resulting from each pulse of gas. The reactions that can be studied include reduction and oxidation of solids and heterogeneous catalytic processes on solid surfaces. The technique has the advantage that the solid reactant can be brought to the desired temperature under an inert atmosphere before the reactive gas is injected. Reaction thus takes place at a well-defined temperature. The incremental amounts of reaction can be controlled by the amount of reactant gas injected in a pulse.

As an example, Maciejewski *et al.* [5] used the isothermal reduction of CuO by hydrogen at 450°C, see Figure 8.9. Each pulse extended the fractional reaction by 0.035. The MS signal for water ($m/z = 18$) shows that the desorption of water produced during CuO reduction is slow.

Figure 8.9
The isothermal reduction of CuO by hydrogen at 450°C [5]. (With the permission of Thermochimica Acta.)

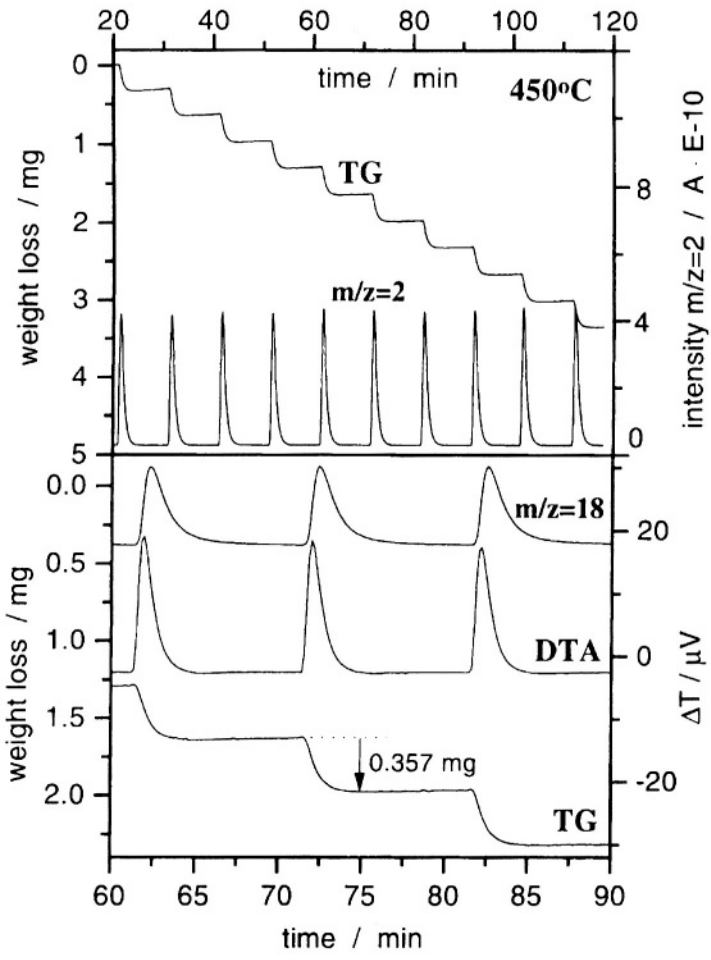

References

1. J. Mullens, “Handbook of Thermal Analysis and Calorimetry”, Vol.1, (Ed. M.E. Brown), Elsevier, Amsterdam, 1998, Ch.12.
2. E. Kaiserberger (Ed.)”Coupling Thermal Analysis and Gas Analysis Methods”, Special Issue of Thermochim. Acta, 295 (1997) 1-186.
3. P.K. Gallagher, “Thermal Characterization of Polymeric Materials”, (Ed. E.A. Turi), Academic, San Diego, 2nd Edn, 1997, Ch. 1.
4. S.B. Warrington in “Thermal Analysis: Techniques and Applications”, (Eds E.L. Charsley and S.B. Warrington), Royal Society of Chemistry, Cambridge, 1992, p.84.
5. M. Maciejewski, C.A. Müller, R. Tschan, W.D. Emmerich and A. Baiker, Thermochim. Acta, 295 (1997) 167.
6. E. Kaiserberger and E. Post, Thermochim. Acta, 295 (1997) 73.
7. A. Hallbrucker and E. Mayer, J. Thermal Anal., 35 (1989) 1733.
8. W.D. Emmerich and E. Kaiserberger, J. Thermal Anal., 17 (1979) 197; Proc. 7th ICTA, Vol.1, (Ed. B. Miller) Wiley, Chichester, 1982, p.279.
9. G. Szekely, M. Nebuloni and L.F. Zerilli, Thermochim. Acta, 196 (1992) 511.
10. E. Kaiserberger and E. Post, Thermochim. Acta, 324 (1998) 197.
11. K. Jaenicke-Rossler and G. Leitner, Thermochim. Acta, 295 (1997) 133.
12. B. Roduit, J. Baldyga, M. Maciejewski and A. Baiker, Thermochim. Acta, 295 (1997) 59.
13. M. Maciejewski and A. Baiker, Thermochim. Acta, 295 (1997) 95.
14. J.M. Criado, C. Real, A. Ortega and M.D. Alcala, T. Thermal Anal., 36 (1990) 2531.
15. R.L. Schmid and J. Felshe, Thermochim. Acta, 59 (1982) 105.
16. M. Statheropolous, S. Kyriakou and N. Tzamtzis, Thermochim. Acta, 322 (1998) 167.
17. I.D. Sills and S. He, Thermochim. Acta, 339 (1999) 125.
18. S.A. Liebman, D.H. Ahlstrom and P.R. Griffiths, Appl. Spectrosc., 30 (1976) 355.
19. W.M. Groenewoud and W. de Jong, Thermochim. Acta, 286 (1996) 341.
20. D.J. Morgan, J. Thermal Anal, 12 (1977) 245.
21. J.H. Slaghuis and P.M. Morgan, Thermochim. Acta, 175 (1991) 135.
22. H. Hachenburg, "Industrial Gas Chromatographic Trace Analysis", Heyden, London, 1973.
23. B. Thompson, "Fundamentals of Gas Analysis by Gas Chromatography", Varian, Palo Alto, 1977.
24. T.J. Lever, D.M. Price and S.B. Warrington, Proc. 28th NATAS, (2000) 720.
25. D. Roedolf, T.J. Lever, D.M. Price and K. Schaap, Proc. 12th ICTAC, (2000) paper PI-9.
26. D.M. Price, M. Reading, T.J. Lever, A. Hammiche and H.M. Pollock, Proc. 12th ICTAC, (2000) paper O-20.
27. D.M. Price, M. Reading and R.M. Smith, Proc. 28th NATAS, (2000) 705.

28. S.B. Warrington and P.A. Barnes, Proc. 6th ICTA, Vol.1, (Ed. H.G. Wiedemann), Birkhaeuser Verlag, Basel, 1980, p.327.
29. P.K. Gallagher, E.M. Gyorgy and W.R. Jones, J. Thermal Anal., 23 (1982) 185.
30. P.K. Gallagher and E.M. Gyorgy, Proc. 6th ICTA, Vol.1, (Ed. H.G. Wiedemann), Birkhaeuser Verlag, Basel, 1980, p. 113.
31. R. Cote, C.W. Bale and M. Gauthier, J. Electrochem. Soc., 131 (1984) 63.
32. E. Knaepen, J. Mullens, J. Yperman and L.C. van Poucke, Thermochim. Acta, 284 (1996) 213.
33. L. Dei and G.G.T. Guarini, J. Thermal Anal., 50 (1997) 773.
34. K.G.H. Raemaekers and J.C.J. Bart , Thermochim. Acta, 295 (1997) 1.
35. J. Mullens, R. Carleer, G. Reggers, M. Ruysen, J. Yperman and L.C. Van Poucke, Bull. Soc. Chim. Belg., 101 (1992) 267.
36. A. Kettrup, G. Matuschek, H. Utschick, Ch. Namendorf and G. Bräuer, Thermochim. Acta, 295 (1997) 119.
37. G. Reggers, M. Ruysen, R. Carleer and J. Mullens, Thermochim. Acta, 295 (1997)107.

LESS-COMMON TECHNIQUES

9.1 Introduction

Some of the techniques of thermal analysis, based on the monitoring of less-obvious properties of a sample and often requiring more specialized equipment, are grouped, for convenience, under the heading of less-common techniques [1], These techniques include Emanation Thermal Analysis (ETA), Thermoelectrometry and Thermosonimetry. A few interesting techniques that are difficult to classify are described at the end of this Chapter, under Miscellaneous.

9.2 Emanation Thermal Analysis (ETA) [1-10]

9.2.1 Introduction

Emanation thermal analysis (ETA) involves the measurement of the release of inert (and usually radioactive) gas from an initially solid sample, while the temperature of the sample, in a specified atmosphere, is programmed. The rate of release of gas is used as an indication of the changes taking place in the sample. Comparison of ETA results with those from thermogravimetry (TG) and evolved gas analysis (EGA) provides information about the microstructure of the sample.

Most of the solids to be studied do not naturally contain inert gas and the solubility of inert gases in inorganic solids is small. The inert gases are trapped at lattice imperfections and these defects can serve as both traps and diffusion pathways. The migration of inert gases in solids is discussed in reference [3].

9.2.2 Sample preparation

There are several techniques for incorporating inert gas in a solid sample. These techniques can be divided broadly into two groups: (A) techniques for introducing the *parent* nuclide of the inert gas, e.g.

$$^{228}\mathrm{Th} \xrightarrow{\alpha} {}^{224}\mathrm{Ra} \xrightarrow{\alpha} {}^{220}\mathrm{Rn}$$

(see Figure 9.1) or (B) techniques for introducing the inert gas itself. Labelling with parent nuclide gives a sample which is stable for longer as far as a source of inert gas is concerned. Gas is being formed continuously and will not all be lost in a single run on the sample. The recoil mechanism associated with the release of the inert gas has to be taken into account. The following methods have been used:

Figure 9.1
Sample labelling by recoil ion implantation [1,2]. ^{228}Th and ^{224}Ra were adsorbed on the surface and ^{220}Rn was produced by the sequence ^{228}Th → ^{224}Ra → ^{220}Rn.
(With the permission of Thermochimica Acta.)

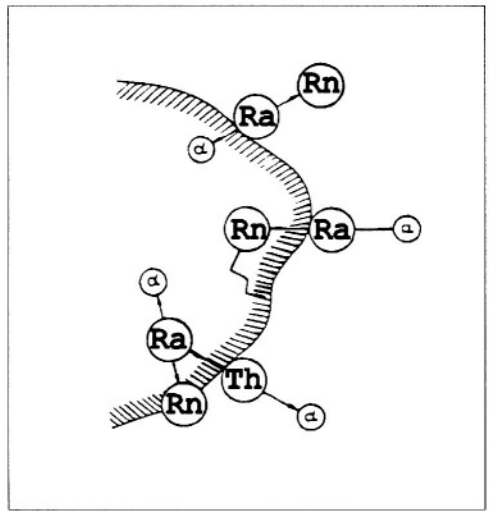

A1: Coprecipitation of parent isotopes. The disintegration process ensures a random distribution of the products.

A2: Impregnation of the sample with a solution of parent isotope. This method is used when coprecipitation is not possible. Parent atoms are distributed only on the surface. Disintegration results in penetration of the daughter atoms into crystallites but, unless the crystallites are small, the distribution is non-uniform. The distribution may be improved by annealing the sample.

A3: Nuclear reactions may be used to produce the parent nuclide or the inert gas, e.g.,

$$^{88}\mathrm{Sr} \xrightarrow{n,\alpha} {}^{85}\mathrm{Kr}$$

$$^{44}\mathrm{Ca} \xrightarrow{n,\alpha} {}^{41}\mathrm{Ar}$$

$$^{127}\mathrm{I} \xrightarrow{n,p} {}^{128}\mathrm{I} \rightarrow {}^{128}\mathrm{Xe}$$

B1: Ion bombardment is a common method of implanting inert gas atoms in solids. The ions may be generated in vacuum using an electrical discharge or a microwave plasma. The quantity of gas absorbed depends on the gas used, the energy of bombardment and the nature of the solid.

B2: Diffusion at high temperature and/or pressure is also sometimes possible. ^{85}Kr is usually used. (Solids labelled with ^{85}Kr are called kryptonates. $t_{½}$ = 10.76 years for β-emission).

B3: Crystallization or sublimation of the sample in an inert gas atmosphere may be more effective in incorporating the gas.

9.2.3 Apparatus for measurement of gas release

ETA is usually carried out in conjunction with other TA techniques, e.g. NETZCH markets ETA/DTA/EGA apparatus. Carrier gas, at an accurately controlled flow-rate is used to carry released gas to suitable counting chambers. Rn, an α-emitter, requires a scintillation counter, or an ionization chamber or semi-conductor detector, while Geiger counters are used for Kr, Xe and Ar (β-emitters). For experiments lasting a long time compared with the half-life of the inert gas used, the decay of the measured gas should be taken into account. A typical ETA apparatus is shown schematically in Figure 9.2.

Figure 9.2
Schematic diagram of an ETA apparatus (based on reference [6]).

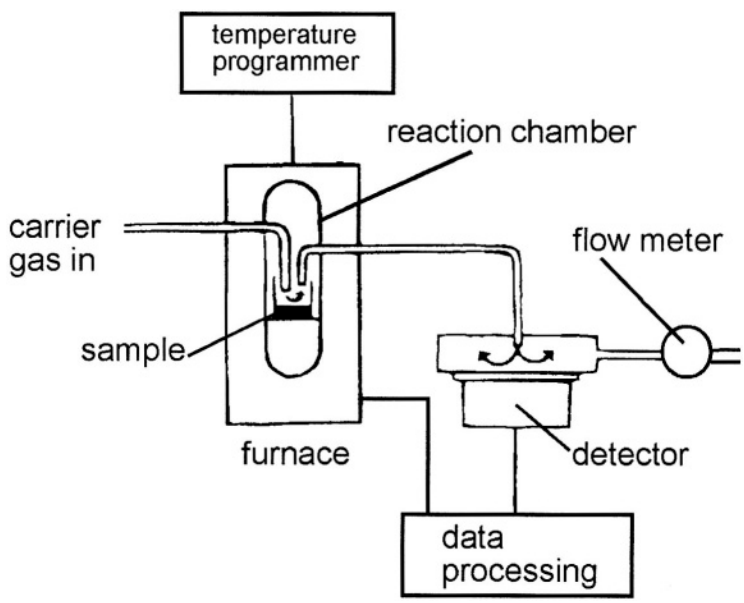

9.2.4 Rate of gas release

Details of the gas release are very dependent upon the way in which the sample was originally labelled. Release may involve either bulk or defect diffusion. There may also be recoil ejection. The emanating power, E, is defined as:

$$E = (dN_{rel} / dt)/(dN_{form}/dt)$$

where dN_{rel} / dt is the release rate and dN_{form}/dt is the formation rate. dN_{form}/dt may be measured by dissolution of the sample in acid or other solvent and measurement of the gas released.

It is of interest that TG and EGA curves obtained during release of gaseous products of thermal decomposition may not correlate exactly with ETA curves. Beckman and Balek [8] have used gas percolation theory to model gas release during ETA experiments. Their latest model [8] for the sample consists of three solid components with different gas diffusion coefficients and extends their earlier two-component model [7]. The initial solid reactant has a low diffusion coefficient, as does the final, stable product. The solid intermediate is highly disordered and permeable. The initial distribution of inert gas in the sample is not assumed to be uniform, whereas the formation of gaseous products by thermal decomposition is assumed to be uniform. The total emanating power of the sample is taken to be the sum of the values for the three individual components.

During the initial stages of reaction [8], isolated clusters of the intermediate phase are totally surrounded by reactant but, later, these clusters become interconnected allowing gaseous products to migrate. The intermediate phase converts to the final product and, in the final stages of decomposition, isolated clusters of residual reactant and/or intermediate phase can be totally surrounded by stable product.

Isothermal gas-release curves for the three-component model were calculated [8] (see Figure 9.3) for different proportions of each of the three components. The shapes of the curves are strongly dependent upon the values of E_1, E_2 and E_3, as well as upon the rate coefficient for the thermal decomposition reaction and a structural relationship factor [8]. This makes ETA a sensitive, although possibly difficult to interpret, means of exploring microstructural changes during solid state reactions.

Figure 9.3
Calculated isothermal gas-evolution curves for the three-component model [8] with various contributions, E_1: E_2: E_3 from the components: 1 (reactant), 2 (intermediate) and 3 (product). (a) 0.4 : 0.4 : 0.4 ; (b) 0.04 : 1.0 : 0.4 ; (c) 0.4 : 1.0 : 0.04 ; (d) 1.0 : 0.05 : 1.0; (e) 0.1 : 0.1 : 1.0. (With the permission of the Journal of Thermal Analysis and Calorimetry.)

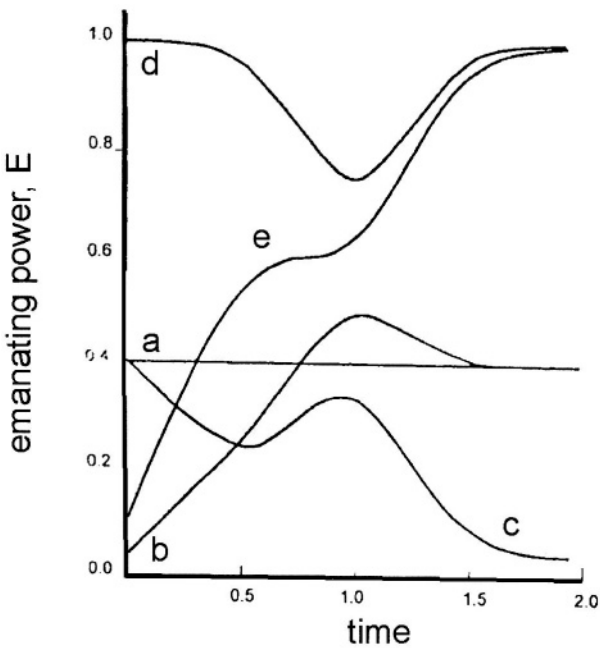

9.2.5 Applications of ETA

One of the major uses of ETA is in the characterization of powders. Emanating power is related to surface area and hence changes in grain size and the occurrence of sintering during heating may be detected.

Figure 9.4 shows a series of isothermal ETA curves for NiO samples, prepared from the carbonate. These curves, obtained in a nitrogen atmosphere, were used [3] to determine the kinetic parameters for sintering of the samples. The apparent activation energy of 276 kJ mol^{-1} was decreased to 155 kJ mol^{-1} when a similar series of runs were done in oxygen. Phase changes also show up as changes in emanating power, e.g. the orthorhombic to rhombohedral phase transition of KNO_3 at 128°C is seen in Figure 9.5.

Figure 9.4
A series of isothermal ETA curves for NiO samples in nitrogen [3]. (With the permission of Elsevier, Amsterdam.)

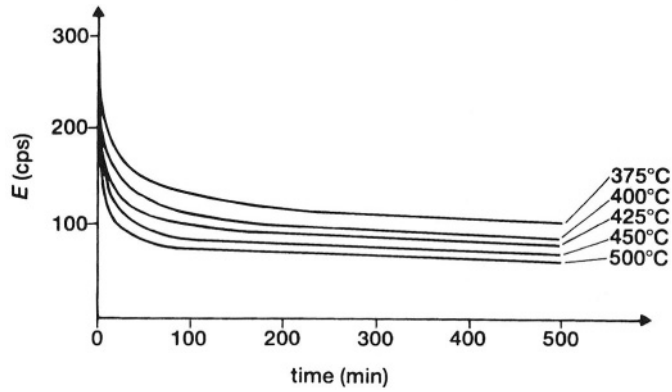

Figure 9.5
ETA curves for the heating (1) and cooling (2) of KNO_3 through the orthorhombic-rhombohedral phase transition at 128°C [3,4]. (With the permission of Elsevier, Amsterdam.)

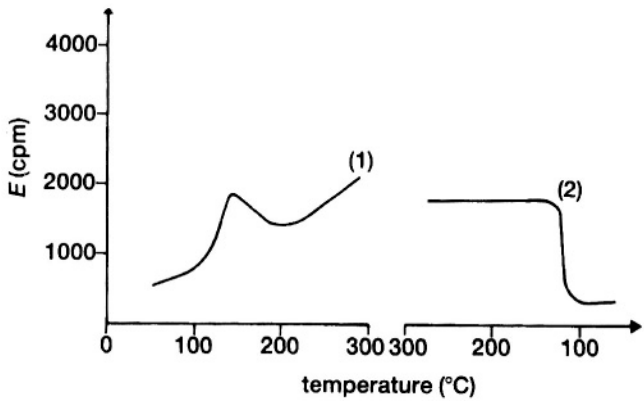

Solid-gas reactions have also been studied [1], e.g. the oxidation of labelled metals or reduction of labelled oxides. ETA and EGA curves are in good agreement. Information on solid-liquid reactions, e.g. the hydration of cement, has been obtained. In both solid-gas and solid-liquid reactions the formation of a layer of solid product may hinder emanation.

For solid-solid reactions such as spinel formation [3,5], e.g.,

$$ZnO(s) + Fe_2O_3(s) \rightarrow ZnFe_2O_4(s)$$

with ZnO labelled with ^{228}Th, the emanation of the individual components is checked first. ETA traces for the reaction are shown in Figure 9.6. The oxides interact in a series of stages. Product begins to form by surface diffusion between 250 and 400°C as shown by the increased emanation (curve 3). The DTA and thermodilatometry (TD) curves (curves 2 and 1 in Figure 9.6) show no changes at these temperatures. Sharp changes in all of the curves in Figure 9.3 are observed at 670 to 700°C. The exotherm on the DTA curve is small, but the increased emanation (curve 3) shows up clearly. This corresponds to interaction by volume diffusion. The reaction is complete by about 800°C. The dilation shown in curve 1 is suggested [3] to be caused by the formation of a very finely powdered product which sinters at higher temperatures. The ETA curve during the second heating of the reaction mixture (curve 4) shows that reaction was complete during the first heating. The reactivities of different preparations of Fe_2O_3 have been compared using this technique [3],

Figure 9.6
Spinel formation by the reaction: $ZnO(s) + Fe_2O_3(s) \rightarrow ZnFe_2O_4(s)$
Curve 1 is the thermodilatometric (TD) measurement, curve 2 the DTA, and curve 3 the ETA trace. The ETA trace during reheating of the reacted mixture is shown in curve 4 [3,5]. (With the permission of Elsevier, Amsterdam.)

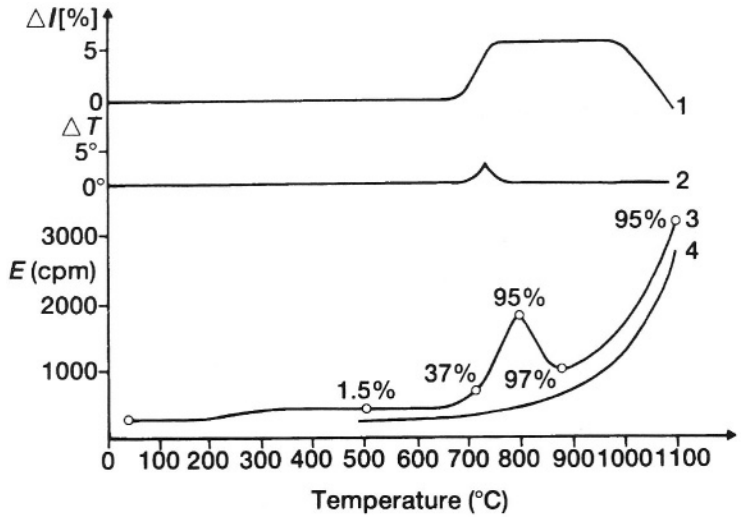

The main drawback about ETA is that preparation and handling of samples requires all the usual radiochemical facilities and precautions. The amounts used in samples are so small that evolved gas, after dilution with carrier, does not form a hazard. Inert gases are not incorporated biologically and the decay products are stable, so hazards are reduced.

9.3 Thermosonimetry (TS) and Thermoacoustimetry

9.3.1 Introduction

In thermosonimetry (TS), sound waves emitted by a sample (acoustic emission) [11,12] are measured as a function of temperature during a controlled heating programme. The sounds emitted arise from the release of thermal stresses in the sample, e.g., movement of dislocations, generation and propagation of cracks, nucleation of new phases, relaxation processes and discontinuous changes in physical properties. At the glass transition temperature, a discontinuous change in free volume generates elastic waves which cause an acoustic effect. The limit of detection of a burst of acoustic emission has been estimated [11] as about 1 fJ and the frequencies involved range from audio to several MHz. The stress-relief processes described above are not generally detectable by the more conventional thermal analysis techniques, on account of their low energy, and thus TS may be used, amongst other applications (see below), to assess radiation damage, defect content and the degree of annealing of samples. It is also a sensitive technique for detecting the mechanical events associated with dehydration, decomposition, melting, etc. [13,14].

In thermoacoustimetry, the characteristics of imposed acoustic waves after passing through a sample, are measured as a function of temperature while the sample is subjected to a controlled temperature programme.

9.3.2 Apparatus for thermosonimetry

The sounds are emitted as mechanical vibrations prior to and during thermal events in the sample. This sonic activity in the sample is picked up and transmitted by means of a specially adapted stethoscope. The mechanical waves are converted to electrical signals by conventional piezoelectric transducers. The stethoscope is made of fused silica (up to 1000°C), or ceramics or noble metals for higher temperatures. The sample is held in the sample head which acts as an acoustic transformer and is connected via a transmitting rod to a piezoelectric sensor, fixed on a heavy recoil foundation and a seismic mount to prevent interference from external noise. A schematic diagram of the apparatus [15,16] is shown in Figure 9.7. The properties of the transducer may vary with temperature, so the waveguiding system is used to transmit the acoustic emissions from the heated sample to the transducer at ambient temperature. Contact surfaces must be well polished and thin films of silicone oil improve signal transfer. Direct insertion of a thermocouple in the sample can cause severe mechanical damping, so the thermocouple is usually placed as close as possible to the sample without actually touching it.

Figure 9.7
Schematic apparatus for thermosonimetry [15,16].

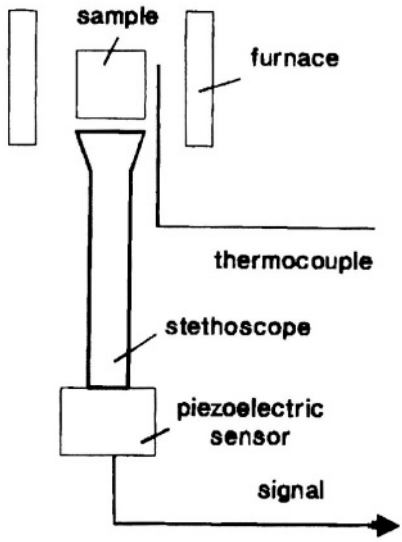

Simultaneous TS - DTA measurements have been reported [17-20]. Such a system has been used [18] to examine the transitions in the ICTAC standards. Lee *et al.* [21] have combined thermodilatometry and TS.

9.3.3. Interpretation

The output from a thermosonimetry experiment consists of a rapid cascade of decaying signals, which may be recorded as: (i) the number of signals of peak amplitude greater than a set threshold value in a given time; or (ii) the time for which the signal amplitude exceeds the threshold value; or (iii) the number of times that signals pass through a chosen voltage level in a positive direction; or (iv) the root-mean-square amplitude level (energy); or (v) as a set of frequencies. The Nyquist theorem requires that the sampling frequency should be at least twice that of the maximum frequency component present in the signal. Because chemical acoustic emission usually occurs in bursts, continuous recording of high frequency data is usually replaced by data acquisition only when the signal exceeds a set threshold. Choice of this threshold relative to the background noise is discussed by Wade *et al.* [22].

Frequency distributions of the TS signals are obtained [18] by timing the intervals between the amplitude components of the decaying signal. The time intervals are converted into pulse heights which are fed to a multi-channel analyzer to give a display of the frequency distribution.

Wentzell and Wade [23] investigated (i) the reproducibility of power spectra from a given chemical system; (ii) the dependence of the spectra on the transducer used; and (iii)

whether the information obtained in the spectra was sufficient to distinguish amongst the different processes which could be occurring. They found that reproducibility of spectra obtained with the same transducer was good, but that reproducibility between transducers was not as good. Transducer response remained reasonably constant over several months of use.

Relationships have been sought between the frequency distributions and the processes occurring in the sample. In the simplest case, frequency distributions can be used as 'fingerprints' of sample origin. Detailed interpretation is complex and empirical pattern recognition methods have been suggested [24,25]. Wentzell *et al.* [24] evaluated possible descriptors obtained from AE signals for use in characterizing the processes giving rise to the signals. Descriptors were grouped into four categories: (i) those associated with the absolute magnitude of the signal; (ii) those related to the rate of decay of the signal; (iii) those measuring the central tendency of the power spectrum, and (iv) those characterizing the dispersion of the power spectrum. The conclusion reached [24] was that "acoustic emission will present a challenge to modern pattern recognition methods", and the subtlety of the information obtainable was emphasized.

Although interpretation of power spectra is complicated by distortion of the acoustic signal by instrumental factors, the main features of the spectra could be associated [23] with fundamental processes occurring in the systems examined, e.g., bubble release was associated with low frequencies and crystal fracture with high frequencies.

The particle size, mass, chemical nature and form (e.g., single crystals, powder) of the sample all affect the TS signal and the TS curves also vary with the resonance frequency of the piezoelectric sensor [19]. The resonance frequencies of the sensors used by Shimada [19] were 140 kHz, 500 kHz, 1 MHz and 1.5 MHz. For power spectra, a wideband sensor (300 kHz to 2 MHz) was used.

9.3.4 Apparatus for thermoacoustimetry

In the apparatus used by Mraz *et al.* [26], a pair of lithium niobate transducers are in contact (under a constant pressure of about 300 kPa) with opposite faces of the sample (Figure 9.8). One transducer induces the incident acoustic signal and the other detects the transmitted signal. Thermal expansion of the sample during the heating programme is monitored continuously with a linear variable differential transformer (LVDT), so that changes in sample dimensions can be allowed for in the calculations. Arrangements are made for atmosphere control around the sample.

Figure 9.8
Schematic apparatus for thermoacoustimetry [26]. (With the permission of Elsevier, Amsterdam.)

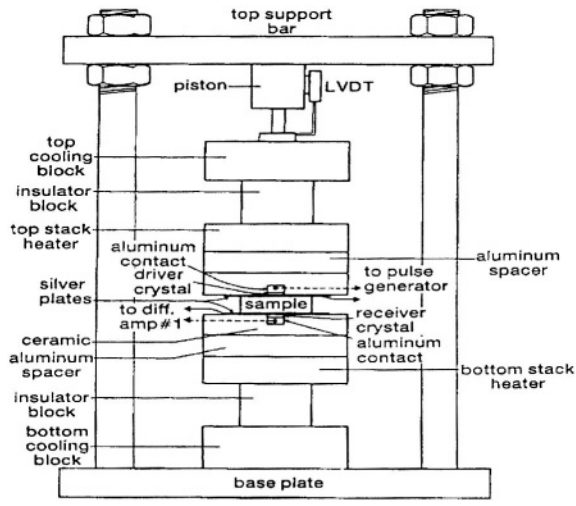

The incident signal is generated by a pulse generator. The transmitted signal received by the second transducer is inverted and amplified and an attenuated version of the driving pulse is added to this output signal. This summation procedure enables detection of the first-arrival times of both the compressional (P) and shear (S) waves. The velocities of the P and S waves and hence the various elastic moduli are then computed at set temperature intervals, and the final result is a plot of velocity or modulus against temperature. The instrument was calibrated with an aluminium standard for which the P and S wave velocities were accurately known.

The apparatus described by Kasap and Mirchandan [27] (Figure 9.9) operates from room temperature to 350°C. The sample is loaded between two identical glass rods, one of which is stationary and the other vertically movable. Transducers and thermocouples are attached to the rods and not the sample.

Figure 9.9
Schematic apparatus for thermoacoustimetry [27].

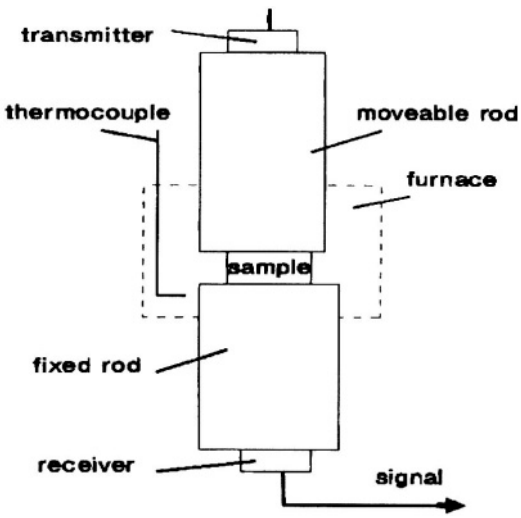

Samples are in the form of sheets or pellets. Blank experiments are carried out with the two glass rods in contact. The ultrasonic transit time through the sample is obtained from the time delay between the through signal and the echo signal. The through signal travels the length of both rods plus the sample length. The echo signal travels the length of the top rod and back, allowance also has to be made for travel time through the coupling regions at the interfaces. Absolute determination of the ultrasonic velocity is usully unnecessary - only the variation with temperature. The use of the through and echo signals eliminates the influence of temperature variations in the glass rods.

The change in attenuation, V_a, of the ultrasonic waves with temperature is obtained by measuring the peak-to-peak amplitude of the through signal, $V_{p\text{-}p}(T)$, at temperature T and relating it to the value at a reference temperature, T_o.

$$V_a = - (1/L_S) \ln [V_{p\text{-}p}(T)/V_{p\text{-}p}(T_o)]$$

(where L_S is the path length through the sample). Kasap and Mirchandan [27] illustrated the operation of their system with curves of $\ln [v_T/v_{300}]$ and of V_a against T (where v_T is the ultrasonic velocity at T) for various materials exhibiting glass transitions. The $\ln [v_T/v_{300}]$ plots showed distinct changes in slope at T_g, while the V_a plots showed peaks. The features of the thermoacoustic curves were clearly related to DSC and microhardness measurements.

Ravi Kumar *et al.* [28] have given a detailed description of the thermoacoustical parameters of polymers.

9.3.5 Applications of thermosonimetry and thermoacoustimetry

TS curves are usually used in combination with other thermoanalytical results to characterize a sample. TS curves on kaolins [15] show two regions of increased activity (Figure 9.10). Comparing results obtained by TS with those obtained by TG and DTA, these regions have been identified as dehydroxylation (500-600°C) followed by recrystallisation (980-985°C) to the metakaolin structure. TS examination of the thermal decomposition of a powdered sample of brucite ($Mg(OH)_2$) [15], suggested that dehydroxylation occurs in a stepwise fashion with successive bursts of reaction as the sample breaks up. The barrier effect which has to be overcome was not identified.

Figure 9.10
TS curve for a kaolin sample [15], showing two regions of increased activity. (With the permission of John Wiley & Sons, Chichester.)

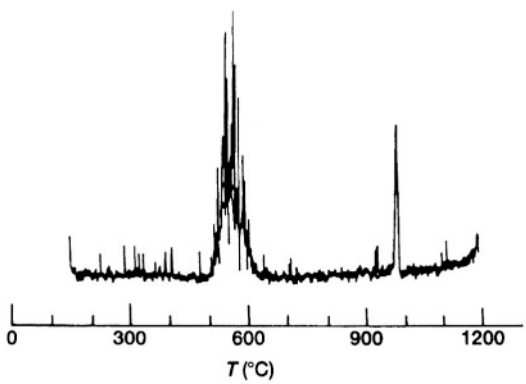

The frequency distributions obtained [18] on heating samples of K_2SO_4 (a) and $KClO_4$ (b) to their transition temperatures of 582°C and 299°C, respectively, are shown in Figure 9.11. The pre-transition activity in $KClO_4$ involves release of included fluid, while that in K_2SO_4 corresponds to generation of micro-cracks. The frequency distribution for K_2SO_4 shows fewer low frequency components. Frequency distributions for the dehydration steps in $CuSO_4.5H_2O$ are qualitatively similar to those of $KClO_4$, again through the fluid loss processes. A combined TS - DTA study of $KClO_4$ [17] identified the two regions of increased acoustic activity with the phase transition (orthorhombic to cubic) (200 to 340°C) and melting accompanied by decomposition (560 to 660°C). The onset of the lower temperature TS peak was well below the transition temperature (298 ° C) indicating that mechanical changes occur in the sample particles prior to the transition. Solidification of the KCl product of decomposition was detectable by TS but not on the DTA curve.

In a series of further papers, Shimada *et al.* [16,17] showed that the low temperature TS signals decreased with decreasing sample mass, which confirmed that acoustic emission was from the whole sample and not just from particles in contact with the sample holder. Resolution of the peaks in the higher temperature signal was better at low sample masses. The low temperature peak decreased with particle size and was undetected below 75 μm diameter particles. Optical and scanning electron microscopy showed that the low temperature TS peak results from fracture of large particles and/or release of liquid from their surfaces. $CsClO_4$ behaves similarly, but TS curves for $NaClO_4.H_2O$ were complicated by dehydration in two steps (55 to 80 °C and 155 to 200 °C). The DTA curve for $KClO_3$ [16] showed melting at 340 to 380°C and two successive exotherms due to decomposition (540 to 610°C). The TS curve showed four main peaks. The first two (360 to 480°C and 485 to 520°C) arise from post-melting events, while the last two (530 to 570°C and 570 to 620°C) correspond to the decomposition stages $KClO_3 \rightarrow KClO_4 \rightarrow$ KCl. The first two TS peaks were shown by high temperature microscopy to be related to the formation and evolution of gas bubbles in the melt.

The phase transitions (α orthorhombic → β trigonal 128 °C; $\beta \rightarrow \gamma$ trigonal on cooling 124°C) occurring on heating and cooling powdered and single crystal samples of KNO_3 were also investigated [20] using simultaneous TS - DTA, supported by microscopy. The γ phase has useful ferroelectric properties. The $\gamma \rightarrow \alpha$ transition was affected by the temperature from which the samples were cooled. This observation was interpreted as resulting from annealing of defects formed by the $\alpha \rightarrow \beta$ transition. The TS signals for the $\gamma \rightarrow \alpha$ transition were stronger than for the $\alpha \rightarrow \beta$ or $\beta \rightarrow \gamma$ transitions

Lee *et al.* [21] have used TS - dilatometry to study the phase II → phase III transition of hexachloroethane in great detail. Agreement between integrated acoustic emission and the dilatometric plots was good. Emission was less intense during heating than during cooling, on account of supercooling. Different acoustic 'signatures' for the processes of nucleation and of growth could not be assigned.

Figure 9.11
The TS frequency distributions obtained [18] on heating samples of K_2SO_4 (a) and $KClO_4$ (b) to their transition temperatures of 582°C and 299°C, respectively. (With the permission of John Wiley & Sons, Chichester.)

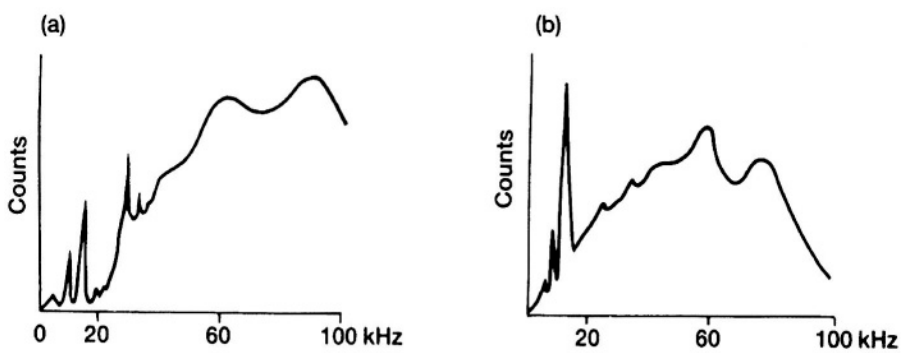

Thermoacoustimetry has been used [26] to distinguish between grades of oil shales. Both the P and the S wave velocities decrease with increasing temperature and with increasing organic content (Figure 9.12). Results are very reproducible. Discontinuities and peaks in the plots are related to loss of water and decomposition of some hydrocarbon fractions. Thermoacoustimetry has also been used [29], in combination with DTA, to examine the characteristics of synthetic fibres (Figure 9.13). The increases in signal occur firstly at the glass-transition temperatures and then prior to melting. The glass fibre shows no changes in this temperature range.

Figure 9.12
Thermoacoustimetry curves of oil shales [26]. (With the permission of Elsevier, Amsterdam.) (gpt = gallons per ton).

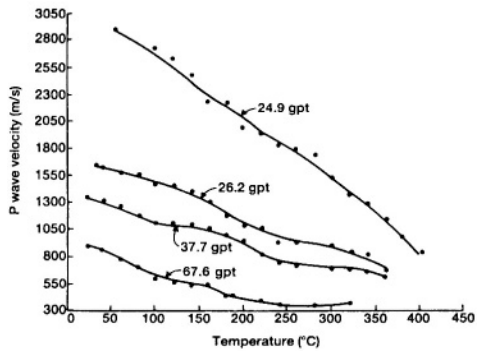

Figure 9.13
Thermoacoustimetry curves of synthetic fibres [29]. (With the permission of John Wiley & Sons, Chichester.)

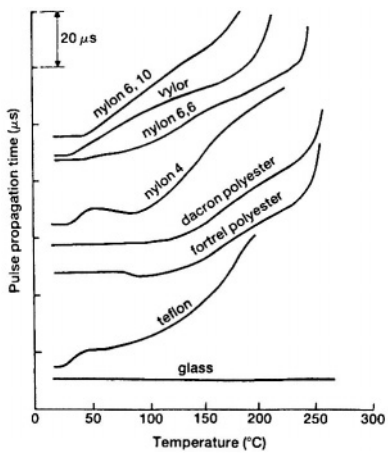

9.4 Thermoelectrometry (or Thermoelectrical Analysis, TEA)

9.4.1 Introduction

The main electrical properties of the sample which may be measured as a function of temperature are dc or ac conductance, capacitance and dielectric properties [30,31]. Measurements may be made in the presence or absence of an electric field, for example, measurement of the emf generated when two dissimilar metal electrodes are in contact with the sample during a heating programme, is known as thermovoltaic detection, TVD [31]. After a sample has been exposed to a static electric field, measurements may be made of the thermally stimulated discharge current, TSDC. Dielectric analysis measures changes in properties of the sample as it is subjected to a periodic field [31] and in dielectric thermal analysis, DETA, the sample is also subjected to a temperature programme.

Most thermoelectrometry studies are carried out simultaneously with other techniques, especially DTA. TG studies on the decomposition of solids have also been carried out in the presence of applied electrical fields.

9.4.2 Apparatus

There is an excellent and comprehensive review of all aspects of thermoelectrometry in the book by Wendlandt [30]. Gallagher [31] has reviewed the apparatus developed for thermoelectrometry and Bidstrup Allen [32] has provided a detailed theoretical background to dielectric measurements.

A DSC cell that has been modified [33] for simultaneous measurements of dc conductance is shown in Figure 9.14. The DSC cell base is insulated from the rest of the cell with a thin glass slide. A thin piece of asbestos was used in the reference position to compensate for the heat capacity of the sample. Platinum foil was used to form an electrical connection from the bottom of the sample to the top of the reference. Glass-insulated platinum wire electrodes contact the tops of the sample and the reference. The current through the sample was recorded as a function of temperature. The dimensions of the sample were then used to calculate the resistivity. Sample surfaces were coated with colloidal graphite to overcome contact resistance. The sensitivity of the DSC was reduced considerably by the presence of the glass slide.

Figure 9.14
TA Instruments DSC cell modified for simultaneous measurements of dc conductance [33]. (With the permission of Elsevier, Amsterdam.)

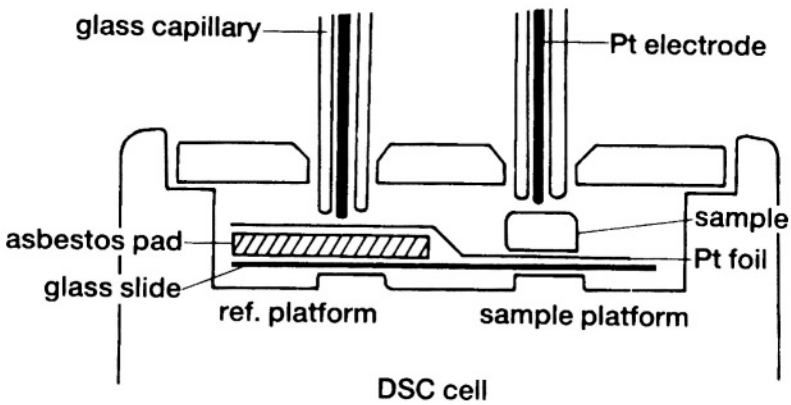

Dielectric thermal analysis, DETA, involves measurements of both the capacitance and the conductance of the sample as functions of time, temperature and frequency. The capacitance is a measure of the material's ability to store charge, while the conductance is a measure of the ease of transfer of charge.

Four major properties are reported during dielectric analysis: the permittivity ($\dot{\varepsilon}$) (also called the dielectric constant); the loss factor ($\ddot{\varepsilon}$); the dissipation factor, tan $\delta = \ddot{\varepsilon}/\dot{\varepsilon}$; and the ionic conductivity (σ^{-1}). The permittivity, which measures the alignment of dipoles, and the loss factor, which represents the energy required to align dipoles and move ions, both provide valuable information about molecular motion. As in most TA techniques, it is the changes in these properties that accompany thermal events in the sample that are usually of more interest than absolute values of the electrical properties.

A sample cell for concurrent dielectric measurement and DTA [34] is illustrated in Figure 9.15. A coaxial-type two terminal electrode configuration is used. The inner electrode is a silver rod positioned symmetrically with respect to the outer electrode, which is a thin silver foil pressed against the walls of the cavity in the nickel block. The sample may be a liquid, a powder or a machined solid. Approximately 500 mg of sample is required. A separate smaller (50 mg) sample is used for concurrent DTA. The sample is connected to the inverting input of an operational amplifier, configured as a current-to-voltage converter with capacitive feedback. The measured phase-shift and attenuation of this network can be related [34] to the dielectric properties of the sample.

Figure 9.15
Sample cell for concurrent dielectric measurement and DTA [34]. (With the permission of the American Chemical Society.)

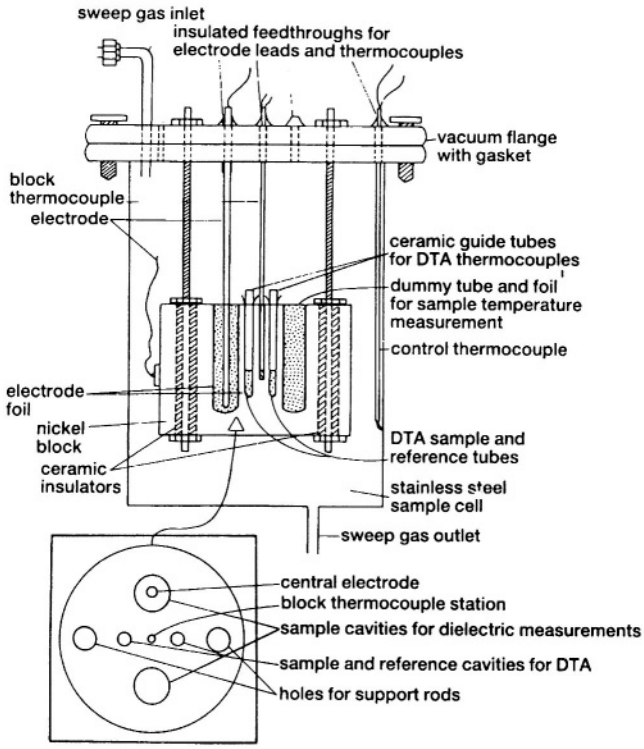

The apparatus can be operated in two modes: either using a continuous range of frequencies (50 Hz to 1 MHZ) at selected temperatures, or over a continuous range of temperatures at selected frequencies. Changes in the dielectric properties of the sample, brought about by phase transitions or chemical reactions are better resolved using the second mode. The instrument was calibrated with standard organic liquids.

The TA Instruments DEA 2970 Dielectric Analyzer is shown in Figure 9.16. It consists of a sensor and a ram/furnace assembly. Different shapes of ceramic sensors can be mounted in the ram/furnace assembly, which provides the controlled experimental conditions (heating, cooling, atmosphere and applied force). The ram is driven by a stepper motor and can apply a constant force or maintain a constant distance between plates, based upon the information fed back from the force transducer and the linear variable differential transformer (LVDT). The high sensitivity of DEA makes it able to detect transitions that are not visible using other TA techniques, for example, the final stages of polymer cure.

Figure 9.16
TA Instruments DEA 2970 Dielectric Analyzer (with the permission of TA Instruments).

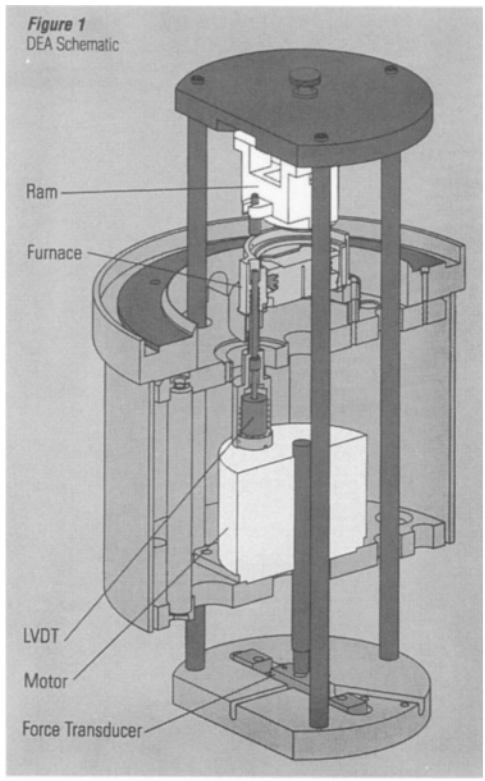

9.4.3 Applications of thermoelectrometry

Electrical conductivity measurements are useful in detecting the appearance of liquid phases in the reactions between initially solid reactants. It is also possible to monitor the loss of chemisorbed OH groups in quantities too small to be detected by TG. Changes in electrical conductivity during heating have also been attributed to changes in concentrations of crystal defects.

Measurements of resistivity against temperature for polymers [33] show sharp drops in resistivity at about the glass-transition temperature. The formation of conductive carbon chains by cross-linking and cyclization within the polymer can be detected by the gradual decrease of resistivity with increasing temperature. Such processes are not shown up by TG or DSC. A curve for PVC is shown in Figure 9.17, with the glass transition and the region of dehydrochlorination marked. Thermoelectrometry is also useful in studying the effect of carbon black additives on the properties of polymers [33].

Figure 9.17
Thermoelectrometry curve for PVC [33]. (With the permission of Elsevier, Amsterdam.)

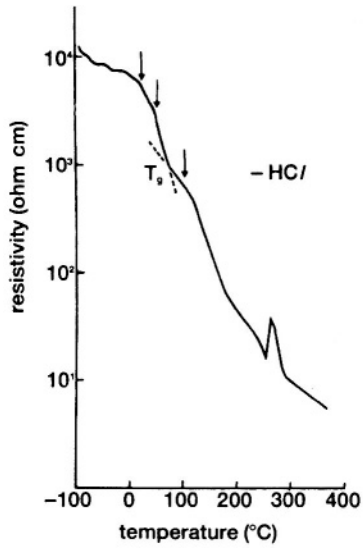

The thermal decomposition of oil shales has been shown [34], using thermoelectrometry, to be a two-step process involving the breakdown of an outershell polar bridge (180-350°C) and cleavage of an inner naphthenic structure (350-500°C).

AC electrical conductivity measurements (up to 350°C) on the Group 1 metal and ammonium perchlorates [34] showed that identical charge conduction mechanisms attributed to movement of interstitial cations were present in all these salts.

Changes in the dielectric constant of a material with temperature can arise from changes in molecular orientation brought about by phase transitions or chemical reactions. A curve of dielectric constant against temperature for $CuSO_4.5H_2O$ [35] has the same form as the TG curve (see Chapter 3). The curve for $NaNO_2$ (120-200°C) shows a peak at about 165°C, of a form similar to that observed in the DTA curve, for the order-disorder crystal transition. This peak is attributed to Debye relaxation behaviour as N atoms diffuse along the *b*-axis in the crystal. Comparing the two curves, it was proposed that removal of H_2O from the copper sulphate crystals is a very fast diffusion process, so no dielectric relaxation is observed. Thus significant additional information is provided by the dielectric measurements. Extension of the above studies [35] to include another known order-disorder ferroelectric crystal, $K_4Fe(CN)_6.3H_2O$, showed that there was an endothermic DTA peak at 105°C with accompanying mass loss showing removal of $3H_2O$. Curves of dielectric constant against temperature show that prior to the dehydration, the H_2O molecules are involved in diffusion, similar to the order-disorder transition in $NaNO_2$, but escape of the H_2O leads to an ordered anhydrous compound.

The power of DETA in separating multiple transitions is illustrated for polymethylmethacrylate (PMMA) [36] in Figure 9.18. A series of curves of loss factor against temperature at different frequencies shows that the α transition (which involves motion in long segments of the main polymer chain) and the β transition (which involves rotation of short-chain ester side groups) become more clearly separated as the test frequency is decreased.

Figure 9.18
The separation of the α and β transitions of polymethylmethacrylate (PMMA)as the test frequency is decreased [36], using the TA Instruments DEA 2970 Dielectric Analyzer (with the permission of TA Instruments).

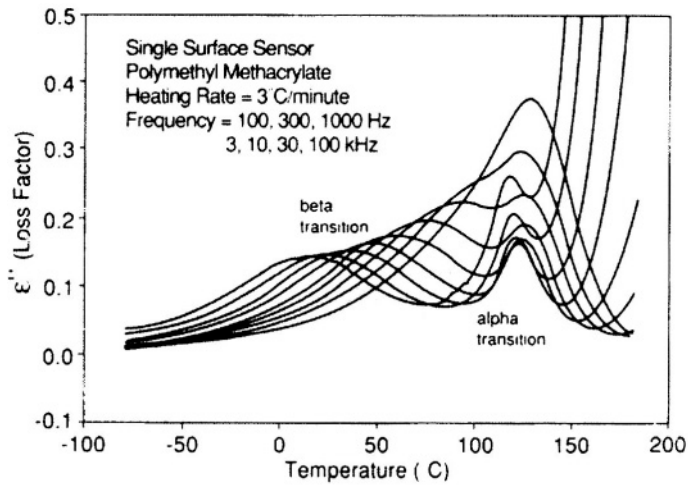

9.5 Miscellaneous Techniques

Mandelis [37] has reviewed photothermal applications in the thermal analysis of solids. Thermal waves may be optically induced in solid samples by modulated irradiation. The thermal waves then interact with the sample before being detected by suitable sensors. Acoustic waves may be simultaneously induced and then detected. Details of the theory and experimental techniques are given in the review [37]. Applications include accurate measurement of thermal transport properties such as thermal conductivity, difffusivity and effusivity and, indirectly, specific heat capacity. Use of these techniques can add significantly to the information obtainable from other thermal analysis techniques, particularly in determining the mechanisms of phase transitions.

A recent paper by Parkes and co-workers [38] describes a new technique of microwave thermal analysis (their suggested abbreviation is MWTA). The advantages of such a

technique are that the microwave radiation heats by direct molecular interaction rather than conduction or convection as in conventional heating and so temperature gradients in the sample are decreased. The uniformity of heating can improve the resolution of thermal events. MWTA depends upon changes in the dielectric properties of the sample and the information obtained is complementary to other techniques.

Epple and Cammenga [39] have illustrated the use of temperature-resolved X-ray diffractometry in thermal analysis. The structural information provided is not accessible through thermoanalytical techniques and is essential in the formulation of mechanisms for solid state reactions. Speyer [40] gives a useful case study of the complementary use of X-ray diffractometry in examining fusion in glass preparation.

References

1. V. Balek and M.E. Brown in "Handbook of Thermal Analysis and Calorimetry", Vol.1 (Ed. M.E. Brown), Elsevier, Amsterdam, 1998, Ch. 9.
2. V. Balek, Thermochim. Acta, 22 (1978)1; 7th ICTA, Vol.1, Wiley, New York, 1982, p.371; Thermochim. Acta, 110 (1987) 222.
3. V. Balek and J. Tolgyessy, "Emanation Thermal Analysis", Comprehensive Analytical Chemistry, Vol.XIIC, Elsevier, Amsterdam, 1984.
4. V. Balek and K.B. Zaborenko, Russian J. Inorg. Chem., 14 (1969) 464.
5. V. Balek, J. Amer. Ceram. Soc., 53 (1970) 540.
6. V. Balek, Thermochim. Acta, 192 (1991) 1.
7. V. Balek and I.N. Beckman, Thermochim. Acta, 318 (1998) 221.
8. I.N. Beckman and V. Balek, J. Thermal Anal. Calorim., 55 (1999) 123.
9. V. Balek, T. Mitsuhashi, J. Šubrt, P. Bezdička and J. Fusek, J. Thermal Anal. Calorim., 60 (2000) 691.
10. T. Sato, M. Hubáček, V. Balek, J. Šubrt, O. Kriz and T. Mitsuhashi, J. Thermal Anal. Calorim., 60 (2000) 661.
11. D. Betteridge, M.T. Joslin and T. Lilley, Anal. Chem., 53 (1981) 1064.
12. R.M. Belchamber, D. Betteridge, M.P. Collins, T. Lilley and A.P. Wade, Anal. Chem., 58 (1986) 1873.
13. P.K. Gallagher, "Thermal Characterization of Polymeric Materials", (Ed. E.A. Turi), Academic, San Diego, 2nd Edn, 1997, pp. 168-177.
14. W.W. Wendlandt, "Thermal Analysis", Wiley, New York, 3rd Edn, 1986, pp.734-739.
15. K. Lonvik and co-workers, 4th ICTA (1975) Vol.3, p1089; 6th ICTA (1980) Vol.2, p313; 7th ICTA (1982) Vol.1, p306; J. Therm. Anal., 25 (1982) 109; Thermochim. Acta, 72 (1984)159,205; 110 (1987) 253; 214 (1993) 51.
16. S. Shimada, Thermochim. Acta, 163(1990)313; 196 (1992) 237; 200 (1992) 317; 255(1995)341; J. Thermal Anal, 40 (1993) 1063.
17. S. Shimada and R. Furuichi, Bull. Chem. Soc. Jpn, 63 (1990) 2526; Thermochim. Acta, 163 (1990) 313.
18. G.M. Clark, 2nd ESTA (1981) p85; Thermochim. Acta, 27 (1978) 19.
19. S. Shimada, Y. Katsuda and R. Furuichi, Thermochim. Acta, 183 (1991) 365; 184(1991)91.

20. S. Shimada, Y. Katsuda and M. Inagaki, J. Phys. Chem., 97 (1993) 8803.
21. O. Lee, Y. Koga and A.P. Wade, Talanta, 37 (1990) 861.
22. A.P. Wade, K.A. Soulsbury, P.Y.T. Chow and I.H. Brock, Anal. Chim. Acta, 246(1991)23.
23. P.D. Wentzell and A.P. Wade, Anal. Chem., 61 (1989) 2638.
24. P.O. Wentzell, O. Lee and A.P. Wade, J. Chemomet., 5 (1991) 389.
25. I.H. Brock, O. Lee, K.A. Soulsbury, P.D. Wentzell, D.B. Sibbald and A.P. Wade, Chemomet. Intell. Lab. Syst, 12 (1992) 271.
26. T. Mraz, K. Rajeshwar and J. Dubow, Thermochim. Acta 38 (1980) 211.
27. S.O. Kasap and V. Mirchandan, Meas. Sci. Technol., 4 (1993) 1213.
28. M. Ravi Kumar, R.R. Reddy, T.V.R. Rao and B.K. Sharma, J. Appl. Polym. Sci., 51(1994)1805.
29. P.K. Chatterjee, 4th ICTA, (Ed. I Buzas), Heyden, London, 1974, Vol. 3, p835.
30. W.W. Wendlandt, "Thermal Analysis", Wiley, New York, 3rd Edn, 1986, pp.697-733; Thermochim. Acta, 73 (1984) 89.
31. P.K. Gallagher, "Thermal Characterization of Polymeric Materials", (Ed. E.A. Turi), Academic Press, San Diego, 2nd Edn, 1997, Ch.1.
32. S.A. Bidstrup Allen in "Handbook of Thermal Analysis and Calorimetry", Vol.1 (Ed. M.E. Brown), Elsevier, Amsterdam, 1998, Ch. 7.
33. A.K. Sircar, T.G. Lombard and J.L. Wells, Thermochim. Acta, 37 (1980) 315.
34. K. Rajeshwar and co-workers, Thermochim. Acta, 33 (1979) 157; 26 (1978) 1; Anal. Chem., 51 (1979) 1149; Nature (London), 287 (1980) 131; J. Chem. Phys., 72 (1980) 6678; J. Phys. Chem. Solids, 41 (1980)271; Phys. Status Solidi, 58 (1980)245.
35. A. Bristoti, I.R. Bonilla and P.R. Andrade, J. Thermal Anal., 9 (1976) 93; 8 (1975) 387.
36. TA Instruments Brochure TA-057B: The DEA 2970 Dielectric Analyzer.
37. A. Mandelis, J. Thermal Anal, 37 (1991) 1065.
38. G.M.B. Parkes, P.A. Barnes, G. Bond and E.L. Charsley, Thermochim. Acta, 356 (2000) 85.
39. M. Epple and H.K. Cammenga, J. Thermal Anal., 38 (1992) 619.
40. R.F. Speyer, "Thermal Analysis of Materials", Marcel Dekker, New York, 1994, Ch.5.

REACTION KINETICS FROM THERMAL ANALYSIS

10.1 Introduction

The main reasons for measuring rates of reactions are: (i) to obtain information about the *reaction mechanism,* which may prove useful in modifying the course of that reaction or in predicting the behaviour of similar, as yet untested, reactions; and/or (ii) to determine values of the *kinetic parameters* (see below) for the reaction of interest, which may allow rates of reaction under conditions of reaction different from those for which the measurements were made, to be calculated by interpolation or (with less certainty) extrapolation.

These two aims are seldom unrelated, because the reaction mechanism, which is used here in the sense of the detailed *chemical* steps involved, can usually only be inferred from the overall picture constructed from the results of the mathematical side of kinetic analysis (the *kinetic model*) and as much complementary evidence (e.g., spectroscopy, chemical and structural analysis, etc.) as possible.

The rate of a general *homogeneous* reaction of the form:

$$A \rightarrow B + C$$

is conventionally measured by following the decrease in concentration of reactant A or the increase in concentration of either product B or C at constant temperature. A rate equation of the form:

Rate = k f(concentrations of reactants & products) (T constant)

is then determined from experiment. The rate coefficient, k, is a function of temperature, usually assumed to be given by the Arrhenius equation [1]:

$$k = A \exp(-E/RT) \quad (\text{or } k = AT^m \exp(-E/RT))$$

where T is the temperature in kelvin, and the Arrhenius parameters, E the activation energy and A the pre-exponential or frequency factor, can be determined by carrying out a series of experiments over a range of different but constant temperatures. An Arrhenius plot is a plot of ln k (or log k) against $1/T$.

In thermal analysis experiments, the reactions studied are almost invariably *heterogeneous* reactions involving at least one initially solid reactant [2,3] and the reaction temperature is usually being continuously increased or decreased according to some set

(usually linear) programme. The rate equations which are likely to apply in heterogenous reactions are considerably different from those familiar in homogeneous kinetics (see below) and programmed temperature experiments require a different approach to kinetic analysis, often referred to in general as *nonisothermal kinetics* (NIK). The principles developed for NIK analysis have been applied to homogeneous kinetics, but because of the influence of thermal analysis techniques and their main use in the study of initially solid samples, the emphasis has been on heterogeneous systems.

Vyazovkin [4] has given an excellent review, from an historical perspective, of the extent to which the concepts of homogeneous kinetics have influenced the language and practice of heterogeneous kinetics. One of the most limiting concepts has been that of a single-step reaction. Real solid-state reactions occur in multiple steps that will usually have different kinetic parameters, e.g. formation and growth of nuclei. As a result of this oversimplification, the kinetic models currently in use for solid-state reactions (and described in detail below) are in many ways similar to the "ideal gas law" that has long been used for describing the behaviour of real gases with varying degrees of success. Better descriptions are needed, but the quality of the data being analysed has got to warrant the effort.

Another limiting concept [4] has been the assumption that the Arrhenius parameters, E and A, are constants and do not depend upon the extent of reaction . The methods of kinetic analysis developed by Vyazovkin and others, described below, have enabled this assumption to be checked and it is shown not to hold in many solid-state reactions.

Much effort has been directed at obtaining kinetic information from the results of thermal analysis experiments [5]. A brief history of the development of nonisothermal kinetic analysis has been given [6] and contributions to the field continue to appear in the current literature. In this introductory account only the main approaches will be outlined. More detail can be found in various reviews [5, 7-9]. Most methods of analysis are referred to by the names of their proposers and it becomes an impossible feat of memory to associate them with their mathematical principles.

Garn [10] expressed some initial reservations concerning the nonisothermal approach. These included problems of measurement of sample temperature when allowance has to be made for heat transfer from the furnace to the outer regions of the sample and then into the sample; the self-cooling or self-heating of the sample during reaction, and the removal of evolved product gases from the vicinity of the sample and the influence of these products on the rate of reaction when the reaction has a high degree of reversibility. Many of these reservations, however, are applicable to solid state kinetics in general.

10.2 Heterogeneous reactions

When a solid sample is heated, one of the many possible changes which it may undergo, is decomposition (see Table 2.1). Information on the kinetics and mechanisms of solid decompositions is of both practical and theoretical importance [3,4]. For a heterogeneous reaction of the type:

$$A(s) \rightarrow B(s) + C(g)$$

e.g., $CaCO_3(s) \rightarrow CaO(s) + CO_2(g)$

the concept of reactant (or product) concentration does not play the significant role that it does in homogeneous reactions and the progress of reaction has to be measured in some other way. Usually the fractional reaction, α, is, defined in terms of the change in mass of the sample ($\alpha = (m_o - m)/(m_o - m_f)$) where m is the mass at that stage, m_o is the initial mass and m_f the mass of the sample when reaction is complete), or equivalent definitions in terms of amounts of gas evolved or heat absorbed or evolved.

α has to be carefully defined in relation to the reaction stoichiometry. Serious problems of definition may arise if the composition of the products varies with the extent of reaction, or if the gaseous products of a reversible reaction are not being effectively and completely removed from the neighbourhood of the sample, or if the reactant melts or sublimes.

Several other factors, which have no analogy in homogeneous reactions, have to be taken into account when solids are involved as reactants and/or products. These include possible variations in properties with direction (anisotropy) in the crystal structure of a single pure solid, as well as the presence of numerous impurities and structural defects, such as surfaces, edges, dislocations and point defects, in any real solid sample. Although such features form only a small proportion of the mass of a solid, they have marked effects on many of the physical properties and, especially, thermal stability [11].

Numerous observations confirm that decomposition of solid reactants generally is initiated at defective regions of the crystal such as the surface or, more specifically, points of emergence of dislocations at the surface. Nuclei of solid product, B, are thus formed, the gaseous product escapes (sometimes with difficulty) and the resulting disruption causes strain in the neighbouring regions of unreacted A, resulting in growth of the nuclei (see Figure 10.1). The shape of these nuclei will be governed by the crystal structure, in that decomposition in some directions will occur more readily than in others. The detailed geometry of the processes of nucleation and growth [12,13] leads to specific predictions of the rate at which the product gas is evolved. In addition to considering the geometry of the reactant/product interface, account has to be taken of the chemical reactions taking place at or near the interface and physical processes such as diffusion and heat transfer.

10.3 Formulation of the problem

10.3.1 Introduction

A kinetic study thus involves measurement of α either as a function of time, t, at constant temperature, or as a function of temperature, T, which is increased according to some heating programme (usually linear), $\beta = dT/dt$. The isothermal method, α against t, corresponds to the conventional curve of concentration against t familiar from homogeneous kinetics, while the dynamic method, i.e. measurement of α against T, is the basis of thermal analysis, see Figures 10.2 and 10.3.

Figure 10.1
Formation and growth of nuclei of product in the decomposition of solids: (a) nucleation sites; (b) first nuclei formed; (c) growth and further nucleation; (d) overlap of nuclei; (e) ingestion of a nucleation site; (f) continued growth.

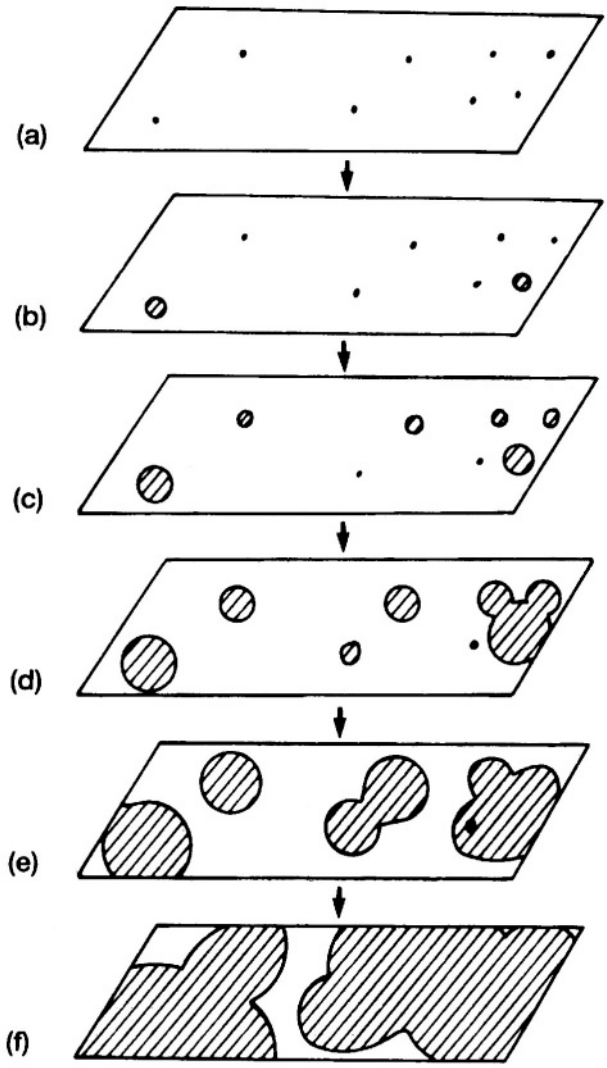

The *reproducibility* of the sets of α, t or α, T data under fixed conditions of isothermal temperature, or at a constant heating-rate, needs to be examined, including any influence of the sample mass on the data. Some experimental techniques may produce relatively noisy α, t or α, T traces and some *smoothing* of the data may be advisable. The extent of mathematical smoothing can always be monitored, while the smooth experimental traces from other measurement techniques may contain an unknown amount and type of instrumental damping.

Krís and Sesták [14] have pointed out that both α and T may vary with position in the sample and that heat and mass transport effects are seldom taken into consideration, even in DTA where the real temperature deviation from the programmed temperature is recorded [15].

10.3.2 Conversion functions and reaction models

Kinetic analysis of both isothermal and dynamic results involves attempting to relate the experimentally observed α, t or α, T values with values predicted for a limited set of models [3,4] based on processes of nucleation and growth (see Figure 10.1), diffusion or some simpler geometrical forms of progress of the reactant/product interface.

In the literature, there is considerable ambiguity in the use of the term *reaction mechanism.* Sometimes it has the meaning, common to homogeneous kinetics, of describing the **chemical** steps by which reactants are converted to products. Often, however, the term is used to describe the rate equation and, by implication, the geometrical or other model on which the rate equation is based. In homogeneous kinetics, one would not imply that the fact that the experimental data could be described by, for example, a second-order rate equation revealed much about the mechanism other than the possibility of control by a bimolecular reaction step. The chemical nature of such a step would be referred to as the reaction mechanism. In solid state reactions, information on the chemical steps involved can be very difficult to obtain and many kinetic studies do not proceed beyond identification of the most appropriate rate equation (or kinetic model) from a rather limited selection.

The expressions derived from these models can all be written in their integral forms (at constant T):

$$g(\alpha) = k\,(t - t_o)$$

or differential forms:

$$d\alpha/dt = k\,f(\alpha)$$

where $f(\alpha)$ and $g(\alpha)$ are known as *conversion functions* (see Table 10.1 and Figures 10.2, and 10.3).

What constitutes the most acceptable description of the experimental α, t or α, T data is still a matter of debate. At least two main aspects need to be considered: (i) the purely mathematical "fit" of the experimental data to the relationship between α and t, $(d\alpha/dt)$ and

Table 10.1

THE MOST IMPORTANT RATE EQUATIONS USED IN KINETIC ANALYSES OF SOLID STATE REACTIONS

	$g(\alpha) = k(t' - t_0) = kt$	$f(\alpha) = (1/k)\,(d\alpha/dt)$	$\alpha = h(t)$
1. Acceleratory α-time curves			
P1 power law	$\alpha^{1/n}$	$n(\alpha)^{(n-1)/n}$	
E1 exponential law	$\ln \alpha$	α	
2. Sigmoid α-time curves			
A2 Avrami-Erofeev	$[-\ln(1-\alpha)]^{1/2}$	$2(1-\alpha)(-\ln(1-\alpha))^{1/2}$	
A3 Avrami-Erofeev	$[-\ln(1-\alpha)]^{1/3}$	$3(1-\alpha)(-\ln(1-\alpha))^{2/3}$	
A4 Avrami-Erofeev	$[-\ln(1-\alpha)]^{1/4}$	$4(1-\alpha)(-\ln(1-\alpha))^{3/4}$	
An Avrami-Erofeev	$[-\ln(1-\alpha)]^{1/n}$	$n(1-\alpha)(-\ln(1-\alpha))^{(n-1)/n}$	$1 - \exp[-(kt)^n]$
B1 Prout-Tompkins	$\ln[\alpha/(1-\alpha)]$	$\alpha(1-\alpha)$	$\{1 + 1/[\exp(kt)]\}^{-1}$

Table 10.1 (Contd)

	$g(\alpha) = k(t' - t_o) = kt$	$f(\alpha) = (1/k)\ (d\alpha/dt)$	$\alpha = h(t)$
3. Deceleratory α-time curves			
3.1 Geometrical models			
R2 contracting area	$1 - (1 - \alpha)^{1/2}$	$2(1 - \alpha)^{1/2}$	$1 - (1 - kt)^2$
R3 contracting volume	$1 - (1 - \alpha)^{1/3}$	$3(1 - \alpha)^{2/3}$	$1 - (1 - kt)^3$
3.2 Diffusion models			
D1 one-dimensional	α^2	$1/2\alpha$	$(kt)^{1/2}$
D2 two-dimensional	$(1 - \alpha)\ln(1 - \alpha) + \alpha$	$[-\ln(1 - \alpha)]^{-1}$	
D3 three-dimensional	$[1 - (1 - \alpha)^{1/3}]^2$	$3/2(1 - \alpha)^{2/3}[1 - (1 - \alpha)^{1/3}]$	$1 - (1 - (kt)^{1/2})^3$
D4 Ginstling-Brounshtein	$1 - (2\alpha/3) - (1 - \alpha)^{2/3}$	$3/2[(1 - \alpha)^{-1/3} - 1]^{-1}$	

Table 10.1 (Contd)

	$g(\alpha) = k(t' - t_0) = kt$	$f(\alpha) = (1/k)\ (\mathrm{d}\alpha/\mathrm{d}t)$	$\alpha = h(t)$
3.3 'Order of reaction' models			
F0 zero order	α	1	kt
F1 first order	$-\ln(1 - \alpha)$	$1 - \alpha$	$1 - \exp(-kt)$
F2 second order	$[1/(1 - \alpha)] - 1$	$(1 - \alpha)^2$	$1 - (kt + 1)^{-1}$
F3 third order	$[1/(1 - \alpha)^2] - 1$	$(1 - \alpha)^3$	$1 - (kt + 1)^{-1/2}$

NOTES:

(1) Rate coefficients, k, are different in each expression and times, t, are assumed to have been corrected for any induction period, t_0.

(2) The units of k are always expressed as $(\text{time})^{-1}$. In those equations incorporating an exponent, the correct notation is $\alpha = k^n t^n$ and NOT $\alpha = k\, t^n$.

t or $(d\alpha/dt)$ and α, required by the functions listed in Table 10.1, together with the range of α across which this expression satisfactorily represents the data (whether the fit varies with temperature is also important) and (ii) the evidence in support of the kinetic model upon which the conversion function is based, obtained by complementary techniques such as optical and electron microscopy, spectroscopy, etc.

Figure 10.2
Isothermal α - time curves for the conversion functions listed in Table 10.1: (a) sigmoid models; (b) geometrical models; (c) reaction order (RO) models; and (d) diffusion models. (For comparison, all curves are based on $\alpha = 0.98$ at $t = 100$.)

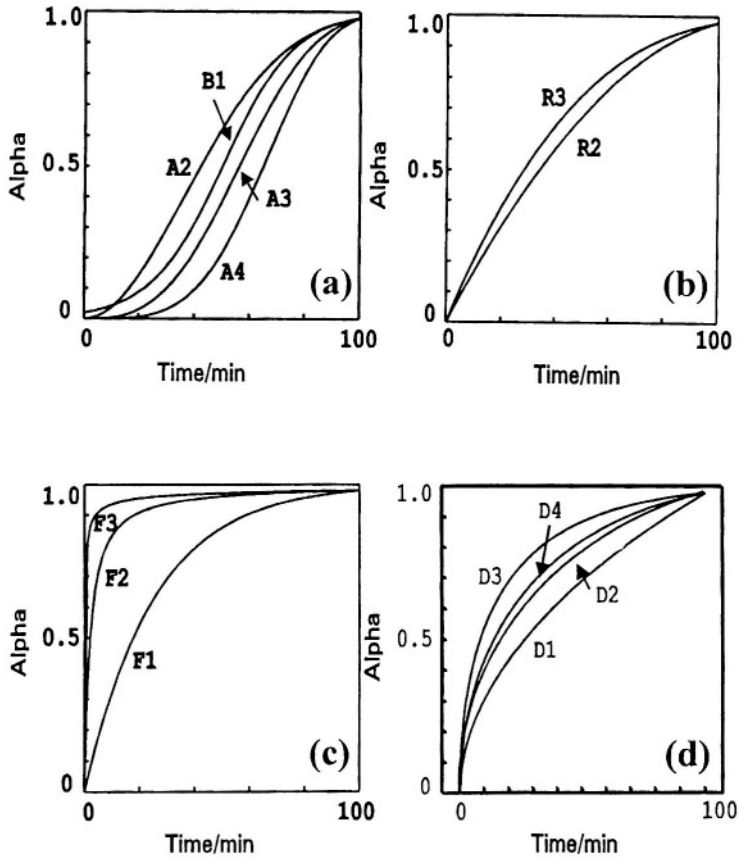

Figure 10.3
Some of the isothermal relative rate [$= (d\alpha/dt)/(d\alpha/dt)_{max}$] - time curves for the conversion functions listed in Table 10.1: (a) sigmoid models, (b) deceleratory models. (For comparison, all curves are based on $\alpha = 0.98$ at $t = 100$.) (The curves for the F3 and the diffusion models are not illustrated. They are too deceleratory for useful comparison here.)

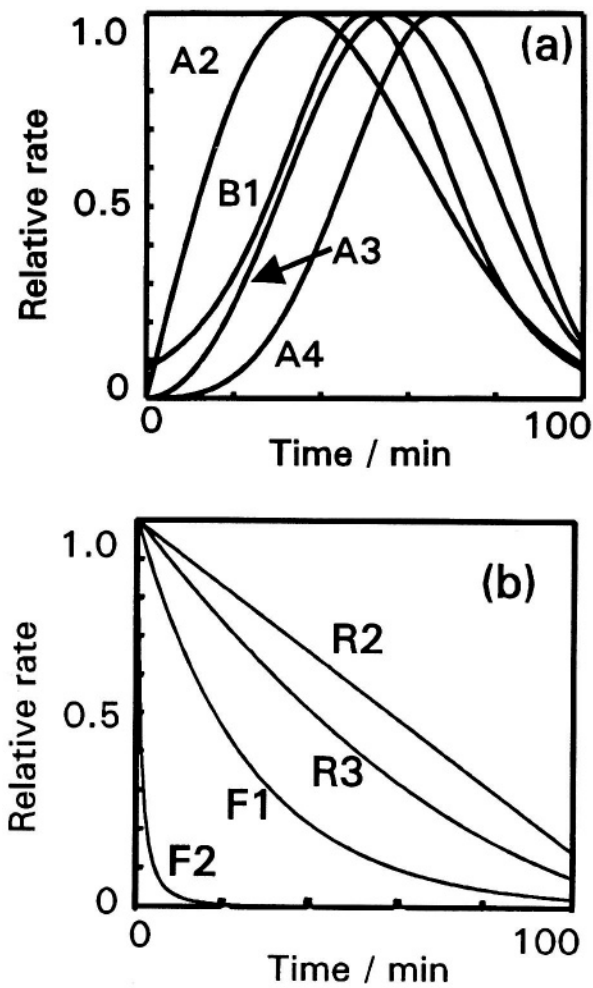

10.3.3 The Effect of Temperature

The effect of temperature is introduced through use of the Arrhenius equation (see above) so that:

$$d\alpha/dt = A \exp(-E/RT)\, f(\alpha)$$

The validity of applying the Arrhenius equation to heterogeneous reactions has been questioned [10,16], but the parameters E and A do have practical value even if their theoretical interpretation is difficult [17]. Laidler [1] has described alternative empirical functions that have been proposed and concludes that they have no significant advantages.

For reversible reactions, the rate of reaction will depend on the partial pressure, p, of the gaseous product. The rate equation should thus include allowance for this, in terms of some function $h(p)$

$$d\alpha/dt = A \exp(-E/RT)\, f(\alpha)\, h(p)$$

This complication is usually ignored and this may be justifiable when working in vacuum or with a strong flow of inert gas through the sample.

For dynamic measurements, the usual approach is to write:

$$d\alpha/dT = (d\alpha/dt).(dt/dT) = (d\alpha/dt).(1/\beta)$$

where $\beta = dT/dt$, is the heating rate. The heating rate is usually maintained constant, although other programmes have been considered [18,19]. Reading *et al.* [20] have developed a technique referred to as constant rate thermal analysis (CRTA) (see Chapter 3) in which the the sample is heated in such a way that reaction takes place at constant rate, and Ortega *et al.* [21] have extended this idea to control the temperature so that the reaction proceeds at a constantly increasing rate (acceleration).

A *temperature-jump* or *step-wise* programme has also been suggested [22,23] in which, during a single experiment, the temperature is rapidly changed ("jumped") from one value to another and the rates at the two (or more) temperatures are measured and used to calculate Arrhenius parameters for that particular α value. This method assumes that α does not change significantly during the time taken to measure the two rate values.

Modulated temperature DSC (see Chapter 4), in which the programmed temperature follows small regular oscillations, is a relatively new technique for distinguishing reversible and irreversible contributions to the thermal behaviour of samples and kinetic applications are beginning to appear.

The relationship between $d\alpha/dT$ and $d\alpha/dt$ is one of the areas of controversy [24-28] but if the above procedure is accepted, and most treatments proceed on that basis, then:

$$d\alpha/dT = (1/\beta).(d\alpha/dt) = (A/\beta)\exp(-E/RT)\, f(\alpha) \qquad (10.1)$$

Separating variables:

$$d\alpha/f(\alpha) = (A/\beta) \exp(-E/RT)\, dT$$

Integrating between the limits, $\alpha = 0$ at $T = T_o$ and $\alpha = \alpha$ at $T = T$:

$$\int_0^{\alpha} (1/f(\alpha))d\alpha \simeq \int_{To}^{T} (A/\beta) \exp(-E/RT)\ dT$$

$$g(\alpha) = \int_{To}^{T} (A/\beta) \exp(-E/RT)\ dT = \int_{o}^{T} (A/\beta) \exp(-E/RT)\ dT \qquad (10.2)$$

(because $\int_{o}^{To} (A/\beta) \exp(-E/RT)\ dT = 0$)

10.3.4 The Temperature Integral

Use of equation (10.2) obviously involves evaluation of the temperature integral:

$$\int_{o}^{T} \exp(-E/RT)\ dT$$

The problem is simplified by introducing the variable $x = E/RT$ so that:

$$\int_{o}^{T} \exp(-E/RT)\ dT = (E/R)\int_{o}^{\infty} (e^{-x}/x^2)dx = (E/R)p(x)$$

Then equation (10.2) becomes:

$$g(\alpha) = (AE/R\beta)\, p(x)$$

Tables of values of the integral $p(x)$ have been provided [29,30]. A lot of attention has been directed at finding suitable approximations for the above temperature integrals [5,6,31-33]. Gorbachev [34] has suggested that there is little value in trying to find more accurate approximations considering the nature of the original α, T data. The three main approaches to evaluation of the temperature integral [31] are : (i) use of numerical values of $p(x)$; (ii) use of series approximations for $p(x)$, and (iii) use of approximations to obtain an expression which can be integrated [5], for example, Doyle's approximation [35] (for $x > 20$) is:

$$\log_{10} p(x) \approx -2.315 - 0.4567x$$

Flynn [36] has commented that the computer power now available has decreased the need for approximations.

10.3.5 The "Inverse Kinetic Problem" (IKP)

The unknowns are thus *A, E* and the form of the conversion function, either $f(\alpha)$ or $g(\alpha)$. (Note that there is no standardization on this terminology and in some papers $f(\alpha)$ and $g(\alpha)$ are used in exactly the opposite sense to that given here.) Often, following homogeneous kinetics, $f(\alpha)$ is taken to be $(1 - \alpha)^n$, so that *n,* the apparent "order of reaction", becomes the third unknown. A more general conversion function, suggested by Sestak and Berggren [37] is:

$$f(\alpha) = \alpha^m (1 - \alpha)^n (-\ln(1- \alpha))^p$$

which increases the number of unknowns, but allows for all the usual models of solid state reactions. The unknowns then have to be determined from experimental measurements which can be converted to values of α and/or $d\alpha/dt$ at temperatures *T,* obtained at a set heating rate β.

Militký and Sesták [38] have expressed the "inverse kinetic problem" (IKP) as the necessity to determine up to six unknown constants, *b1, b2, b3, d1, d2* and *d3* in the expression

$$d\alpha/dt = b1\ T^{b2} \exp(-b3/RT)\ \alpha^{d1} (1 - \alpha)^{d2} [-\ln(1 - \alpha)]^{d3}$$

The simpler form of the Arrhenius equation, i.e. $b2 = 0$, is generally used because a temperature dependent term in the pre-exponential factor [39,40] only adds a further adjustable parameter. When *d3* is zero, $f(\alpha) = \alpha^{d1} (1 - \alpha)^{d2}$, is the Sesták-Berggren equation (see above), or if $d1 = d2 = 1$, the Prout-Tompkins or Austin-Rickett equation results (see Table 10.1).

It is also usually assumed that a single rate expression, $f(\alpha)$ or $g(\alpha)$, applies over a wide range of α values (ideally $0 < \alpha < 1.0$) and that the values of the Arrhenius parameters, *A* and *E,* are constant over at least that α range. If the rate expression and/or the Arrhenius parameters vary with α, i.e. the reaction mechanism changes (see below), the kinetic analysis becomes more complicated. Budrugeac and Segal [41] have, for example, used the assumption that *E* may be a function of α of the form:

$$E = E_0 + E_1 \ln(1 - \alpha)$$

where E_0 and E_1 are constants, together with the assumption of a compensation relationship (see below) between *E* and A. This effectively introduces four more adjustable parameters.

Before proceeding further with the kinetic analysis of nonisothermal data, the simpler and more conventional isothermal approach will be outlined.

10.4 Kinetic Analysis of Isothermal Data

The main approaches which have been used in kinetic analysis of isothermal data for decompositions and other reactions of solids are listed below [2,3]. These are all based on the initial assumption that a single conversion function and a single set of Arrhenius parameters, *A* and *E,* apply over the full range of α. It is always necessary to watch for any indications, such as curved Arrhenius plots, that may indicate that these assumptions are not valid.

(i) The linearity of plots of $g(\alpha)$ (from Table 10.1) against time is determined,

(ii) Plots of α against measured values of reduced-time are compared with similar plots calculated for the rate equations in Table 10.1. Measured time values are corrected by subtraction of t_o, the induction period to onset of the main reaction (also including the time required to heat the reactant to temperature, *T*). Experimental time values, $(t - t_o)$, can then be scaled by the reduced-time factor, $t_{red} = (t - t_o)/(t_{0.5} - t_o)$, where $t_{0.5}$ is the time at which $\alpha = 0.50$ and $k(t_{0.5} - t_o) = 1.0$. Plots of measured values of α against t_{red} , for all experiments including those at different isothermal temperatures, should then all fall on a single curve. This composite curve can be compared with the calculated curve for each conversion function from Table 10.1. Such calculated curves are expressed in the form, $\alpha = k(t_{red})$ and deviations $(\alpha_{THEOR} - \alpha_{EXPTL})$ for each point can be determined. Comparisons of the magnitudes, and variations with α, of these differences are then used to identify the rate equation giving the most acceptable kinetic fit to the data and its range of applicability. Any systematic change in the shape of the α-time curve with temperature can be identified during preparation of the composite curve. The magnitude of $(t_{red})^{-1}$ is proportional to the rate coefficient at temperature *T,* so that the reciprocals of the time scaling factors can be used as quantitative measures of *k* to calculate the activation energy, without the necessity for identifying the kinetic model [42]. The reference value of α is not always selected at 0.50 because this often corresponds to the region of maximum rate and, hence, this choice introduces error into the determination of $t_{0.5}$. When there is an initial reaction, or uncertainty in the length of the induction period, it may be appropriate to use two common points for the scaling, for example [43] $t_{red} = 0.00$ at $\alpha = 0.20$ and $t_{red} = 1.00$ at $\alpha = 0.90$. Other aspects of analysis by the reduced-time method have been discussed by Jones *et al.* [44].

(iii) Plots of measured values of $(d\alpha/dt)$ against either α or *t* are compared with similar curves calculated for the rate equations in Table 10.1.

(iv) The linearity of plots of $(d\alpha/dt)$ against $f(\alpha)$ (from Table 10.1.) is determined. Various standard statistical criteria, e.g. the correlation coefficient, *r*; the standard error of the slope of the regression line, s_b; or the standard error of the estimate of $g(\alpha)$ from *t*, s_{yx}, are used to quantify the deviation of a set of experimental points from the calculated regression line. The use of a single parameter to express the deviation of the data from the least-squares line does not, however, reveal whether deviations are systematic or approximately random. The magnitudes and directions of such deviations and their variations with α can, however, be useful [42] in identifying the most appropriate rate equation, and plots of residuals, $[g(\alpha)_{EXPTL} - g(\alpha)_{PREDICTED}]$, against time have been recommended. Each kinetic model within similar groups may then be associated with the alternative model with which it is most likely to be confused. Note that high values of the

correlation coefficient, *r,* are obtained on analysis using the incorrect expression, even over the wide range $0.05 < \alpha < 0.95$. When the range used in the analysis is shortened [42] to $0.20 < \alpha < 0.80$, distinguishability becomes even more difficult.

Once a satisfactory fit has been obtained for a rate equation, $g(\alpha) = k(t - t_0)$, the value of k and its standard error, s_b, may be determined from the slope of the plot. If the form of the conversion function $g(\alpha)$ does not change with temperature, the values of k at a series of isothermal temperatures, *T,* can be used in a conventional Arrhenius plot to calculate values for E and A.

10.5 Kinetic Analysis of Nonisothermal Data

10.5.1 Introductory Comments

The changes in experimental conditions on going from isothermal to programmed temperature measurements are neither minor nor trivial. The "warm up" period required to reach isothermal conditions is a well-known source of kinetic distortion, but experiments at different heating rates can result in different temperature gradients in the samples which unless corrected for may also lead to erroneous kinetic conclusions. There has also been extensive discussion [45,46] of the applicability under nonisothermal conditions of the Avrami-Erofeev (or JMAEK) equation (see Table 10.1), which is based on a model that includes contributions from the distinct processes of nucleation and of product growth which may have very different temperature dependences.

10.5.2 Classification of Methods

The traditional classification of methods used in the analysis of the nonisothermal kinetic data has usually been to distinguish *differential* methods, based on use of equation (10.1), from *integral* methods, based on use of equation (10.2). Vyazovkin and Lesnikovich [47] criticized this conventional classification because it refers to the type of experimental data used. They suggested instead a classification based on the method of calculation of the kinetic parameters, which involves either *"discrimination",* i.e. identification of the kinetic model $f(\alpha)$ or $g(\alpha)$, or a *"non-discriminatory"* method. An alternative name for non-discriminatory methods is "model-free methods", but this tends to give the unfortunate and incorrect impression that the kinetic model $f(\alpha)$ or $g(\alpha)$ is not necessary for characterization of a reaction. The best description is as "isoconversional methods" and these extremely effective and highly recommended methods are described in more detail below.

Methods involving discrimination can be further sub-divided into methods of *"analysis",* where a single model is sought to describe the experimental data, or methods of *"synthesis",* where several models are combined to give a better description of the data.

10.5.3 The uniqueness of experimentally determined kinetic parameters

After years of debate about whether the form of $f(\alpha)$ or $g(\alpha)$ and the magnitudes of E and A can be obtained from measurements from *a single programmed temperature experiment,* Criado *et al.* [48] clearly showed that the same TG curve could be generated using three different kinetic models with different Arrhenius parameters. This is illustrated in Figure 10.4.

Figure 10.4
A set of α, T data that can be described by three different kinetic models: F1 with $E = 167$ kJ mol^{-1} and $A = 1.6 \times 10^{6}$ s^{-1}; or A2 with $E = 76$ kJ mol^{-1} and $A = 12$ s^{-1}; or D3 with $E = 308$ kJ mol^{-1} and $A = 6 \times 10^{12}$ s^{-1} [48]. (With the permission of Thermochimica Acta.)

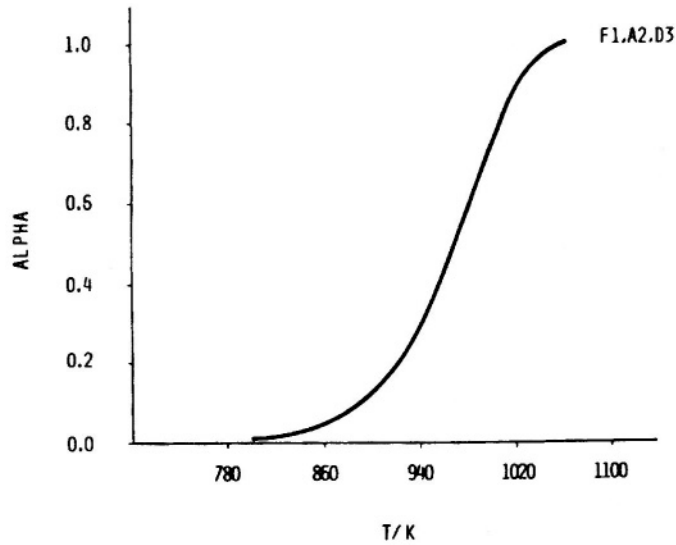

Agrawal [49] had earlier discussed some of the problems of the uniqueness of the derived parameters. Non-unique kinetic parameters may be an explanation for some reported, apparent compensation effects (see below).

Vyazovkin and Lesnikovich [47,50,51] emphasize that all inverse problems have ambiguous solutions that arise from attempts to determine too many unknown constants from limited data, or when a set of experimental data can be alternatively described by different formal models and kinetic constants.

Málek [52] has given an excellent account of the correlation between kinetic parameters and the kinetic models from which they are derived. As a consequence of the correlation between E and A (the so-called "compensation effect" (see below)) a TA curve can be described by a kinetic model and an associated apparent E value, instead of the true model and true E value, where:

$$(E)_{app} = F.\,(E)_{true}$$

and the multiplying factor, F, is characteristic of the true kinetic model. Values of such factors are given.

10.5.4 Isoconversional Methods [4,7,53-58]

In retrospect, it is interesting to note how much effort was put into attempts to extract kinetic parameters from experiments at a single heating-rate. Since the clear demonstrations, described above, of the non-uniqueness of such kinetic parameters, papers based on such methods continue to appear. When data from several *dynamic* experiments at different heating rates, β, are available (and this should become the only acceptable norm for kinetic investigations using TA techniques, other than sets of α - time data at a series of different but constant temperatures, or constant-rate studies) the approach is usually to temporarily eliminate the unknown form of the model $f(\alpha)$ or $g(\alpha)$ by comparing measurements made at a common value of α under the different heating-rate conditions. Such methods of kinetic analysis have been classified as "*isoconversional*", or "model free", or "non-discriminatory" (see above), and much of their development and promotion is due to Vyazovkin and co-workers [4,7,53-58]. To avoid discarding potentially significant information, the parameters obtained from the initial stages of the isoconversional methods should be used with the original data to determine the conversion function (kinetic model), which Sesták [59] regards as the major goal of kinetic studies, although this is sometimes not done. Maciejewski [60] has clearly shown that a reaction must be described by, at very least, a complete kinetic triplet (E, A and $f(\alpha)$ or $g(\alpha)$). Knowledge of only one of the Arrhenius parameters, such as a value for E, is insufficient to characterise the kinetics of a reaction. More complex reactions may require several sets of kinetic triplets for complete characterization.

Isoconversional methods are based upon the assumption that the rate of reaction at a constant extent of reaction, α, is only a function of the temperature:

$$\mathrm{d}\ln(\mathrm{d}\alpha/\mathrm{d}t)_\alpha / \mathrm{d}T^{-1} = -E_\alpha/R \qquad (10.3)$$

where the subscript α indicates the values at that extent of reaction. From integration of equation (10.3):

$$\ln(\mathrm{d}\alpha/\mathrm{d}t)_\alpha = -E_\alpha/RT + \text{constant} \qquad (10.4)$$

A plot of $\ln(\mathrm{d}\alpha/\mathrm{d}t)_\alpha$ against T^{-1} is the basis of the **Friedman** [61] method. Vyazovkin [53] points out that, like other differential methods, measurements of instantaneous rates are very sensitive to experimental noise, and recommends use of an integral method, based on a more general form of integration of equation (10.2):

$$g(\alpha) = A \int_0^{t_\alpha} \exp(-E/RT(t))\ \mathrm{d}t$$

where $T(t)$ is the heating programme. For linear heating programmes, use of one of the many approximations for the temperature integral (see discussion above) leads to relationships of the form:

$$\ln(\beta) = \text{constant} - E_\alpha / RT_\alpha$$

Plots of $\ln(\beta)$ against $1 / T_{\alpha}$ are the basis of the methods of **Flynn and Wall** [62] and **Ozawa** [63]. Vyazovkin [53] has discussed the various comparisons that have been made between Friedman's differential method and the Flynn, Wall and Ozawa integral method. Because of differences that may arise, Vyazovkin has suggested and tested an "advanced" isoconversional approach where integration is carried out over small intervals of α [53].

A main advantage of isoconversional methods is identified [53] as being the calculation of consistent activation energies which are in good agreement with values from isothermal experiments. Variations of E with extent of reaction, α, are usually an indication of a complex conversion function. A disadvantage of the approach is that the value of A cannot be determined without knowledge of the model $f(\alpha)$. A good guide to the adequacy of a kinetic analysis is the ability to reconstruct a set of calculated α - time or α-temperature curves for comparison with the experimental data.

In summary then, classification of methods of kinetic analysis as either differential or integral methods is not of great practical use because data can be transformed readily from one form to the other by use of numerical methods of differentiation and integration.. The isoconversional approach eliminates the need to identify the rate equation, or kinetic model, during the initial stages of a kinetic analysis. The values of the Arrhenius parameters for many reactions are relatively insensitive to the rate equation applicable, but for a complete analysis the values of A and E obtained in this first stage may then be used in identifying the conversion function.

Several approaches involve use of the second derivative of equation (10.1), or the version with $f(\alpha) = (1 - \alpha)^n$, with respect to temperature [7,31] or with respect to time [31], in spite of the problems of obtaining accurate values of second derivatives. Using

$$d\alpha/dT = (A/\beta) \exp(-E/RT) (1 - \alpha)^n \qquad (10.5)$$

gives:

$$(d^2\alpha/dT^2) = (d\alpha/dT)[(E/RT^2) - n (d\alpha/dT)/(1 - \alpha)]$$

and, because this second derivative must be zero at the inflexion point of a TG curve or the maximum of a DSC peak::

$$E/(RT^2_{max}) = (d\alpha/dT)_{max} (n/(1 - \alpha_{max})) \qquad (10.6)$$

from which E may be calculated if n is known and T_{max}, $(d\alpha/dT)_{max}$ and α_{max} are measured [64]. Combining equations (10.5) and (10.6) gives:

$$(A/\beta) \exp(-E/RT_{max}) n (1 - \alpha)^{(n-1)} = E/RT_{max}^2$$

and, because $(1 - \alpha_{max})$ is a constant for a given value of n, the **Kissinger** [65] method of obtaining a value for E is to plot $\ln(\beta/T^2_{max})$ against $1/T_{max}$ for a series of experiments at different heating rates, β. The slope of such a plot is $-E/R$.

Augis and Bennett [66] have modified the Kissinger treatment for use with the Avrami - Erofe'ev model, which applies in so many solid-state reactions. They plot $\ln(\beta/(T_{max} - T_o)$ against $1/T_{max}$ where T_o is the initial temperature at the start of the heating programme, instead of $\ln(\beta/T^2_{max})$ against $1/T_{max}$. Elder [67] has generalized the Kissinger treatment to make is applicable to the full range of kinetic models. The generalized equation is:

$$\ln(\beta/T^{m+2}_{max}) = \ln(AR/E) + \ln (L - E/RT_{max})$$

where m is the temperature exponent of the preexponential term in the modified Arrhenius equation and is often taken as zero, and

$$L = - f(\alpha_{max})/(1 + mRT_{max}/E)$$

This correction term was found to be relatively small, but helps in distinguishing between similar models. The values of E obtained were not very sensitive to incorrect choice of model.

The **Ozawa** treatment [63] is also applicable to derivative curves and is similar to the Kissinger method. $\ln \beta$ is plotted against $1/T_{max}$ and the slope of this plot is again $-E/R$.

Van Dooren and Muller [68] studied the effects of sample mass and particle-size on the determination of kinetic parameters from DSC runs using the methods of Kissinger and of Ozawa. It was found that both sample mass and particle size could influence the values of the kinetic parameters, but the extent of these effects varied from one substance examined to another. The two methods gave similar values for E with slightly lower precision for the Kissinger method. It was suggested that temperatures at $\alpha = 0.5$ (half conversion) should be used in place of T_{max}.

The "non-parametric kinetics (NPK)" method [69] of **Serra, Nomen and Sempere** is based on the usual assumption that the reaction rate can be expressed as a product of two independent functions, $f(\alpha)$ and $h(T)$. $h(T)$, the temperature dependence, need not be of the Arrhenius-type. The reaction rates, $d\alpha/dt$, measured from several experiments at different heating-rates, β, are organised as an n x m matrix whose rows correspond to different (constant) degrees of conversion, and whose columns correspond (by interpolation) to different (constant) temperatures. The NPK method then uses the Singular Value Decomposition (**SVD**) algorithm [70] to decompose matrix **A** into the two vectors **a** and **b**. These vectors can then be further analysed by examining the resulting plots of rate against α (to determine the kinetic model) and of rate/$f(\alpha)$ against temperature (to check on Arrhenius-type behaviour and to determine Arrhenius parameters when appropriate). The NPK method uses a large number of points and a wide range of temperatures. This is a model-free method in the sense that it allows for isolating the temperature dependence of the reaction rate (and, therefore, the activation energy) without making any assumptions about the reaction model.

10.6 The influences of various parameters on the shapes of theoretical thermal analysis curves

With there being so many parameters in equations (10.1) or (10.2), it is useful to see what effect varying one of these parameters at a time has on the shape of a TG or DSC curve [5,6,31,71]. The most fundamental variable is the form of the conversion function $f(\alpha)$ or $g(\alpha)$ (see Table 10.1). The shapes of the theoretical isothermal α, time curves for various model conversion functions [2,3,5,72] are shown in Figure 10.3. It is not always an easy task to distinguish amongst the models, even under isothermal conditions [73]. The shapes of these curves are, of course, considerably altered under nonisothermal conditions and theoretical α, temperature curves [31,67] for the various models are given in Figure 10.5. (These curves were constructed using the Doyle approximation [29] for the temperature integral, $p(x)$, see below.) The models based on apparent order of reaction, *n,* (even if fractional) i.e. F1, F2, R2 and R3, Figure 10.5(b), are difficult to distinguish at low values of α. Distinguishability improves for higher orders at higher values of α. The diffusion models, D2, D3 and D4, give generally lower onset temperatures and flatter curves (Figure 10.5(c)) than the *n*th-order group, while the Avrami-Erofeev models have higher onset temperatures and steeper curves. Figure 10.6 shows the differential curves corresponding to the integral curves given in Figure 10.5.

The next sets of comparisons are done with a fixed model and this is used to examine the influence of the other variables, the heating rate β, the activation energy, *E,* and the pre-exponential factor, *A*. Elder [67] has provided similar curves and Zsakó [71] has shown similar influences for the first-order (F1) model. Although the F1 model is not a very realistic representation, it is often assumed to apply as an approximation. Figure 10.7 shows the regular effect on the theoretical contracting-volume R3 curve, of doubling the heating rate in the range $\beta = 1$ to 16 K min^{-1}. Changing the pre-exponential factor by factors of ten in the range $A = 1.9 \times 10^{17}$ to 1.9×10^{13} min^{-1} also affects mainly the onset temperature and the acceleratory position of the curves, Figure 10.8, with the remaining segments being almost parallel. Very similar behaviour is observed for curves with the activation energy increasing in steps of 5 kJ mol^{-1}, in the range 90 to 110 kJ mol^{-1}, as shown in Figure 10.9. The overall shape of the thermal analysis curve is thus determined by the conversion function, $f(\alpha)$ or $g(\alpha)$, applying, while the position of this curve on the temperature axis is determined by the values of *E, A* and, to a lesser extent, the heating rate β.

Figure 10.5
Theoretical alpha-T curves for various kinetic models.
β = 1.0 K min^{-1}, E = 100 kJ mol^{-1}, A = 1.9 x 10^{15} min^{-1}.
(a) the Avrami-Erofeev (JMAEK) models, An,
(b) models based on apparent order of reaction, n, and contracting geometry, F1, F2, F3, R2 and R3, and
(c) diffusion models, D1, D2, D3 and D4.

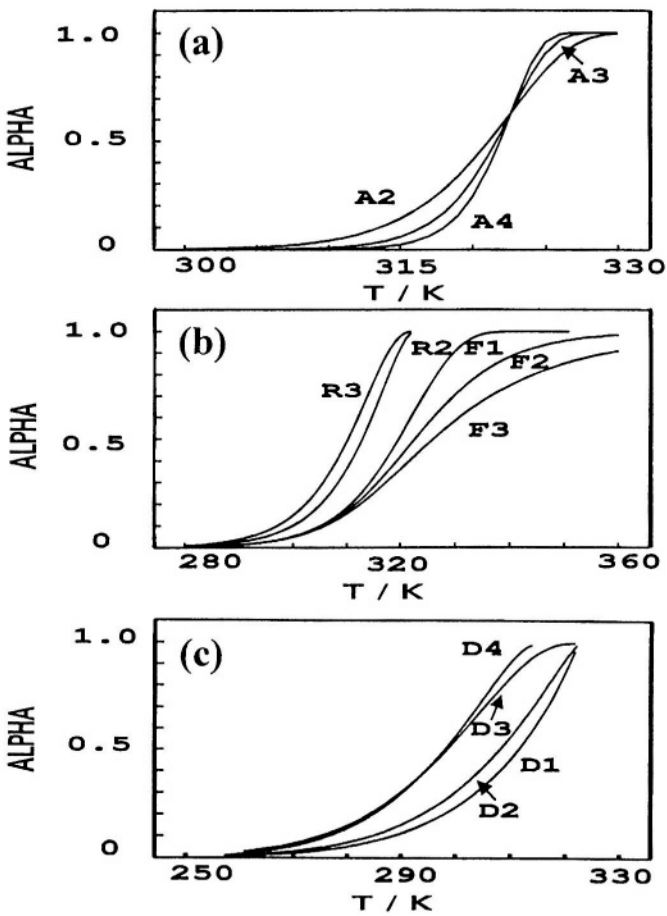

Figure 10.6
Theoretical curves of $d\alpha/dT$ against T for various kinetic models.
β = 1.0 K min^{-1}, E = 100 kJ mol^{-1}, A = 1.9 x 10^{15} min^{-1}.
(a) the Avrami-Erofeev (JMAEK) models, An,
(b) models based on apparent order of reaction, n, and contracting geometry, F1, F2, F3, R2 and R3, and
(c) diffusion models, D1, D2, D3 and D4.

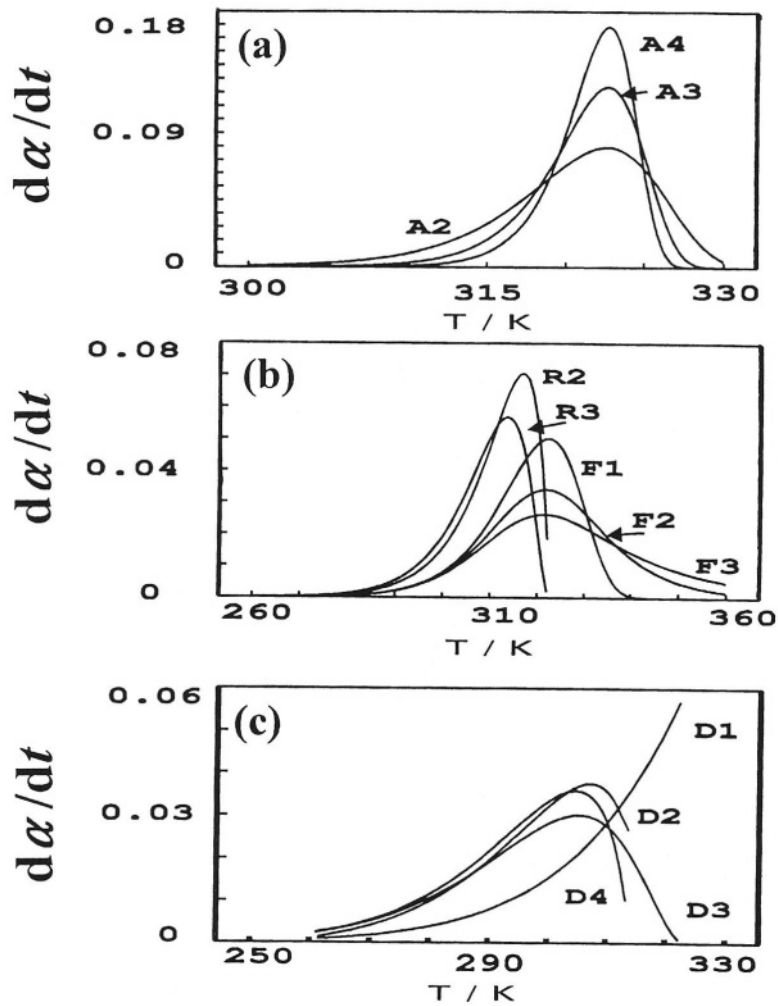

Figure 10.7
Influence of heating rate, β, (in the range 1 to 16 K min^{-1}) on the shape of theoretical alpha-T curves for the R3 model. (E = 100 kJ mol^{-1}, A = 1.9 x 10^{15} min^{-1}.)

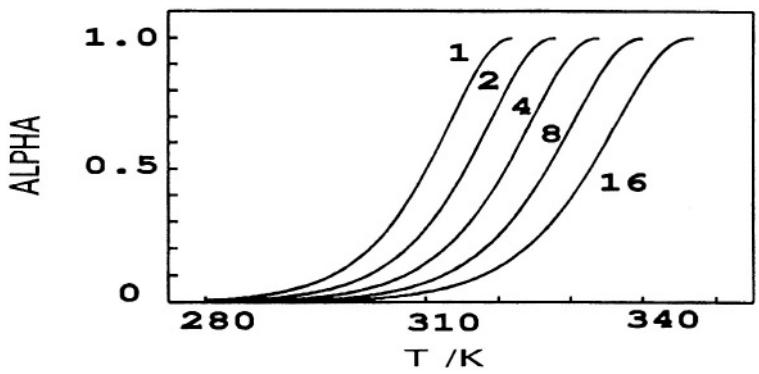

Figure 10.8
Influence of pre-exponential factor, A, (in the range 1.9 x 10^{17} to 1.9 x 10^{13} min^{-1}) on the shape of theoretical alpha-T curves for the R3 model. (E = 100 kJ mol^{-1}, β = 1.0 K min^{-1}.)

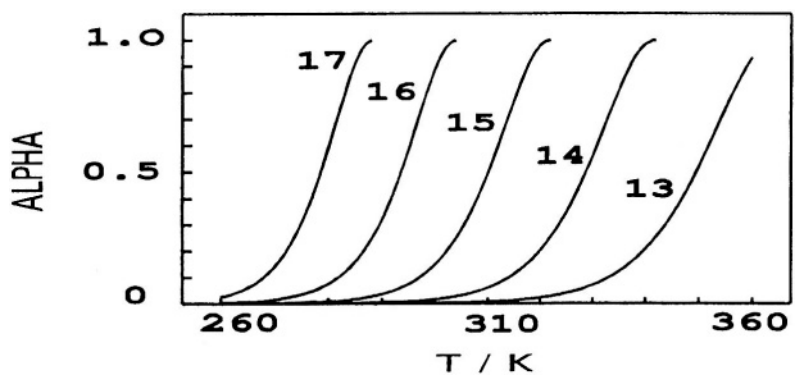

Figure10.9
Influence of activation energy, E, in the range 90 to 110 kJ mol^{-1}, on the shape of theoretical alpha-T curves for the R3 model. (A = 1.9 x 10^{15} min^{-1}, β = 1.0 K min^{-1}.)

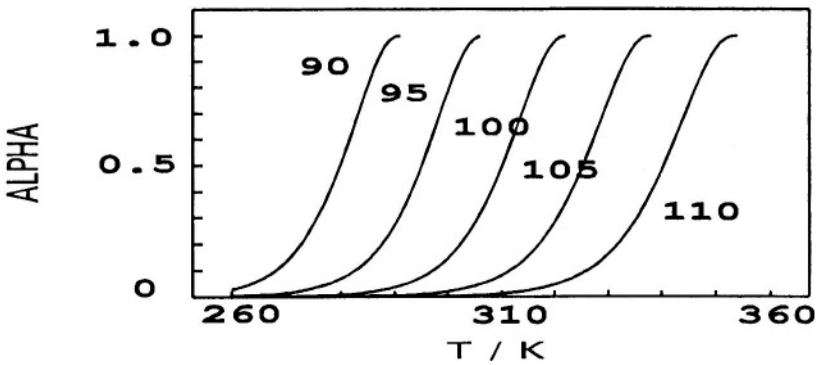

10.7 The Compensation Effect

Sometimes, for a series of closely related, but *not* identical reactions, the experimental Arrhenius parameters, determined by similar procedures, have been reported to conform to an equation of the form:

$$\ln A = aE + b \qquad (10.5)$$

where a and b are constants. This is known as " a compensation effect"[2,3,74,75] because the decrease in reaction rate resulting from an increase in activation energy, E, is offset by an increase in the magnitude of ln A. This is also known as the *isokinetic effect* because, for the set of (A, E) values that fit equation (10.5), there exists a temperature, T_K, at which all rate coefficients are equal. For many reactions, the value of T_K is at, or within, the temperature ranges of the kinetic measurements exhibiting the compensation behaviour. A similar effect has also been observed for a series of closely related, but *not* identical, experiments on a single chemical reaction, where the differences in the experimental conditions, including the physical state and history of the solid reactant, may result in a relationship of the form of equation (10.5) between the apparent Arrhenius parameters.

A huge volume of literature [75] has grown around this seemingly simple relationship. None of the many theoretical explanations [74] suggested for compensation behaviour has received general acceptance. There are good reasons for suspecting that many reported instances of compensation effects may be computational artefacts [76-81].

10.8 Complex reactions

The behaviour of any real, initially-solid sample is going to be considerably more complex than the idealized description given above. The success that has been achieved using this limited set of models can only be attributed to an averaging effect over the variety of processes occurring at the molecular level. When some of these processes have very different kinetic characteristics, none of the models may provide an adequate description of the experimental results.

There are several useful indicators of the possible occurrence of complex reactions [49]. From the experimental side, a lack of correspondence between DSC and DTG results indicates that the rate of change of enthalpy is not directly proportional to the rate of mass loss. Experiments at different heating rates also show up complexities.

Another important indication is the dependence of the value obtained for E upon the extent of reaction, α [81]. It is thus essential to use a method of kinetic analysis that allows such a dependence to be detected. In isothermal studies, the occurrence of complex reactions may be detected by Arrhenius plots that are curved or give two linear regions [81]. The shapes of plots of α against reduced-time also vary systematically with temperature.

The contributions to complex reactions are most easily separated when the activation energies of the individual reactions are considerably different. Reactions with low E values dominate the kinetics at low temperatures and slow heating rates, while those with high E values dominate at high temperatures and high heating rates. At the isokinetic temperature the rates of the participating reactions are equal.

Elder [82] has modelled several multiple reaction schemes, including mutually independent concurrent first-order reactions, competitive first-order reactions, mutually independent n-th order reactions, and mutually independent Avrami-Erofeev models with $n = 2$ or 3.

Vyazovkin and Lesnikovich [81] have discussed the identification of the type of complex process encountered in nonisothermal experiments by examination of the shape of the curve of the dependence of the apparent value of E on α, found by isoconversional methods. Concurrent reactions are characterized by an increasing dependence of E on α, but detailed shapes are dependent on the ratios of the contributing rates. A decreasing dependence of E on α, was found for intermediate reversible processes [81].

Contributions from individual reactions with similar E values are not separable by changing the heating rate, so deconvolution has to be attempted by mathematical methods [83]. Many such methods proposed in the literature are restricted to RO models. Criado *et al.* [83] proceed on the basis of summing the individual contributions. The overall reacted fraction α is defined as:

$$\alpha = \sum w_i \alpha_i$$

where w_i is the fraction of the total mass loss due to contributing reaction i (with Arrhenius parameters, A_i and $(E)_i$). A method is then presented which uses non-linear optimization combined with a version of the Kissinger method to deconvolute up to 15 contributing processes.

Ozawa and Kanari [84] have also discussed the kinetic analysis of competitive reactions for which measurements of the extents of conversion and rates of production of individual products are required. Suitable data could be obtained by combining evolved gas analysis with TG or DSC.

Vyazovkin [85] has treated the problem of a reaction complicated by diffusion as consecutive reactions involving the formation of a surface layer followed by diffusion through that layer.

10.9 Prediction of kinetic behaviour

An important practical aspect of kinetic studies is the prediction of kinetic behaviour under conditions other than those used in the original experimental measurements [86], for example, the estimation of shelf-lives of drugs under normal storage conditions, from accelerated tests at higher temperatures. For predictions to be reasonably reliable, the values of the kinetic parameters, E, A and the forms of the conversion functions, $f(\alpha)$ (or $g(\alpha)$), should not vary with T. The precision of the estimates of E and A also needs to be known [87]. Vyazovkin and Linert [87] and Maciejewski [60] have described some of the implications of attempting to predict kinetic behaviour when the kinetic model $g(\alpha)$ or $f(\alpha)$ has been incorrectly chosen (such as when non-unique kinetic triplets have been determined by single heating-rate experiments), and when the reactions are complex.

Flynn [88] has reviewed the prediction of service lifetimes of polymeric materials, at lower temperatures, from decomposition parameters obtained at relatively high temperatures. Reasons for the failure of predictions are discussed. These include extrapolation beyond temperatures at which phase changes (and accompanying changes of physical properties) occur.

10.10 Kinetics Standards

Attempts to find a reaction which could serve as a standard for comparison of kinetic measurements have not been successful. The major requirements for such a reaction have been specified by Gallagher [89] as: (i) an irreversible reaction taking place in a single stage, with (ii) a low value of the enthalpy of reaction, to minimize self-heating or self-cooling effects; (iii) the temperature range required for reaction to proceed at a slow, but measurable rate should not be too low, so as to avoid large temperature calibration errors; (iv) there should be no reaction of the sample with the surrounding atmosphere; (v) no dependence of reaction on the method of sample preparation, pretreatment or particle size and distribution; and (vi) the changes to be measured to follow the course of reaction, e.g., mass, amounts of evolved gases, enthalpy change, should be large, to permit the use of

small samples. Some of these requirements are not compatible with each other, so compromises are necessary.

The dehydration of lithium sulfate monohydrate as a kinetic standard was suggested, but ruled out [89], because: (i) the reaction is reversible at low temperatures, and (ii) is moderately endothermic; (iii) the reaction takes place at temperatures below 3 70 K and TG instruments are difficult to calibrate accurately in this range; (iv) rates of the reaction are very dependent upon particle-size and prehistory; (v) overall dehydration involves several rate processes, e.g., chemical reaction, diffusion, recrystallization, and the rate-determining step may not remain the same during the course of experiments; and (vi) the overall rate of dehydration is influenced by the presence of water vapour in the surrounding atmosphere.

Sbirrazzuoli et al. [90] have proposed and discussed an electronic means of simulating DSC signals according to set kinetic laws for comparison with experimental results.

10.11 Kinetic Test Data

It is also useful to be able to test different methods of kinetic analysis on a "reference" data set. Isothermal and nonisothermal data sets have been provided [91]and the kinetic analysis of these data sets by a variety of volunteer participants, using computational methods of their choice, has been discussed in considerable detail [92]. Some of the sets are actual experimental results for the thermal decompositions of ammonium perchlorate and calcium carbonate. The data sets 7 and 8 (illustrated in Figures 10.10 and 10.11, respectively) were simulated using a system of two equally-weighted, parallel, first-order reactions:

$$\frac{d\alpha}{dt} = \frac{1}{2}\left(\frac{d\alpha_1}{dt} + \frac{d\alpha_2}{dt}\right) = \frac{1}{2}\left[k_1(T)(1-\alpha_1) + k_2(T)(1-\alpha_2)\right]$$

The Arrhenius parameters of the individual steps were taken to be $A_1 = 10^{10}$ min^{-1}, $E_1 =$ 80 kJ mol^{-1}; $A_2 = 10^{15}$ min^{-1}, $E_2 = 120$ kJ mol^{-1}.

The kinetic results produced from data sets 1 -4 are discussed by Maciejewski [60] and for data sets 5-8 by Vyazovkin [93]. There is ample computational machinery available for testing the "goodness-of-fit" of experimental data to the limited set of kinetic equations. Provided that the methods of kinetic analysis are computationally sound, they should be seen as complementary. Confidence in the resulting parameters is vastly increased if similar values are obtained using different approaches It is a considerable advantage to remove the influence of the kinetic model from the kinetic analysis while estimating the Arrhenius parameters, but a full kinetic analysis should consider the problems of identification of the function or functions (however complex these may turn out to be) which determine the extent of reactant conversion. The introduction of additional kinetic parameters to improve the goodness of fit can only be justified if they can be given some physical significance.

The emphasis on computational aspects of kinetic analysis has not been matched by effort put into better planning of experiments and the difficulties of interpretation of results.

Figure 10.10
Simulated alpha-temperature curves (Set 7 [91]) calculated at heating rates of : 0.5, 1.0, 2.0, 4.0 and 8.0 K min^{-1}.

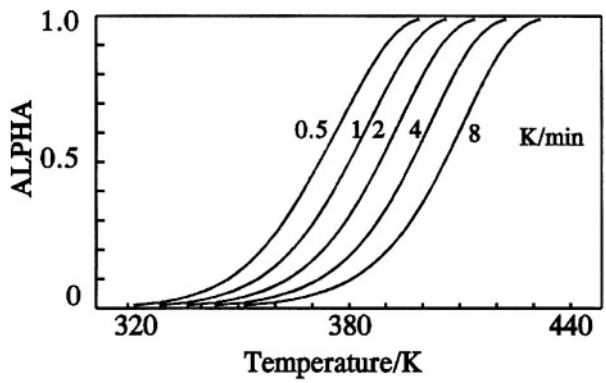

Figure 10.11
Simulated isothermal alpha-time curves (Set 8 [91]) calculated at temperatures of : a=380, b=375, c=370, d=365 and e=360 K.

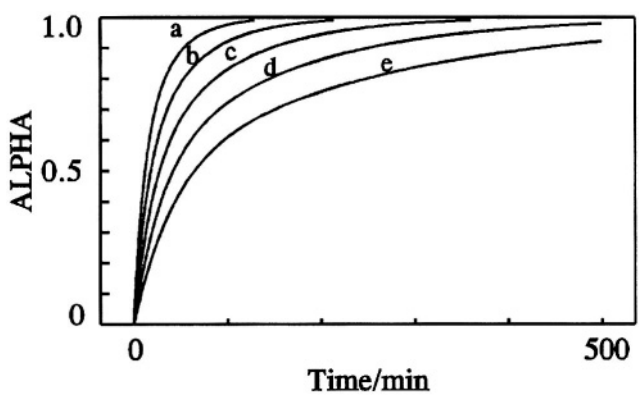

10.12 Publication of Kinetic Results

The final and very important stage of any research project is the reporting of kinetic results in written form [5]. Some of the essential information that should be provided in such reports includes: (1) the reasons for undertaking the research; (2) a review of the relevant literature, especially work by other authors; (3) complete description of the materials used (supplier, method of preparation or manufacture, structural information and particle sizes and distributions, analytical results including purity and the nature and concentrations of any impurities, reactant pretreatment); (4) full details of the equipment and methods used and their calibration (calibration materials and procedures, heating rates, base-line corrections; dimensions, geometry and material of the reactant container; pressures, flow rates and purities of all gases). (5) The stoichiometry of the reaction(s) to which the kinetic measurements refer and, hence, the basis of definition of the extent of reaction, α need to be specified (analysis of the residual solid product may be necessary). (6) The reproducibility of the data measured for kinetic analysis should be specified. (7) The methods used for determining the kinetic parameters by fitting the data to kinetic expressions should be recorded, including the criteria for acceptability of fit, and the range of fit of the equations considered. Some of the commercially available programs for kinetic analysis do not even specify the algorithms on which they are based, while other packages use kinetic expressions restricted to the reaction order (RO) type. (8) Characterization of a reaction by a complete and unique kinetic triplet is essential. Such a triplet cannot be estimated from experiments done at a single heating-rate, so the many published methods based on this unacceptable approach should be abandoned in favour of isoconversional methods on data obtained at different heating rates. (It is interesting that no one would contemplate complete kinetic analysis of a single isothermal experiment.) (9) Values of the Arrhenius parameters, E and A, reported should also include their standard errors. The number of significant figures used to report numerical values (± errors) must be realistic. (10) Results obtained should be discussed critically and interpreted in the context of all relevant work, including citation of related studies by other workers. Advances should be explained and discussed realistically and directions for possible future advances should be indicated.

10.13 Conclusions

Two reasons given [5] for possible failure of a method of kinetic analysis are: (i) the approximations used may not be valid, and (ii) the model used in deriving the mathematics may not take into account physically real factors of the experiment such as the heat transfer and atmosphere control problems.

Arguments about the relative value of non-isothermal and isothermal methods of kinetic analysis are generally unproductive. The complementary use of the two approaches can provide valuable insights into the processes occurring, provided that the experimenter is critically aware of the shortcomings and limitations of each approach. Vyazovkin and Lesnikovich [47] point out that the kinetic parameters calculated from isothermal data are

not very dependent upon the kinetic model chosen, while the opposite is true for non-isothermal methods. Thus, ideally, one could determine the Arrhenius parameters from isothermal measurements and the kinetic model from nonisothermal measurements.

The use of derivative methods avoids the need for approximations to the temperature integral (discussed above). Measurements are also not subject to cumulative errors and the often poorly-defined boundary conditions for integration do not appear in the calculation [62]. Numerical differentiation of integral measurements normally produces data which require smoothing before further analysis. Derivative methods may be more sensitive in determining the kinetic model [94], but the smoothing required may lead to distortion [95].

The reported lack of agreement amongst kinetic parameters calculated from the same set of experimental data using different methods of mathematical analysis [5,93,96] is disturbing. The set of models from which the 'best model' is to be chosen has been criticized [47] as being is too limited. Even if the set does not contain the true model, one of the set is probably going to appear to be the 'best model' for lack of alternatives. Modification of the models in attempts to account for all the features of real processes, however, generally results in an increased number of adjustable parameters, for which physical interpretations are difficult to find. Vyazovkin and Lesnikovich [97] have suggested that different aspects of the real process may be best described by a synthesis of individual features of ideal models from the existing set.

Vyazovkin and Lesnikovich [47] have warned against the practice of forcing the model to be of the reaction order (RO) type where the value of n may not possess physical significance. They have also shown [50] that the Avrami - Erofeev model is equivalent to linear combinations of some of the other formal models and hence may serve as a generalized description. Coincidence of the parameters calculated by alternative methods confirms only the equivalence of the methods of calculation and not the validity of the parameters obtained.

The use of non-linear regression methods [98-105], where minimum deviation between experimental and theoretical data is sought, is preferable to methods that involve linearization of the appropriate rate equation [47], usually through a logarithmic transformation which distorts the Gaussian distribution of errors.

As a final word, it is essential that a complete kinetic triplet be determined to characterize a reaction. Such a complete and unique set cannot be determined from experiments done at a single heating rate.

References

1. K.J. Laidler, J. Chem. Educ., 49 (1972) 343; 61 (1984) 494.
2. M.E. Brown, D. Dollimore and A.K. Galwey, "Reactions in the Solid State", Comprehensive Chemical Kinetics, Vol.22, Elsevier, Amsterdam, 1980.
3. A.K. Galwey and M.E. Brown, “Thermal Decomposition of Ionic Solids”, Elsevier, Amsterdam, 1999.
4. S. Vyazovkin, Int. Rev. Phys. Chem., 19 (2000) 45.
5. A.K. Galwey and M.E. Brown, “Handbook of Thermal Analysis and Calorimetry, Vol.1, Principles and Practice”, (Ed. M.E. Brown), Elsevier, Amsterdam, 1998, Ch. 3.
6. J. Sestak, V. Satava and W.W. Wendlandt, Thermochim. Acta, 7 (1973) 447.
7. S. Vyazovkin and C.A. Wight, Int. Rev. Phys. Chem., 17 (1998) 407; Annu. Rev. Phys. Chem., 48 (1997) 125.
8. M. Maciejewski, J. Thermal Anal., 38 (1992) 51; 33 (1988) 1269.
9. A.K. Burnham and R.L. Braun, Energy Fuels, 11 (1997) 88.
10. P.D. Garn, Crit. Rev. Anal. Chem., 3 (1972) 65.
11. V.V. Boldyrev, Thermochim. Acta, 100 (1986) 315; (Ed.)“Reactivity of Solids: Past, Present and Future”, IUPAC, Blackwell Science, Oxford, 1996.
12. A.K. Galwey, Proc. 7th Int. Conf. Thermal Analysis, Wiley-Heyden, Chichester, 1982, Vol. 1, p.38.
13. A.K. Galwey, Thermochim. Acta, 96 (1985) 259.
14. J. Krís and J. Sesták, Thermochim. Acta, 110 (1987) 87.
15. M.W. Beck and M.E. Brown, J. Chem. Soc., Faraday Trans., 87 (1991) 711.
16. M. Arnold, G. E. Veress, J. Paulik and F. Paulik, Thermochim. Acta, 52 (1982) 67; Analyt. Chim. Acta, 124 (1981) 341.
17. A.K. Galwey and M.E. Brown, Proc. R. Soc. London, A450 (1995) 501.
18. G. Varhegyi, Thermochim. Acta, 57 (1982) 247.
19. C. Popescu and E. Segal, J. Thermal Anal., 24 (1982) 309.
20. M. Reading,” Handbook of Thermal Analysis and Calorimetry, Vol. 1, Principles and Practice”, (Ed. M.E. Brown), Elsevier, Amsterdam, 1998., Ch.8.
21. A. Ortega, L.A. Pérez-Maqueda and J.M. Criado, Thermochim. Acta, 239 (1994) 171; J. Thermal Anal., 42 (1994) 551.
22. O. Toft Sørensen, Thermochim. Acta, 50 (1981) 163.
23. J.H. Flynn and B. Dickens, Thermochim. Acta, 15 (1976) 1.
24. G. Gyulai and E. J. Greenhow, Talanta, 21 (1974) 131.
25. J. R. MacCullum, Thermochim. Acta, 53 (1982) 375.
26. P. D. Garn, J. Thermal Anal., 6 (1974) 237.
27. J. Sestak and J. Kratochvil, J. Thermal Anal., 5 (1973) 193.
28. J. Sestak, "Thermophysical Properties of Solids", Comprehensive Analytical Chemistry, Vol. XIID, Elsevier, Amsterdam, 1984.
29. C.D. Doyle, J. Appl. Polym. Sci., 5 (1961) 285.
30. J. Zsako, J. Phys. Chem., 72 (1968) 2406.
31. J. Zsako, "Thermal Analysis", (Ed. Z.D. Zivkovic), University of Beograd, Bor, Yugoslavia, 1984, p. 167.

32. J. Blazejowski, Thermochim. Acta, 48 (1981) 125.
33. A. J. Kassman, Thermochim. Acta, 84 (1985) 89.
34. V. M. Gorbachev, J. Thermal Anal., 25 (1982) 603.
35. C. D. Doyle, Nature, London, 207 (1965) 290.
36. J.H. Flynn, Thermochim. Acta, 300 (1997) 83.
37. J. Sestak and G. Berggren, Thermochim. Acta, 3 (1971) 1.
38. J. Militký and J. Sesták, Thermochim. Acta, 203 (1992) 31.
39. A.A. Zuru, R. Whitehead and D.L. Griffiths, Thermochim. Acta, 164 (1990) 285.
40. D. Dollimore, G.A. Gamlen and T.J. Taylor, Thermochim. Acta, 54 (1982) 181.
41. P. Budrugeac and E. Segal, Thermochim. Acta, 260 (1995) 75.
42. M.E. Brown and A.K. Galwey, Anal.Chem., 61 (1989) 1136.
43. B.R. Wheeler and A.K. Galwey, J.Chem.Soc., Faraday Trans.I, 70 (1974) 661.
44. L.F. Jones, D. Dollimore and T. Nicklin, Thermochim. Acta, 13 (1975) 240.
45. D.W. Henderson, J. Thermal Anal., 15 (1979) 325.
46. J.W. Graydon, S.J. Thorpe and D.W. Kirk, J. Non-crystalline Solids, 175 (1994) 31.
47. S.V. Vyazovkin and A.I. Lesnikovich, J. Thermal Anal., 35 (1989) 2169.
48. J.M. Criado, A. Ortega and F. Gotor, Thermochim. Acta, 157 (1990) 171.
49. R.K. Agrawal, Thermochim. Acta, 203 (1992) 93, 111.
50. S.V. Vyazovkin and A.I. Lesnikovich, J. Thermal Anal., 36 (1990) 599.
51. S.V. Vyazovkin, A.I. Lesnikovich, E.A. Gunin and V.G. Guslev, Thermochim. Acta, 130 (1988) 269.
52. J. Málek, Thermochim. Acta, 200 (1992) 257.
53. S.V. Vyazovkin, J. Comput. Chem., 22 (2001) 178.
54. S. Vyazovkin and C.A. Wight, Anal. Chem., 72 (2000) 3171.
55. S. Vyazovkin and C.A. Wight, Thermochim. Acta, 340/341 (1999) 53.
56. S. Vyazovkin and C.A. Wight, J. Phys. Chem., 101 (1997) 8279.
57. S. Vyazovkin and D. Dollimore, J. Chem. Inf. Comp. Sci., 36 (1996) 42.
58. S. Vyazovkin, Int. J. Chem. Kinet., 28 (1996) 95.
59. J. Sesták, J. Thermal Anal., 16 (1979) 503.
60. M. Maciejewski, Thermochim. Acta, 355 (2000) 145.
61. H. Friedman, J. Polym. Sci., 50 (1965) 183.
62. J. H. Flynn and L. A. Wall, J. Res. Nat. Bur. Stand., 70A (1966) 487.
63. T. Ozawa, Bull. Chem. Soc. Japan, 38 (1965) 1881; J. Thermal Anal., 2 (1970) 301.
64. R. M. Fuoss, O. Sayler and H. S. Wilson, J. Polym. Sci., 2 (1964) 3147.
65. H. E. Kissinger, J. Res. Nat. Bur. Stand., 57 (1956) 217; Anal. Chem., 29 (1957) 1702.
66. J. A. Augis and J. E. Bennett, J. Thermal Anal., 13 (1978) 283.
67. J. P. Elder, J. Thermal Anal., 30 (1985) 657; "Analytical Calorimetry", Vol. 5, ed. P.S. Gill and J. F. Johnson, Plenum, New York, 1984, p.269.
68. A. Van Dooren and B. W. Muller, Thermochim. Acta, 65 (1983) 269.

69. R. Serra, R. Nomen and J. Sempere, Thermochim. Acta, 316 (1998) 37; J. Thermal Anal., 52 (1998) 933.
70. G.E. Forsythe, M.A. Malcolm and C.B. Moler, "Computer Methods for Mathematical Computations", Prentice-Hall, Englewood Cliffs, N.J., USA, 1977, Ch. 9.
71. J. Zsako, J. Thermal Analysis, 2 (1970) 145; J. Phys. Chem., 72 (1968) 2406.
72. M. E. Brown and C. A. R. Phillpotts, J. Chem. Educ., 55 (1978) 556.
73. M. E. Brown and A. K. Galwey, Thermochim. Acta, 29 (1979) 129.
74. N. Koga, Thermochim. Acta, 244 (1994) 1.
75. A. K. Galwey and M. E. Brown, Thermochim. Acta, 300 (1997) 107.
76. G.C. McBane, J. Chem. Ed., 75 (1998) 919.
77. A. K. Galwey and M. E. Brown, Thermochim. Acta, submitted (2001).
78. J. Norwisz and J. Plewa, J. Thermal Anal., 17 (1979) 549.
79. J.M. Criado and M. Gonzalez, Thermochim. Acta, 46 (1981) 201.
80. R.V. Muraleedharan, J. Thermal Anal., 41 (1994) 53.
81. S.V. Vyazovkin and A.I. Lesnikovich, Thermochim. Acta, 165 (1990) 273.
82. J.P. Elder, J. Thermal Anal., 29 (1984) 1327; 34 (1988) 1467; 35 (1989) 1965; 36 (1990) 1077.
83. J.M. Criado, M. González, A. Ortega and C. Real, J. Thermal Anal., 34(1988) 1387.
84. T. Ozawa and K. Kanari, Thermochim. Acta, 234 (1994) 41.
85. S.V. Vyazovkin, Thermochim. Acta, 223 (1993) 201.
86. S.V. Vyazovkin and A.I. Lesnikovich, Thermochim. Acta, 182 (1991) 133.
87. S.V. Vyazovkin and W. Linert, Anal. Chim. Acta, 295 (1994) 101.
88. J.H. Flynn, J. Thermal Anal., 44 (1995) 499.
89. M.E. Brown, R.M. Flynn and J.H. Flynn, Thermochim. Acta, 256 (1995) 477.
90. N. Sbirrazuoli, L. Vincent and S. Vyazovkin, Chemometrics Intell. Lab. Systems, 52 (2000) 23.
91. M.E. Brown, M. Maciejewski and S. Vyazovkin, Thermochim. Acta, 307 (1997) 201; J. Thermal Anal., 51 (1998) 327.
92. M.E. Brown, M. Maciejewski, S. Vyazovkin, R. Nomen, J. Sempere, A. Burnham, J. Opfermann, R. Strey, H.L. Anderson, A. Kemmler, R. Keuleers, J. Janssens, H.O. Desseyn, Chao-Rui Li, Tong B. Tang, B. Roduit, J.Malek and T. Mitsuhashi, Thermochim. Acta, 355 (2000) 125.
93. S. Vyazovkin, Thermochim. Acta, 355 (2000) 155.
94. J.M. Criado, J. Málek and J. Sesták, Thermochim. Acta, 175 (1991) 299.
95. J.H. Flynn, J. Thermal Anal., 37 (1991) 293.
96. J. Málek and J.M. Criado, Thermochim.Acta, 175 (1991) 305.
97. S.V. Vyazovkin and A.I. Lesnikovich, Thermochim. Acta, 122 (1987)413.
98. J. Militký and J. Sesták, Thermochim. Acta, 203 (1992) 31.
99. J. Madarász, G. Pokol and S. Gál, J. Thermal Anal., 42 (1994) 559.
100. S.V. Karachinsky, O. Yu. Peshkova, V.V. Dragalov and A.L. Chimishkyan, J. Thermal Anal., 34 (1988) 761.

101. J. Opfermann, F. Giblin, J. Mayer and E. Kaiserberger, Amer. Lab., (Feb. 1995) 34.
102. J. Opfermann, J. Thermal Anal. Calorim, 60 (2000) 641.
103. H.L. Anderson, A. Kemmler and R. Strey, Thermochim. Acta, 271 (1996) 23.
104. H.J. Flammersheim and J. Opfermann, Thermochim. Acta, 337 (1999) 141.
105. F. Baitalow, H.-G. Schmidt and G. Wolf, Thermochim. Acta, 337 (1999) 111.

PURITY DETERMINATION USING DSC

11.1 Introduction

Measurements of the depression of the melting point [1] of a sample are often used to determine its purity [2]. Melting endotherms, recorded using differential scanning calorimetry (DSC), are routinely used to recognize the occurrence of melting and to measure the melting temperature of the sample. With a bit more effort, as discussed below, it is possible to determine the purity of the sample by analyzing, in detail, the shape of the melting endotherm. There is no need to have a high-purity sample of the substance under investigation for comparison, although a sample of any very pure material, such as indium metal, is needed to determine the thermal performance of the particular instrument being used. Because such materials are used, in any case, to calibrate the instrument for temperature and enthalpy measurements, this last requirement is readily achievable. Calculations are based on the assumptions that solid solutions are not formed and that the melt is an ideal solution. Melting must not be accompanied by decomposition or sublimation. The assumptions made apply only to relatively pure (>98%) materials.

The practical aim of purity determinations is usually to decide whether or not the sample meets certain specifications, determined by the intended further uses of the sample. Special Technical Publication 838 of the ASTM [3] is an important source of information on purity determination. In it, a review by Brennan and co-workers [4] outlines the history of the DSC method and emphasizes A.P. Gray's pioneering work in this area.

The melting endotherm for a pure substance recorded on a DSC is illustrated in Figure 11.1. T_o is the melting point of the sample and the area ABC is proportional to the enthalpy of fusion, ΔH_{fus}, of the sample. The presence of an impurity in the sample (the solvent) generally lowers the melting point of the solvent and also broadens the melting range, giving a broader DSC endotherm as illustrated in Figure 11.2 (inset). From endotherms such as illustrated in Figures 11.1 and 11.2, melting points and enthalpies of fusion may readily be determined. In suitable cases, as mentioned above, an estimate of the purity of a compound can be obtained, from analysis of the detailed shape of its melting endotherm, e.g., Figure 11.2, without reference to compounds containing known amounts of impurities.

Figure 11.1
Idealized DSC record of the melting of pure indium. Slope AB ($=1/R_0$) is used to correct for the thermal lag. T_o is the melting point of the sample and the area ABC is proportional to the enthalpy of fusion, ΔH_{fus}, of the sample [2]. (With the permission of the Journal of Chemical Education.)

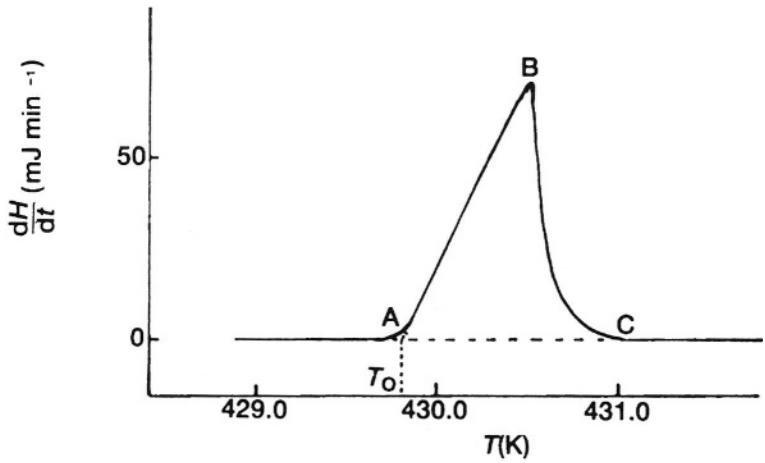

Figure 11.2
Idealized DSC record of melting of an impure sample. The slope of BF (=slope of AB in Figure 11.1) is used to correct the programmed temperature, T_p, to the sample temperature, T_s. T_m is the melting point. The area ABC is proportional to the enthalpy of fusion, ΔH_{fus}, of the sample. The fraction melted, F_n, at temperature T_n = area ADE/area ABC = a_n/A [2]. (With the permission of the Journal of Chemical Education.)

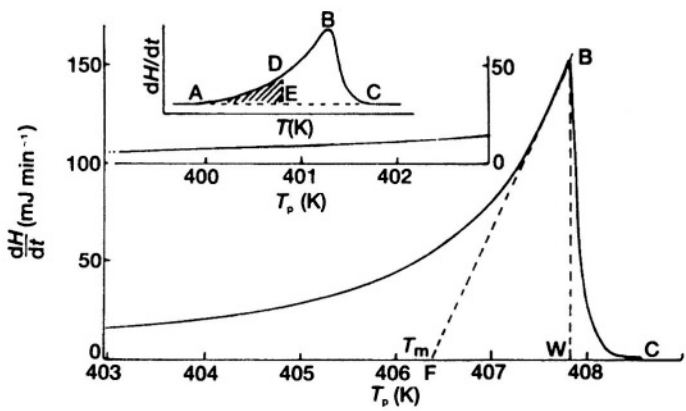

11.2 Phase equilibria

The simplest system to consider is that in which the impurity forms an ideal solution in the melt, i.e. a eutectic system. If the impurity is labelled, in the customary way, as component 2 and the solvent as component 1, then for equilibrium (at constant pressure) between pure 1 in the solid and 1 in the solution (or "melt") at activity a_1, there must be equality of the chemical potentials (μ) of 1 in the two phases:

$$\mu_1^\circ(\mathrm{s}) = \mu_1(\ell)$$

$$\mu_1^\circ(\mathrm{s}) = \mu_1^\circ(\ell) + RT \ln a_1 \qquad (11.1)$$

(where the superscript ° refers to standard conditions, i.e. unit activities). Differentiating equation (11.1) with respect to temperature, T:

$$\mathrm{d}\mu_1^\circ(\mathrm{s})/\mathrm{d}T = (\mathrm{d}\,\mu_1^\circ(\ell)/\mathrm{d}T) + R \ln a_1 + RT\,(\mathrm{d}(\ln a_1)/\mathrm{d}T)$$

and because $\mathrm{d}\mu/\mathrm{d}T = -\bar{S}$ (where the bar represents a molar quantity)

$$-\bar{S}_1^\circ(\mathrm{s}) = -\bar{S}_1^\circ(\ell) + R \ln a_1 + RT\,(\mathrm{d}(\ln a_1)/\mathrm{d}T) \qquad (11.2)$$

From equation (11.1)

$$R \ln a_1 = (\mu_1^\circ(\mathrm{s}) - \mu_1^\circ(\ell))/T$$

so equation (11.2) on rearranging, becomes:

$$\mathrm{d}(\ln a_1)/\mathrm{d}T = [-(\mu_1^\circ(\mathrm{s}) - \mu_1^\circ(\ell))/RT^2] - [(\bar{S}_1^\circ(\mathrm{s}) - \bar{S}_1^\circ(\ell))/RT]$$

$$= \{[(\mu_1^\circ(\ell) + T\bar{S}_1^\circ(\ell)] - [\mu_1^\circ(\mathrm{s}) + T\bar{S}_1^\circ(\mathrm{s})]\}/RT^2$$

or

$$\mathrm{d}(\ln a_1)/\mathrm{d}T = (\bar{H}_1^\circ(\ell) - \bar{H}_1^\circ(\mathrm{s}))/RT^2 = \Delta\bar{H}_{\mathrm{f},1}^\circ/RT^2 \qquad (11.3)$$

because $H = G + TS$ and $\bar{G}^\circ = \mu^\circ$. Integrating equation (13.3) between the limits $a_1 = 1$ at $T = T_o$ (because solid solutions are not formed) and $a_1 = a_1$ at $T = T$, assuming that $\Delta H_{\mathrm{f},1}^\circ$ is independent of temperature over the range:

$$\ln a_1 = (\Delta\bar{H}_{\mathrm{f},1}^\circ/R)[(1/T_o) - (1/T)]$$

For an ideal solution $a_1 = x_1$ (the mole fraction of 1). Hence

$$\ln a_1 = \ln (1 - x_2) = (\Delta \bar{H}_{f,1}^{\circ} / R)[(1/T_o) - (1/T)]$$

For a dilute solution, i.e. small values of x_2,

$$\ln (1 - x_2) \approx - x_2$$

$$x_2 = (\Delta \bar{H}_{f,1}^{\circ} / R)[(1/T) - (1/T_o)] \qquad (11.4)$$

Equation (11.4) forms the basis of melting-point depression calculations, as follows. At $T = T_m$, the melting point of the impure sample:

$$x_2 \approx (\Delta \bar{H}_{f,1}^{\circ} / R)[(T_o - T_m)/(T_o T_m)] = (\Delta \bar{H}_{f,1}^{\circ} / R)[\Delta T_f / (T_o T_m)] \qquad (11.5)$$

If ΔT_f is small, $T_o \approx T_m$ and $T_o T_m \approx T_o^2$. Also $x_2 = n_2/(n_1 + n_2) \approx m M_1/1000$, where m is the molality of the solute and M_1 the molar mass of the solvent. Hence:

$$\Delta T_f = [(R T_o^2 M_1)/(\Delta \bar{H}_{f,1}^{\circ} 1000)]\, m = K_f m$$

where K_f is termed the cryoscopic constant.

Only when the sample is completely melted, i.e. at $T >> T_m$, is the mole fraction of impurity in the liquid, x_2, the same as that in the original sample, x_2^*. From the phase diagram for a simple eutectic system (Figure 11.3) it may be seen that the value x_2^* is the minimum value which x_2 attains. At $T < T_m$ (see Figure 11.3), when the fraction of sample that has melted, F, is less than unity, the composition of the melt is closer to that of the eutectic, i.e., $x_2 > x_2^*$. When melting commences, the first liquid has the eutectic composition.

If F is the fraction melted at temperature T, then, assuming a linear initial segment of the liquidus curve (Figure 11.3), and using equation (11.4):

$$F = n_l/(n_l + n_s) = x_2^*/x_2 = (T_o - T_m)/(T_o - T) = (x_2^* R T_o^2)/[\Delta \bar{H}_{f,1}^{\circ} (T_o - T)] \qquad (11.6)$$

Rearrangement yields:

$$T = T_o - [x_2^* R T_o^2 / \Delta \bar{H}_{f,1}^{\circ}](1/F) \qquad (11.7)$$

If F can be determined at various temperatures, T, a plot of T against $1/F$ should yield a straight line, provided that $\Delta \bar{H}_{f,1}^{\circ}$ is independent of temperature. If the values of T_o and $\Delta \bar{H}_{f,1}^{\circ}$ are known, x_2^* can be determined from the measured slope of the line. The DSC curve is capable of providing values of F at temperatures T for use in such a plot.

Figure 11.3
Low concentration region of a simple eutectic phase diagram (inset) [2]. By the lever rule: $BC/AB = n_{solid}/n_{liquid}$. C is the composition of the melt in equilibrium with pure solid at T. Here $x_2 > x_2^*$. $F = n_\ell/(n_\ell + n_s) = AB/(AB + BC) = AB/BC = x_2^*/x_2$. (With the permission of the Journal of Chemical Education.)

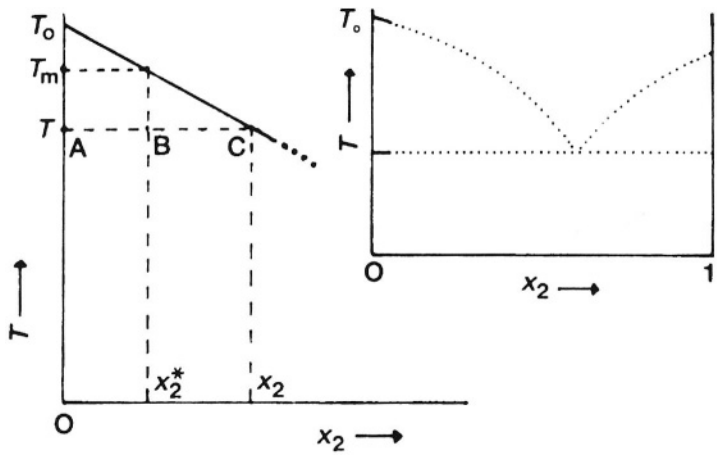

11.3 The DSC melting curve

The DSC measures the thermal energy per unit time, dH/dt, transferred to or from the sample as the temperature of the sample holder, T, is changed at a constant rate, $dT/dt = \beta$. Thus the output from the DSC is directly proportional to the heat capacity of the system, dH/dT.

$$dH/dt = (dH/dT)(dT/dt) \tag{11.8}$$

For an absolutely pure compound with zero melting range, dH/dt would become infinite at the melting point, T_o. For an impure compound, dH/dT is finite and is a function of T.

When the fraction melted, F, is zero, the heat capacity of the sample is that of the solid mixture, and when $F = 1$ the heat capacity of the sample is that of the ideal solution. Intermediate behaviour is obtained as follows:

$$dH/dT = (dH/dF)(dF/dT)$$

dF/dT is obtained from equation (11.6) as:

$$dF/dT = (x_2^* RT_o^2)/[\Delta\bar{H}_{f,1}^\circ (T_o - T)^2]$$

It is also assumed that, because of the restriction to consideration of ideal eutectic systems and to the formation of ideal solutions on melting, that:

$$H_F = F\,\Delta\bar{H}_{f,1}^{\circ}$$

and therefore:

$$dH/dF = \Delta\bar{H}_{f,1}^{\circ}$$

Combining these results:

$$dH/dT = (x_2^* RT_o^2)/(T_o - T)^2 \qquad (11.9)$$

Equation (11.9) then gives the variation of the heat capacity of the sample during melting as a function of T. The upper limit of the melting process is $T = T_m$ (when $F = 1$). Therefore, equation (11.7) becomes:

$$T_m = T_o - [x_2^* RT_o^2/\Delta\bar{H}_{f,1}^{\circ}]$$

The lower limit of the melting process is $T << T_o$, when $dH/dT \approx x_2^* R = C_s$, i.e. the heat capacity of the sample is approximately constant. In the idealized DSC curves given in Figs. 11.1 and 11.2, it has been assumed that the heat capacity of the liquid just above the melting temperature is the same as that of the solid at lower temperatures (i.e., both equal to C_s).

Equation (11.9) can be written as:

$$dH/dT = [x_2^* R(T_o/T)^2]/(T_o/T - 1)^2$$

so that, within the limits of the assumptions made above, the heat capacity during melting depends only on the mole fraction of impurity, x_2^* and the temperature relative to the melting point of the pure substance, T_o/T.

Because dH/dt is proportional to dH/dT, plots of dH/dT against T represent the initial part of an idealized DSC melting curve. Such curves for phenacetin and for benzamide, with values of x_2^* from 0.0050 to 0.3000, have been given by Marti *et al.* [5,6].

The real DSC melting curve, because of factors such as thermal lag, which is discussed in more detail below will look more like the curve in Figure 11.2, inset. The total area under the curve, i.e. area ABC, is proportional to the enthalpy of fusion, $\Delta H_{f,1}^{\circ}$. The actual value of $\Delta\bar{H}_{f,1}^{\circ}$ can be obtained by calibration of the instrument with a standard of known $\Delta H_{f,1}^{\circ}$ (Figure 11.1). The feature sought for the present discussion, the fraction of the sample melted, F, at temperature T, is obtained directly from the fractional area under the curve, i.e. F = area ADE/area ABC. The range of F values used in practice is usually restricted to $0.1 < F < 0.4$. Even with this restricted range, the linearity of plots of T against $1/F$ (equation (11.7)) is often poor. Corrections have to be made for thermal lag and for undetected premelting as discussed below.

11.4 Corrections

11.4.1 Thermal Lag

Flow of thermal energy from the holder at the programmed temperature, T_p, to the sample at a slightly lower temperature, T_s, is governed by Newton's law:

$$T_p - T_s = (dH/dt)\, R_o \qquad (11.10)$$

where R_o is the thermal resistance. The value of R_o for the instrument may be obtained [7] from the melting curve of a high purity standard (Figure 11.1). This will melt over a very narrow temperature range, so that as the programmed temperature continues to increase with time, the sample temperature, T_s, will remain constant, i.e. $dT_s/dt = 0$. From equation (11.10):

$$(dT_p/dt) - (dT_s/dt) = R_o\, [d(dH/dt)/dt]$$

Hence:

$$(dT_p/dt) = R_o\, [d(dH/dt)/dt] = R_o\, (dT/dt)\, [d(dH/dt)/dT] = R_o\, \beta\, [d(dH/dt)/dT]$$

and

$$d(dH/dt)/dT = R_o$$

R_o may thus be determined from the slope, AB, of the DSC melting curve for the high purity standard (Figure 11.1). The value of R_o is then used graphically or analytically to correct the programmed temperature, T_p, to the true sample temperature, T_s. T_s then, rather than T_p, is plotted against $1/F$.

11.4.2 Undetermined Premelting

Even with correction for thermal lag, the linearity of the plots of T_s against $1/F$ is often not good, and corrections have to be made to the measured areas, for melting which has occurred at lower temperatures and which is difficult or impossible to measure. This is evident in the small but cumulatively significant deviation from the ideal baseline illustrated in Figure 11.2.

If the undetermined area under the curve is ϵ, the measured partial areas up to temperatures $T_1, T_2 \ldots\ldots T_n$ are $a_1, a_2 \ldots\ldots a_n$, respectively, and the measured total area is A, the true value of F_n is:

$$F_n = (a_n + \epsilon)/(A + \epsilon)$$

or

$$1/F_n = (A + \epsilon)/(a_n + \epsilon) \approx (A)/(a_n + \epsilon)$$

because $A >> \epsilon$, so the effect of including ϵ is to reduce the value of $1/F_n$, see Figure 11.4. In practice ϵ is treated as a parameter whose value is adjusted so that a plot of T_s against the corrected $1/F$ is linear, see Figure 11.4. The restraints are that the final value of $(A + \epsilon)$ should correspond directly to the correct value of $\Delta H_{f,1}^{\circ}$ (if known) and that the value of T_o, determined from the intercept on the T_s axis, should be correct. Once these conditions have been met, the value of x_2^* (= slope x $\Delta H_{f,1}^{\circ}/RT_o^2$) and hence the purity of the sample can be determined. Because melting actually begins at the eutectic temperature, which may be far below the range of temperatures being examined, the correction, ϵ, may sometimes be quite large and values of as much as 30% of the total area are not uncommon [8]. Obviously the approximation, $A + \epsilon \approx A$, cannot then be used. Sondack [9] has suggested an alternative procedure.

Figure 11.4
Correction for undetermined premelting. The correction = 100 x ϵ/A and $F = (a + \epsilon)/(A + \epsilon)$ [2]. (With the permission of the Journal of Chemical Education.)

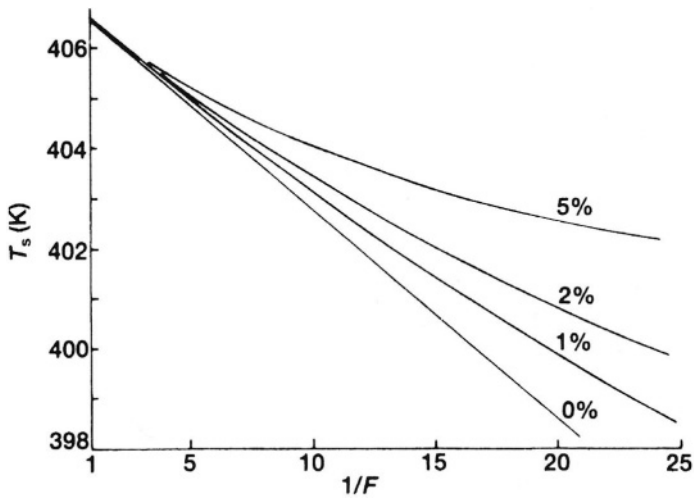

The whole procedure for purity determination is summarized in the flowchart (Figure 11.5). More details on the procedure are given in references [3,9].

Figure 11.5
Flow chart representing the procedure used in purity determination by DSC [2].
(With the permission of the Journal of Chemical Education.)

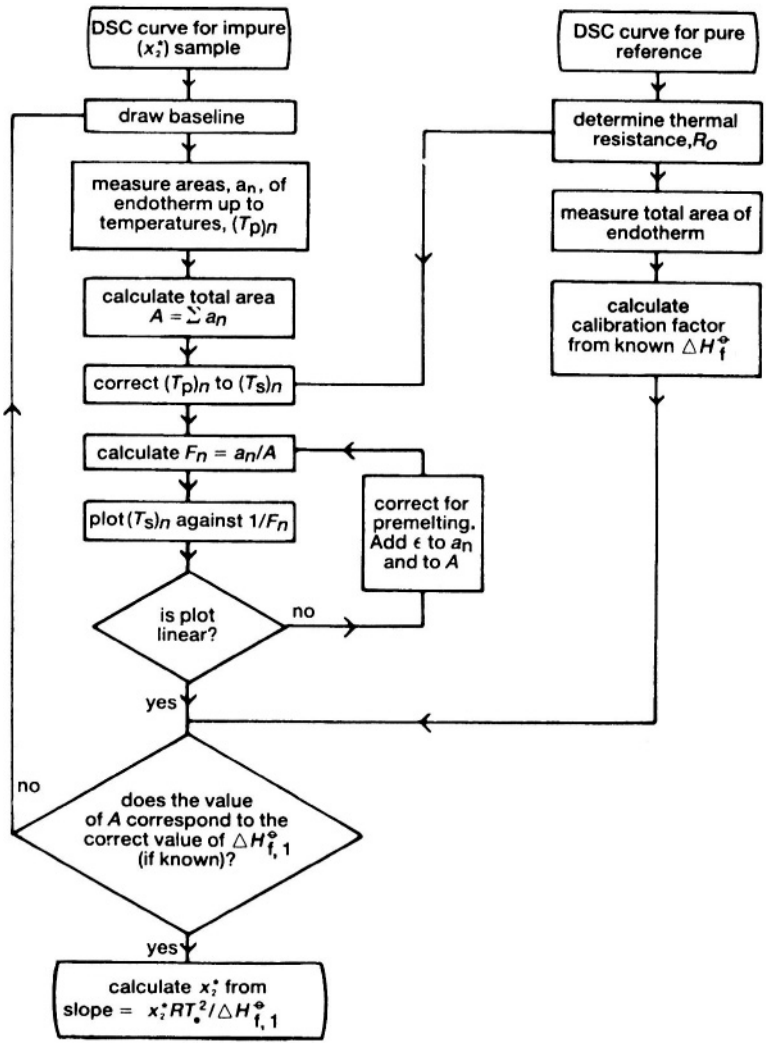

11.5 Step methods

Staub and Perron [10] have shown that a stepped heating technique can extend the working region for purity determination. The sample is heated through the melting region in steps of a few tenths of a degree, thus allowing a closer approach to true thermodynamic equilibrium. The results of such a procedure [11] on an impure phenacetin sample, using a modified DSC-1B are shown in Figure 11.6. There are six steps/5 K and the areas of each peak, obtained by integration, are given. The first eleven peaks and the last three arise from the difference in the heat capacity of the sample and reference. These peaks have approximately constant area and the melting peaks can be corrected for this difference. Because thermal equilibrium is established after each peak, no correction is required for the thermal resistance, R_o, of the system. The corrected areas of all the melting steps are then summed and converted to fractional areas, F and $1/F$ is plotted against T, as before, except that with this procedure [11] all the data are used including the latter part of the melting process. The linearization process for the undetermined premelting still has to be carried out. Gray and Fyans [8] have suggested an alternative procedure to that given above, in which the mole fraction of impurity (x_2^*) is calculated from the areas of two consecutive stepped peaks (a_n and a_{n-1}), the magnitude of the stepping interval (ΔT), and the molar mass (M) and the melting point (T_o) of the pure major component. This method depends upon the applicability of the van't Hoff equation and the relationship derived [8] is:

$$x_2^* = [2M\,\Delta T/\,RT_o^2][(a_n\,a_{n-1})(a_n + a_{n-1})/(a_n - a_{n-1})^2]$$

The melting point (T_o) of the pure solvent may be determined [11] from the areas a_n and a_{n-1}, the step interval ΔT and the final temperature of the step T_n:

$$T_o = T_n + [\,2\,\Delta T\;a_{n-1}/(a_n - a_{n-1})]$$

It is recommended [8] that step increments used should be as large as possible. Elder [12] has compared results obtained using the isothermal step method with those using the dynamic method and discusses the advantages and disadvantages.

11.6 Conclusions

Moros [13] has discussed the design, preparation, and evaluation of phenacetin doped with different amounts of aminobenzoic acid as standards for checking the reliability of purity determinations by DSC. The precision, accuracy and the limits of applicability of the method have been discussed by Hunter and Blaine [14]. Raskin [15], in a critical review of methods of purity determination using DSC, concludes that the accuracy of the method is generally overestimated. A realistic estimate of the accuracy in the range $0.005 < x^{2*} < 0.02$ is given [15] as 30-50% when the sample mass is less than 3 mg and the scanning rate is less than 2 K min^{-1}.

Figure 11.6
Stepwise heating of an impure (96.04 mole %) phenacetin sample [11]. Peak areas are expressed in thousands. (With the permission of the American Chemical Society.)

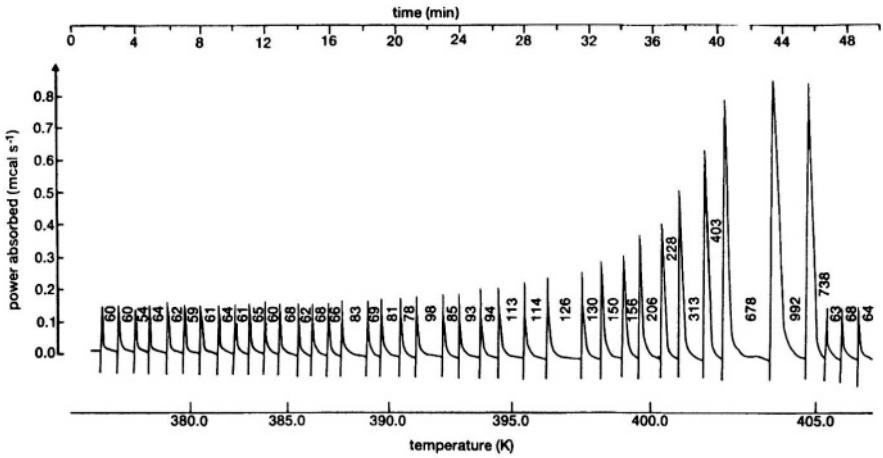

Garn *et al.* [16-18] have discussed the problems that arise when there is appreciable solid solubility. They used NMR to detect the solidus and compared DSC and NMR results. They showed that lack of thermal equilibrium is not a principal source of error in the method and also found that the measured impurity content is sometimes dependent upon the nature of the impurity as well as its concentration. McGhie [19] has provided a very useful discussion of the melting behaviour of solid solutions, using a system consisting of 0 to 20% anthracene in 2,3-dimethyl naphthalene as an example. The normal DSC method is invalid for such systems.

Wiedemann [20] has described the use of simultaneous DSC-thermomicroscopy (see Chapter 5)for purity detemination. The addition of thermomicroscopy allows the various stages of melting to be photographed to show the changes that occur. Flammersheim et al. [21] have discussed the correction of DSC curves for the broadening of peaks caused by the particular apparatus.

Purity determinations by thermal measurements are competitive [22] with other techniques in terms of accuracy, precision, and ease of measurement, and, in many cases, e.g. for crystalline organic compounds, are superior.

References

1. P.W. Atkins, "Physical Chemistry", Oxford University Press, Oxford, 6th Edn, 1998, p.179.
2. M.E. Brown, J. Chem. Educ., 56 (1979) 310.
3. R.L. Blaine and C.K. Schoff (Eds), "Purity Determinations by Thermal Methods", ASTM Special Technical Publication 838, American Society for Testing and Materials, Philadelphia, 1984.
4. W.P. Brennan, M.P. Divito, R.L. Fyans and A.P. Gray, in "Purity Determinations by Thermal Methods", (Eds R.L. Blaine and C.K. Schoff), ASTM Special Technical Publication 838, American Society for Testing and Materials, Philadelphia, 1984, p.5.
5. E.E. Marti, Thermochim Acta, 5 (1973), 173.
6. E.E. Marti, O. Heiber, W. Huber and G. Tonn, Proc. 3rd ICTA, (Ed. H.G. Weidemann), Birkhauser Verlag, Basel, 1971, Vol.3, p.83.
7. Thermal Analysis Newsletters, Nos.5 and 6, Perkin-Elmer Corporation, Norwalk, Connecticut (undated).
8. A.P. Gray and R.L. Fyans, Thermal Analysis Application Study No. 10, Perkin-Elmer, Norwalk, 1973.
9. D.L. Sondack, Anal. Chem., 44 (1972) 888.
10. H. Staub and W. Perron, Anal. Chem., 46 (1974) 128.
11. J. Zynger, Anal. Chem., 47 (1975) 1380.
12. S.A. Moros, in "Purity Determinations by Thermal Methods", (Eds R.L. Blaine and C.K. Schoff), ASTM Special Technical Publication 838, American Society for Testing and Materials, Philadelphia, 1984, p.22.
13. J.E. Hunter III and R.L. Blaine, in "Purity Determinations by Thermal Methods", (Eds R.L. Blaine and C.K. Schoff), ASTM Special Technical Publication 838, American Society for Testing and Materials, Philadelphia, 1984, p.39.
14. J.P. Elder, in "Purity Determinations by Thermal Methods", (Eds R.L. Blaine and C.K. Schoff), ASTM Special Technical Publication 838, American Society for Testing and Materials, Philadelphia, 1984, p.50.
15. A.A. Raskin, J. Thermal Anal., 30 (1985) 901.
16. P.D. Garn, B. Kawalec, J.J. Houser and T.F. Habash, Proc. 7th ICTA, Vol.2, Wiley, Chichester, 1982, p.899.
17. B. Kawalec, J.J. Houser and P.D. Garn, J. Thermal Anal., 25 (1982) 259.
18. T.F. Habash, J.J. Houser and P.D. Garn, J. Thermal Anal., 25 (1982) 271.
19. A.R. McGhie, in "Purity Determinations by Thermal Methods", (Eds R.L. Blaine and C.K. Schoff), ASTM Special Technical Publication 838, American Society for Testing and Materials, Philadelphia, 1984, p.61.
20. H.G. Wiedemann, R. Riesen and G. Bayer, in "Purity Determinations by Thermal Methods", (Eds R.L. Blaine and C.K. Schoff), ASTM Special Technical Publication 838, American Society for Testing and Materials, Philadelphia, 1984, p.107.

21. H.J. Flammersheim, N. Eckhardt and W. Kunze, Thermochim. Acta, 187 (1991) 269.
22. C.K. Schoff, in “Purity Determinations by Thermal Methods”, (Eds R.L. Blaine and C.K. Schoff), ASTM Special Technical Publication 838, American Society for Testing and Materials, Philadelphia, 1984, p. 141.

CONCLUSIONS

12.1 The Range of Thermal Analysis

In the preceding Chapters, only a few selected examples have been given of the vast number of applications of thermal analysis. To get a better idea of the range of applications over all branches of inorganic, organic, physical and industrial chemistry, metallurgy, polymer science, glass and ceramic science, food science, biology, geology, pharmacy, medicine, agriculture and engineering, it is worth scanning the contents pages of some of the proceedings of the International Conferences on Thermal Analysis and Calorimetry (ICTAC), as well as the biennial reviews in Analytical Chemistry (detailed references are given in Appendix A), or any issue of the major journals in the field: Thermochimica Acta and the Journal of Thermal Analysis and Calorimetry.

As suggested in the opening paragraphs of this book, there are very few materials which will not show interesting changes on heating. The materials studied have ranged from kidney stones to synthetic diamonds, and from ancient papyri to the latest polymers and ceramics for very specialized applications. Maximum information can only be obtained by combining the results of the use of several different (preferably simultaneous) thermal analysis techniques with other complementary measurements. The information so obtained has been used to solve old problems and to develop new processes for the future.

12.2 The Future of Thermal Analysis

Reading and colleagues, who have been so active at the forefront of developments in many areas of Thermal Analysis, have published their views of "Thermal Analysis for the 21st Century" [1]. They identify three major problems with current thermal methods: the long time required for measurements; the small size of samples, and the averaged nature of the information obtained. Reading and co-workers have made very considerable contributions to this third problem by their role in the development of modulated temperature DSC (see Chapter 4) that has allowed reversible and irreversible processes to be separated. The introduction of modulated techniques has been a major advance in TA [2] and has been followed by another very promising new direction, that of micro thermal analysis (see Chapter 5), also resulting from the creativity and skill of Reading and his colleagues.

Much of the future of TA lies in the further development of these techniques [3] and the applications that will arise as the equipment required becomes more readily available.

Special issues of both Thermochimica Acta [4] and the Journal of Thermal Analysis and Calorimetry [5] have surveyed the field of TA at the beginning of a new millennium.

The limited information available from the original basic techniques of TG, DSC/DTA, TMA and DMA on their own is inadequate for the full solution of most problems in materials science. TG will have to be operable in highest resolution mode with some form of evolved gas analysis (MS or FTIR) being essential. Information on the effects of modulating the temperature (or other parameters) during examination of a sample is also becoming essential. The various spin-off techniques from atomic force microscopy will permit the real heterogeneous nature of materials to be explored.

Mathot [6] has surveyed the development of thermal analysis and calorimetry in recent years and has sounded a warning about the lack of attention paid by educational institutions to analytical science in general and to training in the techniques of thermal analysis and calorimetry in particular. He forecasts a decreasing competence level of users of the techniques. To counteract this, Mathot suggests that efforts should be made to: use present capabilities to the full; improve existing equipment; develop new equipment (and not leave this entirely to the manufacturers); decrease the "black-box" nature of much of the hardware and software so that users are aware of, and understand, what they are doing; and improve data measurement, processing and presentation. The key to doing this relies on the education provided by institutions, manufacturers and national and international thermal analysis and calorimetry societies.

References

1. M. Reading, D.J. Hourston, M. Song, H.M. Pollock and A. Hammiche, Amer. Lab., January 1998, 13.
2. B. Wunderlich, Thermochim, Acta, 355 (2000) 43.
3. D.M. Price, M. Reading,, A. Hammiche and H.M. Pollock, J. Thermal Anal. Calorim., 60 (2000) 723.
4. W. Hemminger (Ed.), Thermochimica Acta, Vol. 355 (2000).
5. M.E. Brown, N. Koga, J. Malek and J. Mimkes (Eds), Journal of Thermal Analysis and Calorimetry, Vol. 60, No. 3, (2000).
6. V.B.F. Mathot, Thermochim. Acta, 355 (2000) 1.

APPENDIX A: THE LITERATURE OF THERMAL ANALYSIS

An introduction to the vast literature of thermal analysis is given below. See also Hemminger and Sarge in Chapter 1 of Volume 1 of the Handbook of Thermal Analysis & Calorimetry (Ed. M.E. Brown), Elsevier, Amsterdam, 1998.

A.1 Books

R.L. Blaine and C.K. Schoff (Eds), Purity Determinations by Thermal Methods, ASTM Special Technical Publication 838, American Society for Testing and Materials, Philadelphia, 1984.

A. Blazek, Thermal Analysis, Van Nostrand Reinhold, London, 1972.

M.E. Brown (Ed.), Handbook of Thermal Analysis and Calorimetry, Vol.1, Principles and Practice, Elsevier, Amsterdam, 1998.

E.L. Charsley and S.B. Warrington (Eds.), Thermal Analysis: Techniques and Applications, Royal Society of Chemistry, Cambridge, 1992, 296 pp.

T. Daniels, Thermal Analysis, Kogan Page, London, 1973.

J.W. Dodd and K.H. Tonge, Thermal Methods: Analytical Chemistry by Open Learning, Wiley, Chichester, 1987, 337 pp.

C. Duval, Inorganic Thermogravimetric Analysis, 2nd Rev. Edn, Elsevier, Amsterdam, 1962.

C.M. Earnest, Thermal Analysis of Clays, Minerals and Coals, Perkin-Elmer, Norwalk, 1984.

G.W. Ehrenstein, G. Riedel and P. Trawiel, Praxis der Thermischen Analyse von Kunstoffen, Hanser, 1998.

J.L. Ford and P. Timmins, Pharmaceutical Thermal Analysis: Techniques and Applications, E. Horwood, Chichester, 1989, 313 pp.

P.D. Garn, Thermoanalytical Methods of Investigation, Academic Press, New York, 1965.

P.J. Haines, Thermal Methods of Analysis: Principles, Applications and Problems, Blackie Academic and Professional, London, 1995, 286 pp.

V.R. Harwalkar and C.-Y. Ma (Eds.), Thermal Analysis of Foods, Elsevier, London, 1990, 362 pp.

F. Hatakeyama and F. X. Quinn, Thermal Analysis: Fundamentals and Applications to Polymer Science, Wiley, Chichester, 1994, 158 pp.

T. Hatakeyama and Zhenhai Liu, Handbook of Thermal Analysis, Wiley, Chichester, 1998.

K. Heide, Dynamische thermische Analysenmethoden, Deutscher Verlag für Grundstoffindustrie, Leipzig, 2nd Edn, 1982, 311 pp.

W.F. Hemminger and H.K. Cammenga, Methoden der Thermischen Analyse, Springer, Berlin, 1989, 299 pp.

G. Höhne, W. Hemminger and H.-J. Flammersheim, Differential Scanning Calorimetry - An Introduction for Practitioners, Springer, Berlin, 1996, 222 pp.

C.J. Keattch and D. Dollimore, An Introduction to Thermogravimetry, 2nd Edn, Heyden, London, 1975, 164 pp.

R.B. Kemp (Ed.), Handbook of Thermal Analysis and Calorimetry, Vol.4, From Macromolecules to Man, Elsevier, Amsterdam, 1999, 1032 pp.

H. Kopsch, Thermal Methods in Petroleum Analysis, Wiley, New York, 1995.

W. Lodding (Ed.) Gas Effluent Analysis, Arnold, London, 1976, 220 pp.

C. Lu and A.W. Czanderna (Eds), Applications of Piezoelectric Quartz Crystal Microbalances, Elsevier, Amsterdam, 1984.

R.C. Mackenzie (Ed.), Differential Thermal Analysis, Vol.1 and 2, Academic Press, London, 1969.

J.L. McNaughton and C.T. Mortimer, Differential Scanning Calorimetry, Perkin-Elmer Order No.: L-604 (Reprinted from IRS; Phys. Chem. Ser.2 (1975) Vol.10, Butterworths), 44 pp.

E. Marti, H.R. Oswald and H.G. Wiedemann (Eds), Angewandte chemische Thermodynamik and Thermoanalytik, Birkhauser Verlag, Basel, 1979.

V.B.F. Mathot (Ed.), Calorimetry and Thermal Analysis of Polymers, Carl Hanser, München, 1994, 369 pp.

K.P. Menard, Dynamic Mechanical Analysis - A Practical Introduction, CRC Press, Boca Raton, USA, 1999, 208 pp.

O. Menis, H.L. Rook and P.D. Garn (Eds), The State-of-the-Art of Thermal Analysis, NBS Special publication 580, 1980.

R.Sh. Mikhail and E. Robens, Microstructure and Thermal Analysis of Solid Surfaces, Wiley, Chichester, 1983, 496 pp.

F. Paulik, Special Trends in Thermal Analysis, Wiley, Chichester, 1995, 459 pp.

M.I. Pope and M.D. Judd, Differential Thermal Analysis, Heyden, London, 1977.

A.T. Riga and C.M. Neag, Materials Characterization by Thermomechanical Analysis, American Society for Testing and Materials, Philadelphia, 1991.

M.P. Sepe, Thermal Analysis of Polymers, Rapra Review Report No. 95, RAPRA, 1997.

W. Smykatz-Kloss, Differential Thermal Analysis, Applications and Results in Mineralogy, Springer-Verlag, New York, 1974.

W. Smykatz-Kloss and S.St.J. Warne (Eds.), Thermal Analysis in the Geosciences, Springer, Berlin 1991, 379 pp.

R.F. Speyer, Thermal Analysis of Materials, Marcel Dekker, New York, 1994, 285 pp.

J.W. Stucki, D.L. Bish and F.A. Mumpton (Eds), Thermal Analysis in Clay Science, Clay Minerals Society, 1990.

D.N. Todor, Thermal Analysis of Minerals, Abacus Press, Tunbridge Wells, 1976.

E.A. Turi (Ed.), Thermal Characterization of Polymeric Materials, Academic Press, New York, 2nd Edn., 1996.

W.W. Wendlandt, Thermal Analysis, 3rd Edn., Wiley, New York 1986, 814 pp.

W.W. Wendlandt and L.W. Collins (Eds), Thermal Analysis (Benchmark Papers in Analytical Chemistry), Dowden, Hutchinson & Ross, Stroudsbourg, USA, 1976.

W.W. Wendlandt and J.P. Smith, Thermal Properties of Transition Metal Ammine Complexes, Elsevier, Amsterdam, 1967.

G. Widmann, R. Riesen, Thermal Analysis. Terms, Methods, Applications, Hüthig, Heidelberg, 1986, 131 pp.

C.L. Wilson and D.W. Wilson (Eds), Comprehensive Analytical Chemistry, Elsevier, Amsterdam.
Vol.XIIA: Simultaneous Thermoanalytical Examinations by Means of the Derivatograph, J. Paulik and F. Paulik, 1981, 277 pp.
Vol.XIIB: Biochemical and Clinical Applications of Thermometric and Thermal Analysis, N.D. Jesperson (Ed), 1982.
Vol.XIIC: Emanation Thermal Analysis and other Radiometric Emanation Methods, V. Balek and J. Tolgyessy, 1983, 304 pp.
Vol.XIID: Thermophysical Properties of Solids, J. Sestak, 1984, 440 pp.

S.P. Wolsky and A.W. Czanderna (Eds), Microweighing in Vacuum and Controlled Environments, Elsevier, Amsterdam, 1980.

B. Wunderlich, Thermal Analysis, Academic Press, Boston, 1990, 450 pp.

Videotapes

The University of York Electronics Centre, York, England, has produced 3 videotapes of about 25 minutes each, entitled "Thermal Analysis: An Introduction to Principles and Practice", for commercial distribution.

Computer-assisted Courses

ATHAS (Advanced Thermal Analysis System) is a group founded by Professor B. Wunderlich at the University of Tennessee. This site offers computer-assisted courses.

web.utk.edu/~athas/

Many more sites of interest can be found by following the links from the ICTAC website at www.ictac.org

A.2 Conference Proceedings

The proceedings of the International and European Congresses on Thermal Analysis and Calorimetry (ICTAC and ESTAC) are valuable sources.

TABLE A1 ICTA / ICTAC Conferences

NO.	DATE	PLACE	EDITOR	PUBLISHER
12th	2000	Copenhagen, Denmark	O. Toft Sørensen P. Juul Møller	J. Thermal Analysis and Calorimetry, Vol.64 (2001)
11th	1996	Philadelphia, USA	M.Y. Keating	J. Thermal Analysis Vol. 49 (1-3) (1997).
10th	1992	Hatfield, UK	D.J. Morgan	J. Thermal Analysis Vol. 40 (1-3) (1993).
9th	1988	Jerusalem, Israel	S. Yariv	Thermochimica Acta Vols 133-135 (1988); 148 (1988). Pure Appl. Chem. 61 (1989) 1323-1360.
8th	1985	Bratislava, Czechoslovakia	A. Blazek, V. Balek, J. Sestak	Thermochimica Acta Vols 92,93 (1985); 110 (1986).
7th	1982	Kingston, Canada	B. Miller	Wiley (1982).
6th	1980	Bayreuth, FRG	H.G. Wiedemann W. Hemminger	Birkhauser Verlag 1980.
5th	1977	Kyoto, Japan	H. Chihara	Heyden, 1977.
4th	1974	Budapest, Hungary	I. Buzas	Akademai Kiado, 1975.
3rd	1971	Switzerland	H.G. Wiedemann	Birkhauser Verlag
2nd	1968	Worcester, USA	R.F. Schwenker Jr. and P.D. Garn	Academic
1st	1965	Aberdeen, UK	J.P. Redfern	Macmillan, 1965.

TABLE A2 European Symposia on Thermal Analysis and Calorimetry (ESTAC)

NO.	DATE	PLACE	EDITOR	PUBLISHER
7th	1998	Balatonfured, Hungary	J. Kristóf Cs. Novák	J. Thermal Anal. Calorim., 56 (1999) 1-1478.
6th	1994	Grado, Italy	I. Kikic, A. Cesàro, G. Della Gatta	Thermochim. Acta, 269/270 (1995). Pure Appl. Chem., 67 (1995) 1789 - 1890.
5th	1991	Nice, France	R. Castanat, E. Karmazsin	J. Thermal Anal., 38 (1992) 1-1025.
4th	1987	Jena, GDR	D. Schultze	J. Thermal Anal., 33 (1988).
3rd	1984	Interlaken, Switzerland	E. Marti, H.R. Oswald	Thermochim. Acta, 85 (1985) 1-533.
2nd	1981	Aberdeen, UK	D. Dollimore	Heyden, 1981.
1st	1976	Salford, UK	D. Dollimore	Heyden, 1976.

Much valuable information can also be found in the proceedings of the conferences of national societies, especially those of the North American Thermal Analysis Society (NATAS). Many such proceedings are now published as special issues of the Journal of Thermal Analysis and Calorimetry or Thermochimica Acta (see below).

A.3 Journals

The Journal of Thermal Analysis & Calorimetry(Kluwer) and Thermochimica Acta (Elsevier) are the main English language specialist journals, although results of thermal analyses appear in many other journals, especially Analytical Chemistry, Talanta, Analytica Chimica Acta, International Laboratory, Laboratory Practice, Analyst, and the many polymer journals.

At two-year intervals, the journal Analytical Chemistry publishes reviews including detailed references. Analytical Chemistry, 72 (2000) 27R; 70 (1998) 27R; 68 (1996) 63R; 66 (1994) 17R; 64 (1992) 147R; 62 (1990) 44R; 60 (1988) 274R; 58 (1986) 1R; 56 (1984) 250R; 54 (1982) 97R; 52 (1980) 106R; 50 (1978) 143R; 48 (1976) 341R; 46 (1974) 451R; 44 (1972) 513R; 42 (1970) 268R; 40 (1968) 380R; 38 (1966) 443R; 36 (1964) 347R and earlier reviews on DTA.

Both Thermochimica Acta and the Journal of Thermal Analysis and Calorimetry have published special issues on a variety of themes and in honour of leading thermal analysts.

The two references below are of particular historical value:

R.C. Mackenzie, A History of Thermal Analysis, Thermochim. Acta, 73 (1984), 251 - 367.

W.W. Wendlandt, The Development of Thermal Analysis Instrumentation 1955 - 1985, Thermochim. Acta, 100 (1986), 1 - 22.

A.4 Nomenclature

The International Confederation for Thermal Analysis and Calorimetry (ICTAC) has published several recommendations for the standardizing and reporting of results of thermal analysis. Nomenclature is always evolving, as discussed in Chapter 1, as new techniques are introduced and existing techniques are modified. To follow part of this evolution, the following references are suggested. For the latest recommendations it is probably wise to consult the ICTAC website and also follow any links from there to organizations such as ASTM.

R.C. Mackenzie, Talanta, 16 (1969) 1227; Pure Appl. Chem., 37 (1974) 439; Talanta, 19 (1972) 1079;J. Therm. Anal., 8 (1975); Thermochim. Acta., 28 (1979) 1 and 46 (1981) 333.

See also The Metrication of Thermal Analysis or Conversion to SI Units, R.L. BLAINE, Thermochim. Acta, 26 (1978) 217-228.

R.C. Mackenzie, Nomenclature in Thermal Analysis, in: Treatise on Analytical Chemistry (P.J. Elving, Ed.), Part 1, Vol. 12, Wiley, New York, 1983, pp. 1- 16.

International Confederation for Thermal Analysis: For Better Thermal Analysis and Calorimetry, 3rd Ed. (J.O. Hill, Ed.), 1991.

A.5 Manufacturer's Literature

The major manufacturers provide extensive information on thermal analysis, most of which can be downloaded from their websites (see Appendix B).

APPENDIX B: MAJOR SUPPLIERS OF THERMAL ANALYSIS EQUIPMENT

B.1 Choosing Thermal Analysis Equipment

A bewildering array of equipment is available to anyone starting out in thermal analysis and selecting a suitable system is not an easy decision. It is advisable first to visit the websites of the suppliers (see below), or collect the pamphlets and specifications of most systems from the suppliers and then attempt to make a preliminary selection by considering the following factors:

(1) What types of sample are going to be examined both immediately and as far as can be predicted, in the future?

(2) What sort of information on the sample is required, e.g. thermal stability, glass-transitions, percentage crystallinity, mechanical properties, details of gases evolved etc.?

(3) Over what temperature ranges are the changes that are of interest likely to occur?

Answers to the above questions can be used to eliminate definitely unsuitable systems. Unless there are very special requirements such as extreme ranges of temperature, or use of very corrosive atmospheres or strongly exothermic or even explosive samples, there will usually still be a wide choice of instruments. Prices related to budget available will obviously be a further restriction, and modular systems, which can be added to, are attractive.

A most important question to be answered before choosing a system, is the training and service available from the suppliers. This involves seeking out other users and checking on their experiences. At the same time it is worth checking on the prices of spares and accessories (which can be ridiculously high). Even the best equipment (which need not be the most expensive) will be difficult to operate and maintain if the local agents cannot provide informed and rapid service.

B.2 Major Suppliers of Thermal Analysis Equipment

These are listed (in alphabetical order) in the Table following. Because of rapid changes in the market, it is recommended that a search be done if any difficulties are encountered in accessing a website. It is also possible to follow links from the ICTAC website at www.ictac.org

Major Suppliers of Thermal Analysis Equipment (in alphabetical order)

Company	Address	Website
Cahn (see Thermo Cahn)		
Haake (see Thermo Haake)		
Linseis GmbH	Vielitzerstrasse 43, 8672 Selb, FRG	www.linseis.com
Mettler-Toledo Instrumente AG	CH-8606 Greifensee, Switzerland	www.mt.com
Netzch-Geratebau GmbH	P O Box 1460, D-8672 Selb, Germany	www.netzsch.com
Perkin-Elmer Corporation	761 Main Avenue, Norwalk, Connecticut 06856, USA	www.instruments.perkinelmer.com
Polymer Laboratories	Essex Road, Church Stretton , SY6 6AX, England	
Seiko (see Thermo Haake)		
Setaram	7, rue de l'Oratoire, F-69300 Caluire, France	www.setaram.com
Shimadzu Corporation	1, Nishinokyo Kuwabaracho, Nakagyou-ku, Kyoto 604-8511, Japan	www.shimadzu.com www.shimadzu.co.jp
TA Instruments	109 Lukens Drive, New Castle, DE 19720, USA	www.tainst.com
Thermo Cahn	5225 Verona Rd, Madison, WI 5371, USA	www.cahn.com
Thermo Haake	Dieselstr.4, Karlsruhe BW 76227, Germany	www.thermohaake.com

APPENDIX C: DATA PROCESSING IN THERMAL ANALYSIS

C.1 Introduction

Wendlandt [1] and Wunderlich [2] have dealt with some of the historical aspects of the impact of microcomputers on the field of thermal analysis. Changes have been so rapid that methods and equipment described in papers published even a few years ago (including the first edition of this book) have generally become obsolete and the trend will continue with developments such as the Internet, etc..

The manufacturers of thermal analysis equipment offer both the hardware and the software necessary to carry out most thermal analyses, with a high degree of automation, and to calculate the usual parameters from the captured data. These systems are generally specific to the particular manufacturer's equipment and the software may be difficult, or even impossible to modify for one's own requirements. Some calculations, such as the derivation of kinetic parameters under nonisothermal conditions (see Chapter 10), are areas of controversy and continuing development and it is necessary to know the approach and the algorithms being used in such software before any significance can be attached to the output. In this brief appendix, some of the basic procedures involved in data processing are outlined. A more detailed discussion is given in reference [3].

The data processing required for thermal analysis in general, and especially for DSC and DTA, bears many resemblances to that developed for gas chromatography, e.g. the establishment of and correction of the signal for the baseline; detection of onset of peaks, peak maxima and the return to the baseline; resolution of overlapping peaks and determination of areas under peaks by numerical integration. The routines required for TG usually involve smoothing and numerical differentiation, buoyancy corrections, and possibly polynomial regression. All of the above procedures are well documented. Other more specialized procedures, such as kinetic analysis under nonisothermal conditions (Chapter 10), determination of purity by detailed analysis of the shape of melting endotherms (Chapter 11), the determination of glass-transition temperatures and of heat capacities, are usually available from the manufacturers, or may be carried out by importing data files into spreadsheet packages.

C.2 Data processing

The sequence of operations in the capture and processing of data from thermal analysis experiments is usually: (1) data capture and storage; (2) display of data for preliminary examination; (3) manipulation of the data: (a) baseline correction, (b) smoothing, (c) scaling; (4) processing of the data: (a) numerical differentiation, (b) peak integration; (5) other calculations, e.g., (a) kinetic analysis, (b) purity determination, etc.

Data capture, storage and display are too hardware-specific for discussion to be useful. Baseline correction and scaling are usually fairly straightforward to understand from the options available in the software provided.

C.3 Spreadsheet and database packages [5-10]

The availability of powerful spreadsheet packages, such as Microsoft Excel and Corel Quatro, has virtually removed any necessity for the writing or use of dedicated software. Reich and co-workers have published a series of papers on the use of spreadsheets [4-6] and databases [7-9] for kinetic analyses of thermal analysis results. These papers also show how the power of such packages continues to improve.

C.4 Algorithms

Smoothing of data
Whether data has been smoothed and the method, if any, used is seldom easy to ascertain. Very smooth traces with little noise may indicate either excellent instrumentation or heavy smoothing. Various types of numerical filters are available. Savitsky-Golay [10] smoothing involves a least-squares convolution method and weighting factors are given [10] for from 5 to 25-point polynomials. Where it is important not to lose points from the ends of the data sets, a modification developed by Gorry [11] can be used. Ebert et al. [12] have published a spline smoothing program in Basic. Marchand and Marmet [13] have described a binomial filter and Bussian and Hardle [14] a robust filter. The application of some of these smoothing routines to a noisy DSC trace is illustrated in Figure C1.

Numerical differentiation
A DSC or DTA curve is already an example of a differential measurement and so such curves are not usually differentiated further. If an integral measurement such as a TG curve has been recorded, then a DTG curve can be obtained by numerical differentiation. The usual method is that of Savitsky and Golay [10]. Data points must be at equally spaced time intervals. As an example of a 9-point convolution acting on point y_4, with a normalising constant [10] of 60:

$$dy / dt = (- 4\, y_o - 3\, y_1 - 2\, y_2 - y_3 + y_5 + 2\, y_6 + 3\, y_7 + 4\, y_8) / (60\, \Delta t)$$

Peak integration
Peak area determination (see Figure C2) is usually done by numerical integration using either Simpson's rule or the trapezoidal rule. For a large number of closely spaced points, the trapezoidal rule is adequate and simpler. As an example, the cumulative area calculated by the trapezoidal rule is:

$$|(y_1 - y_o)\, \Delta t / 2\,| = a$$

$$|(y_2 - y_1)\, \Delta t / 2\,| + (y_1 - y_o)\, \Delta t + a = b$$

$$|(y_3 - y_2)\, \Delta t / 2\,| + (y_2 - y_o)\, \Delta t + b = c, \text{ etc.}$$

Figure C1
Digital smoothing of DSC traces and the effect of smoothing on the area (517.8 to 597.8 K) under the peak. (a) Original DSC trace(area = 100.0); (b) Savitsky-Golay [10] 5-point filter 1 pass (area = 99.4); (c) Savitsky-Golay 5-point filter after 5 passes (area = 98.4); (d) binomial filter [12] 1 pass (area = 98.1); (e) binomial filter 5 passes (area = 96.0); (f) binomial filter 10 passes (area = 94.9).

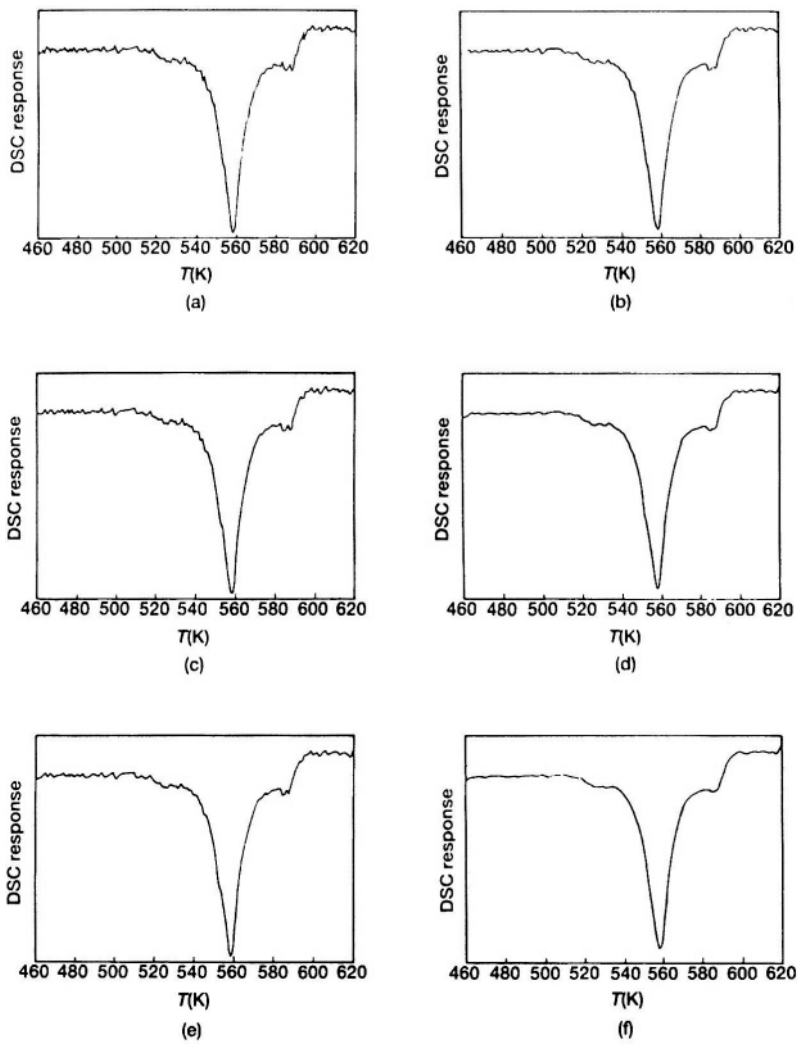

Figure C2
Peak area determination

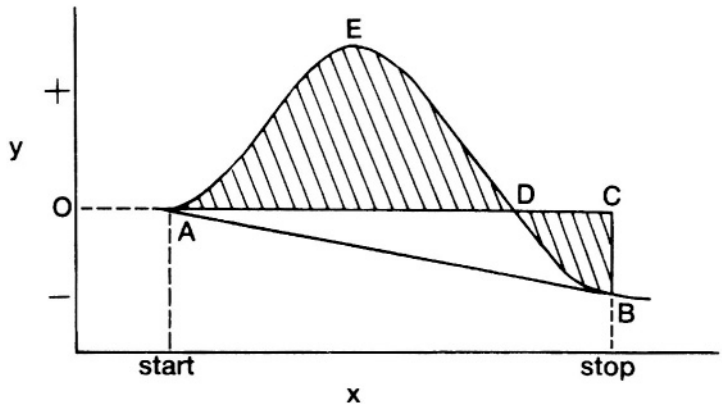

shaded region = area at return = area AEDA − area DCBD
triangle ABC = area correction = area ADBA + area DCBD
corrected area = shaded region + correction
area AEDBA = area AEDA − area DCBD + area ADBA + area DCBD
= area AEDA + area ADBA

References

1. W.W. Wendlandt, Thermochim. Acta, 5 (1973) 225.
2. B. Wunderlich, Int. Lab., October 1982, 32.
3. R.F. Speyer, Thermal Analysis of Materials, Marcel Dekker, New York, 1994, Ch. 4.
4. L. Reich and S.H. Patel, Amer. Lab., 19(9) (1987) 23.
5. L. Reich and S.S. Stivala, Thermochim. Acta, 138 (1989) 177.
6. L. Reich, Thermochim. Acta, 143 (1989) 311; 164 (1990) 1,7; 173 (1990) 253.
7. L. Reich, Thermochim. Acta, 180 (1991) 303; 185 (1991) 205; 195 (1992) 221; 200(1992)349.
8. L. Reich and S.H. Patel, Thermochim. Acta, 222 (1993) 85; 246 (1994) 107.
9. L. Reich, Thermochim. Acta, 231 (1994) 177; 273 (1996) 113.
10. A. Savitsky and M.J.E. Golay, Anal. Chem., 36 (1964) 628.
11. P.A. Gorry, Anal. Chem., 62 (1990) 570.
12. K. Ebert, H. Ederer and T.L. Isenhour, Computer Applications in Chemistry, VCH Verlag, Weinheim, 1989.
13. Marchand and Marmet, Rev. Sci. Instr., 54 (1984) 1034.
14. B-M. Bussian and W. Hardle, J. Appl. Spectrosc., 38 (1984) 309.

APPENDIX D: INTRODUCTORY EXPERIMENTS IN THERMAL ANALYSIS

A selection of introductory experiments is given below. What can be done will obviously be determined by the apparatus available, and constant reference should be made to the manuals supplied with the instruments. Modern computerized instruments will usually operate interactively, providing some of the directions given in the procedures below. Access to simultaneous techniques and/or evolved gas analysis will add to the possibilities suggested below and provide a great deal more information.

D.1 DIFFERENTIAL SCANNING CALORIMETRY (DSC)

A1) *Calibration:* Calibrate a DSC with respect to temperature and heat flow. Check on the reproducibility. Compare the results obtained on different instruments, if possible. Carefully compare the calibration procedures given in the respective manuals for power-compensated and heat-flux instruments.

A2) *Dehydration:* Determine the temperatures and enthalpy changes for the dehydration stages of $CuSO_4.5H_2O$. Carry out similar measurements on some other hydrates, e.g. $BaCl_2.2H_2O$, $Ni(HCOO)_2.2H_2O$ (formate) or $Ni(COO)_2.2H_2O$ (oxalate) and see how the enthalpy of dehydration per mole of H_2O varies from salt to salt. Check the reproducibility of the enthalpy measurements and examine the influence of baseline choice on the values obtained.

A3) *Decompositions*: Study the decompositions of some metal carboxylates, e.g., $Ni(HCOO)_2.2H_2O$ or $Ni(COO)_2.2H_2O$, after first having dehydrated them (see 2). Try to carry out an isothermal DSC run at a suitable temperature. Use the data obtained in programmed temperature experiments at different heating rates to estimate kinetic parameters using some of the procedures described in Chapter 10.

A4) *Phase transitions*: Determine the temperatures and enthalpy changes of phase transitions in salts such as NH_4NO_3, KNO_3, $KClO_4$ or Ag_2SO_4. Study the reversibility of these changes on cooling and comment on the use of these transition temperatures as temperature standards for instrument calibration. Use a hot-stage microscope (HSM) for visual detection of the phase changes.

A5) *Glass transition*: Determine the glass-transition temperatures of several polymers.

A6) *Polymer crystallinity*: Polyethylene (PE) is a semicrystalline thermoplastic. From a DSC curve, determine the temperature range over which melting occurs as well as the enthalpy of melting. The percentage crystallinity is calculated by comparing the measured value with that for 100% crystalline material ($290\ J\ g^{-1}$).

A7) *Polymer stability*: compare the degradation in nitrogen of a suitable polymer with its oxidation in air or oxygen.
Examine the temperature regions before degradation starts to determine the glass-transition temperatures (see 5) and the occurrence of crystallization and/or melting.

A8) *Curing of an epoxy resin*: Do a DSC run on an epoxy glue mixture. Determine the enthalpy change of the exothermic curing process. Rescan the product and determine the glass-transition temperature of the polymer.

A9) *Specific heat capacity*: Determine the specific heat capacity of an inert substance, such as Al_2O_3, relative to that of aluminium metal ($0.900\ J\ K^{-1}g^{-1}$ at 25°C). Comment on the variation of the specific heat capacity with temperature.

A10) *Purity determination*: Compare the melting endotherm of pure indium with that for benzoic acid and estimate the purity of the benzoic acid.

D.2 THERMOGRAVIMETRY (TG)

B1) *Temperature calibration*: Use magnetic standards of known Curie point, to calibrate the temperature of the furnace.

B2) *Dehydration*: Determine the temperatures and mass losses accompanying the dehydration stages of $CuSO_4.5H_2O$. Compare your results with those from the DSC experiment A2 and draw up a full description of the dehydration process.

B3) *Decompositions*: The studies carried out in the DSC experiment A3 can be complemented by determining the mass-losses accompanying the thermal events detected. Kinetics may be determined from non-isothermal experiments at different heating rates, or from a series of experiments at different isothermal temperatures.

B4) *Percentage filler in a polymer*: Decompose a sample of an expoxy putty in nitrogen. The residue is the filler.

B5) *Analysis of coal or of a rubber*: (a) Heat a sample in nitrogen until no further mass-loss occurs. This gives the proportion of volatile material. (b) Change the purge gas to oxygen while holding the sample at the high end of the temperature range. The mass-loss corresponds to the proportion of carbon residue. (c) The mass of the residue in oxygen corresponds to the inorganic ash.

APPENDIX E: EXAMPLES OF EXAMINATION QUESTIONS

1. Answer TWO of the following :

   (a) Describe the problems of and the techniques used for temperature calibration of thermal analysis instruments.

   (b) Discuss the problems of obtaining kinetic parameters from a single thermal analysis experiment.

   (c) Estimates of the purity of a material which melts may be made from analysis of a DSC melting endotherm. Describe the procedure.

---

2. Answer TWO of the following :

   (a) All thermal analysis instruments have features in common. Discuss these common features and the way in which the individual techniques differ from the generalized instrument.

   (b) Describe, with examples, the various types of curves obtained from thermogravimetric (TG) experiments, and discuss their interpretation.

   (c) Make a detailed comparison of the techniques of differential thermal analysis (DTA) and differential scanning calorimetry (DSC) and discuss the relative advantages and disadvantages of the techniques.

---

3. Write a report to the Managing Director of your company, which produces organic polymers, advising him of the advantages (and disadvantages) of introducing thermal analysis techniques into the research and quality-control laboratories.

---

4. Discuss the use of thermomechanical analysis (TMA) and dynamic mechanical analysis (DMA) in studying the physical properties of polymers.

---

5. (a) Explain what is meant by a 'transducer' and describe the transducers used in the main thermal analysis techniques.

(b) Discuss the information obtainable by applying thermal analysis techniques to the study of solid polymers.

---

6. (a) Discuss the possibilities of obtaining kinetic information from two thermal analysis experiments.

(b) Describe the uses of hot-stage microscopy (HSM) and evolved gas analysis (EGA) in extending the information obtainable from differential scanning calorimetry (DSC) or differential thermal analysis (DTA).

---

7. Answer TWO of the following sections :

(a) Discuss the use of a wide range of thermal analysis techniques in the study of the properties of polymers.

(b) Describe the techniques of evolved gas analysis (EGA) and their use in combination with other thermal analysis techniques.

(c) Outline the approach used to estimate the purity of organic compounds using differential scanning calorimetry (DSC).

---

8. Write a concise report (use your imagination) advising a polymer chemist on the possibility and advantages of using the techniques of thermal analysis in his or her research.

---

9. Discuss TWO of the following topics :

(a) Combinations of thermal analysis techniques with themselves and with evolved gas analysis and other complementary techniques.

(b) The principles, interpretation of results, and applications of differential scanning calorimetry.

(c) The use of thermal analysis in obtaining kinetic parameters for solid-state reactions.

(d) The use of thermomechanical analysis and of dynamic mechanical analysis in the characterisation of polymers.

---

10. EITHER

Discuss the possibility of determining the kinetics of a reaction from a single programmed-temperature experiment. Describe the simplifications that occur when experimentation is extended to at least a second programmed-temperature run or an isothermal run.

OR

It is claimed that absolute purities of certain solid substances may be determined using differential scanning calorimetry (DSC). Outline the approach and discuss this claim with particular reference to the underlined words.

---

11. Thermal analysis may be defined as the measurement of changes in properties of materials as a function of temperature. Describe the main properties which have been used and the information which can be obtained from such studies.

---

12. Compare the principles, practical limitations and the quantitative information obtainable from differential thermal analysis (DTA) and differential scanning calorimetry (DSC).

---

13. Answer TWO of the following :

(a) Discuss the similarities and differences between thermomechanical analysis (TMA) and dynamic mechanical analysis (DMA).

(b) Give a definition of "thermal analysis" and discuss this definition in terms of the materials studied, the types of changes taking place in these materials and the properties of these materials used to study these changes.

(c) Describe the techniques used for the analysis of gases evolved during thermal analysis experiments and compare the advantages and disadvantages of these techniques.

---

14. Attempt TWO of the following :

(a) Describe in detail the differences between differential scanning calorimetry (DSC) and differential thermal analysis (DTA).

(b) Describe the principles, apparatus and applications of dynamic mechanical analysis (DMA).

(c) Discuss the possibility of obtaining kinetic information from conventional (i.e. non-isothermal) thermogravimetry (TG).

(d) Describe a method for determining the purity of an organic compound using differential scanning calorimetry (DSC).

(e) Discuss the possibilities and problems of combining thermal analysis techniques and include discussion of evolved gas analysis.

EXPLANATION OF THE SYMBOLS USED IN THE TEXT

A = area; amplitude of vibration; Arrhenius pre-exponential factor; component of binary mixture

B = calibration factor (heat capacity); bulk modulus; sample thickness; component of binary mixture; amplitude of modulation

C = heat capacity; calibration constant; Curie constant

D = thermal diffusivity; amplitude of kinetically hindered response

E = Young's modulus; emanating power; Arrhenius activation energy

E' = storage modulus

E'' = loss modulus

F = force; fraction melted

$F( )$ = averaged function

G = shear modulus, Gibbs energy

H = enthalpy; magnetic field strength

K = instrument constant; heat transfer coefficient

K_f = crysoscopic constant

L = length

M = magnetization; molar mass

P = period of oscillation

Q = heat

R = as constant; thermal resistance

S = entropy; area

T = temperature

V = volume; voltage; attenuation

X = general abcissa

Y = general ordinate

a = constant; partial area; activity

b = constant

c = specific heat capacity; constant

d = diameter; thickness

θ = angle; Weiss constant
$\theta(T)$ = function of temperature
λ = thermal conductivity
μ = chemical potential; micro
ν = ultrasonic velocity
ν_p = Poisson's ratio
ν_r = resonance frequency
ρ = density
σ = stress; ionic conductivity
χ = volume magnetic susceptibility
ω = angular frequency

Subscripts
c = calibrant; completion
C = Curie point
e = eutectic; extrapolated
f = furnace; fusion; final
fus = fusion
g = glass transition
i = initial
m = melting
n = general number
o = initial or at 0 K or at 0°C; melting
p = onstant pressure; peak; programme
p-p = peak-to-peak
r = reference
rm = measured reference
s = sample
sm = measured sample
t = time or temperature in Celsius
1 = refers to solvent
2 = refers to solute
½ = half-step

Superscripts
o = standard
– = molar quantity
* = impurity

e = exponential base
f = frequency
f( ) = conversion function; general function
fus = fusion
g( ) = conversion function
(g) = gas
h( ) = conversion function
h = baseline displacement; height; relative amplitude of vibration
k = rate coefficient
(ℓ) = liquid
m = mass; constant exponent in rate equation
n = apparent order of reaction; number of moles
p = pressure; constant exponent in rate equation
$p(x)$ = temperature integral defined in Chapter 10 ($x = E/RT$)
q = heat
r = thermocouple resistance
s = partial area; mass magnetic susceptibility
(s) = solid
t = time; temperature in Celsius
w = weighting factor
x = mole fraction; dimension; (= E/RT)
x_1 = mole fraction of solvent
x_2 = mole fraction of solute
x_2^* = mole fraction of impurity
y = dimension
z = dimension; charge

Δ = change or finite difference; damping
α = coefficient of linear expansion; fractional reaction; constant for thermocouple
β = heating rate; constant for thermocouple
δ = constant for thermocouple; phase angle
ε = strain; dielectric constant
ϵ = undetermined premelting
η = viscosity coefficient

INDEX

S